The association of circular RNAs with hypertension

Bradley Aaron Woods

Biomedical Science (Honours)

Submitted in total fulfilment of the requirements for the degree of Doctor of Philosophy

Federation University Australia

PO Box 663
University Drive, Mount Helen
Ballarat Victoria 3350
Australia

August 2022

Primary Supervisor: **Prof. Fadi Charchar**

Co-Supervisors: **Dr Sean Byars (Melbourne University) and Associate Professor Simon Conn (Flinders University)**

Associate Supervisor: **Dr. Scott Nankervis**

Declaration of Authorship

This thesis is composed of my original work, and contains no material previously published or written by another person except where due reference has been made in the text. I have clearly stated the contribution by others to jointly authored works that I have included in my thesis.

I have clearly stated the contribution of others to my thesis, including statistical assistance, survey design, data analysis, significant technical procedures, professional editorial advice, and any other original research work used or reported in my thesis. The content of my thesis is the result of work I have conducted since the commencement of my research higher degree candidature and does not include a substantial part of work that has been submitted to qualify for the award of any other degree or diploma in any university or other tertiary institution. I have clearly stated which parts of my thesis, if any, have been submitted to qualify for another award.

I acknowledge that an electronic copy of my thesis must be lodged with the University Library and, subject to the policy and procedures of Federation University Australia, the thesis be made available for research and study in accordance with the Copyright Act 1968 unless a period of embargo has been approved by the Dean of the Graduate School.

I acknowledge that copyright of all material contained in my thesis resides with the copyright holder(s) of that material. Where appropriate I have obtained copyright permission from the copyright holder to reproduce material in this thesis.

Signed: Mr Bradley Aaron Woods

Thesis information

This thesis contains six chapters in total with chapter 1 being a literature overview and chapter 2 being a summary of material and methods. The three results chapters contain all my own work unless stated otherwise and lastly chapter 6 is discussion and conclusions linking together the work undertaken in this thesis.

All the work presented in this Thesis is my own work except the following:

1. Sample collection for the TRANSLATE study was conducted by Professor Maciej Tomaszewski.
2. TRANSLATE RNA sequencing data was provided by Dr James Eales
3. sRNA sequencing (minus analysis) was performed with the assistance of the Australian Genome Research Facility.
4. Bioinformatic analysis of sRNA sequencing data was undertaken with supervision from Dr Sean Byars.
5. RNA-sequencing was performed with the assistance of the Australia Genome Research Facility.

Thesis overview

Background: Hypertension (HT) is a complex condition that affects more than one billion people globally. Despite advances in our understanding of HT pathophysiology and the implementation of more effective treatment and prevention strategies, HT remains one of the world's great public health problems. HT can be classified as either essential or secondary, essential hypertension (EH) is defined as persistent blood pressure (BP) elevation in the absence of identifiable aetiologies. Due to the complex nature of EH this has led researchers to investigate the role of genetics in EH development in particular the role of epigenetics and how they regulate downstream gene expression.

Circular RNAs (circRNAs) are an underexplored class of the non-coding RNAs that have recently gained attention for their role in disease development and progression. Circular RNAs exert their effect through a variety of biological functions, the main functions being 'miRNA sponge' due to their ability to sequester miRNAs thereby inhibiting their effect on mRNAs. The role circRNAs perform in BP regulation is poorly understood with many studies to date focused on utilising circRNAs as a biomarker rather than investigating them as a contributing pathological factor to increased BP.

Hypothesis: The central hypothesis underpinning this PhD thesis is that alterations in hypertensive kidney circRNA expression plays a fundamental role in modulating gene expression involved in the regulation of BP and development of HT.

Aims: This PhD thesis focused on characterising the role of circRNA expression in the hypertensive kidney using sRNA and RNA sequencing methods. Three major aims are addressed.

- Aim 1: To perform a comprehensive sequencing experiment to identify renal circRNAs in a small cohort of hypertensive human kidney samples and to follow up validation in a larger sample.
- Aim 2: To characterize the previously identified circRNAs from Chapter 3 and identify whether they regulate miRNAs utilising sRNA sequencing methodology (Chapter 4).
- Aim 3: To identify downstream mRNAs that are impacted by reduced circRNA expression and the subsequent pathways that are impacted correlating this back to hypertension/blood pressure regulation (Chapter 5).

Results: In Aim 1 ultra-deep RNA sequencing was successful in identifying 12 differentially expressed circRNAs of which 11 had been previously annotated. Further validation of these results in a 65 human kidneys utilising qPCR methodology confirmed the expression of seven circRNAs. Subsequent *in-silico* analysis identified several predicted miRNA interactions for our circRNAs of interest of which expression analysis identified and confirmed the downregulation of two (miR-145 and miR-217). Further networking analysis identified several mRNAs predicted to interact with our two differentially expressed miRNAs of which several of them had a pre-established role in either BP regulation or HT pathophysiology.

For Aim 2 we knocked down the expression of three circRNAs in the HEK293 cell line (*circZNF91*, *circGRB10* and *circRP11-298P3.4*) to investigate their function as a 'miRNA sponge'. qPCR analysis confirmed circRNA knockdown whilst also confirming that the corresponding linear RNA was not downregulated, ensuring that any differentially expression observed it was independent of reduced mRNA expression. .sRNA sequencing identified 110 differentially expressed miRNAs for the *circRP11-298P3.4* model however no statistical significance was observed for the *circZNF91* and *circGRB10* model. Several of the impacted

miRNAs in the *circRP11-298P3.4* model have been identified to play a role in BP regulation or pathophysiology of HT.

Lastly for Aim 3m RNA sequencing was undertaken using the same circRNA knockdown models in the previous aim. RNA sequencing was undertaken and discovered several genes impacted across all three of our circRNA knockdown models. Subsequent pathway analysis identified many biological process were altered by the plethora of genes that were differentially expressed. Of interest was the *circRP11-298P3.4* model with a common biological function being altered was cholesterol synthesis.

Conclusion: This PhD Thesis provides novel evidence for implication of renal circRNA expression in HT pathogenesis and an association between circRNA expression and expression of genes associated with HT and BP. Together, this PhD Thesis provides new insights into the role of renal circRNAs in BP modulation. This thesis provides a framework for circRNA specific epigenetic regulation transcription in the human kidney and points towards circRNAs role in BP regulation and subsequent HT development.

Acknowledgments

What a journey the past 3 and ½ years have been. To undertake a PhD at the best of times is challenging, throw in a global pandemic and for some this would have been considered madness or impossible. However, like many others over the past couple of years I preserved. I would not have been able to complete this monumental task without the love and support from many people in my life.

First, to my primary supervisor Professor Fadi Charchar. Words cannot express the gratitude I have for the opportunity you have offered me. To be able to undertake a PhD was always a goal of mine and you made it come true. Your words of wisdom have helped guide me through what was been at times quite a difficult process but with them I was able to achieve something I never thought possible, especially through 2020/2021 when we were all working from home. To the rest of my supervisory team your support through my PhD journey has not gone unnoticed, to Dr Scott Nankervis, you have been part of my Federation University experience since day dot when I started my undergraduate degree back in 2015 (that feels like an eternity ago) and not long after I finished that you took me on as an honours student and gave me my first exposure to research which in way helped grow my love for the art of scientific research. To Dr Sean Byars your expertise with the RNA sequencing has been a saving grace for me throughout this journey, without your guidance and support I would have been lost and probably given up 10 times over by now and lastly Associate Professor Simon Conn, you are truly the circRNA guru. You provided that next level thinking that had previously gone overlooked over the first year and half of my PhD journey. You got me thinking on a different level and really opened my eyes to the level of thinking and understanding that is required at this level.

Over the past 7 odd years Federation University has been a large part of my life. From the very first day of my undergraduate degree in 2015 to my most recent day I have loved every moment. This is largely due to the people I have had the pleasure to meet and work with over the past 7 years. To everyone that is part of the Charchar lab I cannot thank you enough for your support and friendship over the past few years, especially to Dr Michelle Maier and Dr Priscilla Prestes. You both are truly amazing people and have helped me in more ways than you probably imagine. To all the other PhD students' part of the Charchar Lab, thank you for your support over the past three years. We have all been on this journey together and wish you all the best of luck in competing your PhD and for your future afterwards.

To the members of the Wendouree Fire Brigade, I have said this often, but I consider you all my second family. You have allowed me to escape the pressures of my PhD but usually that involved dealing with the pressures of CFA but to be honest, I did not mind that. I have had the great pleasure of being your 2nd and 1st Lieutenant throughout my PhD journey and I remember a lot of people telling me I was crazy for being an officer during what was already going to be a challenging journey. In hindsight those people were probably right, but would I change it now, absolutely not. I have loved every bit of the past four and a half years, to all the members of the BMT over that span thank you for being understanding of my circumstances and allowing me to succeed in all the positions I have held. To the rest of the membership, thank you for all the support you have given me in the various positions I have held over the past four and a half years. Your support has allowed me to thrive and hopefully bring about great change to the brigade.

To the team at Manse Medical/Sleep Health Group, you are truly the best. Words cannot express how grateful I am for the opportunity you have given me. To Andrew, Jess, and Jimmy, thank you for taking the chance on me to begin with and for continuing to have faith in me. To Taylah, Franz and Ben (Nurse Ben), thank you for taking the time to train me up

which at times could not have been an easy task haha. And lastly, because if I do not mention them, they will think I am the worst, Ash. Even though you think I am a dinosaur doctor you make work that bit more enjoyable. Now that this journey is complete, I look forward to continuing my journey with you all.

But, to save the best for last the biggest thanks has to go to my amazing wife Jenny and son Oliver. Jenny, you have made more sacrifices than I have throughout this journey and for that I cannot express how much it means to me. I have tried my hardest to get the work-life balance right but as you are aware that at times became difficult. From the early mornings and late nights, you tolerated more than some people could ever. You have always been my biggest supporter and helped me through the most difficult of times. I could not have achieved this without your love and support. To Oliver, being your dad is one of the greatest experiences of my life and I hope one day you will understand why Daddy couldn't play with you as much over the past year. I have always wanted to set the best example for you, and I hope that in the future you can look back on this and realise with hard work and dedication anything is possible. You are one of the best things to have happened to me and I can't wait to spend my spare time with both you and Mummy without the guilt of writing this thesis lingering over me.

An Australian Government Research Training Program (RTP) Stipend and RTP Fee-Offset Scholarship through Federation University Australia supported Bradley Aaron Woods

Conference presentations

- "Differentially expressed Circular RNAs in hypertensive patients"- Higher Degrees Research Conference, Federation University Australia, Ballarat, Australia, July 26th, 2019 (Oral Presentation)

- "Circular RNAs are upregulated in hypertensive patients" – Asian Pacific Congress of Hypertension, Brisbane, Australia, November 24th-27th 2019 (Oral Presentation) – **Awarded ISH-NIC (International Society of Hypertension New Investigators Committee) best student oral presentation award.**

- "Characterizing the role of the circular RNA, circRP11-298P3.4 in hypertension" – High Blood Pressure Research Council Australia Annual Scientific Meeting, Online, December 6th – 8th 2021 (Oral Presentation)

Publications arising during candidature

1. Prestes, P. R., Maier, M. C., **Woods, B. A**., & Charchar, F. J. (2020). A Guide to the Short, Long and Circular RNAs in Hypertension and Cardiovascular Disease. International journal of molecular sciences, 21(10), E3666. https://doi.org/10.3390/ijms21103666

Abbreviations

ACE: angiotensin converting enzyme

ACEi: angiotensin converting enzyme inhibitors

AGO: argonaute

AGO2: argonaute 2

AGRF: Australian Genome Research Facility

Alu: arthrobacter luteus

AngI: angiotensin I

AngII: angiotensin II

ANP: atrial natriuretic peptide

ARB: angiotensin receptor blockers

AT1R: angiotensin II type 1 receptors

AT2R: angiotensin II type 2 receptors

ATP2B1: ATPase plasma membrane Ca2+ transporting 1

BNP: brain natriuretic peptide

BP: blood pressure

CAD: coronary artery disease

CCB: calcium-channel blockers

cDNA: complementary DNA

circRNA: circular RNA

ciRNAs: circular intronic RNAs

CKD: chronic kidney disease

CNP: C-type natriuretic peptide

DBP: diastolic blood pressure

dsRNA: double-stranded RNA

DGCR8: DiGeorge syndrome critical region 8

ecircRNAs: exonic circRNAs

ECFV: extracellular fluid volume

EDHF: endothelium derived hyperpolarization factors

EH: essential hypertension

EIciRNAs: exonic-intronic circRNAs

FBS: foetal bovine serum

GFR: glomerular filtration rate

GWAS: genome wide association study

HAEC: human aortic endothelial cells

HBP: high blood pressure

HC: healthy control

HEK293T: human embryonic kidney 293T cell line

HF: heart failure

hiPSCs: human induced pluripotent stem cells

HMGCS1: hydroxymethylglutaryl-CoA synthase

HT: hypertension

hsa: *Homo sapiens*

HUVECs: human umbilical vein endothelial cells

IDI: insulin induced gene 1

IGF-1: insulin-like growth factor 1

IRES: internal ribosome entry site

ISH: international society of hypertension

KEGG: kyoto encyclopaedia of genes and genomes

LVH: left ventricular hypertrophy

m6A: methylated adenosine N6

MBR: miRNA binding region

MI: myocardial infarction

mRNA: messenger RNA

miRNA: micro RNA

MSMO1: methylsterol mono-oxygenase 1

ncRNAs: non-coding RNAs

NLRP3: nucleotide-binding domain like receptor protein 3

NP: natriuretic peptides

NPR-A: natriuretic peptide receptor A

NPR-B: natriuretic peptide receptor B

NPR-C: natriuretic peptide receptor C

NT: normotensive

PARP: poly (ADP-ribose) polymerase

pre-mRNA: pre-messenger RNA

qPCR: quantitative polymerase chain reaction

RAAS: renin-angiotensin-aldosterone system

RBM20: RNA binding motif protein 20

RBP: RNA binding protein

ROS: reactive oxygen species

rRNA: ribosomal RNA

SBP: systolic blood pressure

SD: sprague dawley

SEM: standard error of the mean

SHR: spontaneous hypertensive rat

siRNA: small interfering ribonucleic acid

SP1: specificity protein 1

SNS: sympathetic nervous system

SRY: sex determining region Y

SOD: superoxide dismutase

TRANSLATE: TRANscriptome of Renal Human TissuE

tRNA: transfer RNA

TXA2: thromboxane A2

TXNIP: Thioredoxin-interacting protein

VCAM-1: vascular cell adhesion protein 1

VSMC: vascular smooth muscle cells

WKY: wistar kyoto rat

Physicochemical and Biological Units

°C: degrees Celsius

µg: microgram

min: minutes

mM: millimolar

µM: micromolar

rpm: revolutions per minute

U: Units

Contents

Declaration of Authorship....ii
Thesis information iii
Thesis overview iv
Acknowledgments....vii
Conference presentations x
Publications arising during candidature xi
Abbreviations xii
Physicochemical and Biological Units xvi
Figures....xxii
Tables xxiv

Chapter 1 Literature Review....1
1.0 Hypertension 2
1.0.1 Aetiology of essential hypertension 2
1.1 Mechanisms involved in blood pressure regulation....3
1.1.1 Sympathetic nervous system 3
1.1.2 Renin angiotensin aldosterone system 5
1.1.3 Endothelial dysfunction....6
1.1.4 Natriuretic peptides 8
1.2 The role of kidneys in hypertension....10
1.3 Genetics of hypertension....15
1.4 Non-coding RNAs 17
1.5 Micro RNAs....17
1.5.1 miRNAs and hypertension 18
1.6 Circular RNAs 20
1.6.1 Circular RNA biogenesis 20
1.6.2 Circular RNA functions 24
1.6.2.1 Competitors of Linear RNA splicing and Gene Expression....25
1.6.2.2 MicroRNA Sponges 26
1.6.2.3 Protein Interaction 27
1.6.2.4 Protein Synthesis 28
1.7 Circular RNA and Cardiovascular Disease....28
1.7.1 Circular RNA and hypertension....30
1.7.2 Circular RNAs, myocardial infarction and heart failure 32

1.7.3 Circular RNAs, atherosclerosis and CAD 34
1.8 Conclusion 35
1.9 Hypothesis and Aims 37

Chapter 2 General Methods 39
2.0 Introduction 40
2.1 RNase R treatment and cDNA synthesis 40
2.2 CircRNA primer design 40
2.3 Quantification of circRNA expression using qPCR 41
2.4 TaqMan advanced miRNA cDNA synthesis and assays 42
2.5 Cell Culture 42
2.6 siRNA design and circRNA silencing 42
2.7 RNA Extraction 43
2.8 Linear RNA Primer Design 44
2.9 Linear RNA cDNA synthesis and gene expression analysis 44
2.10 Statistical Analysis 45

Chapter 3 Investigating circRNA expression in hypertensive human kidney samples 46
Abstract 47
3.0 Introduction 48
3.1 Methods 51
3.1.1 TRANscriptome of Renal Human TissuE (TRANSLATE) Study 51
3.1.2 Ultra-deep RNA sequencing 52
3.1.3 Bioinformatic identification of circRNAs and primer design 55
3.1.4 RNase treatment and cDNA synthesis 56
3.1.5 Quantification of circRNA expression using qPCR 56
3.1.6 Quantification of linear isoforms 57
3.1.7 *In-silico* identification of predicted circRNA – miRNA interactions 57
3.1.8 Quantification of miRNA expression using TaqMan Advanced miRNA assays. 58
3.1.9 *In-silico* identification of circRNA-miRNA-mRNA network 58
3.1.10 Quantification of predicted mRNA targets 59
3.1.11 Statistical Analysis 59
3.2 Results 59
3.2.1 Clinical characteristics of TRANSLATE study participants 59

3.2.2 CircRNA sequencing identifies differentially expressed circRNAs within the TRANSLATE cohort 60
3.2.3 qRT-PCR validation of human kidney samples confirms some of the circRNA sequencing data 62
3.2.4 Linear isoforms of circRNAs are not impacted by the differentially expressed circRNAs. 64
3.2.5 Predicted miRNA-circRNA interactions display several miRNAs implicated with hypertension development 66
3.2.6 miRNA expression analysis from the TRANSLATE study identifies several differentially expressed miRNAs of interest 68
3.2.7 *In silico* gene networking outlines several mRNAs previously identified in HT studies interacting with our DE circRNAs and miRNAs 69
3.2.9 mRNA expression from the TRANSLATE study supports potential circRNA-miRNA-mRNA interactions 70
3.3 Discussion 72
3.4 Limitations 77

Chapter 4 Reduced circRNA expression and its impact on miRNA expression profile 78
Abstract 79
4.0 Introduction 80
4.1 Methods 82
4.1.1 Cell culture 82
4.1.2 siRNA design and transfection 82
4.1.3 RNA extraction 82
4.1.4 RNase R treatment and circRNA cDNA synthesis 82
4.1.5 Quantification of circRNA expression using qRT-PCR 83
4.1.6 Linear RNA cDNA synthesis and qPCR 83
4.1.7 Small RNA library prep 83
4.1.8 Small RNA sequencing analysis 84
4.2 Results 85
4.2.1 Successful knockdown of circRP11-298P3.4, circZNF91 and circGRB10 did not impact the linear isoform expression 85
4.2.2 Knockdown of *circRP11-298P3.4* resulted in differentially expressed miRNAs 87
4.2.3 Knockdown of *circZNF91* did not alter the miRNA expression 90
4.2.4 Knockdown of *circGRB10* did not alter the miRNA expression 92
4.2.5 miRNAs of interest from *circRP11-298P3.4* knockdown 94
4.3 Discussion 98

4.4 Limitations 102

Chapter 5 Reduced circRNA expression and its impact on the mRNA expression profile 104
Abstract 105
5.0 Introduction 107
5.1 Methods 109
5.1.1 Cell culture 109
5.1.2 siRNA design and transfection 109
5.1.3 RNA extraction 109
5.1.4 RNase R treatment and circRNA cDNA synthesis 109
5.1.5 Quantification of circRNA expression using qRT-PCR 109
5.1.6 Linear RNA cDNA synthesis and qPCR 109
5.1.7 RNA Sequencing Library Preparation 110
5.1.8 RNA Sequencing Analysis 110
5.1.9 Construction of circRNA – miRNA – mRNA network 111
5.1.10 Pathway Analysis 111
5.2 Results 112
5.2.1 Reduced circZNF91 expression resulted in an altered mRNA expression profile in the absence of differentially expressed miRNAs 112
5.2.2 Reduced circGRB10 expression resulted in an altered mRNA expression profile in the absence of differentially expressed miRNAs 117
5.2.3 Reduced circRP11-298P3.4 expression resulted in an altered mRNA expression profile 122
5.2.4 circRP11-298P3.4 Pathway Analysis 126
5.2.5 circZNF91 Pathway Analysis 128
5.2.6 circGRB10 Pathway Analysis 134
5.2.7 circRNA – miRNA – mRNA networks of interest for circRP11-298P3.4 142
5.3 Discussion 144
5.4 Limitations 149

Chapter 6 Discussion and Conclusions 150
6.0 Overview 151
6.2 Discussion 154
6.4 Future Directions 160

References.....162

Appendix.....175
1) circZNF91 knockdown Gene Ontology pathway analysis 175
2) circZNF91 knockdown Reactome pathway analysis.....180
3) circGRB10 knockdown Gene Ontology pathway analysis.....189
4) circGRB10 knockdown Reactome pathway analysis 210

Figures

Figure 1.1: Renin-Angiotensin-Aldosterone System control of blood pressure.

Figure 1.2: Link between oxidative stress and hypertension

Figure 1.3: Physiology of natriuretic peptides

Figure 1.4: The kidneys response to an increase in blood pressure.

Figure 1.5: Biogenesis of mature messenger RNA (mRNA) and circular RNA (circRNA) from precursor mRNA (pre-mRNA).

Figure 1.6: Models of circRNA biogenesis

Figure 1.7: Function of circular RNAs

Figure 2.1: Designing divergent primers for circRNAs

Figure 2.2: Designing siRNAs for circRNAs

Figure 3.1: CircRNA library preparation flowchart leading to sequencing

Figure 3.2: CircRNA analysis flowchart

Figure 3.3: DE circRNAs from grouped analysis

Figure 3.4: Scatterplot group 1 vs group 2 DE circRNAs.

Figure 3.5: Validation of DE circRNAs in the TRANSLATE study.

Figure 3.6: Next-generation RNA sequencing quantification of mRNA isoforms of our circRNAs of interest

Figure 3.7: DE circRNA predicted interactions with miRNA implicated with hypertension development./progression.

Figure 3.8: Expression of miRNAs predicted to interact with our DE circRNAs.

Figure 3.9: circRNA – miRNA – mRNA network.

Figure 3.10: Differentially expressed mRNAs of interest from the TRANSLATE Study

Figure 3.11: Refined circRNA – miRNA – mRNA predicted interactions from the TRNASLATE Study

Figure 4.1: Knockdown confirmation of circZNF91, circRP11-298P3.4, circGRB10 and corresponding mRNA.

Figure 4.2: Top 50 differentially expressed miRNA heatmap for circRP11-298P3.4 knockdown

Figure 4.3: Top 50 miRNA heatmap for *circZNF91* knockdown

Figure 4.4: Top 50 miRNA heatmap for *circGRB10* knockdown

Figure 4.5: Proposed impact of siRNA knockdown of circRNAs

Figure 4.6: *circRP11-298P3.4* predicted miRNA interactions post miRNA sequencing

Figure 5.1: Smearplot of *circZNF91* knockdown mRNA sequencing

Figure 5.2: Top 50 differentially expressed genes heatmap for *circZNF91* knockdown

Figure 5.3: Smearplot of *circGRB10* knockdown mRNA sequencing

Figure 5.4: Top 50 differentially expressed genes heatmap for *circGRB10* knockdown

Figure 5.5: Smearplot of *circRP11-298P3.4* knockdown mRNA sequencing

Figure 5.6: Top 50 differentially expressed genes heatmap for *circRP11-298P3.4*

Figure 5.7: Gene Ontology biological process impacted by reduced *circRP11-298P3.4* expression

Figure 5.8: Gene Ontology biological process impacted by reduced *circZNF91* expression

Figure 5.9: Gene Ontology biological process impacted by reduced *circGRB10* expression

Figure 5.10: Finalised circRNA – miRNA – mRNA network for *circRP11-298P3.4* model

Tables

Table 1.1: Genome-wide association studies of hypertension

Table 1.2: MicroRNAs found in blood pressure regulation and essential hypertension studies

Table 1.3: Summary of circRNAs implicated in CVDs including species, sample types studied and differential expression direction

Table 3.1: Summary of circRNA EH findings

Table 3.2: CircRNA primer sequences

Table 3.3: miRNAs measured utilising TaqMan™ Advanced miRNA assays

Table 3.4: Clinical characteristics of individuals in the TRANSLATE study

Table 3.5: Clinical characteristic of individuals used in the circRNA sequencing from the TRANSLATE study.

Table 3.6: Details of the DE circRNAs from Group 1 vs Group 2

Table 4.1: Circular RNA siRNA sequence and associated scramble controls

Table 4.2: Linear isoform RT-PCR primer sequences

Table 4.3: Top 50 differentially expressed miRNAs as result of *circRP11-298P3.4* knockdown

Table 4.4: Top 50 miRNAs from *circZNF91* knockdown

Table 4.5: Top 50 miRNAs from *circGRB10* knockdown

Table 4.6: Literature search to identify which differentially expressed miRNAs of interest (from circRP11-298P3.4 knockdown) have previously been identified to be associated with CVD and/or kidney function

Table 5.1: Top 50 Differentially expressed genes as result of *circZNF91* knockdown

Table 5.2: Top 50 Differentially expressed genes as result of *circGRB10* knockdown

Table 5.3: Top 50 Differentially expressed genes as result of *circRP11-298P3.4* knockdown

Table 5.4: Differentially expressed pathways from Gene Ontology pathway analysis from the *circRP11-298P3.4* knockdown model

Table 5.5: Differentially expressed pathways from Reactome pathway analysis from the *circRP11-298P3.4* knockdown model

Table 5.6: Differentially expressed pathways from Gene Ontology pathway analysis from the *circZNF91* knockdown model

Table 5.7: Differentially expressed pathways from Reactome pathway analysis from the *circZNF91* knockdown model

Table 5.8: Differentially expressed pathways from Gene Ontology pathway analysis from the *circGRB10* knockdown model

Table 5.9: Differentially expressed pathways from Reactome pathway analysis from the *circGRB10* knockdown model

Table 5.10 *CircRP11-298P3.4* model mRNAs of interest function

Chapter 1

Literature Review

1.0 Hypertension

Hypertension (HT), also known as high blood pressure (HBP), is a medical condition of persistently elevated arterial blood pressure (BP). As per the International Society of Hypertensions (ISH) guidelines, HT is defined by a systolic blood pressure (SBP) ≥140mmHg and/or a diastolic blood pressure (DBP) ≥90mmHg [1]. A HT diagnosis is made when the average of 2 or more diastolic BP measurements on at least 2 subsequent visits is ≥90 mmHg or when the average of multiple systolic BP readings on 2 or more subsequent visits is consistently ≥140 mmHg [2]. High BP is typically not associated with other symptoms which is why it is often coined with the term 'the silent killer', but prolonged exposure is a major risk factor for coronary artery disease (CAD), stroke, heart failure, atrial fibrillation, peripheral vascular disease, vision loss, chronic kidney disease (CKD), and dementia [3]. HT can be classified as either essential (also coined primary or essential) or secondary. Essential hypertension (EH) is defined as persistent BP elevation in the absence of identifiable aetiologies. Secondary hypertension occurs as result of an underlying condition, such as those directly affecting the kidney e.g., CKD [4]. Remarkably, around 90–95% of cases are classified as EH [5]. In Australia alone, an estimated 4.1 million people aged between 20-69 have been diagnosed with HT accounting for approximately 25.9% of Australia's workforce [6]. Furthermore, the mortality burden associated with HT continues to grow, with the worldwide attributable deaths increasing by 8.6% since 1990 [7]. As a result of the growing morbidity and mortality rates associated with HT the World Health Organisation [8] is aiming to reduce the prevalence of HT by 25% by 2025 [9].

1.0.1 Aetiology of essential hypertension

The origins of EH are still poorly understood. Genetic factors are however believed to play a pivotal role in the development of EH. Within the past 10 years, numerous

large-scale studies have identified several genetic variants associated with risk of HBP [8, 10-17] these are discussed in greater details in sections 1.3 to 1.6. Genetic variations can also interact with several environmental and lifestyle factors that increase BP and progress to EH development. These factors include but are not limited to obesity, insulin resistance, high alcohol intake, high salt intake (in salt-sensitive patients), aging, sedentary lifestyle, stress, low potassium intake, and low calcium intake [2].

1.1 Mechanisms involved in blood pressure regulation

Biological mechanisms involved in the maintenance of normal BP include the sympathetic nervous system (SNS), endothelial dysfunction, the renin-angiotensin-aldosterone system (RAAS) and natriuresis mediation by natriuretic peptides. In a healthy individual, the SNS contributes to the maintenance of adequate BP by promoting cardiac contractility and heart rate (maintenance of adequate cardiac output) and by inducing arteriolar vasoconstriction (maintenance of adequate peripheral resistance) [18]. The RAAS provides an important homeostatic mechanism for maintaining adequate BP and therefore tissue perfusion [19]. The natriuretic peptides include atrial natriuretic peptide (ANP), brain natriuretic peptide (BNP) and C-type natriuretic peptide (CNP). These peptides induce diuresis; enhancement of renal blood flow and glomerular filtration rate (GFR), systemic vasodilation, the suppression of aldosterone; and inhibition of the SNS [20]. The dysfunction of one or more of these biological mechanisms can be involved in the development of EH [21].

1.1.1 Sympathetic nervous system

Increased SNS activity increases BP and contributes to the development and maintenance of hypertension through stimulation of the heart, peripheral vasculature, and kidneys, causing fluid retention and increased cardiac output and vascular

resistance [22]. The factors responsible for increased sympathetic activity in EH have not been fully elucidated. Genetic, behavioural and lifestyle factors however may contribute to an increase SNS activity [23, 24], for example, obesity has been linked to both HT and nervous system dysfunction [25]. Obesity activates the sympathetic nervous system, including the renal sympathetic outflow [26], although the precise mechanisms is unclear.

In early stages of EH the peripheral resistance is not elevated and the increase in BP is caused by elevated cardiac output, which is influenced by sympathetic overactivity [22]. In addition, autonomic imbalance, characterised by increased sympathetic activity accompanied by reduced parasympathetic activity has been associated with many renal, haematological and metabolic abnormalities that result in increased cardiovascular morbidity and mortality [27]. Recent human studies suggest that sustained increases in heart rate is mainly associated with decreased parasympathetic tone, supporting previous findings suggesting that increased SNS activity contributes to the pathogenesis of HT [27]. Furthermore, as DBP is more closely related to vascular resistance than to cardiac function, suggesting that increased sympathetic tone may increase DBP by causing vascular smooth muscle cell (VSMC) proliferation and peripheral vascular remodelling [28]. Chronic sympathetic stimulation induces vascular remodelling and cardiac hypertrophy, presumably by direct and indirect actions of norepinephrine on its own receptors, as well as on release of various trophic factors, including transforming growth factor, insulin-like growth factor 1(IGF-1), and fibroblast growth factors [29]. Clinical studies have shown positive correlations between circulating norepinephrine levels, left ventricular mass, and reduced radial artery compliance (an index of vascular hypertrophy) [30]. Thus, it can be concluded that increased SNS function can be a contributing factor to the pathogenesis of HT.

1.1.2 Renin angiotensin aldosterone system

The RAAS is part of the endocrine system that modulates the control of BP (Figure 1.1). Renin (also known as angiotensinogenase) is secreted from the juxtaglomerular apparatus of the kidney in response to glomerular under perfusion or a reduced salt intake [31]. Renin is also released in response to stimulation from the SNS [29]. Renin is responsible for converting angiotensinogen to angiotensin I (AngI), a physiologically inactive substance which is rapidly converted to angiotensin II (AngII) in the lungs by angiotensin converting enzyme (ACE) [5]. AngII is a potent vasoconstrictor and thus causes an increase in BP to counter glomerular under-perfusion and osmotic alteration in blood volume in salt-depleted states [32]. In addition Ang II stimulates the release of aldosterone from the zona glomerulosa of the adrenal gland, which results in a further rise in BP related to sodium and water retention [33]. Aldosterone is a mineralocorticoid hormone that promotes Na^+ and water retention, which it does so primarily by acting on the mineralocorticoid receptors in the distal tubules and collecting ducts of the nephrons [34]. The circulating components of the RAAS are not thought to be directly responsible for the rise in BP in EH however, as many HT patients have low levels of renin and AngII and drugs that block the RAAS are not particularly effective at treating the HT [19]. There is however increasing evidence that there are important non-circulating “local” RAAS. Local RAAS refers to tissue-based mechanisms of Ang peptide formation that operate separately from the circulating RAAS [35]. These systems appear to control BP and have been reported in the kidney, heart, and the arterial tree where they may have important roles in regulating regional blood flow [35].

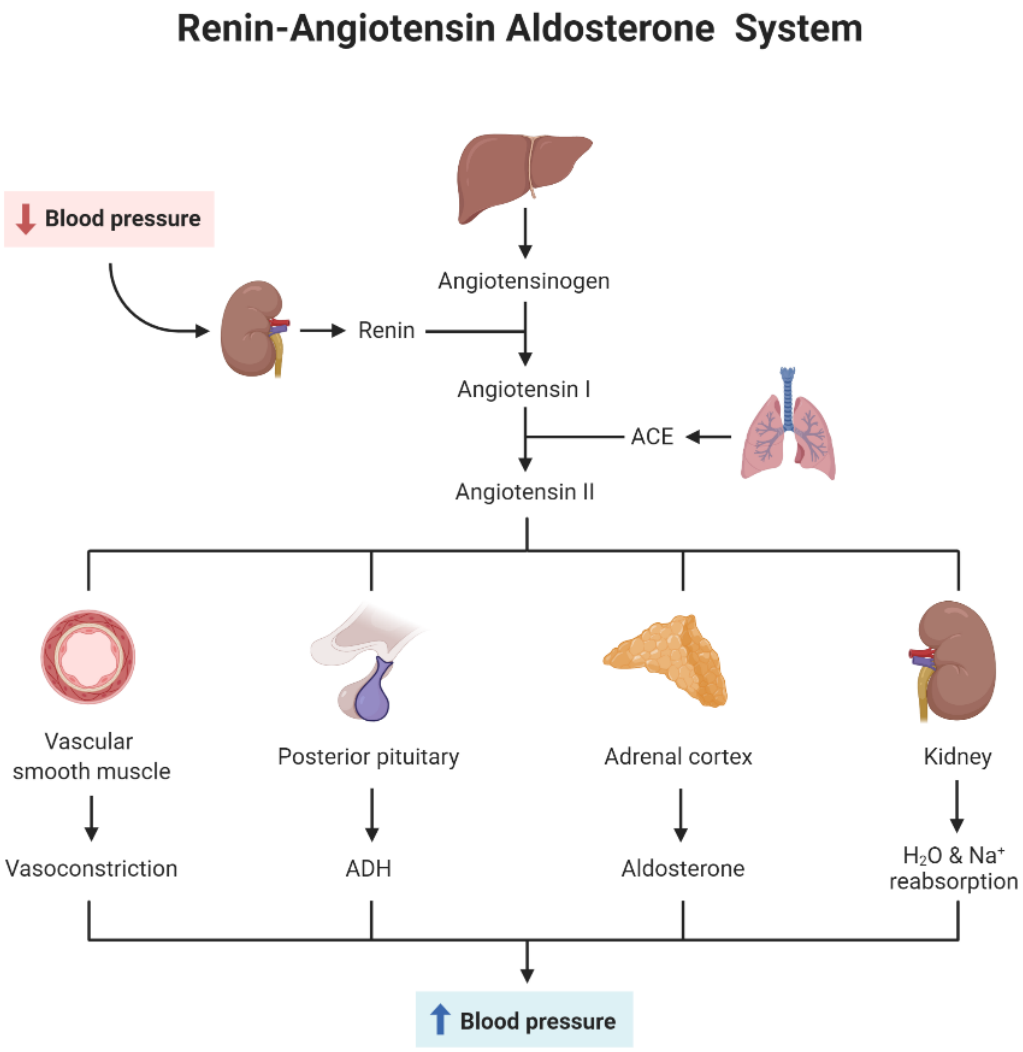

Figure 1.1: Renin-Angiotensin-Aldosterone System control of blood pressure. *A decrease in BP results in Renin production from the kidneys, which converts Angiotensinogen to its active form Ang1. ACE from the lungs converts AngI to AngII, which acts on the blood vessels, kidneys, adrenal gland & the SNS to increase blood pressure. Created with BioRender.com*

1.1.3 Endothelial dysfunction

The vascular endothelium represents a dynamic cellular environment between circulating blood and underlying tissue, acting as an integrator and transducer of the humoral and mechanical stimuli [36]. The vascular endothelium releases two

vasoconstrictor factors, endothelin 1 (ET-1) and thromboxane A2 (TXA2), as well as mediators of vasodilation, such as nitric oxide (NO), prostacyclin, and the endothelium derived hyperpolarization factors (EDHF) [37]. A healthy endothelium responds to stimuli constantly releasing potent vasodilators, which have the potential to reduce vascular resistance. It is however when the vascular endothelium fails to respond/acknowledge these stimuli or experience them in higher concentration, endothelial dysfunction occurs [38]. Endothelial dysfunction is defined as the imbalance between production and bioavailability of endothelium derived vasoconstrictor factors and endothelium-derived vasodilation factors [36]. For example, under normal conditions NO is released by endothelial cells in response to various stimuli, including changes in BP, shear stress, and pulsatile stretch, all of which are side effects of HT. In this way the cardiovascular system in a healthy person is exposed to continuous NO-dependent vasodilator tone, but NO-related vascular relaxation is diminished in HT patients [39]. One of the largest contributors to decreased vascular NO is increased oxidative stress (Figure 1.2). Oxidative stress is the imbalance between the systemic production of reactive oxygen species (ROS) and a biological system's ability to detoxify the reactive intermediates or to repair the resulting damage [40]. Oxidative stress has been demonstrated to play a causal role in different vascular diseases, such as HT [41]. A dominant mechanism of impaired vascular NO bioavailability relates to its oxidative inactivation by ROS and this can subsequently contribute to development of HT (Figure 1.2) [42]. The *in vivo* delivery of superoxide dismutase (SOD) has been observed to reduce BP and by restoring the homeostasis of NO bioactivity [43]. This provides further evidence that oxidative stress contributes to the inactivation of NO and restoration of NO bioavailability can

reverse endothelial dysfunction occurring in Spontaneous Hypertensive Rat (SHR) model of HT [44].

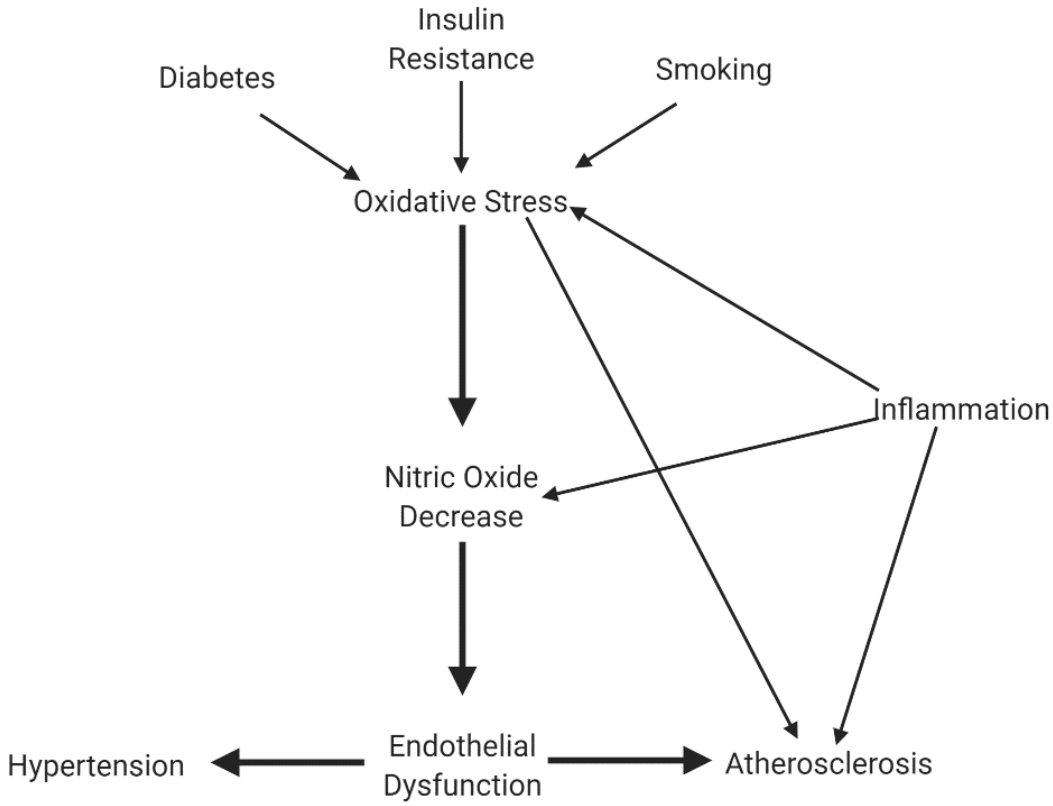

Figure 1.2: Link between oxidative stress and hypertension. *Oxidative stress contributes to a decrease in NO bioavailabity leading to endothelial dysfunction and subsequently cardiovascular disease development. Created with BioRender.com*

1.1.4 Natriuretic peptides

The natriuretic peptides (NPs) are another BP regulatory system that controls renal sodium (Na+) excretion and regulate vascular tone through a variety of mechanisms. The NPs include atrial natriuretic peptide (ANP), brain natriuretic peptide (BNP) and C-type natriuretic peptide (CNP) and interact with three distinct membrane bound receptors; natriuretic peptide receptor-A, B and C (NPR-A, NPR-B and NPR-C) [45]. As with any ligand-receptor interaction there is a preferred binding affinity for each

receptor with ANP and BNP binding selectively to NPR-A, and CNP binds to NPR-B [45]. NPR- A and NPR-B are both guanylyl cyclase coupled transmembrane receptors, when upon ligand binding induces the production of the second messenger cyclic guanosine monophosphate (cGMP) mediating the majority of NPs biological effects [46]. NPR-C however, lacks the guanylyl cyclase activity and it is mainly a clearance receptor for NPs either through degradation or internalization of the NPs [47]. ANP and BNP are both cardiac hormones with ANP produced primarily from the atria and BNP produced primarily in the ventricles of the heart [48]. Both ANP and BNP have similar cardiovascular and metabolic properties such as promoting vasodilation, natriuresis and suppression of the RAAS (Figure 1.3) [49], whereas, CNP is produced by the endothelium and regulates local vascular tone (Figure 1.3) [50]. Dysfunction of NPs in conjunction with RAAS and SNS abnormalities can contribute to an increase in vascular tone and a shift in the pressure-natriuresis relationship subsequently contributing to an observed increase in BP. The important role of the natriuretic peptides in the regulation of BP has been demonstrated in several animal models. For example, early research on transgenic BALB/c mice overexpressing ANP or BNP exhibit hypotension in comparison with genetically normal controls [51, 52]. This observed decrease in BP could be contributed by an increased suppression of the RAAS which is vital in the regulation of BP. Bae *et al*., (2011) supports this hypothesis by demonstrating that mice with Ang II induced HT have increased expression of renal ANP which was explained as a compensatory mechanism to increased RAAS components (Ang II) within the mice [53]. Further to this BNP has been displayed to directly inhibit renal production of renin and reduce the expression of CYP11B2 mRNA, the enzyme responsible to produce aldosterone both of which are key components of the RAAS [54, 55]. These studies outline the

important role that NPs have in BP regulation and how the impairment of these peptides can contribute to the development of HT.

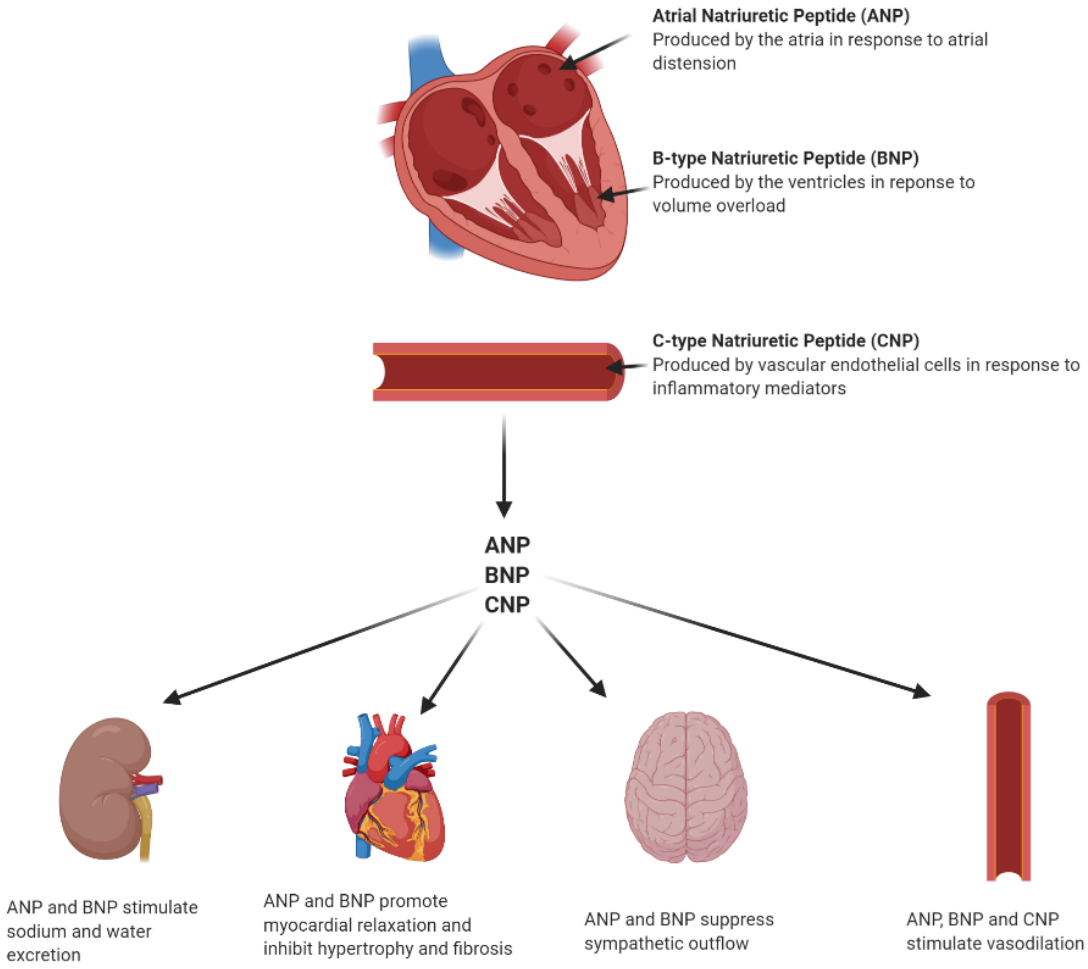

Figure 1.3: Physiology of natriuretic peptides*. The heart produces ANP and BNP with CNP produced within the vasculature. ANP, BNP and CNP exert several mechanistic effects on the kidneys, heart, brain, and vasculature to control BP. Created with BioRender.com*

1.2 The role of kidneys in hypertension

The biological mechanisms controlling BP can be modulated by several organ systems however, one organ is considered the focal point of BP regulation: the kidneys. The kidney has a pivotal role in controlling BP by regulating salt and water homeostasis and is more

commonly known as pressure natriuresis a term coined by Arthur Guyton in 1961 [56, 57]. Under normal conditions, an increase in BP is communicated to the kidney as an increase in renal perfusion pressure, which results in an increased excretion rate of sodium and water (Figure 1.4). The subsequent decrease in the volume of extracellular fluid returns BP back toward homeostasis. However, when this pressure natriuresis becomes impaired there is a decline in kidney function [58]. Importantly, the prevalence of HT is closely associated with the level of kidney function. One such determinant of renal function is the GFR which is calculated as the volume of fluid filtered from the glomerular capillaries into the Bowman's capsule per unit of time [59]. The National Kidney Foundation has outlined that the GFR range in a healthy adult is from 90 to 120 mL/min/1.73 m^2 [60]. Interestingly, it has been reported that the percentage of patients with HT increases in parallel with decreased kidney function irrespective of kidney disease based on data from the National Health and Nutrition Examination Survey III. This survey included 15,600 individuals and discovered that more than 40% of those with a GFR of 60–90 mL/min/1.73 m^2 had a BP level of ≥140/90 mmHg, indicative of a HT phenotype [61]. This observation supports the kidney being the focal point of BP regulations. Nevertheless, the question now becomes what mechanisms impact renal function to the point that HT occurs?

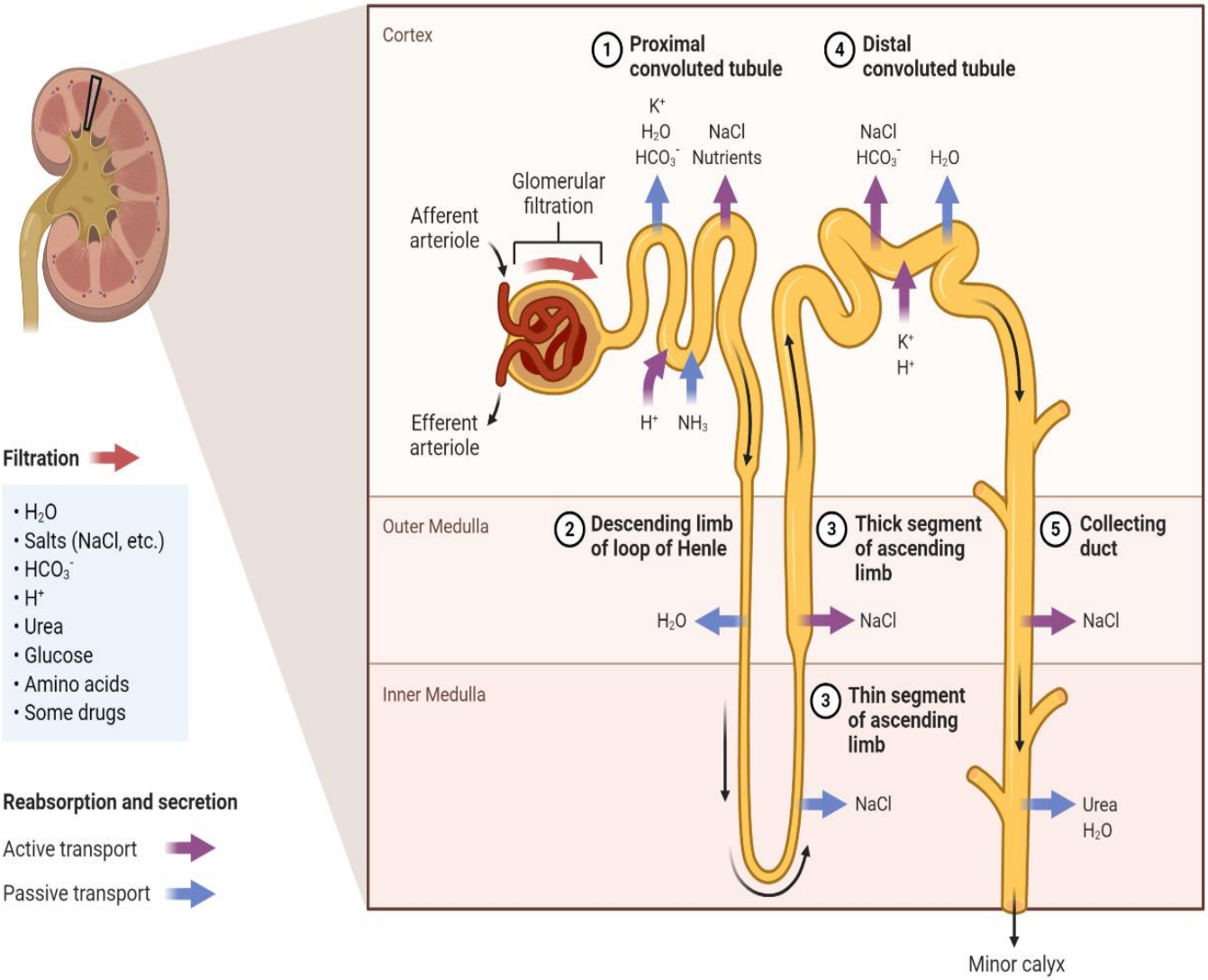

Figure 1.4: The kidneys response to an increase in blood pressure. *Outlining electrolyte and water redistribution throughout the various structures of the kidney to mitigate the increase in blood pressure. Created with BioRender.com*

Several pathways participate in maintaining pressure natriuresis and disturbance of any of these pathways can ultimately contribute to HT development (section 1.1). It is important to note that these pathways do not work in isolation but are inter-related. For example, activation of the SNS contributes to HT development by stimulating the kidney to release renin and subsequently activating the RAAS contributing to an increased BP (Figure 1.1) [62]. Renal SNS activity has long been recognized as a major contributor to the development and progression of HT [62]. Studies involving the SHR model of HT have observed that

signals from the CNS and renal nerve stimulation can induce sodium and water reabsorption within the kidneys, thereby decreasing sodium and water excretion with a subsequent rise in BP. Further to this Klein *et al*., demonstrate that SNS activity was increased in HT patients with autosomal dominant polycystic kidney disease (ADPKD) whereas SNS activity in ADPKD patients without HT were similar to those in the normal control [63]. Taken together, the results from these studies indicate that HT can be mediated by SNS signals arising from the kidneys.

As stated in Section 1.1.2, the RAAS is key regulatory mechanisms for BP control and all components of the RAAS can be synthesized locally in the kidney. Angiotensinogen is synthesized in the cortex and medulla of the kidney and is subsequently converted to Ang I by renin travelling within the vasculature or present in the renal interstitium [64, 65]. ACE is localized within the proximal tubules, distal tubules and collecting ducts, and promotes intrarenal production of Ang II [66]. In addition to its vasoconstrictive properties, Ang II also stimulates release of pro-renin and renin from the collecting duct principal cells [67]. Lastly, aldosterone synthesis primarily occurs in the zona glomerulosa of the adrenal cortex, however, Xue and Siragy (2005) discovered that aldosterone is produced by the glomeruli and proximal tubules of the kidney [68]. This knowledge supports a role for intrarenal RAAS in BP regulation and once again displays the kidney as a focal point behind BP regulation.

ET-1 was originally described as a potent vasoconstrictor produced primarily in the peripheral vasculature; however, ET-1 is now known to be produced by many cell types including the kidney podocyte and has a plethora of functional abilities including renal vasoconstriction, mesangial cell contraction, glomerular cell proliferation, extracellular matrix accumulation, and alterations in nephron fluid and electrolyte transport [69]. ET-1 acts by binding two distinct receptors, the endothelin A, and the endothelin B receptors (ET_AR and ET_BR). The ET_AR promotes vasoconstriction by stimulating water and sodium retention

whilst the ET_BR promotes vasodilation through vascular release of the vasodilator NO and expulsion of water and sodium [70]. In the rat remnant kidney model of chronic renal failure, ET-1 production was observed to increase in renal tissues [71]. These changes in ET-1 expression correlated with an increase in BP and the development of other cardiovascular abnormalities such as cardiac hypertrophy. Further to this finding, in uremic hypertensive rats the expression of ET-1 was increased in the renal cortex in conjunction with a 1.6-fold upregulation of the ET_AR [72]. The same study also identified a significant reduction in the ET_BR, which is responsible for instigating vasodilation and hence reducing BP [72]. Similar results have also been obtained in a number of other rat models of HT such as the Ang II infused [73], Dahl Salt-sensitive rat [74] and DOCA-salt model [75] supporting the overarching hypothesis that over activation of ET_AR and subsequent impairment of the ET_BR pathway is contributing to an increased BP in these rats.

As stated previously, EH is an increased BP without a known cause. This has led researchers to believe that genetics play a significant role in the development of EH, specifically, the genetics involved within the kidney. Several transplantation studies using genetically pre-disposed hypertensive rats have established that the kidneys carry at least a portion of the genetic message for HT. For example, a study conducted by Bianchi *et al*., in 1974 demonstrated that when the normotensive WKY rat is transplanted with a kidney from the genetically pre-disposed SHR they develop an increase in BP with the reverse effect being found in the HT rats that were transplanted with the normotensive kidney. In humans, it has been more difficult to obtain any results, however, a study from 1996 followed 85 patients who received kidney transplantations 8 years after surgery and observed that a person who had received a kidney from a donor with a family history of HT was 10 times more likely to develop HT [76]. Accordingly, a person who was the recipient of a kidney from a donor without a family history of HT was less likely to develop HT [76]. Both studies have outlined

that one of the keys to solving the mystery behind EH development is to better understand the role our genetics play within the kidney and how they influence mechanisms involved in BP regulation.

1.3 Genetics of hypertension

Heritability of BP is estimated to be 50% but there are also substantial environmental factors affecting BP variability [77]. It is assumed that BP is under the control of a large number of genes each of which has only relatively mild effects [78]. Despite this strong heritability, determining the genetic architecture of HT in humans has been challenging, most of the genomic discoveries of common variants affecting BP account for <4% of the between-person variation in the trait [79]. Several genome-wide association studies (GWAS) spanning multiple ethnicity groups have identified a variety of genes associated with BP regulation (Table 1.1). For example, one such GWAS identified uromodulin (UMOD) as a specific gene of interest. UMOD may exert its effects on HT and CVD, at least partly through its effects on renal function. UMOD is expressed primarily in the thick ascending limb of the loop of Henle, which is where most of the sodium excretion occurs within the kidney [15]. As discussed previously maintenance of the pressure-natriuresis relationship is pivotal in the regulation of BP and UMOD may influence this relationship, however, functional studies are required to elucidate the role of UMOD in the kidney and how this participates in HT. To date the largest GWAS undertaken investigating BP was undertaken by Evangelou *et al.*, (2018) in over 1 million people of European ancestry [17]. This study identified 901 loci associated with BP regulation of which 535 were considered novel and highlighted gene regions in systems not previously implicated in BP regulation. Functional analysis undertaken by Evangelou *et al.*, (2018) highlights the importance of several of these loci in vasculature homeostasis. For example, several loci associated with the TGFβ signalling pathway

including SMAD family genes and the TGFβ gene locus itself. This pathway impacts sodium handling in the kidney and ventricular remodelling, while plasma levels of TGFβ have recently been correlated with HT. Although it is estimated that the heritability of BP is 50% attributable to genetic factors, only ≈2% of the phenotypic variance for SBP and DBP can be explained by variants identified through GWAS [79]. This has shifted the focus of researchers from RNAs that code for genes to RNAs that do not code for genes such as the non-coding RNAs (ncRNAs) and how they influence the expression of certain genes and what impact this has on BP regulation.

Table 1.1: Genome-wide association studies of hypertension

Study	*Sample Size (n=)*	*Ethnicity*	*Top Gene*
Levy et al., 2009 [16]	29,136	European	SH2B3
Newton-Cheh et al., 2009 [8]	34,433	European	CNNM2
Kato et al., 2011 [13]	19,608	Asian	HECTD4
Wain et al., 2011 [12]	74,064	European	ATXN2
Ehret et al., 2011 [14]	69,395	European	CSK
Warren et al., 2017 [10]	140,886	European	JAG1
Padmanabhan et al., 2010 [15]	36,386	European	UMOD
Hoffmann et al., 2017 [11]	99,785	Non-Hispanic (81%) Latinos (8%) East Asians (7%) African Americans (3%) South Asians (1%)	Multiple
Evangelou et al., 2018 [17]	757,601	European	Multiple

1.4 Non-coding RNAs

For many years, non-coding RNAs (ncRNAs) were considered part of the 'junk' genome. This is due to them being transcribed from DNA but not undergoing translation into proteins [80]. The first ncRNAs were described in the translation process for messenger RNAs (mRNAs) being the ribosomal RNAs (rRNA) and transfer RNAs (tRNA). ncRNAs are usually stage, tissue, and species specific and their involvement in the regulation of mRNA levels is at a transcriptional and post-transcriptional level. ncRNAs have been classified into either short ncRNAs if less than 30 nucleotides, such as micro RNAs (miRNAs), small interfering RNAs (siRNAs) and piwi-interacting RNAs or long ncRNAs if greater than 200 nucleotides, such as long intergenic ncRNAs and circular RNAs (circRNAs) [81]. ncRNAs have been described as potential biomarkers and therapeutic targets for CVDs due to their increased stability and ability to withstand degradation in the blood stream. This is largely due to their association with proteins, apoptotic bodies, microvesicles, and exosomes which provide protection from various ribonucleases [81]. ncRNAs have already become a diagnostic tool for several diseased states such as cancer and diabetes [82, 83].

1.5 Micro RNAs

miRNAs are small regulatory RNAs approximately 21-25 nucleotides long [84]. miRNAs resemble the siRNAs of the RNA interference (RNAi) pathway, except miRNAs derive from regions of RNA transcripts that fold back on themselves to form short hairpins, whereas siRNAs derive from longer regions of double-stranded RNA [85]. Post miRNA biogenesis and exportation into the cytoplasm they can begin to serve their function as a master gene regulator. miRNAs function as a post-transcriptional gene regulator by targeting mRNA [86], where they have the capability to bind to the 3' untranslated region (3'UTR) of target

mRNAs, initiating either the degradation or inhibition of the target mRNA. In addition to interacting with the 3' UTR it has been reported that miRNAs can interact with other regions, including the 5′ UTR, coding sequence, and gene promoters to exert their function [87], This function of miRNA results in decreased expression of its target gene by preventing translation with many key cellular functions such as development, differentiation, growth and metabolism being impacted [88]. Over 1000 different miRNAs are produced from the human genome and these miRNAs have the potential to regulate at least one-third of all human protein-coding genes [88].

1.5.1 miRNAs and hypertension

MiRNAs have been recorded to last in the circulation of an individual for 4-14 hours with the turnover rate being consistent [89]. This property makes miRNAs an ideal therapeutic target for the treatment of EH, with numerous studies having utilised blood samples to identify circulating miRNAs and linking them to their involvement in EH development (Table 1.2) [90]. A study by Cengiz *et al*., (2015) identified a significant increase of circulating miR-21 in HT individuals [91]. This miRNA was shown to have direct inhibitory effect on endothelial nitric oxide synthase (eNOS), the enzyme responsible for production of NO within the vasculature [91]. The subsequent decrease of freely available NO results in increased peripheral vasoconstriction eventually concluding in the observed increase in BP. Several studies have used varying specimen tissue to identify miRNAs involved in the progression of EH (Table 1.2), and many of these identified miRNAs have been described as contributing to the impairment of mechanisms associated with BP regulation.

Table 1.2: MicroRNAs found in blood pressure regulation and essential hypertension studies

miRNA	*Tissue Type*	*Mechanism Impacted*	*Techniques Used*	*Reference*
miR-let-7e ↑	Blood	Vasculature	qPCR	[92]
miR-192-5p ↓	Kidney (human) Kidney (rat)	Pressure natriuresis	qPCR Knockdown Experiments	[93]
miR-153 ↓	Arteries (Rats)	Vasculature	Luciferase reporter qPCR	[94]
miR-21 ↑	Blood	Vasculature	qPCR	[91]
miR-122 ↑ ***miR-637*** ↑ ***miR-296-5p*** ↓	Blood	Vasculature	qPCR	[95]
miR-335-5p ***miR-26-5p***	Kidney Glomeruli	RAAS	Bioinformatics Predictions	[96]
miR-103a-2-5p ↑ ***miR-585-5p*** ↑	Human Aortic Endothelial Cells (HAEC)	Vasculature	Microarray Bioinformatics Overexpression Studies	[97]
miR-92a ↑	Blood	Vasculature	qPCR	[98]
miR-155-5p ↑	Blood	RAAS Pressure natriuresis Vasculature	qPCR	[99]
miR-510 ↑	Blood	Unknown	Methylation Assay qPCR	[100]
miR-320 ↑ ***miR-26b*** ↓ ***miR-21*** ↓	Aorta (Rats)	Vasculature	Microarray qPCR Validation	[101]
miR-126 ↑	Blood	Vasculature	Microarray Knockdown experiments	[102]
miR-214-3p ↑	Kidney (Rats)	Pressure natriuresis Vasculature	qPCR RNA sequencing Knockdown Experiments	[103]
miR-10a-5p ↑	Blood	Vasculature	qPCR	[104]
miR-223 ↓ ***miR-22*** ↓	Platelets	Unknown	qPCR	[105]
miR-181a ↓ ***miR-663*** ↓	Kidney	RAAS Pressure natriuresis	Microarrays validation with qPCR	[106]

miR-199a-5p ↑	(Human Umbilical Vein Endothelial Cells) HUVECs	Vasculature	qPCR Overexpression Experiment	[107]
miR-505 ↑	Blood	Vasculature	Microarrays validation with qPCR	[108]
miR-506-3p ↑	HUVECs	Vasculature	qPCR Overexpression Studies Bioinformatics Prediction	[109]
miR-151-5p ↑ ***miR-425*** ↑	Blood	Unknown	miRNA Sequencing	[110]

1.6 Circular RNAs

CircRNAs were first identified in RNA viruses in the 1970s [111]. Unfortunately due to inadequate depth of RNA sequencing and molecular techniques, a limited number of circRNAs had been discovered between 1970 to 2010 in plants and humans [112]. With the recent development of RNA deep sequencing technology and bioinformatics circRNAs have since become a molecular target of interest. Currently, more than 25,000 unique circRNAs have been identified in the human genome [113]. CircRNAs, unlike their linear counterpart do not contain the typical 5′ caps and 3′ poly A tails which is due to the covalently closed loop structures they develop with neither 5′–3′polarities nor polyadenylated tails [114]. It is due to this covalent closed-loop structure that circRNAs are protected from degradation by RNases making them more stable than linear RNA counterparts. Recent work has revealed that large numbers of circRNAs are endogenous, abundant, conserved, stable in mammalian cells and prevalent in disease states [111].

1.6.1 Circular RNA biogenesis

In eukaryotes, linear mRNA are formed by processing exons of pre-mRNAs through alternative splicing. Alternative splicing, is a regulated process during gene expression that results in a single gene coding for multiple proteins; splicing occurs through the inclusion/exclusion of different exons from the parental gene which consequently can result in different final protein result [115]. Like the majority of RNAs, circRNAs are transcribed by the RNA polymerase II (Pol II) enzyme, into a pre-messenger RNA (pre- mRNA). These pre-mRNAs are the principal product of transcription, which frequently undertake a splicing process to harvest linear mRNAs. In the case of circRNAs, they undergo an alternative splicing event known as back splicing, promoting the circularization process [116] (Figure 1.5). Back splicing, as the name insinuates is characterized by exons converging onto each other forming the circular nature of the circRNA (Figure 1.5). Consequently, there is a frequently reduced expression of linear mRNAs as circularization occurs, which produces an inverse correlation between the number of regular and circular RNA molecules [117].

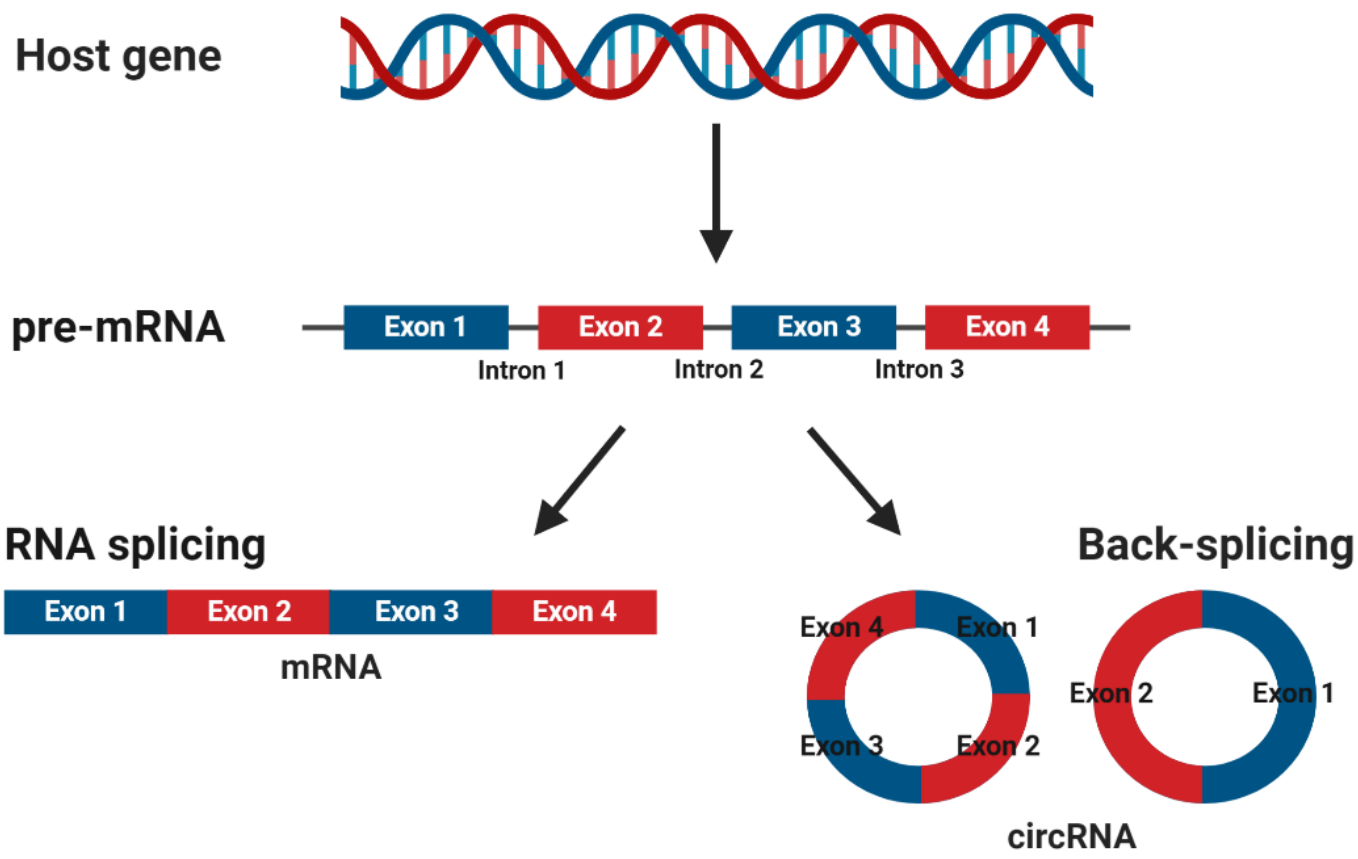

Figure 1.5: Biogenesis of mature messenger RNA (mRNA) and circular RNA (circRNA) from precursor mRNA (pre-mRNA). *Pre-mRNA is synthesised through transcription from the host genes DNA followed by RNA splicing to form a mature mRNA or back splicing to form circRNAs. Created with BioRender.com*

With the optimization of next-generation sequencing technology, several circRNA subtypes have been discovered in recent years. There are three main subtypes of circRNAs: exonic circRNAs (ecircRNAs), which are mainly derived from a singular or numerous exons; circular intronic RNAs (ciRNAs) contain only introns and exonic-intronic circRNAs (EIciRNAs), contain both introns and exons [112]. Currently, most of the identified circRNAs are exonic with the formation mechanisms of these exonic circRNAs strongly regulated [114]. Three models have been proposed for the biogenesis of exonic circRNAs as a product of alternative exon splicing: the

lariat model of circularization, RNA binding protein (RBP) mediated circularization and the back splicing model [114] (Figure 1.6).

Lariat driven circularization occurs when the upstream splice acceptor and downstream donor are close to forming a lariat containing the exons, the introns in the lariat are subsequently cleaved from the circRNA, and the exons are joined by a 5′–3′ phosphodiester bond (Figure 1.6A) [113]. In the RBP mediated model of circularization, interactions between RBPs form a 'bridge' within the upstream and downstream introns, followed by a back-splicing event to form ecircRNAs (Figure 1.6B). During base-pairing-driven circularization, circularization is enhanced by the quantity of Alu element [113]. An Alu element is a short stretch of DNA originally characterized by the action of the Arthrobacter luteus (Alu) restriction endonuclease [118]. If there are many Alu repeats in the downstream splicing donor and the upstream splicing receptor the success of circularization increases exponentially [113]. In this process of circRNA synthesis, the introns either are removed or can also be retained to form an ecircRNA or EIciRNA (Figure 1.6C).

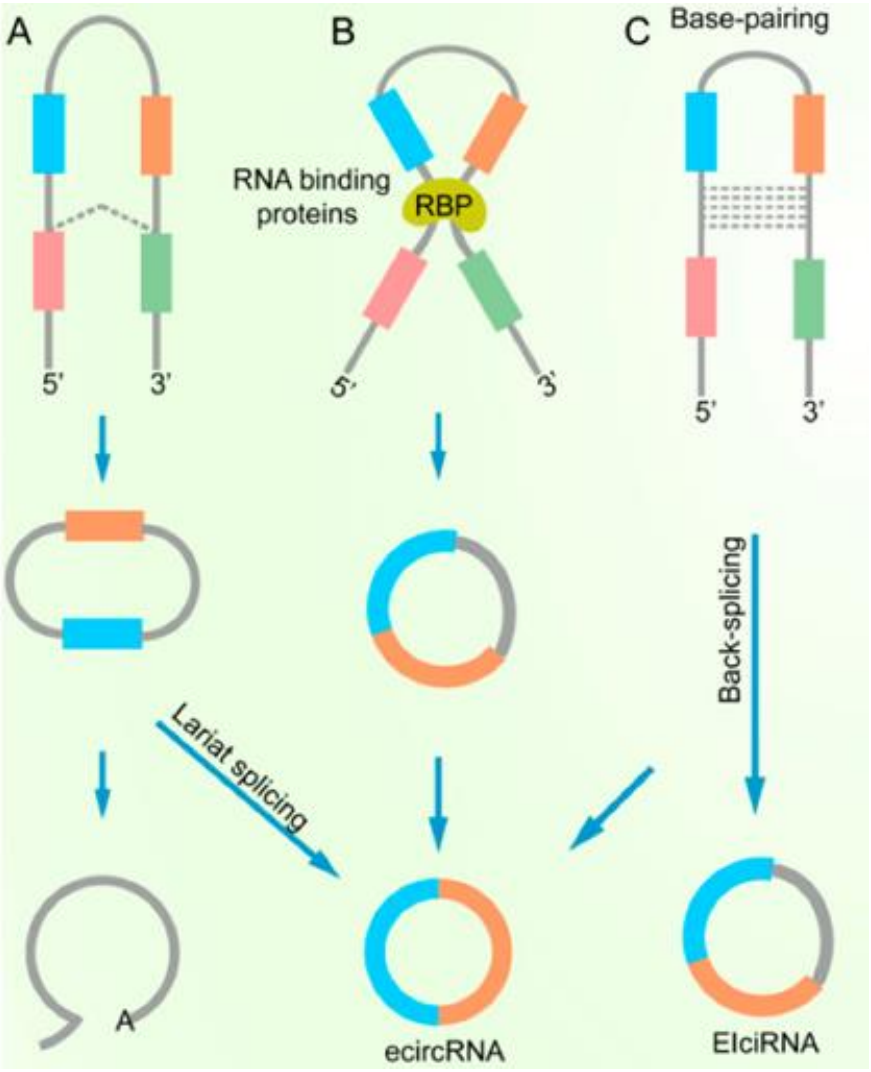

Figure 1.6: Models of circRNA biogenesis*; a) Lariat-driven circularization, b) RBP mediated circularization and c) Back splicing model. Imaged obtained from X. Zhao et al., (2019)*

1.6.2 Circular RNA functions

The function of circRNAs remains unclear. Various analyses have identified numerous exonic circRNAs having conserved circularization sites in orthologous exons [113]. This evolutionary conservation suggests the execution of important roles in an organism and thus numerous possible functions have been suggested. These

plausible functions include acting as a competitor to linear RNA splicing, acting as a miRNA 'sponge', interacting with proteins, and being translated into proteins.

1.6.2.1 Competitors of Linear RNA splicing and Gene Expression

Functional studies of circRNAs have indicated that they are able to regulate the expression of linear mRNA transcripts [119]. One of the first recorded instances of circRNAs regulating the expression of linear mRNA is displayed by the circular form of ANRIL, an antisense RNA from the tumour suppressor INK4 locus which contributes to transcription inhibition. The expression of circular ANRIL RNA is directly linked with INK4/ARF expression levels [120]. This fact has been described as a risk factor for atherosclerosis development and is one the earliest studies to identify a direct link between abnormal circRNA expression and CVD development.

The generation of circRNAs via circularization of exons has been suggested to be a process that competes with the splicing machinery as they perform their function on the same splice-sequence sites [121]. This fact was observed in neural tissue, in which an inverse expression level was described, that is, the circRNAs were more abundantly expressed than their linear counterparts [122, 123]. Similarly, in brain tissue during the aging process, there is an increased expression of circRNAs in comparison to a reduction in levels of linear RNAs [124]. This high level of circRNAs in certain tissues sustains the idea that RNA circularization can control gene expression by displacing the canonical splicing of linear RNAs.

1.6.2.2 MicroRNA Sponges

The vast majority of known circRNAs are enclosed within the cellular cytoplasm after they are transported outside of the nucleus [125]. It has been demonstrated via bioinformatic analyses and luciferase experimentation that circRNAs contain multiple miRNA binding sites allowing them to interact with cellular miRNAs [126]. This fact has prompted researchers to refer to them as "miRNA sponges" as they bind and sequester miRNAs, preventing them from performing their roles on post-transcriptional regulation (Figure 1.7). One of the first studies to observe circRNAs function as a 'miRNA sponge' comes from the Sex determining region Y (SRY) gene, discovered in 1993 [127]. In specific conditions when miR-138 is overexpressed, it co-precipitates with Argonaute 2 (AGO2) and with the SRY circular transcript due to the presence of 16 binding sites for miR-138 within the circRNA sequence [128]. The expression level of miR-138 is negatively correlated with *circSRY*, therefore miR-138 expression is reduced while *circSRY* expression is increased. Another well documented example of circRNAs acting as miRNA 'sponges' can be seen with the circRNA ciRS-7 which functions as a sponge for miRNA-7. This circRNA is expressed in neuronal tissues and contains more than 70 binding sites for miR-7, displaying a high affinity for binding and interaction between the two [128].

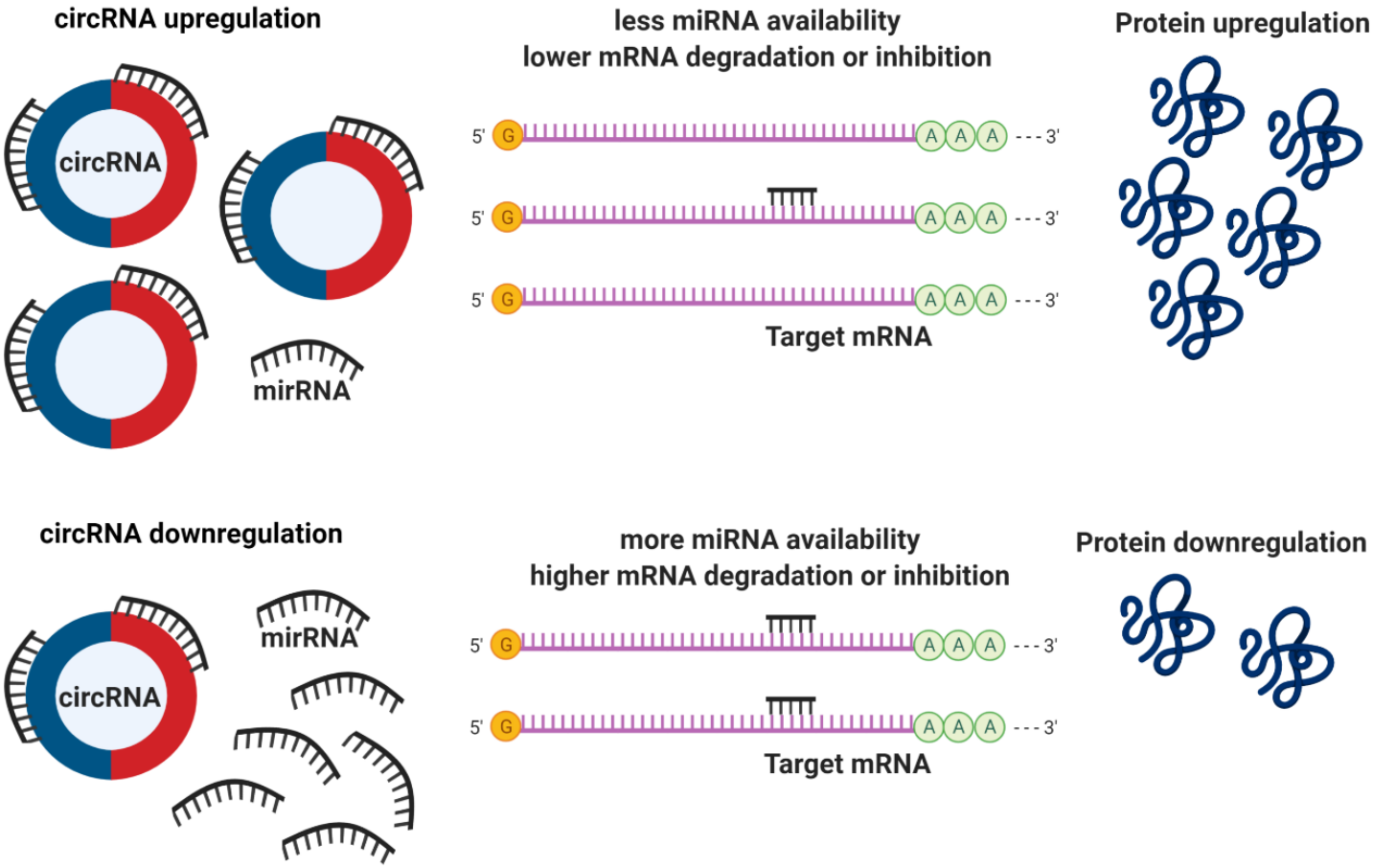

***Figure 1.7: Function of circular RNAs**. The upregulation of circRNAs leads to a decrease in miRNA availability, mRNA degradation or inhibition resulting in an increase of protein translation. Conversely, the downregulation of circRNAs leads to more miRNA available and higher levels of mRNA degradation or inhibition leading to a downregulation in protein translation. Created with BioRender.com*

1.6.2.3 Protein Interaction

Several circRNAs have been revealed to contain protein binding motifs which allows for circRNAs to interact with selected proteins and regulate their function and localization within a cell. For example, circPABPN1 has the ability to interact with the RBP human antigen R (HuR) preventing it from binding with the linear form of PABPN1 and as a consequence, reduces its capacity to be translated [129]. A similar interaction is observed with circMbl

which originates from the gene Muscleblind (Mbl) and contains a recognition motif for the Mbl protein [130]. This interaction between circMbl and Mbl protein regulates the splicing of its own pre-mRNA thereby regulating its expression.

1.6.2.4 Protein Synthesis

Structurally, circRNAs lack the essential elements for cap-dependent translation, such as the 5' cap and poly (A) tail [114]. Due to this circRNAs have widely been considered non-coding in nature, but recent research has detailed that this might not be the case. Pamudurti *et al* (2017) demonstrated that circRNAs that are capable of being translated contain internal ribosome entry sites (IRES) which enables 40S ribosomal subunit to interact and can be then translated in a cap-independent way [131]. Studies by Yang *et al.,* (2017) have shown that circRNAs sequences containing methylated adenosine N6 (m6A) site at the 5' UTR can act as an IRES [132]. M6A modifications are typically associated with processes such as mRNA stability, splicing, and translation but recent evidence has suggested that m6A motifs are enriched in circRNA sequences and that even a single m6A motif can be efficiently transcribed [132].

1.7 Circular RNA and Cardiovascular Disease

Emerging evidence of circRNAs in cardiovascular disorders has demonstrated their differential expression in different CVD states (Table 1.3). However, the relevance of circRNAs to the cardiovascular system remains poorly characterised, and an improvement in understanding of circRNA involvement in CVD will form a basis for the development of these RNAs as biomarkers for discovery, prediction, and therapeutic agents. Importantly, the

combination of genetic sequencing and bioinformatics discovery has enabled the identification of many novel circRNAs with potential implications in CVD development and progression.

Table 1.3: Summary of circRNAs implicated in CVDs including species, sample types studied and differential expression direction

Disease	*Circular RNA*	*Species*	*Sample*	*Expression*	*Reference*
Hypertension	hsa_circ_0005870	Human	Blood	Down	[133]
	hsa_circ_0037909	Human	Blood	Up	[134]
	hsa_circ_0037911	Human	Blood	Up	[135]
	hsa_circ_0126991	Human	Blood	Up	[136]
	hsa_circ_0014243	Human	Blood	Up	[137]
	hsa-circRNA9102-5	Human	Blood	Up	[138]
	CircNr1h4	Mice	Kidneys	Down	[139]
	hsa_circ_0039388	Human	Blood	Up	[140]
	hsa_circ_0038648	Human	Blood	Up	[140]
	hsa_circ_0105015	Human	Blood	Up	[141]
	hsa_circ_0037897	Human	Blood	Up	[142]
Myocardial infarction	mmu_circ_0001878	Mouse	Cardiomyocytes	Up	[143]
	circTtc3	Rats	Cardiomyocytes	Up	[144]
	circNfix	Mouse	Cardiomyocytes	Up	[145]
	circFndc3b	Mouse Human	Cardiomyocytes	Down	[146]
Atherosclerosis	CircRNA-0044073	Human	Blood	Up	[147]
	ocu-ciR-novel-18038	Rabbit	Blood	Down	[148]
	ocu-ciR-novel-18298	Rabbit	Blood	Up	[148]
	ocu-ciR-novel-15993	Rabbit	Blood	Up	[148]
	ocu-ciR-novel-17934	Rabbit	Blood	Down	[148]
	ocu-ciR-novel-17879	Rabbit	Blood	Up	[148]
	ocu-ciR-novel-18036	Rabbit	Blood	Up	[148]
	ocu-ciR-novel-14389	Rabbit	Blood	Up	[148]
	CircANRIL	Human	Blood	Up	[120]
	CircCHFR	Human	VSMC	Up	[149]
	hsa_circ_0003575	Mouse Human	Endothelial Cells HUVEC	Up	[150, 151]
Coronary artery disease	hsa_circ_0001879	Human	Blood	Up	[152]
	hsa_circ_0004104	Human	Blood	Up	[152]
	hsa_circ_0124644	Human	Blood	Up	[153]
	hsa_circ_0098964	Human	Blood	Up	[153]
	hsa_circ_0030769	Human	Blood	Up	[153]
	hsa_circ_0079828	Human	Blood	Up	[153]

hsa_circ_15486-161	Human	Blood	Up	[153]
hsa_circ_0122274	Human	Blood	Up	[154]
hsa_circ_16316-13	Human	Blood	Up	[154]
hsa_circ_0140538	Human	Blood	Up	[154]

1.7.1 Circular RNA and hypertension

Limited studies have explored the association between circRNAs and HT development. Wu *et al*. [133] was the first of its kind to measure the expression of circRNAs in human blood samples of HT patients. Microarrays were used to measure the circRNAs present in the blood samples of five HT patients and five healthy controls (HC) and found 13 downregulated and 46 upregulated circRNAs. Validation of these findings in a larger cohort (54 HT and 54 healthy controls) identified that hsa_circ_0005870 was significantly downregulated in the blood of HT patients [133]. CircRNA-miRNA networking analysis utilizing TargetScan and miRanda software predicted interactions between hsa_circ_0005870 and several miRNAs, including *miR-619-5p*. Interestingly, *miR-619-5p* had the largest number of downstream mRNA targets. Further Kyoto Encyclopaedia of Genes and Genomes (KEGG) pathway analysis of this interaction proposed that the transforming growth factor β (TGFβ) signalling pathway might play a pathological role in HT [133]. One member of the TGFβ signalling family, TGFβ1, has been described to directly interfere with the reabsorption of sodium in the kidney, suggesting that TGFβ1 is critically involved in maintaining pressure natriuresis and subsequently BP [155].

Additional case-control studies identified two unique circRNAs, hsa_circ_0037909 and hsa_circ_0037911, strongly associated with the hypertensive phenotype with BP greater than 140/90mmHg [134, 135]. CircRNA-miRNA networking identified a potential interaction with miR-637, which has been proposed to increase C-reactive

protein (CRP) levels by activating inflammatory pathways in HT patients [156]. Further analysis also identified a positive relationship between hsa_circ_0037911 and serum creatinine. Generally, a high serum creatinine level can be indicative of decreased kidney function [157]. This is important because the kidneys have been shown to play a prominent role in the regulation of BP (Section 1.2). However, a potential mechanism for the increase of serum creatinine and CRP or a possible interplay between the circRNA-miRNA interactions and this change has not been identified.

Two unique circRNAs from separate studies, hsa_circ_0126991 and hsa_circ_0014243, were upregulated in HT patients and were predicted to bind to miR-10a-5p [136, 137]. Further to the predicted interaction, a negative correlation based on expression data between the circRNAs, and miRNA has also been described. Prior to this discovery, miR-10a-5p was identified to be downregulated in other CVDs such as CAD through its effect on the vascular endothelium, a prominent mechanism involved in the regulation of BP [158]. This decreased expression of miR-10a-5p resulted in an increased expression of vascular cell adhesion protein 1 (VCAM1) which promotes other cells to attach to the vessel walls contributing to atherosclerotic plaque formation within blood vessels [159].

One of the limitations with the above-mentioned research is the sole us of blood samples. This is in large part due to how easily obtainable these samples are, however, because of this the literature has focused on using circRNAs as biomarkers instead of understanding the role they have in EH development and progression. This is the advantage that animal models provide over human based studies; it enables researchers to investigate the mechanistic properties of circRNAs at a larger level. One such study explored the expression of the circRNA circNr1h4 in the DOCA-salt induced HT model. This study discovered an increased expression of circNr1h4 in the kidneys of

these mice and further outlined through the use of luciferase reporter assays that miR-155-5p interacts with it [139]. Several studies have shown that miR-155 plays a vital role in not only HT but also various kidney implications. For example, miR-155 is a positive regulator of the nucleotide-binding domain like receptor protein 3 (NLRP3) pathway by inhibiting the FOXO3a gene, and inhibition of the NLRP3 inflammasome has protective qualities for the kidney [160]. However, inhibition of miR-155 has been shown to reduce the damage occurring to the kidneys of pregnant Sprague Dawley (SD) rats with HT via the upregulation of FOXO3a [161].

1.7.2 Circular RNAs, myocardial infarction and heart failure

Myocardial infarction (MI) is characterized by cardiac tissue damage, caused by remodelling of the coronary vasculature due to decreased blood flow in obstructed coronary blood vessels, leading to prolonged myocardial ischemia. MI results in a dysfunctional heart and can ultimately lead to heart failure (HF) and death [162]. Similar to HT several factors can contribute to MI; however, the leading cause is due to individuals with chronically elevated BP [163]. An increase in BP has been repeatedly connected to the development of atherosclerotic lesions, the development of which is the largest contributor to MI occurrence [164]. A microarray study identified 29 upregulated and 34 downregulated circRNAs in C57BL/6J mice where MI was induced by permanent ligation of the left anterior descending coronary artery, which contributed to the development of HF [165]. This was one of the earliest studies investigating circRNAs in MI and has improved our understanding of circRNA dysregulation and CVDs [165].

A circRNA produced from the Cdr1as gene is upregulated in mice with MI-induced injuries with its overexpression aggravating the infarct size *in vivo* leading to cell

apoptosis in mouse cardiomyocytes [143]. Importantly, circCdr1as acts as a sponge for miR-7a and as an indirect result its downstream targets such as poly (ADP-ribose) polymerase (PARP) and specificity protein 1 (SP1) [143, 166]. The upregulation of miR-7a has previously been described to have protective qualities during MI injury which was achieved by reducing SP1-regulated mechanisms such as reduced VEGFA and COL4A1 resulting in inhibition of apoptosis and angiogenesis [143]. Therefore, decreasing expression levels of Cdr1as circRNA may increase levels of miR-7a and could function as a new therapeutic strategy for the treatment of MI.

Interestingly, circTtc3 has also been shown to be upregulated in myocardium after MI [144]. The overexpression of circTtc3-decreased hypoxia induced ATP depletion; which protected cardiomyocytes against apoptotic death post MI whilst reduced expression of circTtc3 through siRNA knockdown enhanced cardiac dysfunction post MI by increasing apoptosis in cardiomyocytes under conditions of cardiac ischemia and dysfunction [144]. These observations indicate that circTtc3 may have protective properties in the heart. These protective effects of circTtc3 are potentially through the circTtc3-miR-15b-Arl2 regulatory cascade [144]. Arl2 in conjunction with ANT1 is involved with regulating cellular ATP levels with previous links being made to heart disease; however, further examination of the molecular functions of these two genes is important though to understanding their potential use as a therapeutic option for MI [167].

CircRNAs are frequently associated with disease progression and development, however recent studies have identified circRNAs that contain cardiac regenerative properties post MI. CircNfix is highly expressed in adult hearts of humans, rats, and mice however, its expression appears to be mediated by a transcription factor bound to a super enhancer [145]. Loss of this superenhancer-regulated circNfix promotes an

increase in cardiomyocyte proliferation and angiogenesis that prevented apoptosis post MI, decreased cardiac dysfunction, and improved cardiac regenerative abilities post MI [145]. Conversely, circFndc3b has been shown to be downregulated in mouse hearts post MI and in human cardiac tissue of ischemic cardiomyopathy patients [146]. Overexpression of circFndc3b in cardiac endothelial cells decreased apoptosis in cardiomyocytes, and improved vascularisation and left ventricular function through its interaction with VEGF which promoted its expression [146]. These examples highlight the possible involvement of circRNAs in cardiac repair, function and remodelling after MI providing a novel therapeutic target for its treatment and prognosis.

1.7.3 Circular RNAs, atherosclerosis and CAD

Recent studies have demonstrated that the upregulation of certain circRNAs can sponge miRNAs influencing the proliferation and invasion of cells involved in CAD. CircRNA-0044073 targets miR-107 [147], while circCHFR targets mir-370 [149] and hsa_circ_0003575 targets multiple miRNAs such as *miR-148a-3p*, *miR-199-3p*, *miR-9-5p*, *miR-377-3p* and *miR-141-3p* [150, 151]. Interestingly, circRNA hsa_circ_0003575 is upregulated in damaged human vein endothelia cells (HUVEC) caused by oxidised low-density lipoprotein (oxLDL), this is important as a damaged endothelium is the starting point in the development of atherosclerosis [151, 168]. The knockdown of hsa_circ_0003575 decreased cellular apoptosis as measured by flow cytometry in HUVECs treated with oxLDL [151]. This study however did not explore the significance of hsa_circ_0003575 knockdown and the implications this has on miRNA expression and subsequently mRNA expression to elucidate why the observed decrease of apoptosis is occurring.

Importantly, with the advancement of RNA sequencing technology thousands of circRNAs have been identified in CAD. Pan *et al*. [169] described 1259 annotated and 381 novel circRNAs in atherosclerotic lesions. The combination of those results and additional histological examination identified 54 circRNAs upregulated and 12 downregulated suggesting a possible involvement to the CAD pathology [169]. Another study, by Yu *et al*. [170] identified 2283 downregulated and 85 upregulated circRNAs in the PBMCs of 70 CAD patients compared to 30 HCs. The top 100 differentially regulated circRNA originated from genes related to metabolism and protein modification. Furthermore, the expression profiles of six circRNAs were validated between atherosclerotic coronary arteries and peripheral blood mononuclear cells warranting further investigation into their use as potential biomarkers. hsa_circ_0001879, hsa_circ_0004104 and hsa_circ_0001445 have been suggested as novel biomarkers for CAD after experimental validation showed an upregulation in the atherosclerotic coronary arteries of patients when compared to controls [152, 171].

1.8 Conclusion

With recent advancement in technologies, circRNAs have only become a topic of interest within the research community recently. CircRNAs are an underexplored class of ncRNAs that have recently gained interest through ability to regulate gene expression by interacting with proteins, functioning as a miRNA sponge, and competing with splicing machinery. The significance of circRNAs in the cardiovascular system remains poorly understood, and an improvement in understanding circRNAs is necessary to understand their part in CVD development. This thesis will aim to fill some of the gaps that exist in this research field by exploring the expression of circRNAs in a large cohort of HT kidneys and outline the role

circRNAs have in BP regulation and HT development by identifying the mechanism by which specific circRNAs exhibit their effect on gene expression.

1.9 Hypothesis and Aims

What we know CircRNAs have been described in conditions such as cancer to through their function as miRNA sponges.' There is emerging evidence that circRNAs play a key role in regulating and maintaining BP and strong evidence that differentially expressed circRNAs influence an individual's risk to developing EH. The majority of circRNA studies into EH have utilised blood samples and have identified several differentially expressed circRNAs, however, this research has only investigated circRNAs for a diagnostic purpose rather than a causation approach.

What we do not know Limited research has been conducted on the link between circRNA expression and the development of EH. Most research in the field has centred around identifying circRNAs in circulation of EH patients and utilizing them as a diagnostic tool. To date, no published data has explored kidney specific circRNA expression and the implications they have on BP regulation. As discussed earlier the kidneys play an important role in the regulation of BP through various mechanisms and understanding the way circRNAs are involved in the regulation of these mechanisms may provide valuable information and understanding to why EH occurs.

Project hypothesis: Differentially expressed, kidney-specific circRNAs play a fundamental role in controlling gene expression contributing to EH development/progression.

Aims: Identifying differential expression circRNAs in the kidney of HT individuals and characterising their function using a variety of molecular biology and RNA sequencing techniques to determine their role in BP regulation and subsequently EH development.

Aim 1: To identify differentially expressed circRNAs in a large cohort of hypertensive human kidney samples (Chapter 3).

Aim 2: To characterize the previously identified circRNAs from Chapter 3 and identify potential miRNA interactions utilising RNA sequencing methodology (Chapter 4).

Aim 3: To identify downstream mRNAs that are impacted by reduced circRNA expression and the subsequent pathways that are impacted correlating this back to hypertension development or blood pressure regulation (Chapter 5).

To address the abovementioned aims, several classic molecular biology techniques, as well as contemporary next-generation sequencing approaches have been employed. These molecular techniques, as well as the human population they are applied to, are outlined in the following General Methods chapter (Chapter 2).

Chapter 2
General Methods

2.0 Introduction

This chapter outline the general methodology used in the major studies of this thesis. Detailed methodology specific to each study will be included in the individual chapters.

2.1 RNase R treatment and cDNA synthesis

For RNase R treatment 2 µg of total RNA was incubated with 6U of RNase R (Lucigen) for 30 min at 37°C. Post incubation, the samples were placed immediately on ice to stop the reaction, and this was followed directly by complementary DNA (cDNA) synthesis. RNase R treated total RNA was stored at -80ºC until use.

cDNA was synthesized from RNase-treated RNA in a 3-step process using 100µM random hexamer primers (Applied Biosystems) and 50U Maxima RT H minus reverse transcriptase (ThermoFisher) on a thermal cycler. This process comprised an initial 25 ˚C incubation for 10 minutes to denature the template, followed by a 50˚C incubation for 30 minutes to anneal the template, and completed with an extension cycle for 5 minutes at 85 ˚C. The newly synthesised cDNA was diluted to 20ng/µL and stored at -20 ˚C until use.

2.2 CircRNA primer design

Designing specific primers for quantification of circRNA using qPCR amplification can be challenging since the mature circRNA sequences after splicing are not readily available in many cases and the primers must be divergent and must span the back splice junction (BSJ) (Figure 2.1) [172]. Utilizing CircInteractome (https://circinteractome.nia.nih.gov/) we obtained the circRNA BSJ sequences and exported them to NCBI primer design tool to obtain five sets of divergent primer pairs for each circRNA with sizes ranging from 120–200 bp spanning the BSJ. Primers were selected based on similarities between melting

temperatures (58° to 60°C) to enable all PCR reactions to be run with the same annealing temperature. These primers were purchased from Integrated DNA Technologies.

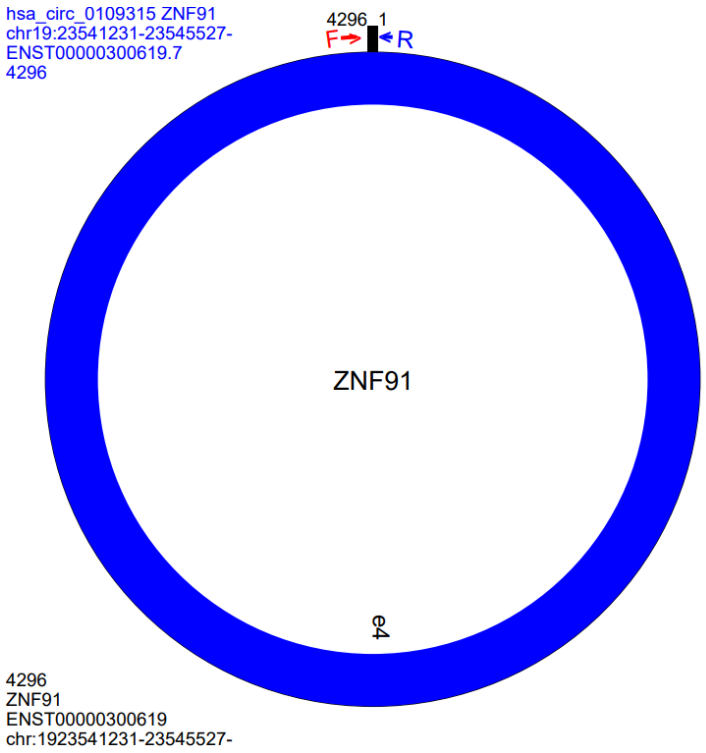

Figure 2.1: Designing divergent primers. *Divergent primers (F and R) located either side of the backsplice junction*

2.3 Quantification of circRNA expression using qPCR

CircRNA expression was measured utilizing real-time quantitative polymerase chain reaction (qPCR) methodology, this is considered the gold standard for circRNA expression analysis [173]. qPCR was performed using the SensiFAST^{TM} SYBR Low-ROX kit (Bioline) following the manufacturer's recommendations. The primer sequences are outlined in each chapter where this methodology is adopted, and all primers were synthesized by Integrated DNA Technologies. qPCR reactions were performed on a QuantStudio^{TM} ViiA7^{TM} qPCR system (Applied Biosystems) with the following cycling conditions 95°C for 5 min, and 45

cycles of 95°C for 10 sec, 58°C for 20 sec and 72°C for 20 sec. PCRs for each sample were performed in triplicate. For each replicate and each sample, a melting curve analysis was performed, and the presence of a single melting curve peak was indicative of a single product. Circular GAPDH was utilised as the house-keeping gene.

2.4 TaqMan advanced miRNA cDNA synthesis and assays

TaqMan™ Advanced miRNA cDNA synthesis kit (Applied Biosystems) was used to reverse transcribe miRNA to cDNA following manufacturer's instructions. miRNA expression was measured using TaqMan™ Advanced miRNA assays by qPCR on the QuantStudio™ ViiA7™ qPCR system (Applied Biosystems). Cycling conditions were as follows: 95°C for 20 secs, and 40 cycles of 95°C for 1 sec and 60°C for 20 secs. Detailed information on the TaqMan™ Advanced miRNA assays will be described in subsequent chapters (Table 3.3) with hsa-miR-215-5p being utilised as the house-keeping gene.

2.5 Cell Culture

The human embryonic kidney 293 (HEK 293) (ATCC) cell line was utilised in the silencing studies to decrease circRNA levels included in chapter 4s and 5 of this thesis. Cells were cultured in Dulbecco's Modified Eagle Medium (DMEM) supplemented with 10% Foetal Bovine Serum (FBS) (Bovogen) and 1% Penicillin/Streptomycin (ThermoFisher Scientific). HEK 293 cells were grown to approximately 80% confluency and then seeded at approximately 10^7 into six-well plates for the investigation of knockdown circRNAs using siRNA transfection.

2.6 siRNA design and circRNA silencing

CircInteractome was used to design siRNA specific to circRNAs of interest, generating sequences of 21-nt long targeting junctional sequences spanning 5–16 nt on either side of the

back splice junction (Figure 2.2). We used cultivated HEK293 cells to decrease the levels of our circRNAs of interest and evaluate its downstream effectors. HEK293 cells were cultivated as per Section 2.5 and transfected with a custom designed siRNA and a scramble control using lipofectamine RNAiMAX (Thermo Fisher Scientific) following manufacturer's instructions. Briefly, HEK293 cells were grown in 6-well plates to approximately 70% confluence and transfected with 25pmol of either siRNA or scramble control. The cells were maintained in myocyte growth medium for 72h. All transfection experiments were performed in triplicates.

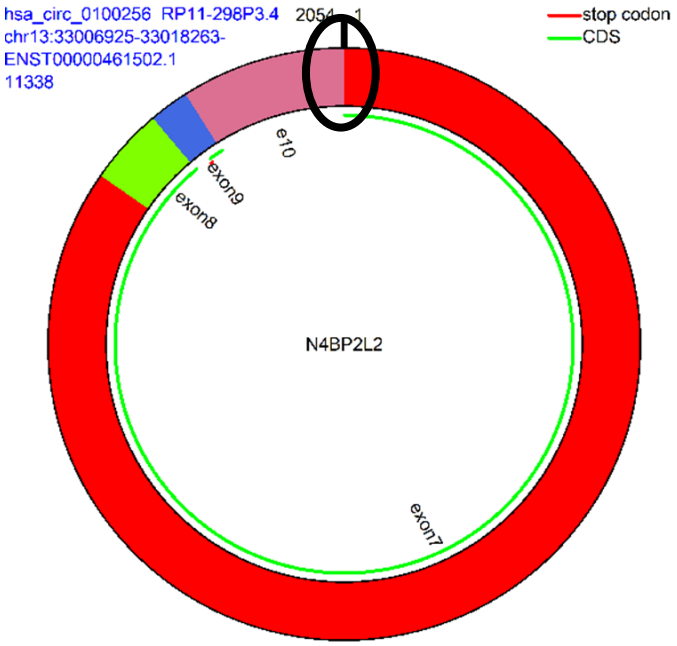

Figure 2.2: Designing siRNAs for circRNAs*. siRNAs target the back splice junction of the circRNA highlighted by the circle on the above image.*

2.7 RNA Extraction

Total RNA was extracted utilizing mirVana^{TM} RNA Isolation Kit (Invitrogen) per the manufacturer's instructions. Following the 72 hours transfection of the HEK293 cell line with either siRNA or the scramble control, the cells were washed with 1µL PBS and then had 600µL of lysis/binding solution added to each well, thus beginning the lysis process and

removing the adherent cells from the bottom of the 6-well plates. The cell/lysis buffer cocktail was then transferred to Eppendorf tubes and vortexed to assist with the lysing process. The remainder of the RNA extraction process was performed as per the manufacturer's instructions (Invitrogen). After completion of the extraction RNA samples were quantitated using the Qubit HS RNA kit (Thermo Fisher Scientific) with a Qubit 3.0 Fluorometer (Thermo Fisher Scientific), following manufacturer's instructions. The 260/280 and 260/230 ratios of absorbance values were used to assess the purity of RNA using a Nanodrop ND-1000 spectrophotometer (Thermo Fisher Scientific).

2.8 Linear RNA Primer Design

Linear RNA primers were designed using the NCBI primer blast tool (http://www.ncbi.nlm.nih.gov/tools/primer-blast/index.cgi) and synthesised by Integrated DNA Technologies. All primer pairs were submitted to a BLAST analyses to ensure specificity to RNA expressed from the gene targeted and spanned exon-exon junctions. Detailed primer information will be presented in following chapters (Table 4.2)

2.9 Linear RNA cDNA synthesis and gene expression analysis

The Vertti thermal cycler (Applied Biosystems) was used to synthesise cDNA from total RNA in a 4-step process using a High-Capacity Reverse Transcription Kit (Applied Biosystems). Step 1, RNA was heated to 25℃ for 10 minutes to denature the template. Step2, RNA was heated to 37°C for 120 minutes to anneal the template. Step3, an extension cycle for 5 minutes at 85°C. Finally, the newly synthesised cDNA was diluted to 20ng/µL and was stored at -20°C until used.

The Via 7 PCR system (Applied Biosystems) was used for all qPCR experiments in this thesis. The qPCR was set up according to manufacturer's instructions. Each reaction tube

contained Master Mix reagent, 2xSensiFAST SYBR® (Bioline), 200ηM each primer, 1µL cDNA and nuclease free H_2O The reaction conditions were as follow; denaturation, 95°C for 5 seconds; annealing, 58°C for 15 seconds; and extension, 72 °C for 10 seconds. This was performed for 40 cycles after an initial polymerase activation step of 95°C for 2 minutes. GAPDH was utilised as the housekeeping gene in this experiment.

2.10 Statistical Analysis

Relative expression of circRNA, mRNA and miRNA was determined using the 2-ΔΔCT method [174]. Statistical analysis was assessed by unpaired T-test with Welch's correction using GraphPad PRISM 9 software. Significance was set as a $P < 0.05$. Analyses related to experiments using human tissue samples, a univariate analysis of variance (ANOVA) was performed to correct for confounding factors such as age, gender and BMI using SPSS software (Version 26). GraphPad PRISM 9 software was used for graphing results. Data is presented as mean ± standard error of the mean (SEM). Statistical significance is represented as *P<0.05, ** P<0.01, ***P<0.001.

Chapter 3

Investigating circRNA expression in hypertensive human kidney samples

Abstract

CircRNAs are an underexplored class of the ncRNAs that can regulate gene expression. However, circRNAs and their involvement in EH have yet to be fully elucidated. EH is a multifactorial disorder and is one of the most common diseases impacting on the cardiovascular system and the kidney has been hypothesized to be involved in the development of EH due to its ability to regulate BP through salt and water homeostasis. The aim of the present study was to identify, at the transcriptome-wide level, circRNAs that were differentially expressed between kidneys of EH individuals and NT individuals from the TRANSLATE study. By using ultra-deep RNA sequencing technology, we identified 12 differentially expressed circRNAs in kidneys of EH individuals. We then validated the expression of these circRNAs in a larger cohort of kidney samples (N=65) by qPCR and established that *circZNF91, circRP11-298P3.4, circGRB10, circKATNAL1, circUBR2, circCARHSP1* and *circLIFR* were indeed differentially expressed in EH kidneys ($P<0.05$). RNA-seq data generated from the same TRANSLATE study samples confirmed that the linear isoform of the circRNAs were not differentially expressed ($P>0.05$). *In-silico* analysis then identified several miRNAs of interest that are predicted to interact with our differentially expressed circRNAs including miR-21, miR-145, miR-155, miR-217, miR-510 and miR-663b, of which, only miR-145 and miR-217 were differentially expressed in the same kidney samples used in the validation step ($P<0.05$). The present results identify several differentially expressed circRNAs in HT human kidney samples. Further to this, it can be presumed that the differentially expression we observed is independent of the linear isoform expression. The future chapters of this thesis will aim to elucidate the specific roles that our circRNAs of interest play in the development of EH and overall regulation of BP.

3.0 Introduction

EH is a form of HT that has no identifiable secondary cause and it is the most common type affecting approximately 85% of those with HT [175]. The remaining ~15% is accounted for by various underlying pathophysiology's such as diabetes, atherosclerosis and endocrine dysfunction that contribute to what is known as secondary HT [175]. Due to the absence of an underlying condition contributing to the increased BP, it is more than likely that this abnormality is determined genetically and is likely to be the consequence of an interaction between environmental and genetic factors [23]. Genetic factors contribute to 30 to 50% of variation in BP [176].Mechanisms controlling gene expression including epigenetic mechanisms have been examined to try an explain the total heritability of elevated BP. Of recent years have there has been an increasing interest in studying ncRNAs a particular epigenetic modulation which includes but is not limited to circRNAs.

Emerging evidence of circRNAs in CVDs has demonstrated differential expression between healthy and diseased states (Section 1.7, Table 1.3). However, the function of circRNAs in the cardiovascular system remains poorly characterised. Understanding circRNAs' involvement in the cardiovascular system will elucidate their role in development and progression of CVD and subsequently clarify many of the mysteries that currently exist between genetics and CVD. Recent publications investigating circRNAs have established them as critical epigenetic regulators in various pathological conditions such as various types of cancers [177], however, their functional relevance to the development and progression of HT is only beginning to surface. Recent investigations have provided evidence that circRNAs can be detected in various tissues and body fluids from HT patients (Table 3.1). In summary, many of these studies have investigated circRNAs in human blood samples to determine their ability to be utilised as a diagnostic tool rather than determining a biological mechanism that might exist [133-142]. Currently, there are no studies that have explored the biological

mechanisms that are impacted by differential circRNA expression in HT let alone investigated the expression of circRNAs in a large cohort of kidney tissue samples. The kidney plays a pivotal role in controlling BP by regulating salt and water homeostasis, making them an organ/system of interest when HT development/progression is considered. This chapter of my thesis contains my first study where we investigate the expression of circRNAs in a large cohort of renal tissue samples from HT patients. The aim of this study is to identify differentially expressed circRNAs in kidney samples from the TRANSLATE study and determine whether there is an association with BP regulation and/or HT development making this study the first of its kind to be undertaken.

Table 3.1: Summary of HT studies investigating circRNA expression

Reference	***Tissue type/Sample size***	***Findings***
Wu et al. [133]	Human: PBMC; 108; 54 controls, 54 EH	hsa_circ_0005870 significantly downregulated in patients with EH.
Bao et al. [134]	Human: PBMC; 96; 48 controls, 48 EH	hsa_circ_0037911 through a potential interaction with miR-637 may be a significant biomarker for diagnosis of EH. hsa_circ_0037909 may affect Scr or LDL in the blood leading to the development of EH.
Bao et al. [135]	Human: PBMC; 200; 100 controls, 100 EH	hsa_circ_0037911 significantly up regulated in patients with EH and expression was closely related to the concentration of Scr
Liu et al. [136]	Human: PBMC; 178; 89 controls, 89 EH	hsa_circ_0126991 correlated with an increased risk of developing EH, serving as a potential biomarker for early diagnosis.
Zheng et al. [137]	Human: PBMC; 178; 89 controls, 89 EH	Levels of hsa_circ_0014243 are upregulated in the blood of EH patients. Predicted to interact with miR-10a-5p and is significantly associated with age, HDL levels and blood glucose levels.
Zheng et al. [138]	Human: PBMC; 192; 96 controls, 96 EH	hsa-circRNA9102-5 may play a crucial role in EH development through sponging miR-150-5p.
Lu et al. [139]	Mouse: Kidney collecting duct cell line	Decreased expression of circNr1h4 was observed which in part contributed to the up-regulation of miR-155-5p and subsequently the downregulation of Far1. This molecular mechanism is hypothesized

		to contribute to kidney injury because of HT.
Yin et al. [140]	Human: PBMC; 128; 65 controls, 63 EH	hsa_circ_0039388 and hsa_circ_0038648 are highly co-expressed with both WNT3 and CMK2N2 mRNAs
He et al. [141]	Human: PBMC; 96; 48 controls, 48 EH	Upregulation of hsa_circ_0105015 is strongly associated with inflammatory pathways in EH. Predicted to interact miR-637.
Tao et al. [142]	Human: PBMC; 184; 92 controls, 92 EH	Upregulation of hsa_circ_0037897 may be a risk factor for the development of EH.

3.1 Methods

3.1.1 TRANscriptome of Renal Human TissuE (TRANSLATE) Study

All analyses conducted in this chapter used human kidney samples collected from participants of the TRANSLATE study. The TRANSLATE study is a unique cohort of 265 kidney samples collected from white European patients who underwent an elective unilateral nephrectomy due to the presence of a non-invasive renal cancer in one of three nephrology-urology centres: Silesian Renal Tissue Bank [178], TRANSLATE P (recruitment conducted in Western Poland) and TRANSLATE Z (recruitment conducted in Southern Poland) [179]. The TRANSLATE study consists of adults (aged >18 years) with no previous history of kidney disease. All participants of the TRANSLATE study underwent detailed clinical phenotyping, which consisted of documentation of clinical history (via coded questionnaire), basic anthropometry as well as triplicate measures of BP by mercury sphygmomanometer. Individuals who had elevated BP greater than >140/90 mmHg on at least two separate occasions and/or were taking antihypertensive medications were identified as hypertensive. RNA was extracted from all kidney tissues using the miRNeasy kit (Qiagen) and stored at –80°C.

The potential effect of coexistent cancer on the transcriptome of the TRANSLATE "healthy" renal tissue was discussed in detail by Marques *et al.* [106], where the global expression profiles of three different cohorts was compared. The three groups contained either healthy tissue from nephrectomy due to cancer, noncancerous kidney tissue, or clear cell renal carcinoma tissue. These sections were analysed using hierarchical clustering analysis and RNA-sequencing. Results from this study showed tight clustering of global expression patterns between healthy tissue from

nephrectomy and subjects who did not have cancer. Highlighting that it was unlikely that the transcriptome of the 'healthy' renal tissue was not affected by the neighbouring renal cell carcinoma.

3.1.2 Ultra-deep RNA sequencing

Limited experimental methodologies exist to profile the expression of circRNAs within a population, however, one of the most utilised methodologies is ultra-deep RNA sequencing (100x)[180]. Comparing circRNAs to mRNAs the quantity is significantly less, hence the depth of sequencing required to detect circRNAs is much higher than that of conventional RNA sequencing. With the advancements of sequencing technology and bioinformatic understanding of circRNAs, sequencing for these novel forms of RNA has become easier to perform.

As a discovery experiment ultra-deep RNA sequencing was conducted by the Beijing Genomic Institute on four human kidney samples from the TRANSLATE study (PKPOZ_18, PKPOZ_36, PKPOZ_44 and PKPOZ_46) with there being two HT samples (PKPOZ_44 and PKPOZ_46) and two normotensive (NT) samples (PKPOZ_18 and PKPOZ_36). The ribosomal rRNA was first removed from the total RNA from these samples using a biotin-labelled specific probe (Ribo-ZeroTM rRNA Removal Kit (Illumina)). After purification, the RNA was fragmented at a temperature and ionic environment. The cDNA strand was then synthesized using random primers and reverse transcriptase in the TruSeq® Stranded kit (Illumina), and then the double-stranded cDNA was synthesized using DNA polymerase I and RNaseH. During cDNA double strand synthesis, the RNA template was removed and dTTP was replaced by dUTP. The double-stranded cDNA product was subsequently

ligated with an “A” base and a linker. The ligation product was amplified for our final cDNA library. Finally, the constructed sequencing library was sequenced (Figure 3.1).

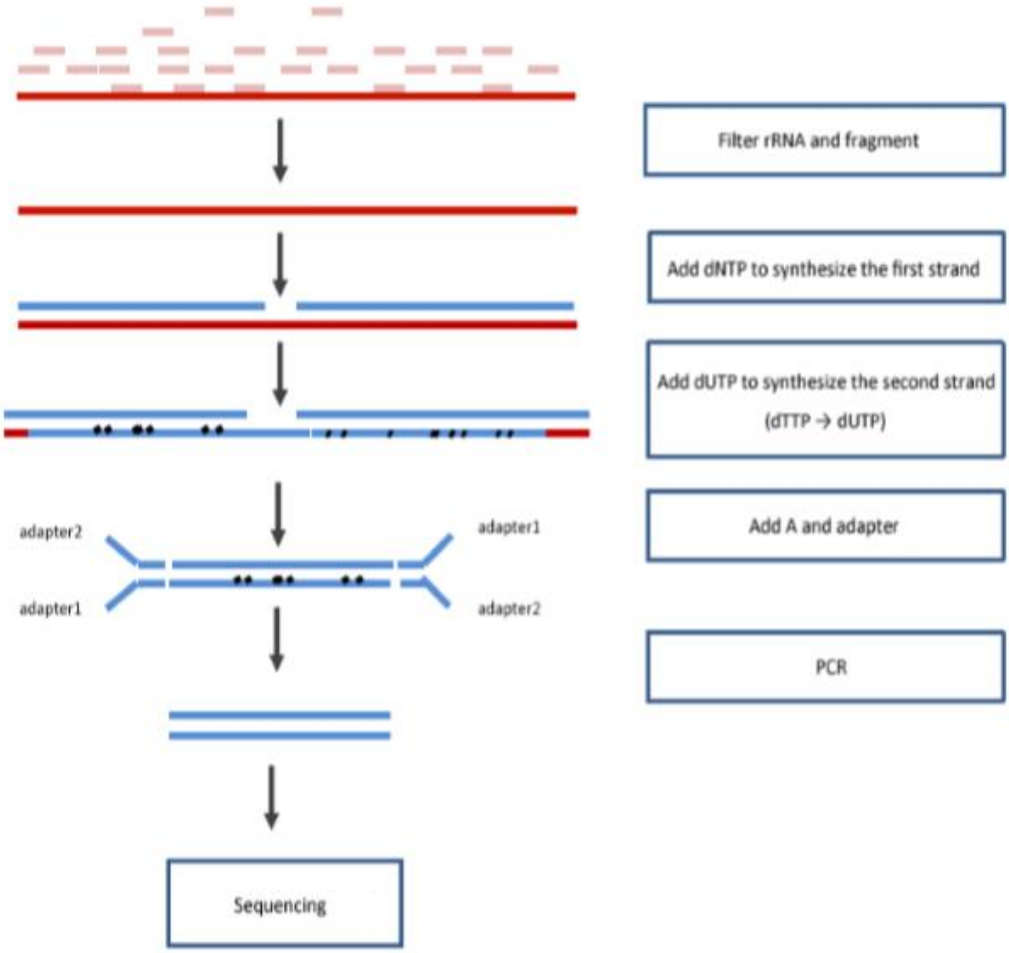

Figure 3.1: *CircRNA library preparation flowchart leading to sequencing*

The raw data generated by this sequencing was filtered to eliminate low quality, joint contamination, and reads with an excessively high base N content using SOAPnuke software [181]. This filtered data is called clean reads and was able to be analysed further. The clean reads are then compared to the reference genome (hg19) and the circRNA is predicted by the CIRI, find_circ software. CIRI is software based on the BWA-MEM genome alignment algorithm used to detect circRNA by generating two scans of the SAM (Sequence Alignment/Map) file. The two parts before and after the

same read were cross aligned to the genome to prove that they are junction reads at both ends of the circRNA (junction reads). Whereas find_circ is a software based on the Bowtie2 comparison genome. First, find_circ discards reads that are contiguous and full-length aligned to the genome. Then, extract 20 bp from the two ends of the remaining reads and then align the genome. Those sequences that can be cross aligned to the exon can prove the existence of circRNA. After combining the results of the two software's, quantitative and differential expression analysis of circRNA was performed using the DEGseq and Deseq2 algorithms for differential circRNA detections. Statistical significance for DEGseq and Deseq2 was defined as a fold change (FC) ≥ 2 and a corrected P value ≤ 0.05. P-values were adjusted for multiple testing using the Benjamini-Hochberg correction with an FDR q-value <0.05 cut-off. The analysis consisted of three separate comparisons which are group 1 (PKPOZ_18 vs PKPOZ_44), group 2 (PKPOZ_36 vs PKPOZ_46) and the comparison of interest, group (group 1 vs group 2) which tested the in-common circRNAs found previously. The complete bioinformatic workflow is outlined in Figure 3.2.

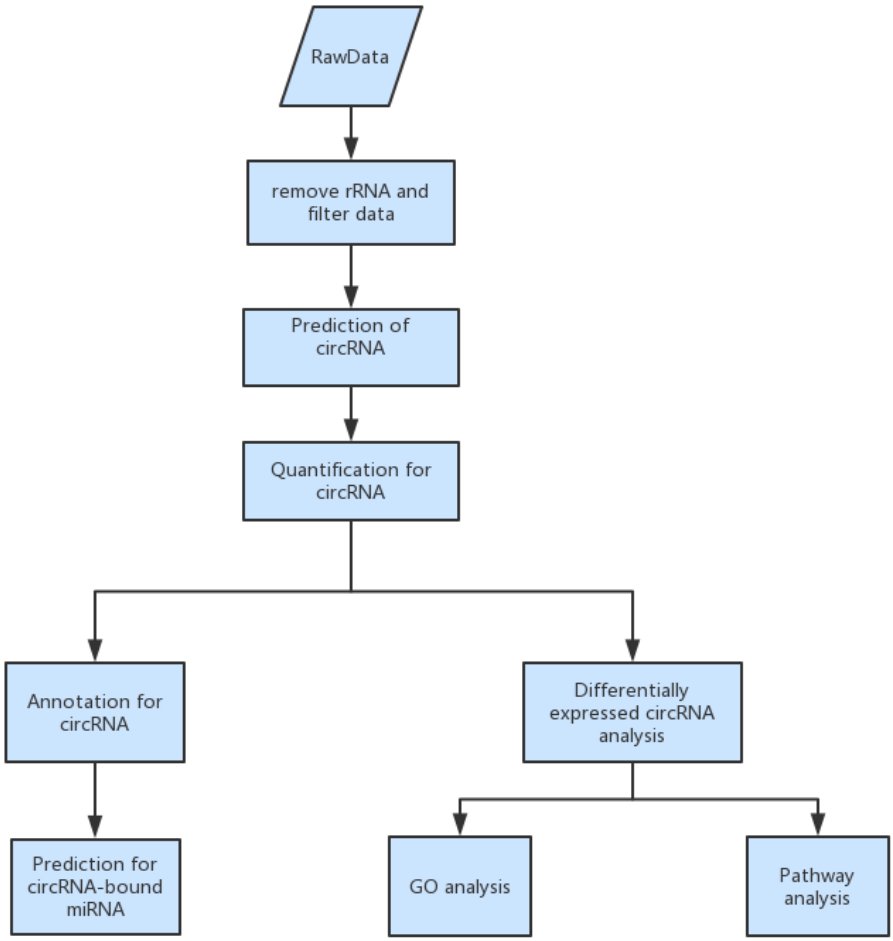

Figure 3.2: *CircRNA analysis flowchart*

3.1.3 Bioinformatic identification of circRNAs and primer design

.

Several databases and tools have been established to provide key bioinformatic knowledge about circRNAs. For instance, circBase (http://www.circbase.org/) informs the user about circRNA identity and tissue specificity based on RNA-seq data [182] and CircInteractome (https://circinteractome.nia.nih.gov/) can be used to design divergent primers and siRNAs and can identify potential interacting factors, including microRNAs and RBPs. [172, 183]. Using the CircInteractome database, we designed specific primers for quantification of our circRNAs. CircInteractome incorporates

primer design tools from Primer345 and NCBI primer design tool and uses a template sequence that spans the circRNA junction to ensure that the circRNA is amplified specifically by reverse transcription followed by qPCR analysis [173].

3.1.4 RNase treatment and cDNA synthesis

Treatment of RNA with RNase R and cDNA synthesis was conducted as previously described (Chapter 2, section 2.1).

3.1.5 Quantification of circRNA expression using qPCR

Expression of circRNAs was measured by quantitative PCR as described previously (Chapter 2, section 2.2). 65 human kidney samples from the TRANSLATE study were utilised in this experimentation. A larger number was not able to be used due to sample availability at Federation University. The circRNAs of interest were measure using the primer sequences outlined in Table 3.2.

Table 3.2: CircRNA primer sequences

Circular RNA	*Primer Sequence*	*Amplicon Length (Base pairs)*
circRP11-298P3.4	5'-GAGACGTACCCGTTGGATACC-3' 5'-TGCCCAGTTTTCTTCAAAACTCTT-3'	121
circUBR2	5'-TGGATGAATTACAGCTCCCTGA-3' 5'-GGGGCAAAGGAATTCTCCG-3'	146
circSRPK2	5'-GAGCAGTCCATCCCATGACA-3' 5'-CCAATAACTCAGCCTGCCTCT-3'	135
circZNF91	5'-AGCATTACAAATATGAAGAGGCATT-3' 5'-ATCTTCCATGCTCTGCTCTGG-3'	102
circKATNAL1	5'-ATTTCCCGTGGGACATTGATGA-3' 5'-CTTTCAAGGGCTTCCACCAGA-3'	167
circGRB10	5'-CACGCCGGGTTCTTTACCTC-3' 5'-CATGCTGCAGGCCGAGTACA-3'	120
circFBXL17	5'-CGGCCAGTGTTACAAGATCTCA-3' 5'-AATGATGCGGAAAGGCAACG-3'	141

circCARHSP1	5'-CGTCTACAAAGGAGTCTGCAAAT-3' 5'-AGGCTCAGATGACATGGCTGA-3'	121
circBORCS7-ASMT	5'-AACAAGTGCTTCAGGAGGCATA-3' 5'-GCAATCTCTGCCACTTCCACT-3'	120
circEVI5	5'-TCCAAGCAGCTTACCAAGTCA-3' 5'-TCGACACAAGAGAAGAGCCAC-3'	123
circLIFR	5'-ACATCATCAGCGTAGTGGCT-3' 5'-CCAGGATGGTCGTTTCAAACAT-3'	136
circGAPDH	5'-ACCCACTCCTCCACCTTTGAC-3' 5'-ACCCTGTTGCTGTAGCCAAATT-3'	104

3.1.6 Quantification of linear isoforms

Quantification of the linear isoforms associated with our circRNAs of interest was achieved through previously generated next-generation RNA sequencing data from the same kidney samples we used from the TRANSLATE study. The methodology surrounding how this was conducted is outlined in the following article published by Marques *et al*., (2015) [106].

3.1.7 *In-silico* identification of predicted circRNA – miRNA interactions

Like other information on circRNAs, identifying circRNA-miRNA interactions is not readily available. CircInteractome is one of the only circRNA databases that readily provides predicted circRNA-miRNA interactions. This is achieved by aligning circRNAs in the TargetScan Perl Script to predict the miRNAs that have sequences complementarity with circRNA [183]. CircInteractome has incorporated into it the ability to search using the TargetScan algorithm, which predicts miRNAs that target circRNA by surveying for 7-mer or 8-mer complementarity to the seed region as well as the 30 ends of each miRNA. A survey of miRNA target sites in circRNAs revealed the presence of numerous target sites for a specific miRNA.

3.1.8 Quantification of miRNA expression using TaqMan Advanced miRNA assays.

Expression of miRNAs was measured by qPCR as described previously (Chapter 2, section 2.3). Table 3.3 outline the TaqMan™ Advanced miRNA assays utilised and the corresponding assay number.

Table 3.3: miRNAs measured utilising TaqMan™ Advanced miRNA assays

miRNA	***Assay No.***
rno-miR-145-3p	rno480937_mir
hsa-miR-155-5p	483064_mir
hsa-miR-215-5p	478516_mir
hsa-miR-217-5p	478773_mir
hsa-miR-383-5p	478079_mir
hsa-miR-510-5p	478968_mir
hsa-miR-526b-3p	478997_mir
hsa-miR-578	479058_mir
hsa-miR-663b	479416_mir

3.1.9 *In-silico* identification of circRNA-miRNA-mRNA network

Identification of the circRNA-miRNA interactions is described in section 3.1.7. The miRNA – mRNA interactions were identified by use of TargetScan (https://www.targetscan.org/vert_80/), miRDB (http://www.mirdb.org/) and TargetMiner (https://www.isical.ac.in/~bioinfo_miu/targetminer20.htm) databases. mRNAs that were present across all three databases were considered 'potential' interactions for the miRNAs of interest. The following list of 'potential' mRNA interactions was overlayed with GWAS data for SBP, DBP and HT from https://www.ebi.ac.uk/gwas/, giving us a final list of mRNAs, that have been identified to be involved BP regulation and potentially regulated by our circRNAs of

interest. This circRNA-miRNA-mRNA network was illustrated using Cytoscape V3.9.1 software.

3.1.10 Quantification of predicted mRNA targets

The expression of predicted mRNA targets was measured using the same methodology outlined in Section 3.1.6 of this chapter.

3.1.11 Statistical Analysis

Statistical analysis utilised for experimentation this chapter is outlined in Chapter 2 Section 2.10.

3.2 Results

3.2.1 Clinical characteristics of TRANSLATE study participants

Table 3.3 provides characteristics of those samples used in the ultra-deep RNA sequencing. Further to this, Table 3.4 outlines the clinical characteristics of the 65 individuals from the TRANSLATE study included in the circRNA and miRNA expression analysis.

Table 3.4: Clinical characteristic of individuals used in the ultra-deep RNA sequencing from the TRANSLATE study.

Variables	*Normotensive (mean ± SD)*	*Hypertensive (mean ± SD)*
N	2	2
Age (years)	61 ± 0	70 ± 2.83
Sex (M/F)	1/1	0/2
Body mass index (kg/m^2)	26 ± 0.42	26.1 ± 2.97
Clinical systolic BP (mmHg)	129.65 ± 13.65	151.6 ± 1.41
Clinical diastolic BP (mmHg)	79.2 ± 3.54	92.9 ± 1.20
Antihypertensive treatment	N/A	1 (50%)

Table 3.5: Clinical characteristics of individuals in the TRANSLATE study

Variables	*Normotensive (mean ± SD)*	*Hypertensive (mean ± SD)*	*P-Value (NT vs HT)*
N	22	43	N/A
Age (years)	55.59 ± 8.17	63.86 ± 10.31	<0.05
Sex (M/F)	9/13	27/16	<0.05
Body mass index (kg/m^2)	25.74 ± 3.50	28.06 ± 4.24	<0.05
Clinical systolic BP (mmHg)	126.98 ± 7.60	150.19 ± 11.96	<0.05
Clinical diastolic BP (mmHg)	77.42 ± 5.88	89.36 ± 8.52	<0.05
Antihypertensive treatment	N/A	35 (81.4%)	N/A

3.2.2 CircRNA sequencing identifies differentially expressed circRNAs within the TRANSLATE cohort

Four renal samples from the TRANSLATE study were included in the circRNA sequencing analysis in the human kidney. The clinical characteristics of the TRANSLATE study participants used are outlined in Table 3.4. The circRNA sequencing identified from all three comparisons several differentially expressed circRNAs ($P<0.05$); 6248 circRNAs were found differentially expressed in group one with 2841 up-regulated and 3407 down-regulated, 8502 circRNAs were differentially expressed in group two with 4594 up-regulated and 3908 down-regulated and the overall analysis of group 1 and group 2 found 12 differentially expressed circRNAs with 6 up-regulated and 6 down-regulated ($P<0.05$, FC > 2) (Figure 3.3 and Table 3.6).

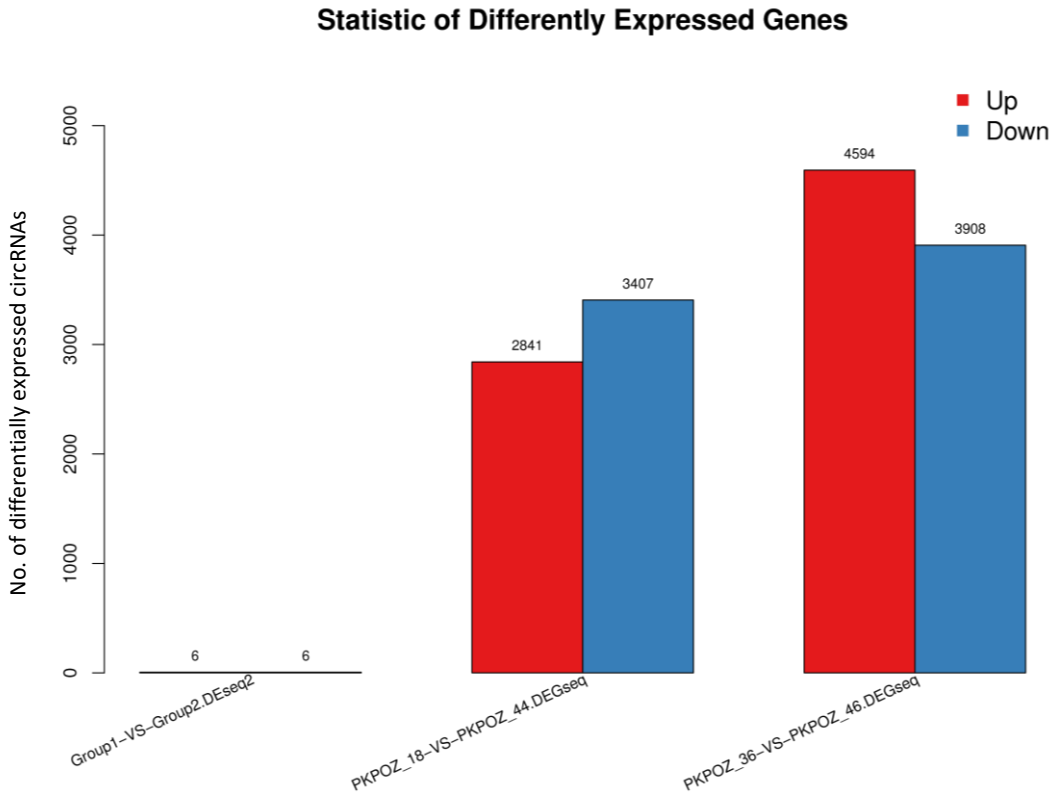

Figure 3.3: DE circRNAs from grouped analysis. *Group 1 (PKPOZ18 vs PKPOZ44) discovered 2841 upregulated and 3407 downregulated, group 2 (PKPOZ36 vs PKPOZ46) discovered 4594 upregulated and 3908 downregulated and group 3 (group 1 vs group 2) discovered 6 upregulated and 6 downregulated.*

Table 3.6: Details of the differentially expressed circRNAs from Group 1 vs Group 2

Chromosome Location (Hg19)	*CircBase ID*	*Gene of Origin*	*Product Size (base pairs)-As per circBase*	*Fold Change*
Chr13: 33006925-33018263	hsa_circ_0100256	RP11-298P3.4	11,338	3.61
Chr6: 42630995-42633983	hsa_circ_0002906	UBR2	2,988	-4.15
Chr7: 104782454-104783777	hsa_circ_0081828	SRPK2	1,323	4.82
Chr19: 23541231-23545527	hsa_circ_0109315	ZNF91	4,296	-4.32
Chr13: 30801548-30815223	hsa_circ_0003587	KATNAL1	13,675	1.61
Chr7: 50737418-50742355	hsa_circ_0008334	GRB10	4,937	-4.55
Chr5: 107684099-107703654	hsa_circ_0001518	FBXL17	19,555	-3.83

Chr16: 8952206-8953192	hsa_circ_0000669	CARHSP1	986	-3.83
Chr10: 104632204-104634418	hsa_circ_0019773	BORCS7-ASMT	2,214	4.05
Chr1: 93159358-93170301	hsa_circ_0013171	EVI5	10,943	-3.94
Chr5: 38496483-38530768	hsa_circ_0072305	LIFR	34,285	4.93
Chr7: 141754553-141778808	Not annotated	MGAM	24,255	8.40

3.2.3 qRT-PCR validation of human kidney samples confirms some of the circRNA sequencing data

Validation of the circRNA sequencing results in kidney samples from the TRANSLATE study confirmed seven circRNAs were differentially expressed in a larger cohort with those being *circCARHSP1, circKATNAL1, circGRB10, circLIFR, circRP11, circUBR2* and *circZNF91* ($P<0.05$) with the remaining four circRNAs *circBORCS7-ASMT, circEVI5, circFBXL17* and *circSRPK2* showing no statistical significance ($P>0.05$) (Figure 3.5). Clinical measurements such as the age, gender and BMI of an individual were co-analysed with the circRNA expression data using a univariate ANOVA to determine that if these clinical measurements were impacting on the expression data presented below. The univariate ANOVA identified that age, gender, and BMI did not influence the expression of the differentially expressed circRNAs.

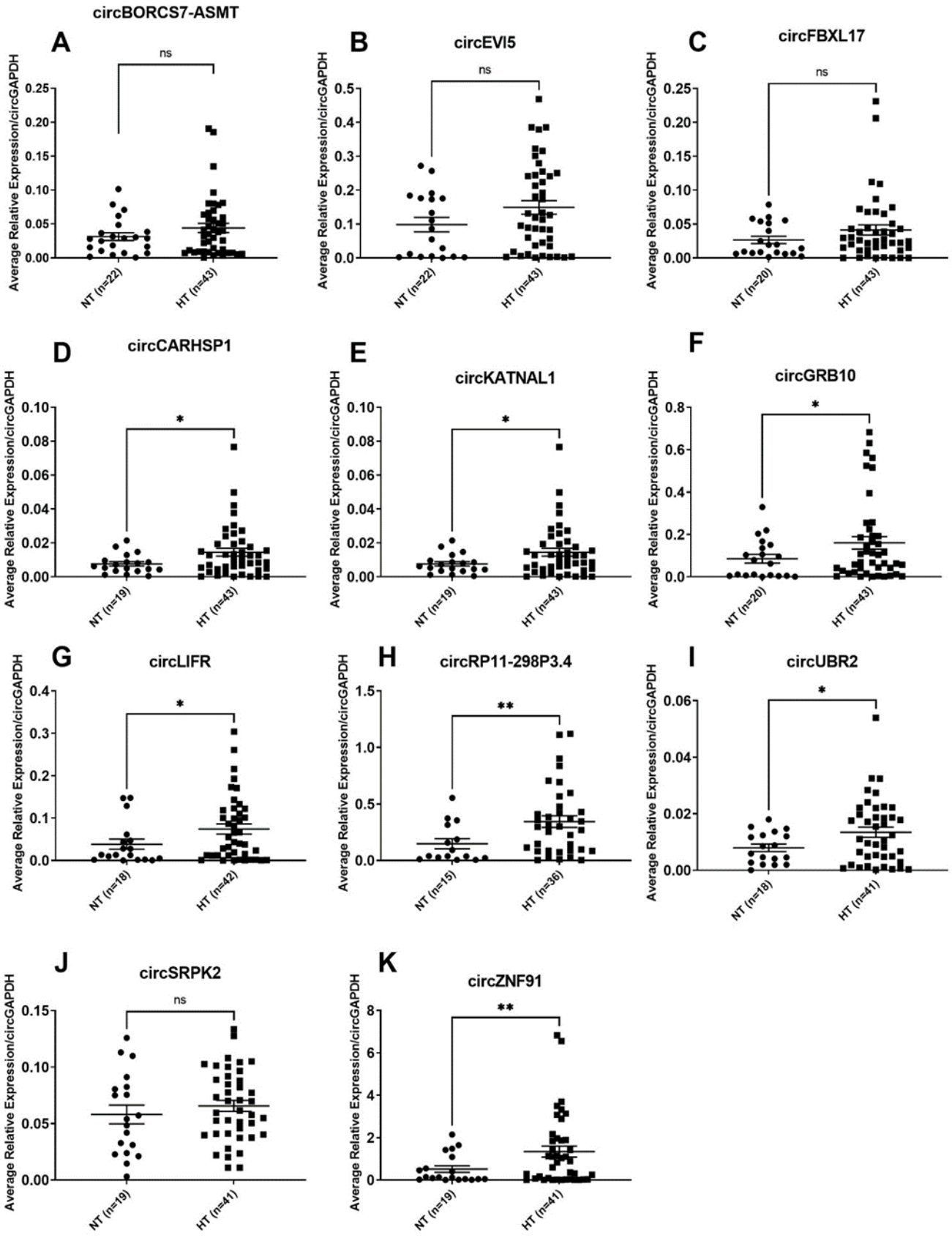
circBORCS7-ASMT
A
ns
Average Relative Expression/circGAPDH
0.25
0.20
0.15
0.10
0.05
0.00
NT (n=22)
HT (n=43)
B
circEVI5
ns
0.5
0.4
0.3
0.2
0.1
0.0
NT (n=22)
HT (n=43)
C
circFBXL17
ns
0.25
0.20
0.15
0.10
0.05
0.00
NT (n=20)
HT (n=43)
D
circCARHSP1
*
0.10
0.08
0.06
0.04
0.02
0.00
NT (n=19)
HT (n=43)
E
circKATNAL1
*
0.10
0.08
0.06
0.04
0.02
0.00
NT (n=19)
HT (n=43)
F
circGRB10
*
0.8
0.6
0.4
0.2
0.0
NT (n=20)
HT (n=43)
G
circLIFR
*
0.4
0.3
0.2
0.1
0.0
NT (n=18)
HT (n=42)
H
circRP11-298P3.4
**
1.5
1.0
0.5
0.0
NT (n=15)
HT (n=36)
I
circUBR2
*
0.06
0.04
0.02
0.00
NT (n=18)
HT (n=41)
J
circSRPK2
ns
0.15
0.10
0.05
0.00
NT (n=19)
HT (n=41)
K
circZNF91
**
8
6
4
2
0
NT (n=19)
HT (n=41)

Figure 3.5: Validation of differentially expressed circRNAs in the TRANSLATE study*. A) circBORCS7-ASMT. B) circEVI5. C) circFBXL17. D) circCARHSP1. E) circKATNAL1. F) circGRB10. G) circLIFR. H) circRP11-298P3.4. I) circUBR2. J) circSRPK2. K) circZNF91. NS=not significant (P>0.05), *P<0.05, **P<0.005*

3.2.4 Linear isoforms of circRNAs are not impacted by the differentially expressed circRNAs.

Due to the competition between splicing machinery, it is possible that an inverse relationship exists between circRNA and mRNA expression from a host gene. We used next-generation RNA sequencing generated from the same TRANSLATE samples used in the validation experiments to determine the corresponding host genes mRNA expression. Next-generation RNA sequencing of the human kidney samples from the TRANSLATE study identified no statistical significance of any of the linear isoforms that corresponded with our circRNAs of interest (P>0.05) (Figure 3.6). The linear isoform of *circBORCS7-ASMT* is not included as there was insufficient expression data across all samples to quantify and graph appropriately.

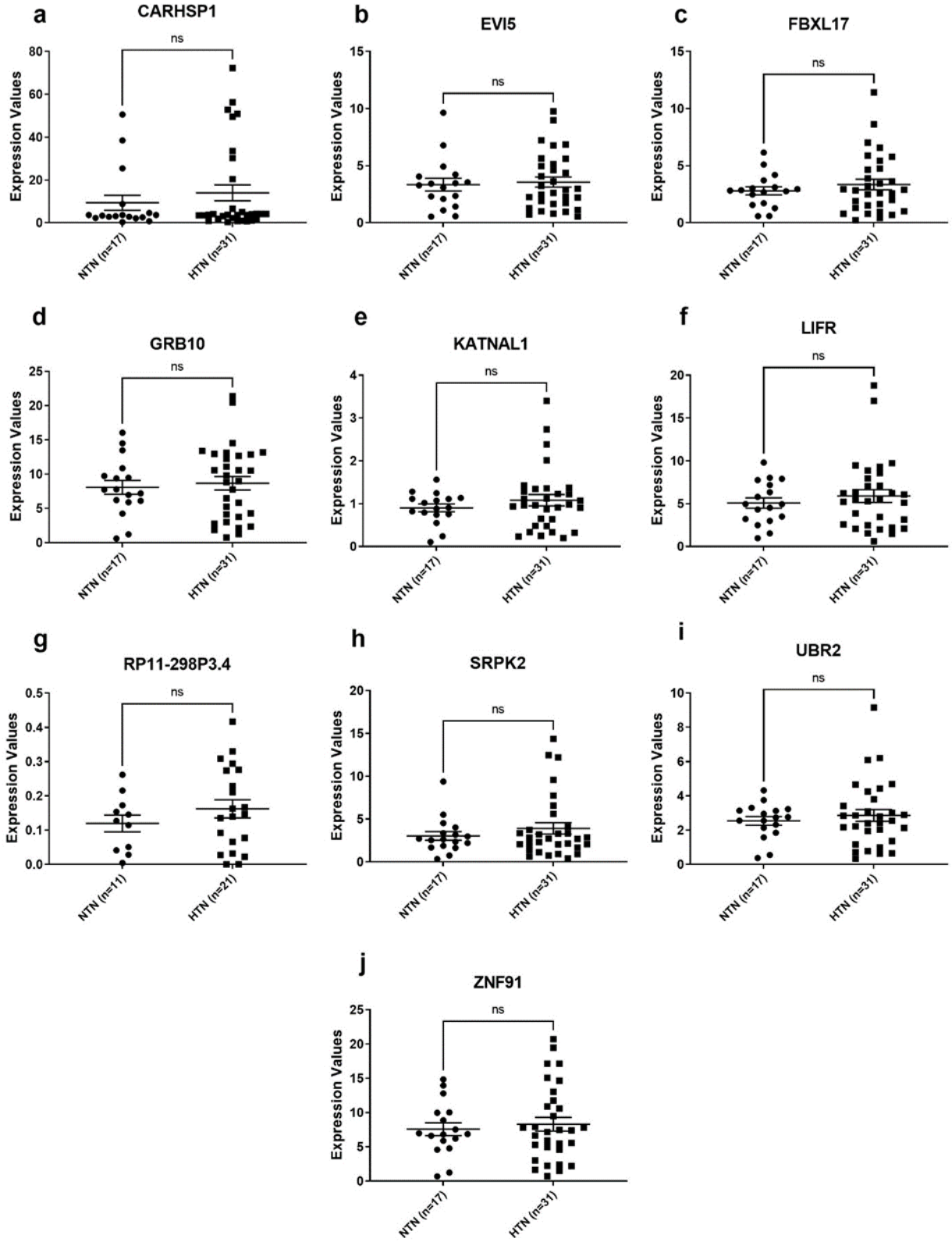

Figure 3.6: Next-generation RNA sequencing quantification of linear isoforms of our circRNAs of interest*. A) CARHSP1. B) EVI5. C) FBXL17. D) GRB10. E) KATNAL1. F) LIFR. G) RP11-298P3.4. H) SRPK2. I) UBR2. J) ZNF91. NS= not significant (P>0.05)*

3.2.5 Predicted miRNA-circRNA interactions display several miRNAs implicated with hypertension development

Utilising the online circRNA database CircInteractome we were able to compile a complex circRNA-miRNA interaction network with miRNAs previously published to have implications in HT development and progression (Section 1.4.2, Table 1.2). The DE circRNAs are predicted to interact with several miRNAs shown to be involved in HT development/progression *circZNF91* is predicted to interact with miR-145, miR-155, miR-383, miR-526b and miR-578, *circCARHSP1* is predicted to interact with miR-146-3p, *circRP11-298P3.4* is predicted to interact with miR-145, miR-155, miR-217, miR-510, miR-526b, miR-578 and miR-663b, *circGRB10* is predicted to interact with miR-217, *circLIFR* is predicted to interact with miR-296-5p, miR-526b and miR-578, *circKATNAL1* is predicted to interact with miR-182, miR-223 and miR-637 and lastly *circUBR2* is predicted to interact with miR-155 and miR-578.

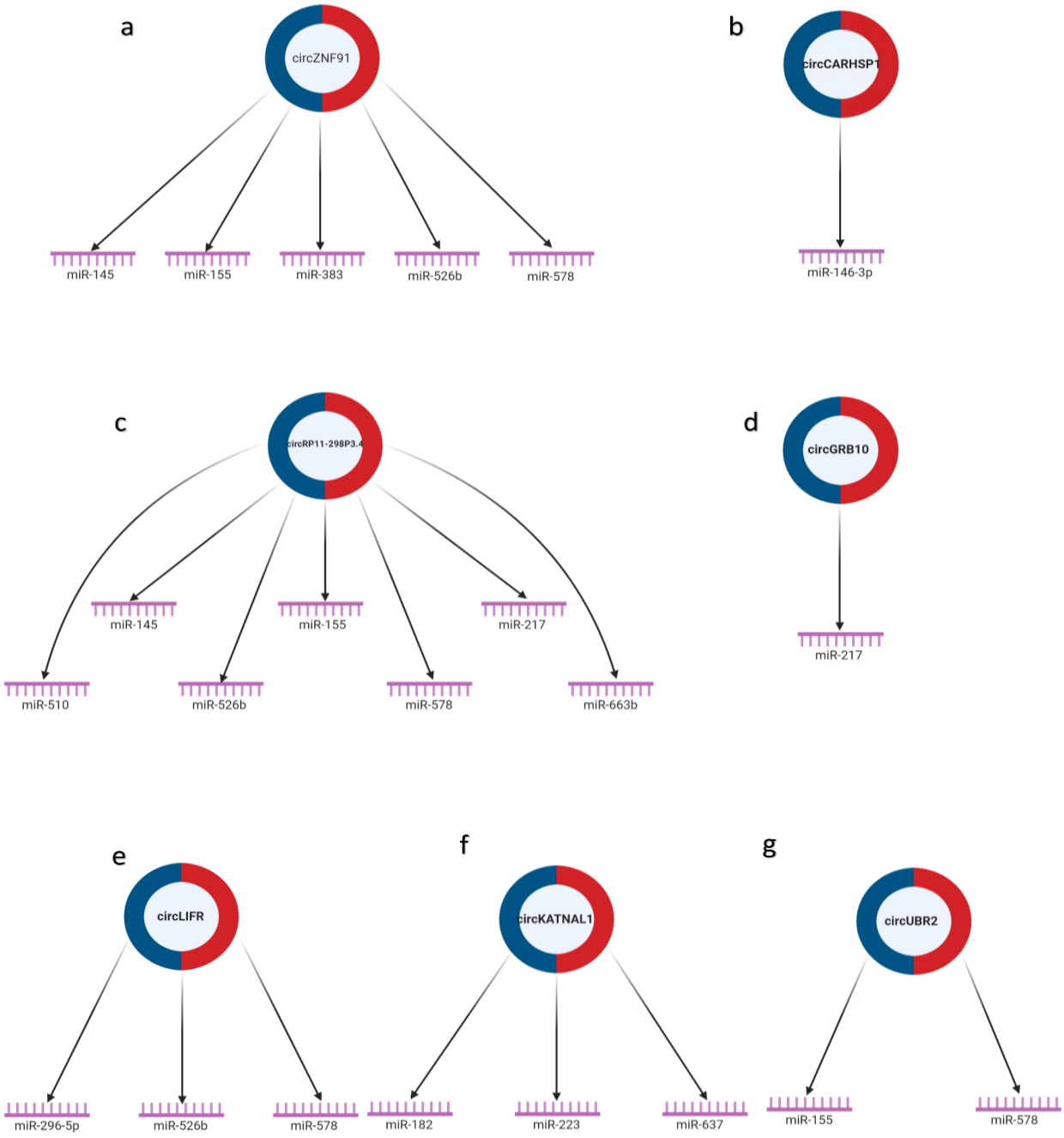

Figure 3.7: CircRNA predicted interactions with miRNAs implicated with hypertension development /progression. *A) circZNF91 is predicted to interact with miR-145, miR-155, miR-383, miR-526b and miR-578. B) circCARHSP1 is predicted to interact with miR-146-3p. C) circRP11-298P3.4 is predicted to interact with miR-145, miR-155, miR-217, miR-510, miR-526b, miR-578 and miR-663b. D) circGRB10 is predicted to interact with miR-217. E) circLIFR is predicted to interact with miR296-5p, miR-526b and miR-578. F) circKATNAL1 is predicted to interact with miR-182, miR-223 and miR-637. G) circUBR2 is predicted to interact with miR-155 and miR-578. Image created using Biorender.*

3.2.6 miRNA expression analysis from the TRANSLATE study identifies several differentially expressed miRNAs of interest

The predicted miRNA interactions with our DE circRNAs were then measured utilising the TaqMan advanced miRNA assays in the same samples utilised in the original validation stage (section 3.2.3). Of the 13 unique miRNAs predicted to interact with our DE circRNAs we identified two with significantly downregulated miRNAs miR-145 and miR-217 in the TRANSLATE samples ($P<0.05$) (Figure 3.8A and C) with another two miR-510-5p and miR-663b (Figure 3.8D and E) displaying a negative trend but no statistical significance ($P>0.05$). Of the 13 miRNAs only one (miR-155) displayed a positive trend in expression in the human renal tissue but no statistical significance was observed ($P>0.05$) (Figure 3.8B). The remaining 8 miRNAs miR-21, miR-146b-3p, miR-182, miR-223, miR-383, miR-526b, miR-578 and miR-637 displayed limited to no expression in the human renal samples to graph appropriately.

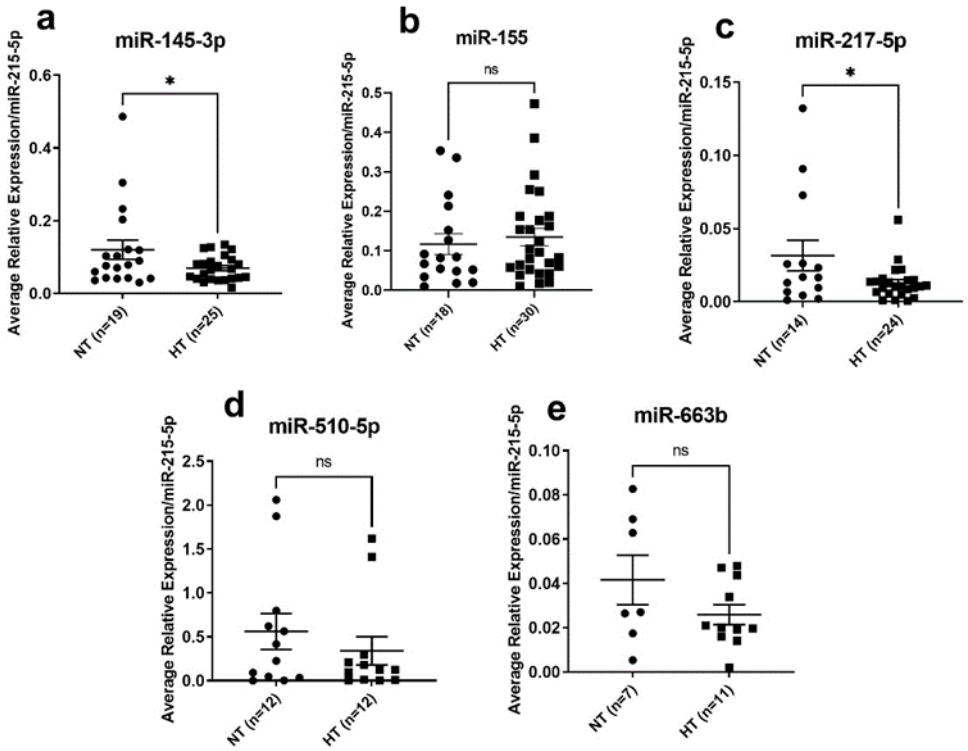

Figure 3.8: Expression of miRNAs predicted to interact with our differentially expressed circRNAs. *A) miR-145-3p. B) miR-155. C) miR-217-5p. D) miR-510-5p. E) miR-663b. No expression was detected for miR-383, miR-578 and miR-663b. NS = Not significant (P>0.05), * P<0.05*

3.2.7 *In silico* gene networking outlines several mRNAs previously identified in HT studies interacting with our DE circRNAs and miRNAs

CircRNA – miRNA interactions are outlined is Figure 3.7. Information of predicted miRNAs interactions was inputted into miRanda and TargetScan to predict target mRNAs. Intersection of target mRNAs from the two software and target genes related to HT, DBP and SBP were cross-matched and were represented in Figure 3.9. *CircZNF91* is predicted to interact with miR-145 which was predicted to interact with 33 mRNAs which have been identified through GWAS. *CircRP11-298P3.4* was also predicted to interact with miR-145 but also miR-217 which was precited to interact with 5 mRNAs which have been identified through GWAS to be of significance in BP/HT.

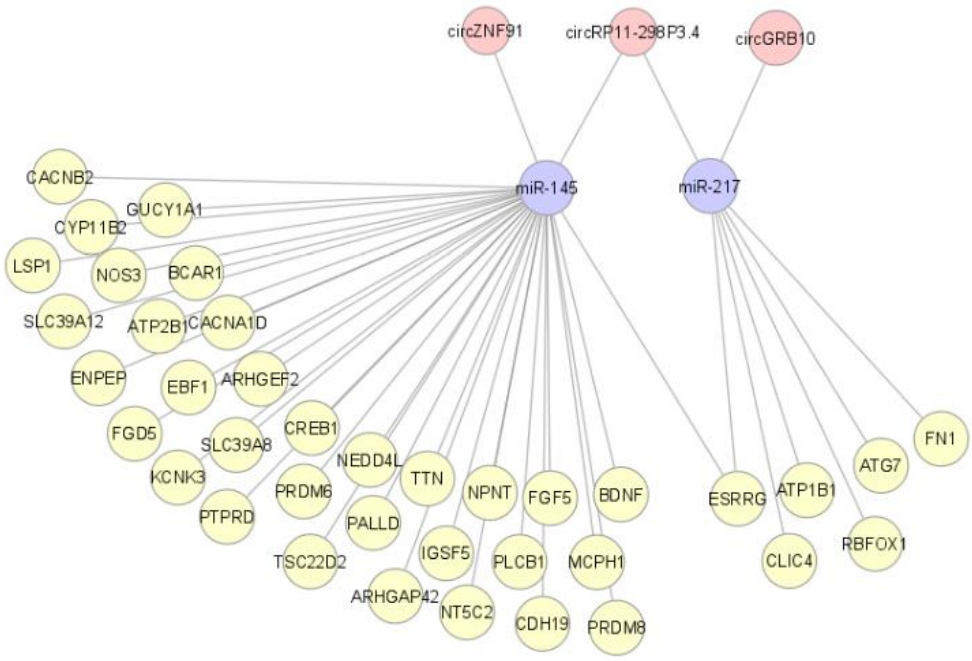

Figure 3.9: circRNA – miRNA – mRNA network. *In silico analysis predicted circZNF91 to interact with miR-145, circRP11-298P3.4 to interact with miR-145 and miR-217 and circGRB10 to interact with miR-217. miR-145 was predicted to interact with 33 mRNAs indemnified through GWAS whilst miR-217 was predicted to interact with 5.*

3.2.9 mRNA expression from the TRANSLATE study supports potential circRNA-miRNA-mRNA interactions

From the 38 total predicted interactions for both miR-145 and miR-217 (Figure 3.9), RNA sequencing data from the TRANSLATE study identified expression in 34 genes (Table 3.). RNA sequencing did not identify expression in *GUCY1A1, CYP11B2, SLC39A12* and *AT1B1*. Of the 34 measurable genes, 10 genes were upregulated in the HT kidneys samples ($P<0.05$) whilst the remaining 24 gene displayed no statistical significance when compared to the NT group ($P>0.05$). The 10 genes that were differentially expressed were *ATP2B1, CLIC4*, *CREB1*, *ESRRG*, *NT5C2, PALLD, PLCB1, SLC39A8, TSC22D2* and *TTN* (Figure 3.10).

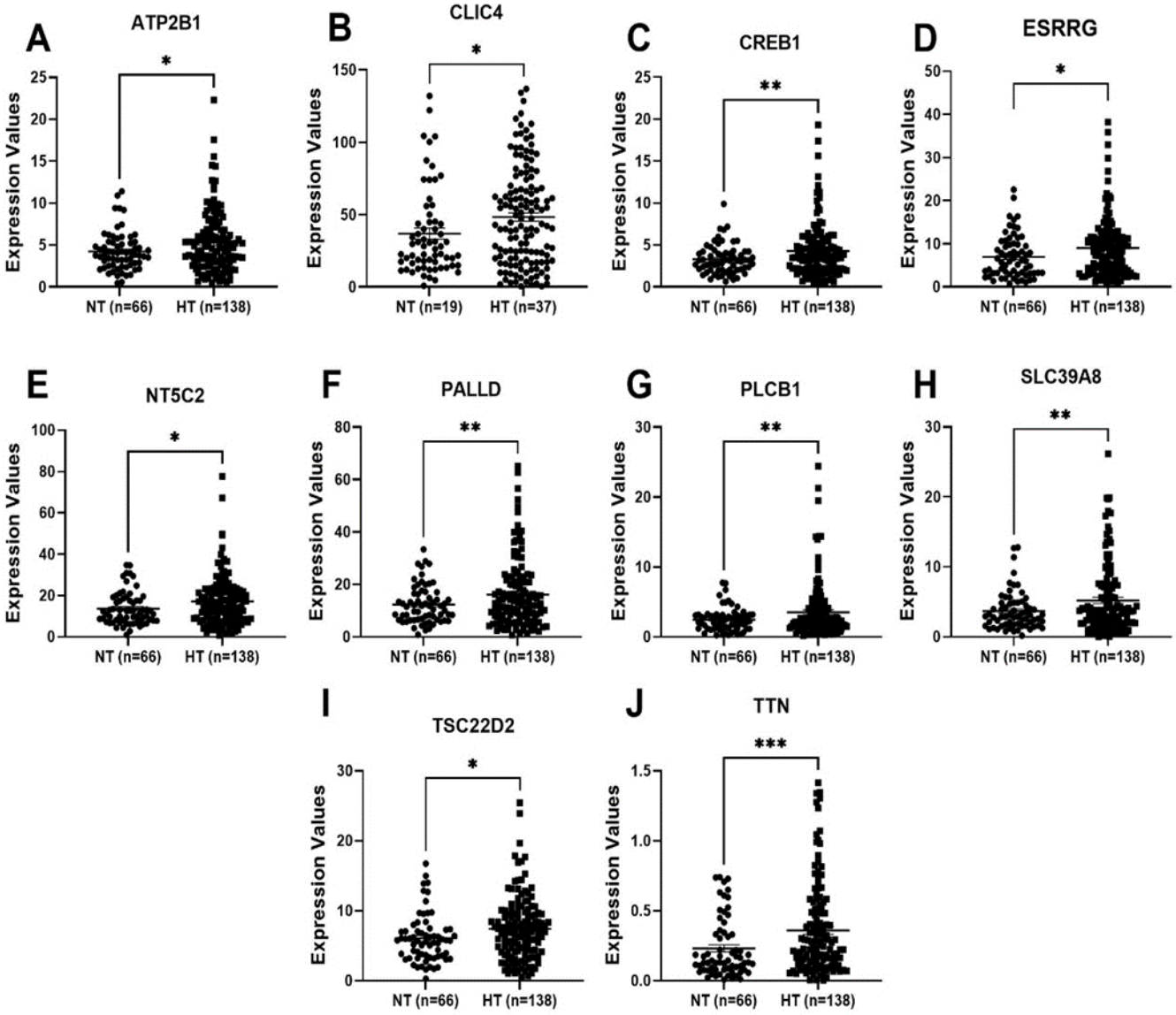

Figure 3.10: Differentially expressed mRNAs of interest from the TRANSLATE Study. A) ATP2B1. B) CLIC4. C) CREB1. D) ESRRG. E) NT5C2. F) PALLD. G) PLCB1. H) SLC39A8. I) TSC22D2. J) TTN. *P < 0.05, **P<0.005, *** P<0.001

3.3 Discussion

This study initially examined the expression of circRNAs utilizing ultra-deep RNA sequencing in a small cohort of human renal samples. This initial sequencing identified 12 differentially expressed circRNAs (Table 3.5), of which 11 had been previously annotated and one has yet to been annotated. However, due to the low sample size that were sequenced we validated the sequencing results in a larger cohort of human renal samples (n=65) utilizing qPCR to ensure the reliability of the results obtained. The validation step confirmed the sequencing results of three circRNAs of interest circKATNAL1, circLIFR and circRP11-298P3.4 (Figure 3.5 E, G and H respectively) which showed that these three circRNAs were significantly upregulated in the EH kidney samples when compared to the healthy controls ($P<0.05$). The validation of *circCARHSP1, circGRB10, circUBR2* and *circZNF91* (Figure 3.5 D, F, I and K respectively) displayed statistical significance ($P<0.05$) but instead of being downregulated as the original sequencing analysis stated we discovered an upregulation of these four circRNAs in the EH kidney samples when compared to the healthy controls. The remaining four circRNAs of interest *circBORCS7, circEVI5, circFBXL17* and *circSRPK2* (Figure 3.5 A, B, C and J respectively) displayed no statistical significance when validated in the larger cohort ($P>0.05$). The circRNA sequencing in conjunction with the validation step is the first experimentation of its kind to examine circRNA expression in the kidney of HT patients.

Due to the competition between splicing machinery an inverse relationship is hypothesized to exist between circRNAs and their corresponding linear transcript [130]. Due to this possibility, we investigated the expression of the linear isoform for our circRNAs of interest to determine if the increased expression we observed previously is due to the pathological state or was contributed too by the competition

between the splicing machinery. We measured the expression of the linear isoform by utilizing previously generated RNA sequencing data from the same samples in the validation stage of this study [106]. This data displayed no statistically significant difference ($P>0.05$) in any of the 11 mRNAs that corresponded with our circRNAs of interest (Figure 3.6). From these findings we can assume that the observed increase in circRNA expression was not contributed too by a subsequent alteration in mRNA expression but is more probably associated with the individual suffering from EH.

One of the proposed primary functions of circRNAs is their ability to act as a miRNA sponge. The circRNA database CircInteractome allowed us to identify several miRNAs that are predicted to interact with our circRNAs of interest (Figure 3.7). Of these miRNAs identified several have been identified in some capacity to be involved with EH/HT development and progression. For instance, *miR-155* is predicted to interact with *circZNF91*, *circRP11-298P3.4* and *circUBR2*. *miR-155* has been shown to critical in HT development and progression through its ability to interact with *FOXO3a*. *FOXO3a* is critical for maintaining cardiac function, regulating BP and anti-oxidative stress [161]. *MiR-155* is also well-known to be upregulated in individuals suffering from CKD, outlining a direct link with renal disease and a potential avenue of exploration [99].

After identifying potential interactions with our circRNAs of interest we measured the expression of these miRNAs in the same sample cohort utilizing TaqMan advanced miRNA assays to determine if there was a downregulation as expected when compared to the specific circRNAs. As mentioned previously, we expect this downregulation due to the upregulation of our circRNAs of interest which are predicted to interact with these circRNAs. We identified that *miR-145* and *miR-217* were significantly downregulated ($P<0.05$) in the HT samples when compared to the

healthy controls (Figure 3.7 A and C respectively). *MiR-145* is predicted to interact with *circZNF91* and *circRP11-298P3.4* whilst *miR-217* is predicted to interact *circGRB10* and *circRP11-298P3.4*. Limited correlations have been made between BP/HT and *miR-217*, however research undertaken by Han *et al* (2015) demonstrated miR-217 mediates a protective property in the proximal tubule cells of the kidney against fibrosis [184]. The protective property is achieved via regulating the expression of Wnt5a, upregulation of *miR-217* resulted in degradation of *Wnt5a* and subsequently downstream *TGFβ1* which acted together to activate epithelial-mesenchymal transition genes such as MMP3, FN1 and Col1a. Provided the apparent protective property that *miR-217* has in the kidney this warrants further investigation into the role of *miR-217* downregulation in BP regulation and HT development given the kidneys serve as a focal point for BP homeostasis.

Although we have identified an inverse relationship between the expression of these circRNAs and miRNA it does not conclude that one is led to by the other. Further validation of these interactions is required before we can confirm fully that what we have observed above is linked or happened by chance. This can be achieved by use of knockdown or overexpression experimentation with the aim of determining if the miRNA profile is altered with the variable circRNA expression, another option is to determine if a miRNA is directly linked to a circRNA through luciferase assays which will determine the presence or lack of binding between miRNAs and circRNAs.

GWAS outlined in Table 1.1 of this thesis provided us with insight to the genes that have a direct link to either HT or BP regulation. These studies provided us with a list of candidate genes to determine if any were predicted to interact with our miRNAs of interest. From there we established a predicted network that our circRNAs of interest might be able to influence BP through (Figure 3.9). We identified 33 genes from a

plethora of GWAS that were predicted to interact with *miR-145* and five genes that were predicted to interact with *miR-217*. Utilizing the same RNA sequencing results from Marques *et al*. (2015) we measured the expression of our predicted mRNA targets. From the 38 genes in total that were of interest we obtained expression data for 34. From the 34 measurable genes 10 were identified to be upregulated in the HT when compared to the control group. With the addition of the mRNA sequencing results for our predicted targets this allowed us to identify circRNA – miRNA – mRNA networks of interest that match the expression profile based on up-regulated circRNA, downregulated miRNA and subsequently upregulated mRNAs (Figure 3.11).

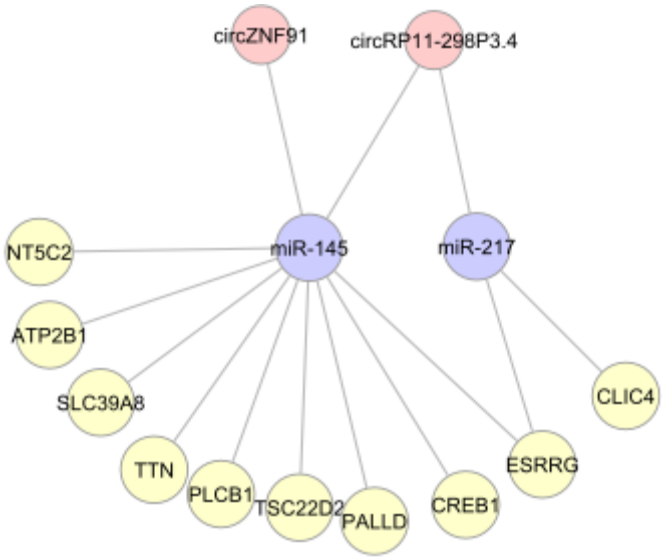

Figure 3.11: Refined circRNA – miRNA – mRNA predicted interactions from the TRANSLATE Study. *Image created using Cytoscape*

For example, we predicted that *CLIC4* interacts with *miR-217*. *CLIC4* overexpression in SHR kidneys contribute to alterations in the proximal tubular compartment resulting in declining kidney function and subsequently contributing to increased BP [185]. *CLIC4* is an early marker of hypoxia-induced pulmonary hypertension and a

component of apoptotic response to oxidative stress, which has previously been shown to be highly upregulated in heart tissue of SHR but considerably downregulated when the animals were treated with BP-lowering medications [186]. Its absence in a CLIC4-null mouse model contributed to impaired renal tubulogenesis in embryos and with aberrant dilation of proximal tubules. The proximal tubule is the major absorptive segment of nephron and accounts for reabsorption of nearly two-thirds of filtered water, sodium, and chloride [187]. Therefore, it can be assumed that CLIC4 plays a pivotal role in the BP regulation through its ability to regulate pressure natriuresis.

Further to this, we predicted that *SLC39A8* or otherwise known as ZiP8 interacts with *miR-145*. ZiP8 is a plasma membrane transporter of divalent metal cations, including the heavy metal cadmium (Cd^{2+}) which in large quantities has been associated with increased BP which is likely to be the consequence of Cd^{2+} induced damage on the kidney and vascular endothelial cells [188, 189]. Studies of mice with an overexpression for ZiP8 has indicated that ZiP8 mediates Cd^{2+} uptake in the kidney proximal tubule and thereby plays an important role in Cd^{2+} toxicity and subsequent kidney failure as a result [188] . ZiP8 has also been identified to regulate NO, this occurs directly through Cd^{2+} accumulation in the endothelial cells of the vasculature which inhibits NO function as a vasodilator (discussed previously in Section 1.1.3) [190]. This demonstrates that ZiP8 by virtue of Cd^{2+} accumulation can manipulate BP regulation through a variety of mechanisms making it a gene of interest moving forward.

The following chapters of this thesis will expand upon the concept that one or many of the above mentioned circRNA – miRNA – mRNA interactions (Figure 3.11) is influencing BP regulation through a renal mechanism, this will be tested by various

means such as knockdown study utilizing siRNAs to decrease the expression of specific circRNAs to elucidate how this impacts on the miRNA profile and subsequently how that impacts the mRNA profile which will further tailor our approach for further experimentation.

3.4 Limitations

As with all scientific research, limitations within the experimental design exist and our research is no different. The first limitation we observed is that our original circRNA sequencing had a limited sample size to start with due to several factors. The main factor was the cost to run this experiment, due to the increased depth of sequencing required to detect circRNAs this significantly increases the cost to run it. This limited the samples we could put forward for the initial sequencing step, being four (n=4). Due to the limited number of samples that were originally sequenced this increased our margin of error when it came to circRNAs that were defined as statistically significant. As Button *et al*. stated, an experiment with a smaller sample size reduces the likelihood that a statistically significant result reflects a true effect. The results in this chapter are only prediction based at this current time. We have identified a number of predicted circRNA-miRNA-mRNA networks of interest (Figure 3.11) using various bioinformatic tools, however the next step is to now validate these networks to definitively state that these types of RNAs are connected and to further explore the role they play in BP regulation.

Chapter 4

Reduced circRNA expression and its impact on miRNA expression profile

Abstract

CircRNAs ability to act as a miRNA 'sponge' is underexplored in the context of EH. Previous studies exploring the role of circRNAs in EH have yet to define a circRNA – miRNA interaction but instead focused on defining circRNAs value as a diagnostic tool. In chapter 3 we identified several circRNAs of interest in the kidneys of individuals with EH, but further work is required to elucidate the role that they might play in disease progression. The aim of the current study was to develop our understanding of *circZNF91*, *circRP11-298P3.4* and *circGRB10*, particularly their ability to function as a 'miRNA sponge'. To investigate this, we first reduced the expression of these circRNAs utilizing siRNA transfection. HEK293 cells were transfected with either siRNAs specific for *circZNF91*, *circRP11-298P3.4* or *circGRB10* with the control groups being HEK293 cells treated with a scramble sequence. Confirmation of circRNA knockdown was achieved by qPCR. To investigate these circRNAs ability to function as 'miRNA sponges' sRNA sequencing was undertaken comparing the siRNA treated groups to the scramble treated groups to identify differentially expressed miRNAs that may have been impacted by the reduced circRNA expression. sRNA sequencing for the *circRP11-298P3.4* knockdown cells identified 109 differentially expressed miRNAs (FDR <0.05) with 72 being down regulated and the remaining 37 upregulated. The sRNA sequencing for *circZNF91* and *circGRB10* did not display any differentially expressed miRNAs (FDR > 0.05). In the *circRP11-298P3.4* knockdown model the upregulated miRNAs become our miRNAs of interest based on the mechanisms of circRNA – miRNA interactions. In the circZNF91 and circGRB10 models, without the presence of differentially expressed miRNAs other circRNA functions need to be considered moving forward. The next chapter of this thesis will aim to elucidate how reduced circRNA expression impacts on mRNA expression, the decisive step in the circRNA-miRNA-mRNA axis.

4.0 Introduction

In chapter 3 of this thesis several circRNAs were identified to be differentially expressed in the kidneys of HT individuals with the miRNAs predicted to interact with them displaying an inverse relationship between their expression. This study aims to build on this knowledge and further of elucidate the functions that our circRNAs of interest might have in overall gene expression regulation.

Of the many circRNA functions, their ability to act as a miRNA 'sponge' is the most detailed. CircRNAs contain miRNA binding regions (MBRs) which are unique nucleotide sequences that allow for circRNAs to interact with miRNAs in a complementary base-pair manner [182]. CircRNAs can consist of one MBR for a specific miRNA to in some cases 70 MBRs, as is the case with ciRS-7 for miR-7 [128]. Upon miRNAs binding with a MBR this inhibits them from binding and suppressing their target mRNAs, thereby, resulting in increased mRNA expression as a result of this mechanism [128]. The circRNA – miRNA interaction can also be achieved through AGO2 proteins located on the circRNA. AGO2 serves as the catalytic engine of the RNA-induced silencing complex (RISC) and plays an important role in sRNAs guided gene silencing processes [191]. This additional method of circRNA – miRNA interaction is observed in *circBIRC6* which interacts with miR-34a and miR-145 through AGO2 located on the circRNA [192].

miRNAs are the most studied type of ncRNA in EH and have previously been described as master gene regulators since they can regulate downstream gene expression by binding to the 3′ UTR of a mRNA [193]. However, since circRNAs serve as a regulator of miRNAs, the question can be asked whether miRNAs that have been previously identified to play a role in EH development and BP regulation are controlled by a higher mechanism; in this case being circRNAs? Numerous studies have explored the possibility for circRNAs to function as

miRNA inhibitors in a HT phenotype, however, a direct interaction between the two has yet to be determined in any of these studies (Refer Tables 1.3 and 3.1).Several methodologies can be adopted to investigate the relationship between circRNAs and miRNAs, the most prevalent one in literature is utilising luciferase assays to identify direct interactions between a circRNA of interest and a miRNA predicted to interact with it. This methodology is advantageous for targeting singular interactions of interest; however, it does not provide a wholistic view of the miRNAs that might be targeted by a specific circRNA. Utilising sRNA sequencing in conjunction with either overexpression or knockdown methodologies would allow us a more comprehensive the complete impact an individual circRNA has on the miRNA profile. In this chapter of my thesis, I investigate the potential miRNA interactions of our most highly expressed circRNAs from chapter 3 *circZNF91, circRP11-298P3.4* and *circGRB10* through siRNA knockdown. In this chapter I hypothesized that siRNA knockdown of kidney specific circRNAs will result in differentially expressed miRNAs which could then serve as candidates for further investigation in EH pathology.

4.1 Methods

4.1.1 Cell culture

The HEK293 cell line were used throughout this chapter of my thesis. Cell culture in this chapter was conducted as per Chapter 2 (Section 2.5). Cells were grown for use in the remaining methodologies in this chapter.

4.1.2 siRNA design and transfection

siRNA design and transfection into HEK293 cells is outlined in Chapter 2 (Section 2.6). The sequences for both the siRNA and associated scramble are outlined in Table 4.1.

Table 4.1: siRNA and associated scramble sequences

Circular RNA	*siRNA sequence*	*Scramble sequence*
circRP11-298P3.4	AACAGAGGAGAGAAAGAGTTT	GAAGGGAAAGAGAACGTATTA
circZNF91	ATGGAAAGGTATATGTCCTCA	GAGTCCAATAATCGGATGTTA
circGRB10	CAAAGCAGAGGATGATGTGGA	GCGAAATTAGGGCGATGAGAA

4.1.3 RNA extraction

Following successful knockdown of circRNA expression the total RNA was extracted using mirVana^{TM} RNA extraction kit as per Chapter 2, section 2.10.

4.1.4 RNase R treatment and circRNA cDNA synthesis

Treatment of total RNA with RNase R and cDNA synthesis was conducted as previously described in Chapter 2, section 2.1.

4.1.5 Quantification of circRNA expression using qRT-PCR

Expression of circRNAs was measured by quantitative PCR as described previously in Chapter 2, section 2.2. Primer sequences for *circZNF91*, *circRP11-298P3.4* and *circGRB10* are outlined in Table 3.2 above.

4.1.6 Linear RNA cDNA synthesis and qPCR

Post RNA extraction cDNA synthesis of total RNA and qPCR utilising this newly created cDNA was conducted as explained in Chapter 2 (Section 2.7). The primers utilised in this experiment are outlined in Table 4.2 below.

Table 4.2: Linear isoform RT-PCR primer sequences

Gene	*Primer Sequences*	*Amplicon Length (base pairs)*
RP11-298P3.4	5'-GGAGGGACGACTGGAGTG-3' 5'-ATGACTGACCAAAGTCGCCA-3'	96
ZNF91	5'-GGACACTGCACAGCAGAATTT-3' 5'-GAGGACATATACCCAGGAAGGC-3'	80
GRB10	5'- GAACAGATGGTTACTTGGTGCC-3' 5'-GGTGTCTGGGTTCCTGCAAA-3'	70
GAPDH	5'-AAGCCTGCCGGTGACTAAC-3' 5'-GCCCAATACGACCAAATCAGAGA-3'	148

4.1.7 Small RNA library prep

Total RNA from *circRP11-298P3.4*, *circZNF91* and *circGRB10* siRNA or associated scramble treated cells (n=3 each) were submitted to the Australian Genome Research Facility (AGRF) for small RNA (sRNA) sequencing. Libraries were prepared using NEBNext® Small RNA library Prep Set for Illumina® (New England Biolabs) and sequenced on the NovaSeq SP Lane, 100 cycles.

4.1.8 Small RNA sequencing analysis

miRNA single-end 50bp Illumina reads were aligned and quantified with Oasis 2.0, an online software package specialised for small RNA-sequencing data including trimming of the adapter sequence from Fastq files, read filtering (15–32 nt) and removal of low abundance reads (< 5 reads). Remaining reads were aligned using the human genome hg38 as reference and Oasis-DB [194], a database containing transcript information of miRNAs and other sRNA types (snRNA, snoRNA, rRNA, piRNAs) derived from miRBase, piRNAbank, Ensembl, sRNA families and predicted novel miRNAs.

Differential expression analysis was performed in the R statistical programming environment (version 4.0.3) using EdgeR [195] (version 3.32.1), which applied a normalisation for library size and trimmed mean of M values (TMM) normalisation where dispersion parameters for each gene are estimated with the Cox-Reid common dispersion method and employed in a negative binomial generalized linear model for each gene. Accounting for gene dispersion ensures that expression differences that are consistent between replicates are more highly weighted than those that are not to ensure differential expression is not driven by outliers. P-values were adjusted for multiple testing using the Benjamini-Hochberg correction with an FDR q-value <0.05 cut-off.

4.2 Results

4.2.1 Successful knockdown of circRP11-298P3.4, circZNF91 and circGRB10 did not impact the linear isoform expression

Due to the competing mechanisms involved in circRNA biogenesis there was a possibility that the siRNAs designed to knockdown the expression of the circRNA could have potentially also impact the expression of the linear isoform. For circRNA expression the siRNA for *circRP11-298P3* (Figure 4.1 C) caused an approximate 70% reduction in expression whilst the siRNAs for *circZNF91 and circGRB10* (Figure 4.1 A & E) caused an approximate 80% reduction in expression compared to the scramble control demonstrating efficient knockdown of our circRNAs of interest. In contrast, the mRNA expression of *RP11-298P3.4, ZNF91* and *GRB10* (Figure 4.1 B, D & F) displayed no significant difference in the siRNA treated groups compared to the scramble controls confirming that the siRNA treatment targets the circRNA specifically.

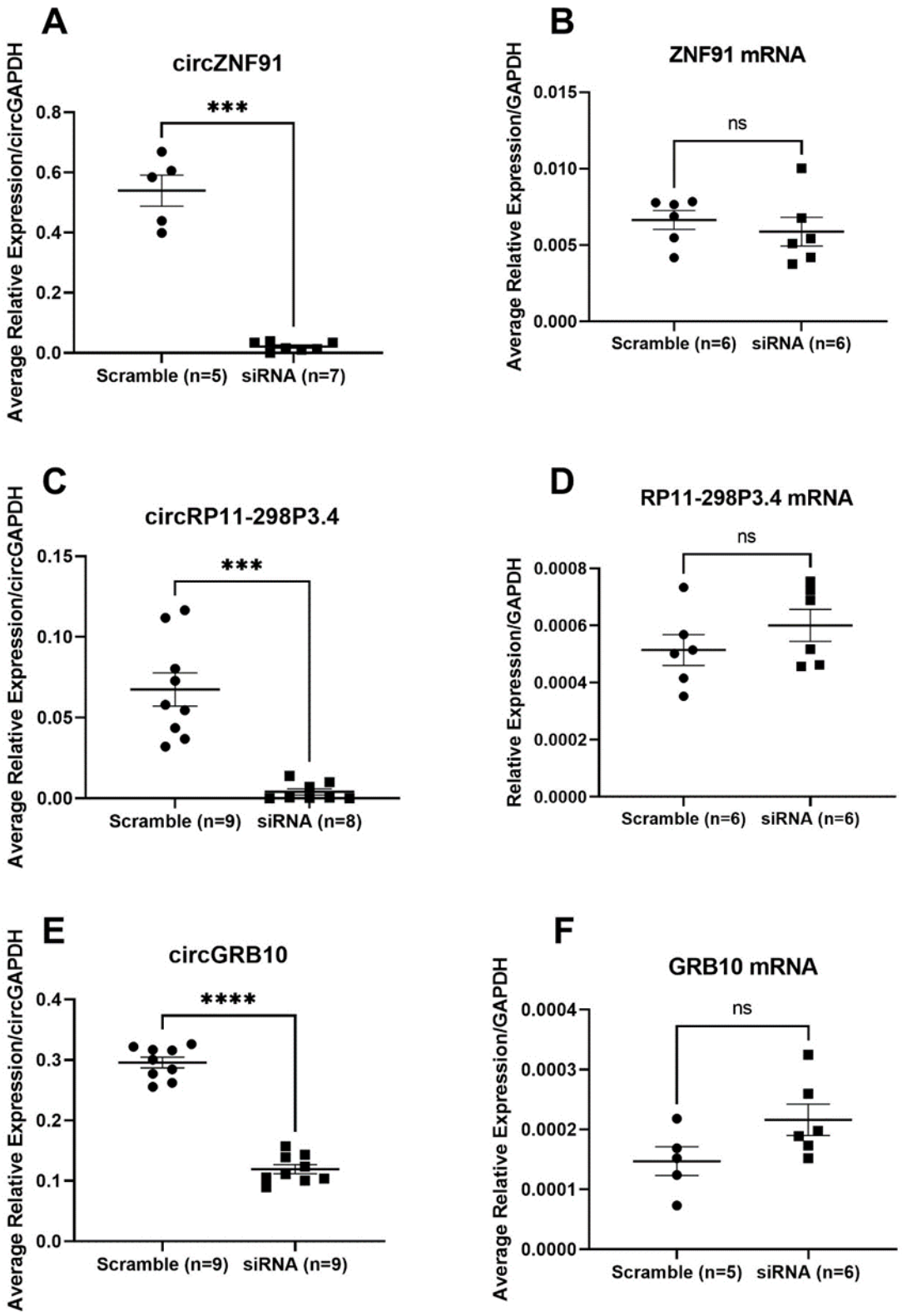

Figure 4.1: Knockdown confirmation of circZNF91, circRP11-298P3.4, circGR10 and corresponding mRNA. A) circZNF91. B) ZNF91 mRNA. C) circRP11-298P3.4. D) RP11298P3.4 mRNA. E) circGRB10. F) GRB10 mRNA. Error bar =SEM, *** P<0.001, **** P<0.0001, NS- Not significant.

4.2.2 Knockdown of *circRP11-298P3.4* resulted in differentially expressed miRNAs

To determine if *circRP11-298P3.4* potentially functions as a miRNA sponge, we reduced its expression via siRNA methodology and undertook sRNA sequencing. This sequencing identified 109 differentially expressed miRNAs (FDR <0.05) with 72 being downregulated and 37 being upregulated when the siRNA treated group was compared to the scramble control (see Table 4.3 below for top 50). Figure 4.2 demonstrates the sample-by-gene differences for the top 50 differentially expressed miRNAs which used unsupervised clustering thus separating the samples by groups based on their differences in differential miRNA expression between them.

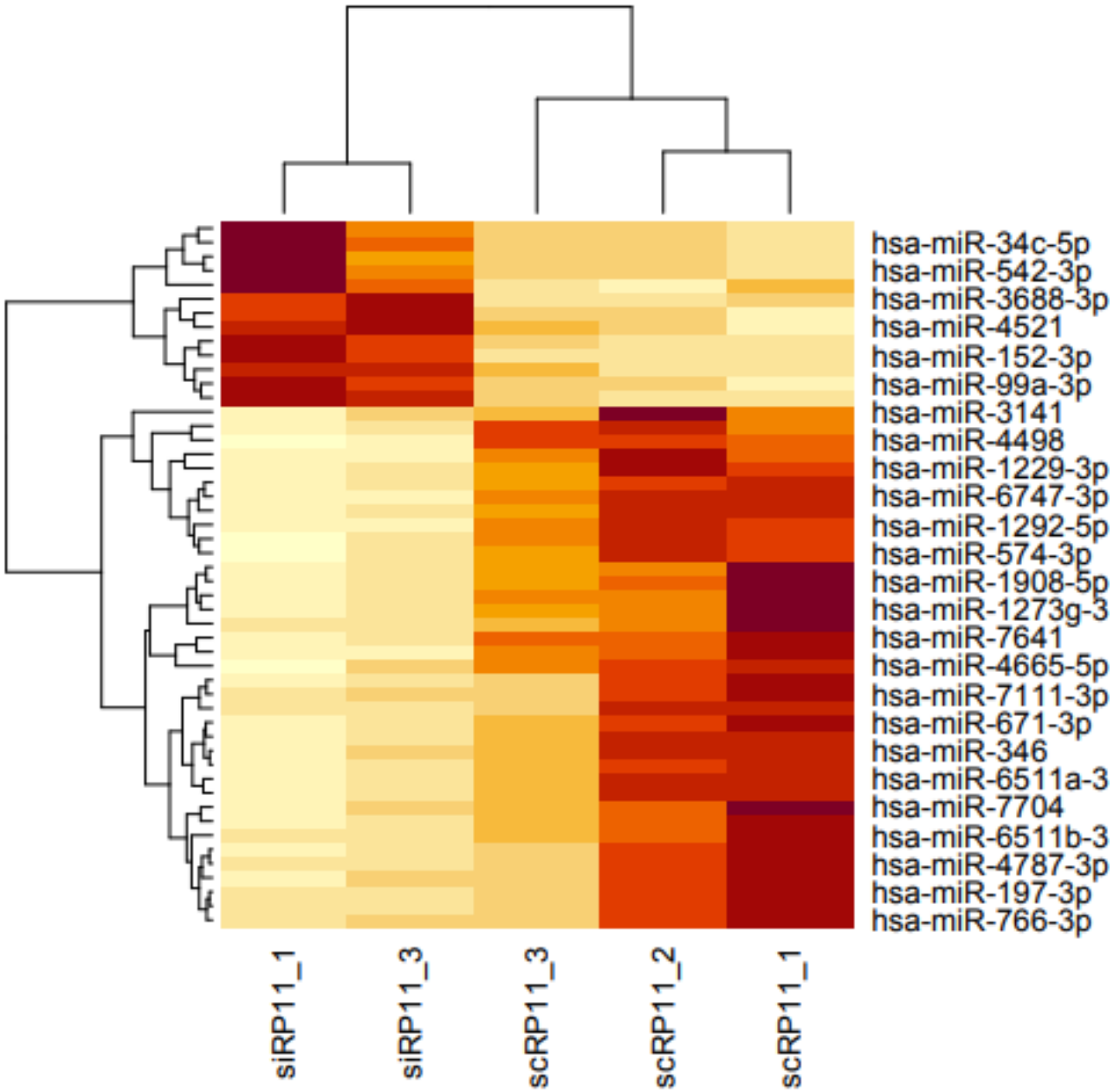

Figure 4.2: Top 50 differentially expressed miRNA heatmap for circRP11-298P3.4 knockdown. *Darker couples represent increased expression whilst lighter colours represent decreased expression*

Table 4.3 Top 50 differentially expressed miRNAs as result of *circRP11-298P3.4* knockdown

miRNA	*LogFC*	*LogCPM*	*FDR*	*Nominal P-Value*
hsa-miR-7641	-1.93722	9.11309	1.67E-09	1.77E-12
hsa-miR-34c-5p	1.309093	7.870263	6.87E-05	1.45E-07
hsa-miR-328-3p	-1.6566	9.796591	8.74E-05	2.77E-07
hsa-miR-4488	-1.59008	4.922766	9.62E-05	4.06E-07
hsa-miR-5585-3p	-1.28284	8.298376	0.00012	7.58E-07
hsa-miR-124-5p	1.295086	5.452996	0.000214	1.58E-06
hsa-miR-1908-5p	-1.78894	3.896672	0.000219	1.84E-06
hsa-miR-615-3p	-1.38108	9.848654	0.00024	2.28E-06
hsa-miR-760	-1.2898	7.39872	0.000283	2.99E-06
hsa-miR-7704	-1.33352	6.64823	0.000692	8.03E-06
hsa-miR-542-3p	1.144322	7.693372	0.000773	1.05E-05
hsa-miR-16-1-3p	1.192568	5.41154	0.000849	1.41E-05
hsa-miR-210-5p	-1.37863	4.721886	0.000849	1.52E-05
hsa-miR-1292-5p	-1.1263	5.876792	0.000881	1.67E-05
hsa-miR-671-3p	-1.1735	8.541244	0.001014	2.03E-05
hsa-miR-34a-5p	1.034448	11.03003	0.001343	2.83E-05
hsa-miR-1273g-3p	-1.12644	6.162219	0.001804	4.00E-05
hsa-miR-1306-5p	-1.20734	7.136994	0.002272	5.53E-05
hsa-miR-6511a-3p	-1.38204	4.375249	0.002272	5.66E-05
hsa-miR-3687	-1.5833	3.282147	0.002272	5.75E-05
hsa-miR-3195	-1.36946	4.750624	0.002483	6.55E-05
hsa-miR-1910-5p	-1.41108	3.980803	0.002683	7.55E-05
hsa-miR-4787-3p	-1.14242	6.739736	0.002683	7.87E-05
hsa-miR-152-3p	0.955818	10.21072	0.002683	8.20E-05
hsa-miR-1249-3p	-1.34623	5.404761	0.002683	8.21E-05
hsa-miR-3615	-1.23422	9.383466	0.002715	8.59E-05
hsa-miR-1229-3p	-1.44193	3.68174	0.002842	9.29E-05
hsa-miR-877-3p	-1.25843	6.751995	0.002917	9.85E-05
hsa-miR-935	-1.03536	7.99208	0.003413	0.000118794
hsa-miR-6511b-3p	-1.23194	4.789898	0.004229	0.000155251
hsa-miR-4492	-1.66166	2.70055	0.004379	0.00017005
hsa-miR-6089	-0.94729	6.229067	0.004379	0.000172868
hsa-miR-5095	-1.36876	3.497858	0.004379	0.000175513
hsa-miR-99a-3p	0.979003	5.218055	0.004801	0.000197497
hsa-miR-4521	0.925523	12.80113	0.004852	0.000204716
hsa-miR-4665-5p	-1.86318	2.488848	0.005224	0.000225929
hsa-miR-766-3p	-1.13059	7.419515	0.005315	0.000235494
hsa-miR-3688-3p	1.852507	1.53619	0.006713	0.000311576
hsa-miR-34a-3p	1.131586	3.789628	0.006858	0.00032553
hsa-miR-101-3p	0.941265	12.47416	0.007123	0.000345632
hsa-miR-346	-0.9574	6.632135	0.007632	0.000378395
hsa-miR-7111-3p	-1.5759	3.285436	0.009127	0.000471774
hsa-miR-424-5p	0.846389	6.769139	0.009195	0.000488203
hsa-miR-574-3p	-0.88214	7.426854	0.009195	0.000494695
hsa-miR-106b-5p	0.845522	11.12664	0.009279	0.000517406
hsa-miR-197-3p	-1.0455	11.01068	0.009279	0.000518758
hsa-miR-3141	-1.33651	4.154182	0.010198	0.000580915
hsa-miR-6747-3p	-1.05114	4.280301	0.010726	0.000622289
hsa-miR-4498	-2.6111	0.937743	0.010816	0.000638931
hsa-miR-6894-5p	-2.90087	0.740588	0.012369	0.000743679

4.2.3 Knockdown of *circZNF91* did not alter the miRNA expression

To elucidate *circZNF91's* ability to function as a miRNA sponge, we reduced the expression of both circRNAs of interest using siRNA methodology. Successful knockdown of *circZNF91* however did not induce a significant decrease in miRNA expression in the siRNA treated groups when compared to scramble control (FDR >0.05) (Figure 4.3 and Table 4.4).

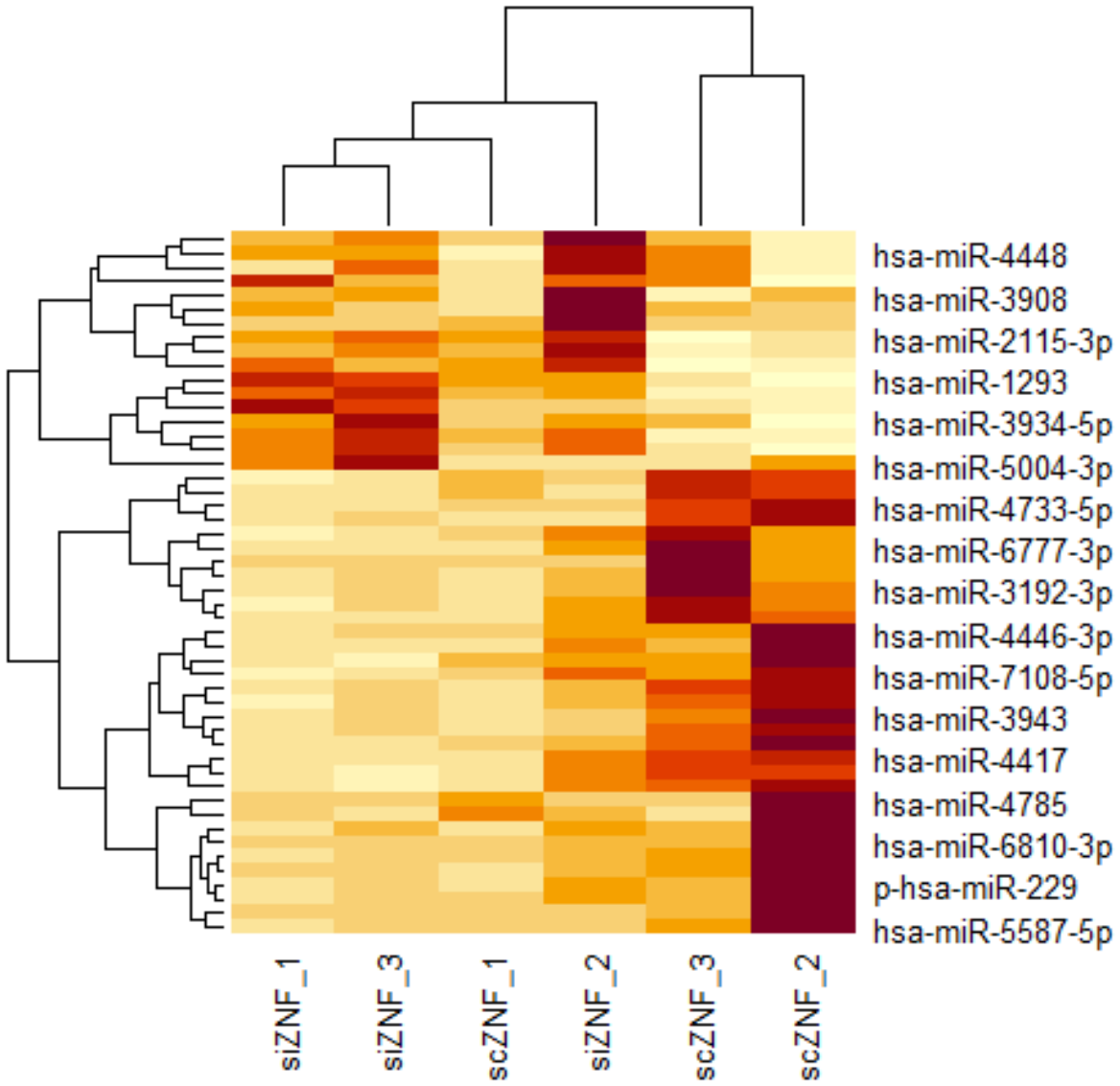

Figure 4.3: Top 50 miRNA heatmap for circZNF91 knockdown. *Darker couples represent increased expression whilst lighter colours represent decreased expression*

Table 4.4 Top 50 miRNAs from *circZNF91* knockdown

miRNA	*LogFC*	*LogCPM*	*FDR*	*Nominal P-Value*
hsa-miR-5587-5p	-2.51167	2.249491	0.998537	0.010425171
hsa-miR-3648	-3.00923	1.687056	0.998537	0.016308153
hsa-miR-4767	-2.86693	1.716584	0.998537	0.019629407
hsa-miR-6793-3p	-2.44959	1.902139	0.998537	0.033454964
hsa-miR-3183	-1.8779	1.187753	0.998537	0.037071112
hsa-miR-1296-5p	-1.69168	10.97768	0.998537	0.04407769
hsa-miR-6810-3p	-2.38441	1.378503	0.998537	0.046938657
hsa-miR-6755-5p	1.807579	0.998986	0.998537	0.049566008
hsa-miR-6765-3p	-1.47648	3.386602	0.998537	0.055388404
hsa-miR-3943	-1.56456	2.977491	0.998537	0.068939336
hsa-miR-1273a	1.230372	4.568199	0.998537	0.07210231
hsa-miR-6861-3p	-1.83985	2.488653	0.998537	0.076938461
hsa-miR-5584-5p	1.854845	0.578648	0.998537	0.077528581
hsa-miR-3202	-1.93209	0.724709	0.998537	0.077626125
hsa-miR-6764-5p	1.368894	1.381089	0.998537	0.078949774
hsa-miR-4426	-1.79771	1.916568	0.998537	0.079685779
hsa-miR-451a	2.266113	1.866156	0.998537	0.08529338
hsa-miR-381-3p	-1.34087	1.672937	0.998537	0.099175382
hsa-miR-4785	-1.37809	1.706677	0.998537	0.102109844
hsa-miR-6840-5p	-1.75749	1.78149	0.998537	0.102875349
hsa-miR-2115-3p	1.368531	2.008459	0.998537	0.103543442
hsa-miR-4448	0.99259	9.447702	0.998537	0.104739167
p-hsa-miR-330	0.908976	11.80783	0.998537	0.110302449
p-hsa-miR-229	-1.65996	4.475859	0.998537	0.111604874
hsa-miR-665	1.296801	1.885121	0.998537	0.113417253
hsa-miR-6515-3p	-1.03035	3.111391	0.998537	0.114183345
hsa-miR-3164	1.288116	1.389663	0.998537	0.114366939
hsa-miR-3908	1.180235	1.996647	0.998537	0.126077352
hsa-miR-296-5p	-1.2294	9.195617	0.998537	0.129862729
hsa-miR-7854-3p	-1.19932	2.558428	0.998537	0.134917677
hsa-miR-4667-3p	-1.72923	0.736818	0.998537	0.137568509
hsa-miR-4743-5p	1.769769	0.363838	0.998537	0.14036484
hsa-miR-1293	1.030541	4.000507	0.998537	0.141264717
hsa-miR-4733-5p	-1.21352	1.404166	0.998537	0.143448011
hsa-miR-4423-5p	1.098926	2.029088	0.998537	0.145711374
hsa-miR-4446-3p	-1.1767	2.783918	0.998537	0.152715312
hsa-miR-6797-5p	-1.59974	1.349624	0.998537	0.15857263
hsa-miR-5004-3p	1.597751	0.832326	0.998537	0.161674134
hsa-miR-6859-3p	-1.25832	1.245017	0.998537	0.163074033
hsa-miR-4417	-1.37948	2.288135	0.998537	0.166845302
hsa-miR-3934-5p	1.005582	2.546762	0.998537	0.171005246
hsa-miR-127-3p	-0.97005	5.213182	0.998537	0.171468338
hsa-miR-7108-5p	-1.69655	1.311243	0.998537	0.172252386
hsa-miR-6515-5p	1.190982	1.465738	0.998537	0.177704795
hsa-miR-2277-3p	-1.17618	5.073269	0.998537	0.179320667
hsa-miR-6893-3p	-1.44176	1.01665	0.998537	0.179604149
hsa-miR-6777-3p	-1.28419	2.298556	0.998537	0.180159746
hsa-miR-3192-3p	-1.36773	1.003346	0.998537	0.182894521
hsa-miR-6735-3p	-1.27083	3.47649	0.998537	0.183335057
hsa-miR-6749-3p	-1.42632	2.326962	0.998537	0.184917484

4.2.4 Knockdown of *circGRB10* did not alter the miRNA expression

To elucidate *circGRB10's* ability to function as a miRNA sponge, we reduced the expression of both circRNAs of interest using siRNA methodology. Successful knockdown of *circGRB10* however did not induce a significant decrease in miRNA expression in the siRNA treated groups when compared to scramble control (FDR >0.05) (Figure 4.4 and Table 4.5).

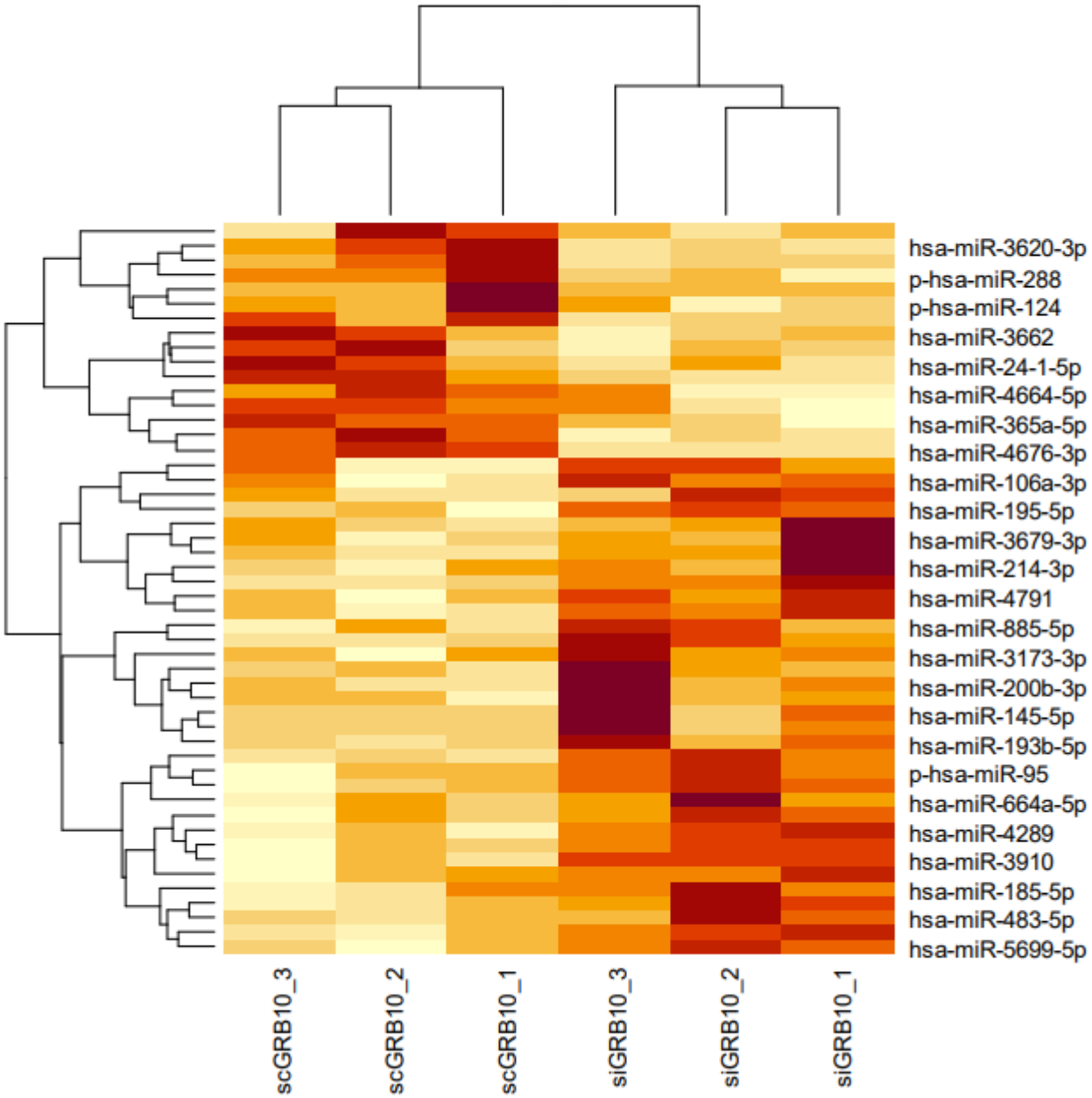

Figure 4.4: Top 50 miRNA heatmap for circGRB10 knockdown. *Darker couples represent increased expression whilst lighter colours represent decreased expression*

Table 4.5 Top 50 miRNAs from *circGRB10* knockdown

miRNA	*LogFC*	*LogCPM*	*FDR*	*Nominal P-Value*
hsa-miR-130a-5p	-1.988796164	0.879034	0.061797357	6.67E-05
hsa-miR-1-3p	0.863429085	9.017964	0.076570532	0.000165
hsa-miR-1273f	1.619218387	0.89079	0.12459089	0.000404
hsa-miR-143-3p	1.394020048	6.654453	0.281489086	0.001216
hsa-miR-3176	-2.682019131	6.818912	0.299507573	0.001617
hsa-miR-4484	0.593518561	4.377896	0.930237397	0.006815
hsa-miR-605-3p	0.568465043	3.894612	0.930237397	0.007032
p-hsa-miR-232	0.682049979	8.972789	0.936095464	0.008307
hsa-miR-3620-3p	-0.637722941	2.810124	0.936095464	0.009296
hsa-miR-106a-3p	1.102160522	1.391673	0.936095464	0.011309
hsa-miR-145-5p	1.251804968	2.393005	0.936095464	0.011521
hsa-miR-185-5p	0.519359136	11.06917	0.936095464	0.012131
hsa-miR-31-5p	0.37918609	9.957318	0.998957698	0.014286
hsa-miR-3910	0.773995975	1.555769	0.998957698	0.016065
p-hsa-miR-95	0.796613529	1.654742	0.998957698	0.019089
hsa-miR-152-5p	-0.523855176	4.011374	0.998957698	0.021489
hsa-miR-4791	0.491866103	9.803838	0.998957698	0.022317
hsa-miR-24-1-5p	-0.752385064	2.449342	0.998957698	0.023652
hsa-miR-193b-5p	0.542456956	3.408181	0.998957698	0.023802
hsa-miR-4676-3p	-0.562386774	2.343919	0.998957698	0.02633
hsa-miR-3192-5p	1.162224889	0.69332	0.998957698	0.026481
hsa-miR-885-5p	0.917979239	1.095519	0.998957698	0.027413
hsa-miR-4664-5p	-1.057536495	0.684243	0.998957698	0.027663
hsa-miR-5699-5p	0.478579839	3.903229	0.998957698	0.03105
hsa-miR-3664-3p	0.782157785	1.840047	0.998957698	0.031122
hsa-miR-3663-3p	0.916118566	0.883468	0.998957698	0.036105
hsa-miR-6812-3p	-1.092934134	0.330044	0.998957698	0.036283
hsa-miR-195-5p	0.415451628	6.890369	0.998957698	0.036599
hsa-miR-3662	-0.536145882	3.141561	0.998957698	0.038978
hsa-miR-3199	0.705310067	1.357661	0.998957698	0.041074
hsa-miR-4289	1.046101831	0.333875	0.998957698	0.042744
hsa-miR-200b-3p	0.498363203	5.714434	0.998957698	0.04367
hsa-miR-4517	0.459732751	3.089333	0.998957698	0.043756
hsa-miR-3691-5p	0.539521468	2.268395	0.998957698	0.043823
hsa-miR-664a-5p	0.544302603	3.565218	0.998957698	0.045181
hsa-miR-204-3p	-1.048681195	0.840827	0.998957698	0.050151
hsa-miR-365a-5p	-0.393049918	4.644644	0.998957698	0.051481
p-hsa-miR-124	-0.846263198	2.090605	0.998957698	0.055036
hsa-miR-214-3p	1.07874827	0.834161	0.998957698	0.058096
hsa-miR-548an	0.533541573	2.259252	0.998957698	0.058998
hsa-miR-3173-3p	0.983495723	0.503664	0.998957698	0.059132
p-hsa-miR-288	-0.398713796	3.899319	0.998957698	0.060885
hsa-miR-483-5p	0.624815388	1.590035	0.998957698	0.063522
hsa-miR-145-3p	0.963954163	0.802083	0.998957698	0.067545
hsa-miR-4699-3p	0.980832573	0.838538	0.998957698	0.069964
hsa-miR-664b-3p	-0.738677289	1.551722	0.998957698	0.071597
hsa-miR-3679-3p	1.037833007	0.366306	0.998957698	0.074717
hsa-miR-508-3p	-0.889507789	0.490951	0.998957698	0.076143
hsa-miR-141-3p	0.764304647	0.851067	0.998957698	0.077979
hsa-miR-3944-3p	-0.584541105	1.591348	0.998957698	0.079278

4.2.5 miRNAs of interest from *circRP11-298P3.4* knockdown

Due to circRNAs function as a miRNA 'sponge' this has garnered them much attention recently. Utilising siRNA knockdown of *circRP11-298P3.4* our aim was to either confirm the miRNAs of interest in Section 3.2.6 or to identify other miRNAs of interest. As outlined in section 4.2.2 we identified 109 differentially expressed miRNAs with the 37 upregulated miRNAs becoming our miRNAs of interest moving forward (Table 4.6). Table 4.6 provides a literature search of the 37 upregulated miRNAs to determine if they have a pre-established role in HT development or overall renal function. Further to this, in section 3.2.6 we identified miR-145 and miR-217 as miRNAs of interest in the TRANSLATE study however, neither of these presented a statistically significant difference (FDR >0.05) in the HEK293 cell line with reduced *circPR11-298P3.4*.

Table 4.6: Literature search to identify which differentially expressed miRNAs of interest (from circRP11-298P3.4 knockdown) have previously been identified to be associated with CVD and/or kidney function

miRNAs	*Association with CVD/Kidney*	*Reference*
hsa-miR-34c-5p	None to date	
hsa-miR-124-5p	Upregulation in circulating miR-124 identified smokers as susceptible to atherosclerosis	[196]
hsa-miR-542-3p	None to date	
hsa-miR-16-1-3p	None to date	
hsa-miR-34a-5p	Circulating levels were significantly related to systolic blood pressure	[197]
hsa-miR-152-3p	None to date	
hsa-miR-99a-3p	None to date	
hsa-miR-4521	None to date	
hsa-miR-3688-3p	None to date	
hsa-miR-34a-3p	None to date	
hsa-miR-101-3p	None to date	
hsa-miR-424-5p	Exerts protective effects against AAA progression	[198]
hsa-miR-106b-5p	miR-106b-5p antagonist reduced the severity of renal injury, decreased cell proliferation in renal tissues	[199]
hsa-miR-29c-3p	Dysregulation of miR-29c-3p plays a role in renal fibrosis	[200]
hsa-miR-205-5p	hsa-miR-205-5p may be notably related to hypertension-related renal cell carcinoma.	[201]
hsa-miR-15a-5p	miR-15a-5p/Smad7 pathway might be a potential target for atrial fibrillation therapy	[202]
hsa-miR-580-3p	None to date	
hsa-miR-30b-5p	Overexpressed miR-30b-5p is being used as a novel therapy for cardiac hypertrophy.	[203]

hsa-miR-151a-5p	Circulating levels of miR-151a-5p can add value on top of traditional risk markers in predicting future myocardial infarction in healthy individuals.	[204]
hsa-miR-651-5p	None to date	
hsa-miR-548ba	None to date	
hsa-miR-4458	miR-4458 in Ang II-treated H9c2 cells was ascribed to its transcriptional enhancement by NRF1, a transcription factor previously identified to be activated in early cardiac hypertrophy.	[205]
hsa-miR-30a-5p	miR-30a-5p inhibits hypoxia/reoxygenation-induced oxidative stress and apoptosis in HK-2 renal tubular epithelial cells by targeting glutamate dehydrogenase 1	[206]
hsa-miR-33a-3p	None to date	
hsa-miR-21-3p	MiR-21-3p mediates metabolism and cell fate alterations of tubular epithelial cells via manipulating AKT/CDK2-FOXO1 pathway	[207]
hsa-miR-381-3p	miR-381-3p targets HMGB1 to suppress the inflammation, oxidative stress, proliferation, and migration of high-glucose-induced VSMCs by targeting HMGB1.	[208]
hsa-miR-579-3p	Overexpression of GAS5 demonstrated protective effects against sepsis-induced renal injury via downregulating miR-579-3p and activating SIRT1/PGC-1α/Nrf2 pathway to inhibit cell pyroptosis.	[209]
hsa-miR-374a-3p	SNHG5 may regulate sepsis-induced AKI via the miR-374a-3p/TLR4/NF-κB pathway, therefore providing a new insight into the treatment of this disease.	[210]
hsa-miR-143-3p	The increase in miR-143-3p was associated with the reduction of BP and arterial stiffness and the increase in skin capillary density.	[211]
hsa-miR-146b-3p	miR-146b-3p represses the proliferation, migration, and phenotype switch of VSMCs induced by PDGF-BB via targeting PIK3CG. Therefore, miR-146b-3p/PIK3CG may be a potential target for the treatment of atherosclerosis.	[212]

hsa-miR-378c	miR-378c-Samd1 circuit participates in two key elements of atherosclerosis, VSMCs phenotypic transition and LDL oxidation.	[213]
hsa-miR-19b-3p	Macrophage-derived extracellular vesicles containing miR-19b-3p accelerate migration and promotion of VSMCs through targeting JAZF1, which promotes the development of atherosclerosis.	[214]
hsa-miR-4664-5p	None to date	
hsa-miR-138-5p	None to date	
hsa-miR-590-5p	miR-590-5p modulates myocardium hypertrophy and myocyte apoptosis in HF by downregulating RTN4.	[215]
hsa-miR-340-5p	Knockdown of XIST up-regulates miR-340-5p to relieve myocardial ischemia-reperfusion injury via inhibiting CCND1	[216]
hsa-miR-450b-5p	None to date	

4.3 Discussion

In chapter 3 *circRP11-298P3.4*, circZNF91 and *circGRB10* were identified in the kidneys of EH individuals as circRNAs of interest. To further investigate the role that the above mentioned circRNAs play in EH pathophysiology we investigated the potential for these circRNAs to function as a 'miRNA sponge' through siRNA knockdown and subsequent sRNA sequencing. Based on the mechanisms of circRNA interaction and function (Figure 4.5) with reduced circRNA expression the hypothesis was that we would view an altered miRNA expression profile with the majority being upregulated. As displayed in sections 4.2.2, 4.2.3 and 4.2.4 respectively, reduced *circZNF91* and *circGRB10* did not induce an altered miRNA expression profile, however *circRP11-298P3.4* knockdown resulted in numerous differentially expressed miRNAs.

Regarding *circZNF91* and *circGRB10*, the lack of differentially expressed miRNAs can be justified by two main theories. Firstly, as observed in Figures 4.3 and 4.4 there is a large amount of variability between samples in each experimental group (discussed in section 4.4 Limitations). Secondly, *circZNF91* and *circGRB10* may not function through 'miRNA sponging' but through alternative methods. CircRNAs can function through a variety of mechanisms such as interacting with miRNAs and RBPs, be translated into proteins and inadvertently compete with linear RNA transcription (As described in Section 1.6.2) [114]. All of these potential functions for circRNAs have the potential to alter the gene expression profile. This hypothesis was supported from the results observed in sections 4.2.2 and 4.2.3 where the miRNA profile was not impacted by reduced circRNA expression. Further experimentation is required to further confirm or disprove our hypothesis and can be achieved by gene

expression analysis, either through RNA sequencing or microarray to identify if reduced *circGRB10* and *circZNF91* induce an altered mRNA expression profile. If this does in fact result in an altered mRNA profile, then the question then becomes how does this occur if the miRNA expression profile is not altered?

Although the knockdown of *circGRB10* and *circZNF91* did not yield any significant results the differential expression of miRNAs after knockdown of *circRP11-298P3.4* suggests that some of these circRNAs may have regulatory functions. Reduced *circRP11-298P3.4* expression induced a notable change in the miRNA expression profile, I observed a total of 109 differentially expressed miRNAs from the sRNA sequencing that was conducted. Of these 110, as described in section 4.2.5 the 37 upregulated miRNAs become the miRNAs of interest based on the mechanisms of circRNA-miRNA interaction (Figure 4.5). CircRNAs are proposed to function as miRNA 'sponges,' based on the reduced circRNA expression induced by the siRNA knockdown our hypothesis was that the lack of freely available circRNAs would consequently result in an increased miRNA expression due to the absence of circRNAs 'sponging' them up and being more freely available. This process is as illustrated in Figure 4.5.

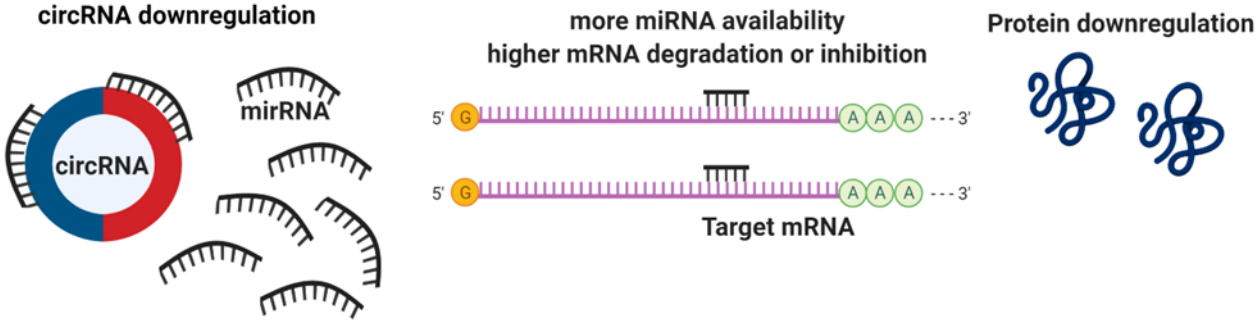

Figure 4.5: Proposed impact of siRNA knockdown of circRNAs. Decreased circRNA expression allows for more freely available miRNAs consequently resulting in decreased target mRNA expression

Several of the upregulated miRNAs from the *circRP11-298P3.4* knockdown have been previously illustrated to play a role in CVD establishment (Table 4.6). For example, in the absence of other cardiometabolic risk factors *miR-34a-5p* was significantly altered in hypertensive compared with normotensive adults [197]. Further to this, *miR-381-3p* and *miR-146b-3p* are both important in the function of VSMCs. *miR-381-3p* targets HMGB1 to suppress the inflammation, oxidative stress, proliferation, and migration of VSMCs by targeting HMGB1 and *miR-146b-3p* represses the proliferation, migration, and phenotype switch of VSMCs induced by PDGF-BB via targeting PIK3CG [208, 212].

Further to several of the miRNAs listed in Table 4.6 playing roles in CVD development several have also been shown to play a role in renal pathophysiology and function. For example, downregulation of *miR-29c-3p* and subsequent upregulation of its target FER tyrosine kinase can aggravate renal fibrosis and hence result in decreased renal function [200]. This is through the activation of extracellular matrix (ECM) genes such as *COL2A1* and *TPM1*. As outlined in section 1.2 reduced renal function can have a severe impact on BP regulation. In addition to *miR-29c-3p*, miR-*30-5p* displayed a significant difference. A study undertaken by He *et al*., (2020) demonstrated that *miR-30-5p* aids the kidney cell line HK-2 to prevent oxidative stress and inhibit apoptosis by negatively regulating *GLUD1* [206].

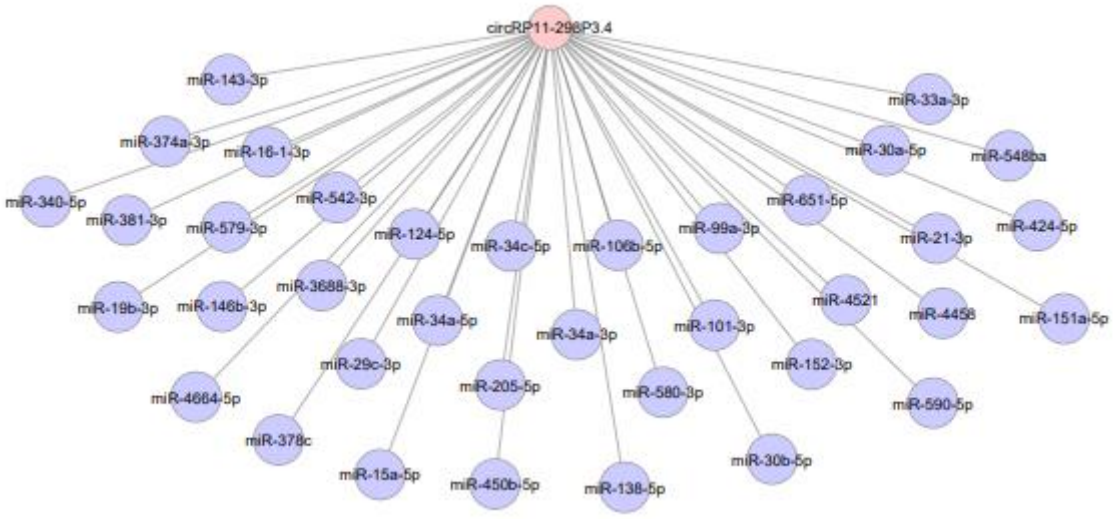

Figure 4.6: circRP11-298P3.4 predicted miRNA interactions post miRNA sequencing . *Image created using Cytoscape*

The following chapter of this thesis will follow on from the work conducted in this chapter. It will further investigate the impact of reduced circRNA expression on mRNA expression. This will complete my experimentation workflow by identifying mRNAs of interest which will allow for construction of circRNA-miRNA-mRNA networks of interest in BP regulation/EH development.

4.4 Limitations

The main limitation that exists were outlined in Figures 4.3 and 4.4 of this chapter. Variability between the samples used in the sRNA sequencing may have been a large contributor to the lack of differentially expressed miRNAs in the *circZNF91* and *circGRB10* siRNA treated groups. This variability could have arisen by various means, the most probable hypothesis is that siRNA transfection between each of the treated wells was not equal. This could be rectified by using a knockdown methodology that is considered 'stable', apart from siRNA knockdown the other methods that could be adopted are utilizing CRISPR-Cas13 [217]. The CRISPR–Cas13 system can be used to knock down circRNAs, without impacting the corresponding mRNAs by designing guide RNAs that target sequences spanning the BSJ.

One further consideration from these results is that none of the predicted circRNA-miRNA interactions from the *circRP11-298P3.4* knockdown have been confirmed and that the ones listed above are predictions. Further experimentation is required to validate the predicted circRNA -miRNA, this can be achieved through luciferase assays. The luciferase reporter assay is commonly used as a tool to study gene expression at the transcriptional level. It also can be utilized to investigate the regulation miRNA complementary to specific circRNA. The luciferase vector is constructed by inserting the specific circRNA sequence in the 3' UTR into the promoter-driven luciferase reported gene. Cell lines are then co-transfected with the luciferase reporter vector and the miRNA mimics to establish the characteristic of circRNA as miRNA sponges by comparing the luciferase activity with the negative controls. Similarly, mutant circRNA sequence could be cloned into luciferase vector to verify the detail binding sites interacted with miRNA.

Furthermore, identifying if the circRNAs of interest contain binding site for the RBP AGO2 could further enhance the circRNA-miRNA interaction hypothesis. This is due to miRNA's

proficiency for binding to AGO2 proteins located on circRNAs [191]. Measuring a circRNAs proficiency for AGO2 binding can be achieved through RNA immunoprecipitation assay (RIP). RIP assays study the physical association between individual proteins and RNA molecules in vivo. This utilises specific antibodies for the protein of interest to pull down the RBPs and target-RNA complexes.

Chapter 5

Reduced circRNA expression and its impact on the mRNA expression profile

Abstract

In Chapter 4 we were able to identify several miRNAs of interest for the *circRP11-298P3.4* model but were unsuccessful in identifying for the *circZNF91* or *circGRB10* model. The aim of this chapter was to investigate whether *circZNF91, circGRB10* and *circRP11-298P3.4* alter mRNA expression. For the *circRP11-298P3.4* model is the last step in the circRNA – miRNA – mRNA network. To investigate this, we first reduced the expression of these circRNAs utilizing siRNA transfection. HEK293 cells were transfected with either siRNAs specific for *circZNF91, circRP11-298P3.4* or *circGRB10.* HEK293 cells treated with a scramble sequence were considered the control groups. Confirmation of circRNA knockdown was achieved by qPCR. To investigate these circRNAs effect on downstream gene expression RNA sequencing was undertaken to compare the siRNA treated groups to the scramble treated groups. Our aim is to identify differentially expressed mRNAs that may have been impacted by the reduced circRNA expression. RNA sequencing for the *circRP11-298P3.4* model identified 32 differentially expressed genes (FDR <0.05) with 17 being down regulated and the remaining 15 upregulated. RNA sequencing for the *circZNF91* model identified 2288 differentially expressed genes (FDR <0.05) with 1642 downregulated and 646 up regulated. RNA sequencing for the *circGRB10* model identified 2907 differentially expressed genes (FDR <0.05) with 574 downregulated and 2333 up regulated. Subsequent pathway analysis utilising the list of differentially expressed genes was undertaken using GOrilla and Reactome databases. Several pathways were identified as significantly altered across each of our models with 11 for *circRP11-298P3.4*, 104 for *circZNF91* and lastly 171 for the *circGRB10* model. For the *circZNF91* and *circGRB10* models several genes had been identified to have a pre-established role in either renal function or BP regulation. However, how either of these circRNAs regulate gene expression is yet to be elucidated with further work required to understand the role they have as a gene regulator. For the *circRP11-298P3.4*

model several differentially expressed genes were identified as key regulators in cholesterol synthesis. The role of cholesterol in renal mediated HT is underexplored but dysregulation of cholesterol synthesis has been shown to impact on overall renal function. Further work is required to confirm the circRNA-miRNA-mRNA interactions concluded in this chapter and to fully elucidate the role these interactions have in cholesterol synthesis in the kidney.

5.0 Introduction

The role of genetics in HT development has been extensively researched with numerous GWAS identifying robust associations between genome loci and BP. The most comprehensive study, conducted in over one million individuals, identifies 901 gene loci that are associated with BP [17]. The same detailed research cannot be said for circRNAs involvement in renal mediated HT development with very little research being undertaken on the relationship between the two. In chapter 4, sRNA sequencing was utilised to identify miRNA targets of interest for *circRP11-298P3.4*, *circZNF91* and *circGRB10*. The *circZNF91* and *circGRB10* models did not display any differentially expressed miRNAs whilst the *circRP11-298P3.4* model did. To further understand the role of these three circRNAs in renal BP regulation/HT development, the next step in the investigative process is to understand the role they play in downstream gene expression.

Although the miRNA sponge function of circRNAs is the most favoured function, it is not the only proposed function that can impact downstream gene expression. Data from the previous chapter supported the notion that *circZNF91* and *circGRB10* did not lead to an altered miRNA expression profile. Outside of circRNAs function as a 'miRNA sponge' they can exert their effect on gene expression through interacting with proteins, being translated into protein and acting as competitors for linear RNA splicing [114]. If the mRNA expression profile is impacted, then the justification for this is more than likely through one of the above-mentioned mechanisms given that we show no evidence for *circZNF91's* and *circGRB10's* ability to function as a 'miRNA sponge'.

In chapter 4 *circRP11-298P3.4* model because we observed an affected miRNA expression profile. As a result, it is expected we will now observe a differentially expressed mRNA profile. Utilising the list of upregulated miRNAs in Chapter 4 and potential downregulated

mRNAs within this chapter our aim of this current study is to construct circRNA-miRNA-mRNA networks of interest and elucidate their role in BP regulation and HT development.

Based on the circRNA -miRNA -mRNA interaction network we expect that reduced circRNA expression would result in increased miRNA expression with subsequently downregulated mRNA expression. After documenting the altered miRNAs (chapter 4) the next step in the investigation process was to determine if the reduced circRNA expression brought about a change in the mRNA expression profile. This was tested using high throughput RNA sequencing. This will allow for further construction of a circRNA-miRNA-mRNA for the *circRP11-298P3.4* model and elucidate *circZNF91's* and *circGRB10's* impact on downstream gene expression.

5.1 Methods

5.1.1 Cell culture

HEK293 cell line was used throughout this chapter of my thesis. Cell culture in this chapter was conducted as per Chapter 2 (Section 2.5). Cells were grown for us in the remaining methodologies in this chapter.

5.1.2 siRNA design and transfection

siRNA design and subsequent transfection into HEK293 cells is outlined in Chapter 2 (Section 2.6). The sequences for both the siRNA and associated scramble are outlined in Chapter 4 (Table 4.1).

5.1.3 RNA extraction

Total RNA was extracted from HEK293 cells treated with si-circZNF91, si-circGRB10, si-circRP11-298P3.4 or their respective scramble control as per Chapter 2, section 2.7.

5.1.4 RNase R treatment and circRNA cDNA synthesis

Treatment of total RNA with RNase R and cDNA synthesis was conducted as previously described (Chapter 2, section 2.1).

5.1.5 Quantification of circRNA expression using qRT-PCR

Expression of *circZNF91*, *circRP11-298P3.4* and circGRB*10* was measured by quantitative PCR as described previously (Chapter 2, section 2.2). The primer sequences utilised are outlined in Table 3.2 above

5.1.6 Linear RNA cDNA synthesis and qPCR

Post RNA extraction cDNA synthesis of total RNA and qPCR utilising this newly created cDNA was conducted as illustrated in Chapter 2 (Section 2.8). The primer sequences of each respective primer are outlined in Table 4.2 above.

5.1.7 RNA Sequencing Library Preparation

Total RNA from siRNA and associated scramble treated samples (n=3 each) were submitted to the Australian Genome Research Facility (AGRF) for RNA sequencing. Libraries were constructed using Illumina's TruSeq stranded RNA sample preparation protocol and sequenced on the NovaSeq SP Lane, 100 cycles.

5.1.8 RNA Sequencing Analysis

The cleaned sequence reads were aligned against the *homo sapiens* genome (HG38). The STAR aligner software (v2.5.3a) was used to map reads to the genomic sequences. The counts of reads mapping to each known gene were summarised. The raw gene counts were used in the R statistical programming environment (version 4.0.3) using EdgeR [195] (version 3.30.3) to determine differentially expressed genes. EdgeR applies a trimmed mean of M values (TMM) normalisation where dispersion parameters for each gene are estimated with the Cox-Reid common dispersion method and employed in a negative binomial generalized linear model for each gene. Accounting for gene dispersion ensures that expression differences that are consistent between replicates are more highly weighted than those that are not to ensure expression is not driven by outliers. P-values were adjusted for multiple testing using the Benjamini-Hochberg correction with an FDR<0.05.

5.1.9 Construction of circRNA – miRNA – mRNA network

CircRNA – miRNA – mRNA networks were established from differentially expressed miRNAs identified from Chapter 4 and differentially expressed mRNAs identified from within this chapter. A similar methodology was adopted from section 3.1.9 to determine the miRNA-mRNA interactions of interest with miRTarBase software utilised to identify interactions between both the differentially expressed miRNAs and mRNAs. The final circRNA-miRNA-mRNA network was illustrated using Cytoscape V3.9.1 software.

5.1.10 Pathway Analysis

To determine how the differentially expressed genes affect cellular function, the differentially expressed genes with FDR < 0.05 were submitted for a pathway's enrichment analysis (www. reactome.com). This program evaluates the submitted list against every pathway from the Reactome database. A binomial test is used to calculate the probability shown for each result, and the p values are corrected for the multiple testing (Benjamini–Hochberg procedure).

Utilising the list of differentially expressed mRNAs generated from RNA sequencing pathway analysis was conducted on each of the circRNA knockdown models. Gene Ontology's GOrilla tool (http://cbl-gorilla.cs.technion.ac.il/#ref) was used for identifying and visualizing enriched GO terms in ranked lists of genes [218].

5.2 Results

5.2.1 Reduced circZNF91 expression resulted in an altered mRNA expression profile in the absence of differentially expressed miRNAs

In section 4.2.3 miRNA sequencing identified no differentially expressed miRNAs following *circZNF91* knockdown. To further investigate the function of *circZNF91* mRNA sequencing was undertaken to elucidate if downstream genes are affected by reduced expression in the absence of altered miRNA expression. mRNA sequencing identified 2288 differentially expressed genes in HEK293 cells with reduced *circZNF91* expression (FDR<0.05). Of these 2288 differentially expressed genes 646 were up-regulated and 1642 were down-regulated (Figure 5.1). Additional information of the top 50 differentially expressed genes are outlined in Figure 5.2 and Table 5.1

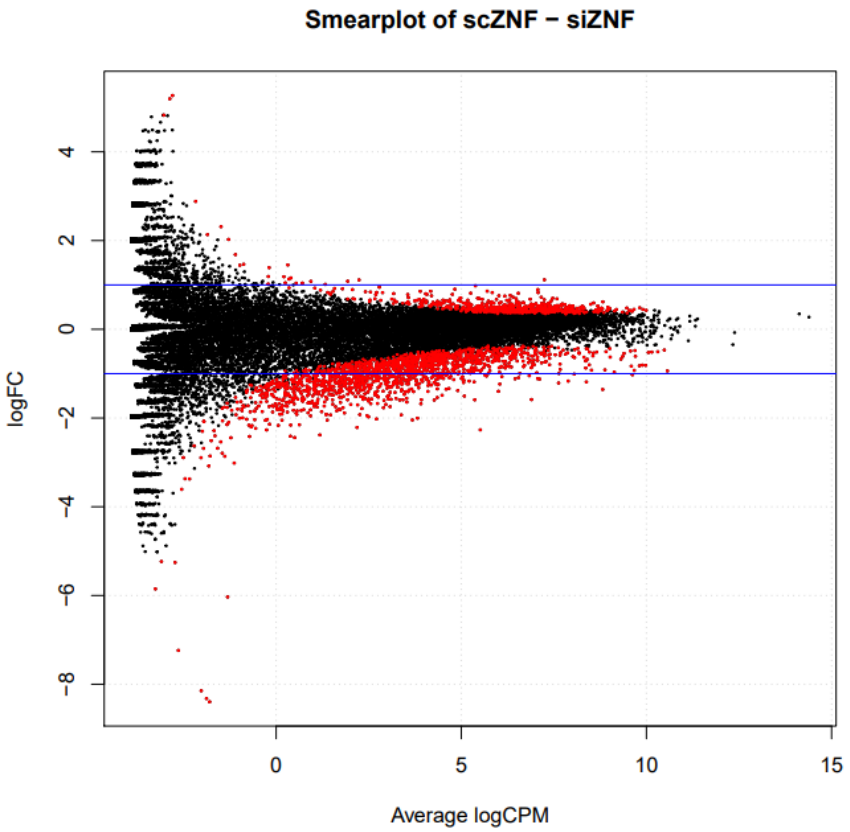

Figure 5.1: Smearplot of circZNF91 knockdown mRNA sequencing – *Identified 646 up-regulated and 1642 down-regulated. Red dots represent differentially expressed genes(FDR < 0.05) and black are those that are not (FDR > 0.05). scZNF = scramble treated, siZNF = siRNA treated*

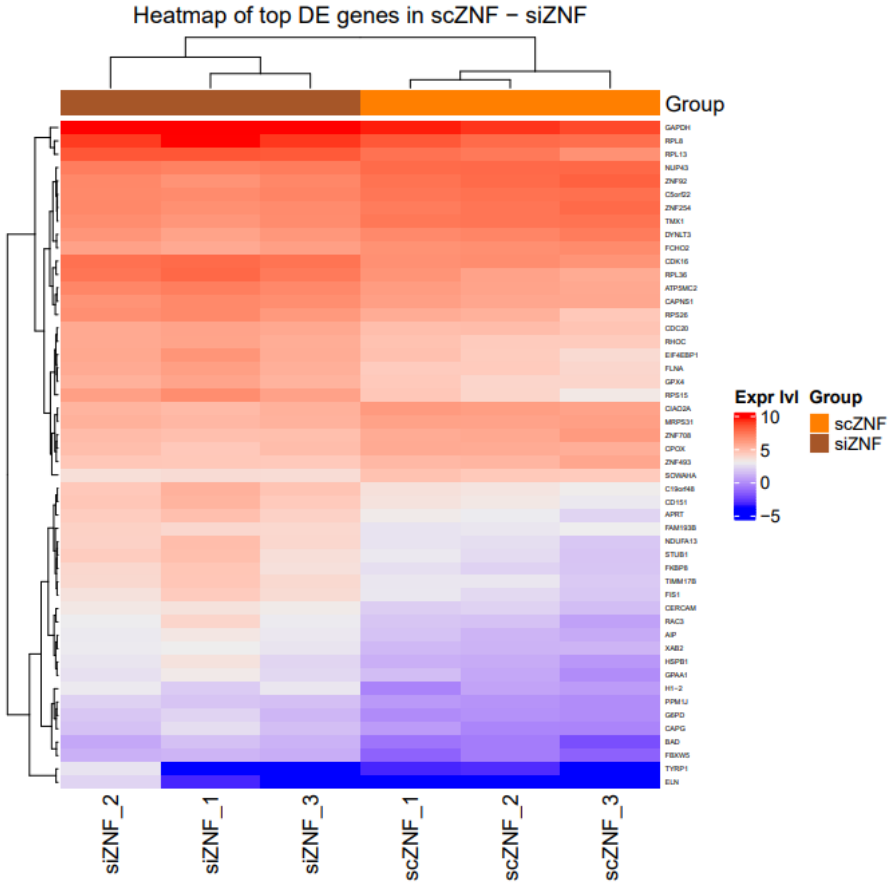

Figure 5.2: Top 50 differentially expressed genes heatmap for circZNF91 knockdown

Table 5.1 Top 50 Differentially expressed genes as result of circZNF91 knockdown

Gene Symbol	*Gene Full Name*	*Chr*	*Gene Start*	*Gene End*	*FDR*	*Expression Change*	*Gene Biotype*
ZNF92	Zinc Finger Protein 92	7	65373854	65401135	7.98E-06	Down	PC
H1-2	H1.2 Linker Histone, Cluster Member	6	26055739	26056469	4.92E-05	Up	PC
RPS15	Ribosomal Protein S15	19	1438395	1440494	4.92E-05	Up	PC
TMX1	Thioredoxin Related Transmembrane Protein 1	14	51240246	51257654	4.92E-05	Down	PC
CIAO2A	Cytosolic Iron-Sulphur Assembly Component 2A	15	64072564	64093837	4.98E-05	Down	PC
CPOX	Coproporphyrinogen Oxidase	3	98569836	98593683	0.00025	Down	PC
CDK16	Cyclin Dependent Kinase 16	X	47217880	47229996	0.00025	Up	PC
ZNF708	Zinc Finger Protein 708	19	21291160	21329425	0.00025	Down	PC
RPS26	Ribosomal Protein S26	12	56041917	56044696	0.000339	Up	PC
NDUFA13	NADH: Ubiquinone Oxidoreductase Subunit A1	19	19516224	19528197	0.000358	Up	PC
FBXW5	F-Box and WD Repeat Domain Containing 5	9	136940434	136944773	0.000358	Up	PC
RPL36	Ribosomal Protein L36	19	5690294	5691874	0.000358	Up	PC
DYNLT3	Dynein Light Chain Tctex-Type 3	X	37838835	37847570	0.000358	Down	PC
BAD	BCL2 Associated Agonist of Cell Death	11	64269827	64284703	0.000381	Up	PC
NUP43	Nucleoporin 43	6	149724314	149746528	0.000381	Down	PC
RAC3	Rac Family Small GTPase 3	17	80031677	82034203	0.000381	Up	PC
HSBP1	Heat Shock Protein Family B (Small) Member 1	16	83807977	83819736	0.00039	Up	PC
GPX4	Glutathione Peroxidase 4	19	1103993	1106778	0.000429	Up	PC
ZNF254	Zinc Finger Protein 254	19	24033415	24129967	0.000429	Down	PC

EIF4EBP1	Eukaryotic Translation Initiation Factor 4E Binding Protein 1	8	38030533	38060364	0.000429	Up	PC
CDC20	Cell Division Cycle 20	1	43358980	43363202	0.000429	Up	PC
G6PD	Glucose-6-Phosphate Dehydrogenase	X	154531389	154547568	0.000429	Up	PC
FLNA	Filamin A	X	154348530	154374633	0.000429	Up	PC
FKBP8	FKBP Prolyl Isomerase 8	19	18531762	18543572	0.000429	Up	PC
FCHO2	FCH And Mu Domain Containing Endocytic Adaptor 2	5	72956040	73090521	0.000429	Down	PC
C19orf48	Chromosome 19 Open Reading Frame 48	19	50797703	508047593	0.000429	Up	Pseudogene
TIMM17B	Translocase Of Inner Mitochondrial Membrane 17B	X	48893446	48898142	0.000429	Up	PC
STUB1	STIP1 Homology And U-Box Containing Protein 1	16	680409	682800	0.000453	Up	PC
CAPG	Capping Actin Protein, Gelsolin Like	2	85394752	85418466	0.000453	Up	PC
APRT	Adenine Phosphoribosyl transferase	16	88809338	88811927	0.000453	Up	PC
RPL13	Ribosomal Protein L13	16	89560656	89566828	0.000455	Up	PC
C5orf22	Chromosome 5 Open Reading Frame 22	5	31532287	31555053	0.000455	Down	Pseudogene
RHOC	Ras Homolog Family Member C	1	112701130	112707407	0.000455	Up	PC
RPL8	Ribosomal Protein L8	8	144789768	144792389	0.000455	Up	PC
FIS1	Fission, Mitochondrial 1	7	101239471	101245080	0.000455	Up	PC
GPAA1	Glycosylphosphatidylinositol Anchor Attachment 1	8	144082633	144086215	0.000455	Up	PC

AIP	Aryl Hydrocarbon Receptor Interacting Protein	11	67468178	67491102	0.000475	Up	PC
FAM193B	Family with Sequence Similarity 193 Member B	5	177519787	177554562	0.000505	Up	PC
ZNF493	Zinc Finger Protein 493	19	21397119	21427577	0.000505	Down	PC
ATP5MC2	ATP Synthase Membrane Subunit C Locus 2	12	53665165	53677545	0.000539	Up	PC
CERCAM	Cerebral Endothelial Cell Adhesion Molecule	9	128405993	128437350	0.000539	Up	PC
SOWAHA	Sosondowah Ankyrin Repeat Domain Family Member A	5	132813302	132816786	0.000567676	Down	PC
CD151	CD151 Molecule (Raph Blood Group)	11	832951	838834	0.000640335	Up	PC
CAPNS1	Calpain Small Subunit 1	19	36140065	36150352	0.000644321	Up	PC
MRPS31	Mitochondrial Ribosomal Protein S31	13	40729127	40771206	0.00065016	Down	PC
XAB2	XPA Binding Protein 2	19	7619524	7629544	0.000651998	Up	PC
PPM1J	Protein Phosphatase, Mg2+/Mn2+ Dependent 1J	1	112709997	112715331	0.000709143	Up	PC
UBC	Ubiquitin C	12	124911645	124914649	0.000727893	Up	PC
LIN52	Lin-52 DREAM MuvB Core Complex Component	14	74084796	74201235	0.000727893	Down	PC
UBE2W	Ubiquitin-conjugating enzyme E2 W	8	73780095	73878861	0.00072929	Down	PC

Position is from GRCh38. Abbreviations: Chr, chromosome; PC, protein coding; ncRNA, non-coding RNA; HPA, human protein atlas

5.2.2 Reduced circGRB10 expression resulted in an altered mRNA expression profile in the absence of differentially expressed miRNAs

In section 4.2.3 miRNA sequencing identified no differentially expressed miRNAs because of *circGRB10* knockdown. To further investigate the function of *circGRB10* mRNA sequencing was undertaken to elucidate if downstream genes are affected by reduced expression in the absence of altered miRNA expression. mRNA sequencing identified 2907 differentially expressed genes in HEK293 cells with reduced *circGRB10* expression (FDR<0.05). Of the 2907 differentially expressed genes 2333 were upregulated and 574 were downregulated (Figure 5.3). Additional information of the top 50 differentially expressed genes are outlined in Figure 5.4 and Table 5.2.

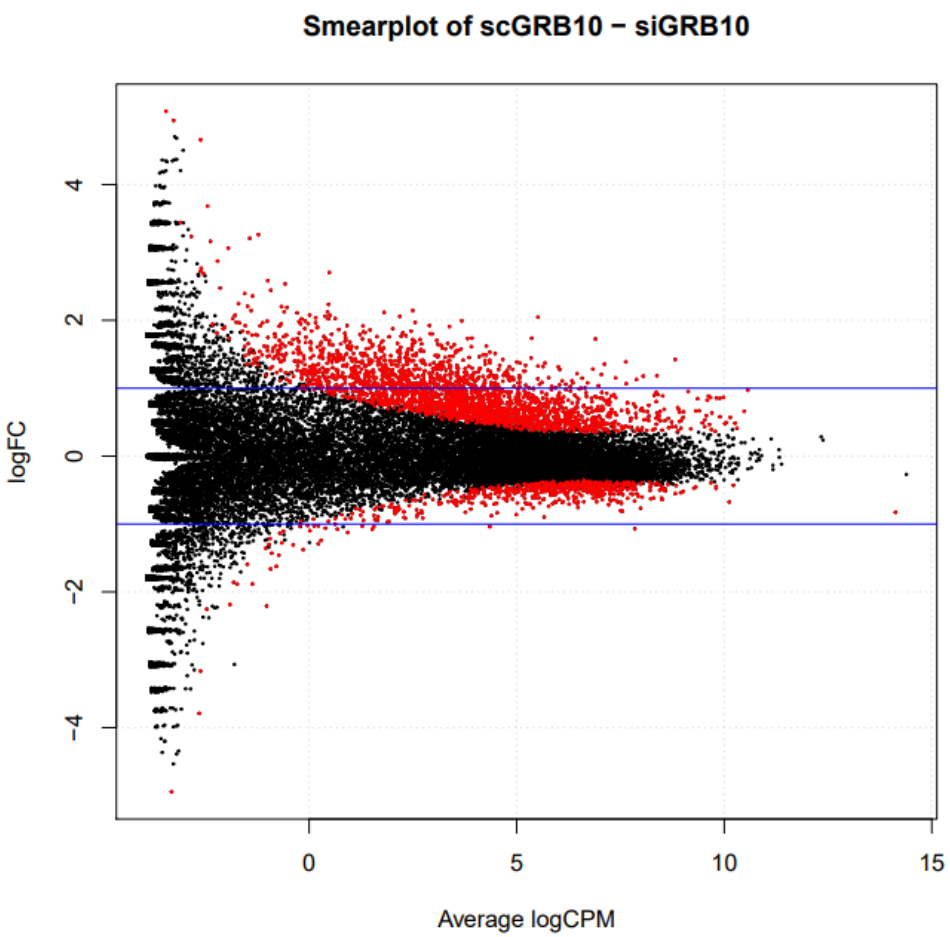

Figure 5.3: Smearplot of circGRB10 knockdown mRNA sequencing – *Identified 2333 up-regulated and 574 down-regulated. Red dots represent differentially expressed genes(FDR < 0.05) and black are those that are not (FDR > 0.05). scGRB10 = scramble treated, siGRB10 = siRNA treated*

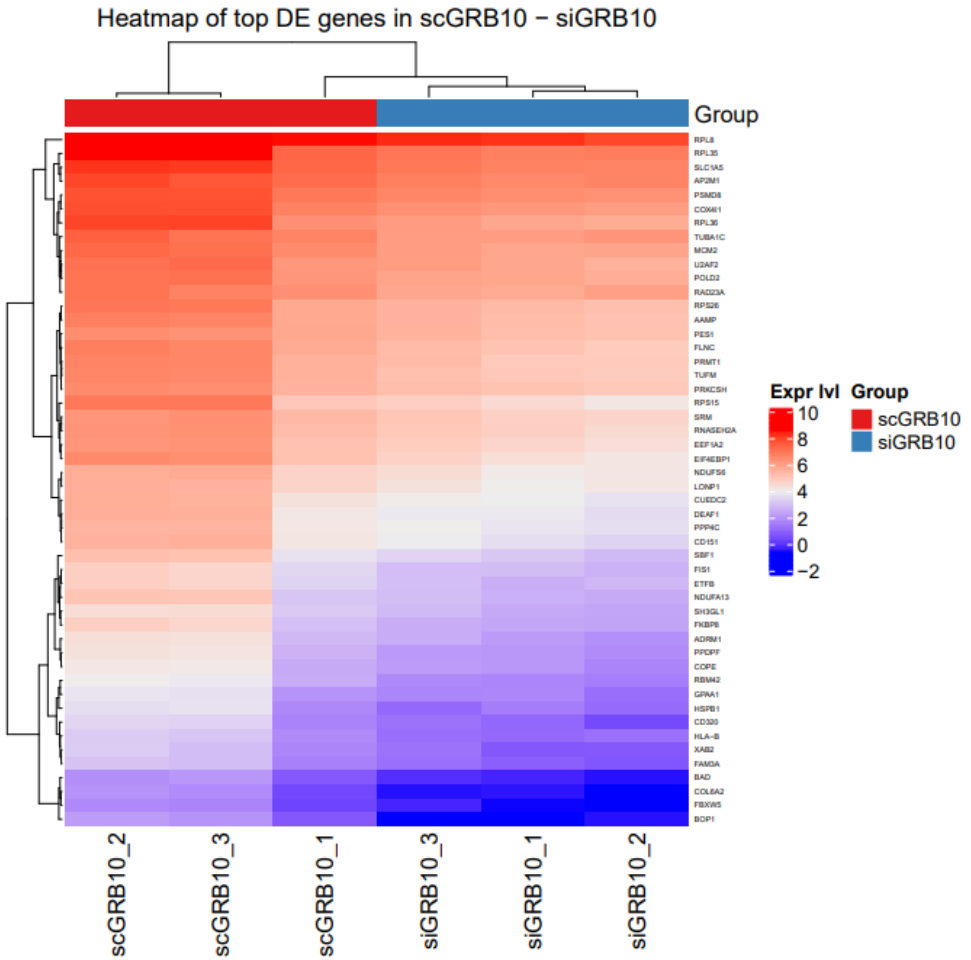

Figure 5.4: Top 50 differentially expressed genes heatmap for circGRB10 knockdown

Table 5.2 Top 50 Differentially expressed genes as result of circGRB10 knockdown

Gene Symbol	*Gene Full Name*	*Chr*	*Gene Start*	*Gene End*	*FDR*	*Expression Change*	*Gene Biotype*
RPL36	Ribosomal Protein L36	19	5690294	5691874	0.00028	Up	PC
RBM42	RNA Binding Motif Protein 42	19	35629035	35637684	0.00028	Up	PC
EIF4EBP1	Eukaryotic Translation Initiation Factor 4E Binding Protein 1	8	38030533	38060364	0.00028	Up	PC
COL6A2	Collagen Type VI Alpha 2 Chain	21	46098070	46132848	0.00028	Up	PC
RPS15	Ribosomal Protein S15	19	1438395	1440494	0.00028	Up	PC
BOP1	BOP1 Ribosomal Biogenesis Factor	8	144262044	144291437	0.00028	Up	PC
TUFM	Tu Translation Elongation Factor, Mitochondrial	16	28842410	28846347	0.00028	Up	PC
XAB2	XPA Binding Protein 2	19	7619524	7629544	0.00028	Up	PC
PRKCSH	Protein Kinase C Substrate 80K-H	19	11435289	11450967	0.00028	Up	PC
COX4I1	Cytochrome C Oxidase Subunit 4I1	16	85799694	85807067	0.00028	Up	PC
NDUFA13	NADH: Ubiquinone Oxidoreductase Subunit A13	19	19516224	19528197	0.00028	Up	PC
SRM	Spermidine Synthase	1	11054588	11060052	0.00028	Up	PC
MCM2	Minichromosome Maintenance Complex Component 2	3	127598410	127622435	0.00028	Up	PC
COPE	COPI Coat Complex Subunit Epsilon	19	18899513	18919386	0.00028	Up	PC
FLNC	Filamin C	7	128830405	128859271	0.00028	Up	PC
RAD23A	RAD23 Homolog A, Nucleotide Excision Repair Protein	19	12945845	12953641	0.000319	Up	PC
RPL8	Ribosomal Protein L8	8	144789768	144792389	0.000319	Up	PC

TUBA1C	Tubulin Alpha 1c	12	49188736	49274600	0.000319	Up	PC
RNASEH2A	Ribonuclease H2 Subunit A	19	12806583	12813639	0.000319	Up	PC
AP2M1	Adaptor Related Protein Complex 2 Subunit Mu 1	3	184174854	184184090	0.000319	Up	PC
U2AF2	U2 Small Nuclear RNA Auxiliary Factor 2	19	55654131	55674715	0.000319	Up	PC
FIS1	Fission, Mitochondrial 1	7	101239471	101245080	0.000319	Up	PC
SBF1	SET Binding Factor 1	22	50444999	50475034	0.000319	Up	PC
EEF1A2	Eukaryotic Translation Elongation Factor 1 Alpha 2	20	63488013	63499082	0.000319	Up	PC
FBXW5	F-Box and WD Repeat Domain Containing 5	9	136940434	136944773	0.000319	Up	PC
FKBP8	FKBP Prolyl Isomerase 8	19	18531762	18543572	0.000319	Up	PC
PPDPF	Pancreatic Progenitor Cell Differentiation and Proliferation Factor	20	63520765	63522206	0.000319	Up	PC
BAD	BCL2 Associated Agonist of Cell Death	11	62269827	64284703	0.000319	Up	PC
SLC1A5	Solute Carrier Family 1 Member 5	19	46774882	46788593	0.000319	Up	PC
NDUFS6	NADH: Ubiquinone Oxidoreductase Subunit S6	5	1801406	1816047	0.000319	Up	PC
POLD2	DNA Polymerase Delta 2, Accessory Subunit	7	44114679	44123667	0.000319	Up	PC
HSBP1	Heat Shock Protein Family B (Small) Member 1	16	83807977	83819736	0.000319	Up	PC
RPS26	Ribosomal Protein S26	12	56041917	56044696	0.000319	Up	PC
ETFB	Electron Transfer Flavoprotein Subunit Beta	19	51345154	51366387	0.000324	Up	PC
CUEDC2	CUE Domain Containing 2	10	102423248	102432573	0.000324	Up	PC
CD320	CD320 Molecule	19	8302126	8308357	0.000324	Up	PC
HLA-B	Major Histocompatibility Complex, Class I, B	6	31353874	31357178	0.000324	Up	PC

SH3GL1	SH3 Domain Containing GRB2 Like 1, Endophilin A2	19	4360368	4400546	0.000324	Up	PC
LONP1	Lon Peptidase 1, Mitochondrial	19	5691833	5720451	0.000324	Up	PC
CD151	CD151 Molecule (Raph Blood Group)	11	832951	838834	0.000324	Up	PC
RPL35	Ribosomal Protein L35	9	124857882	124861956	0.000324	Up	PC
PSMD8	Proteasome 26S Subunit, Non-ATPase 8	19	38374570	38383823	0.000324	Up	PC
PPP4C	Protein Phosphatase 4 Catalytic Subunit	16	30075993	30085376	0.000324	Up	PC
ADRM1	Adhesion Regulating Molecule 1	20	62302060	62308861	0.000324	Up	PC
PRMT1	Protein Arginine Methyltransferase 1	19	49676165	49688446	0.000324	Up	PC
AAMP	Angio Associated Migratory Cell Protein	2	218264126	218270180	0.000324	Up	PC
GPAA1	Glycosylphosphatidylinositol Anchor Attachment 1	8	144082633	144086215	0.000324	Up	PC
DEAF1	DEAF1 Transcription Factor	11	644219	707082	0.000324	Up	PC
FAM3A	FAM3 Metabolism Regulating Signalling Molecule A	X	154506163	154516256	0.000324	Up	PC
PES1	Pescadillo Ribosomal Biogenesis Factor 1	22	30576624	30607012	0.000324	Up	PC

Position is from GRCh38. Abbreviations: Chr, chromosome; PC, protein coding; ncRNA, non-coding RNA;

5.2.3 Reduced circRP11-298P3.4 expression resulted in an altered mRNA expression profile

In section 4.2.2 miRNA sequencing identified 110 differentially expressed miRNAs because of *circRP11-298P3.4* knockdown. To further investigate the function of *circRP11-298P3.4* mRNA sequencing was undertaken to elucidate if downstream genes are affected by the altered miRNA expression. mRNA sequencing identified 32 differentially expressed genes in HEK293 cells with reduced *circRP11-298P3.4* expression (FDR<0.05). Of the 32 differentially expressed genes 15 were upregulated and 17 were downregulated (Figure 5.5). Additional information of the differentially expressed genes are outlined in Figure 5.6 and Table 5.3.

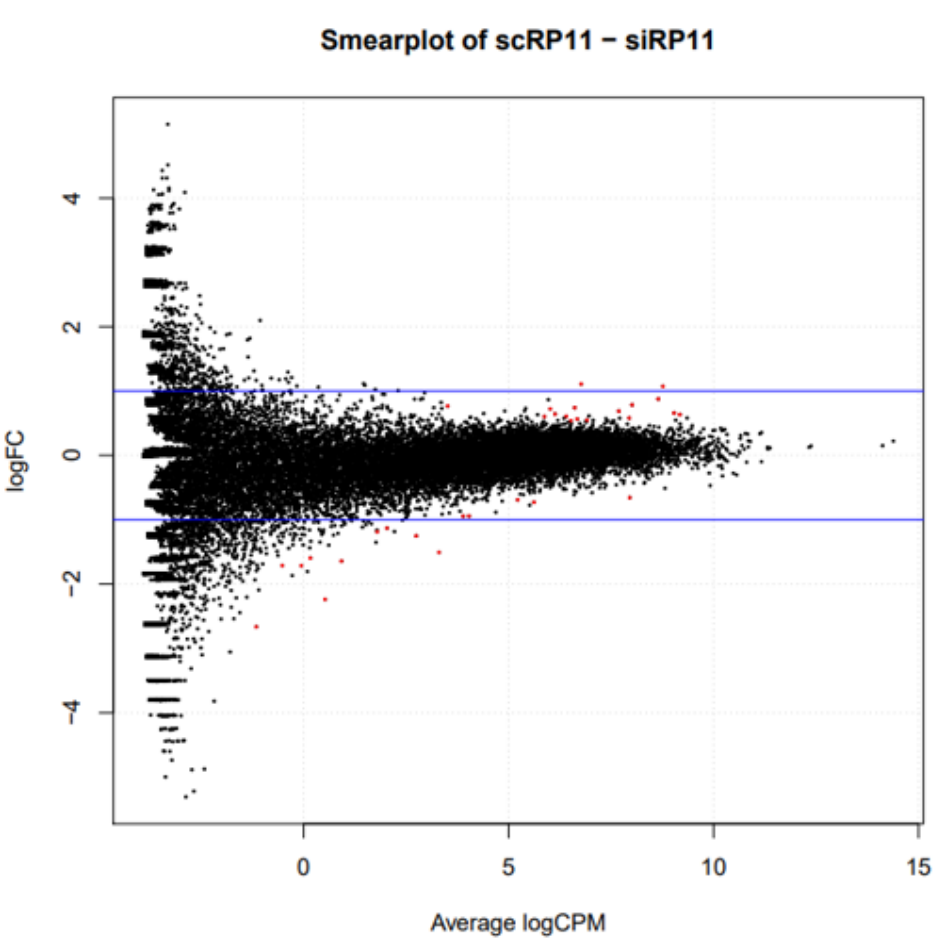

Figure 5.5: Smearplot of circRP11-298P3.4 knockdown mRNA sequencing – *Identified 15 up-regulated and 17 down-regulated. Red dots represent differentially expressed genes(FDR < 0.05) and black are those that are not (FDR > 0.05). scRP11= scramble treated, siZNF = siRNA treated*

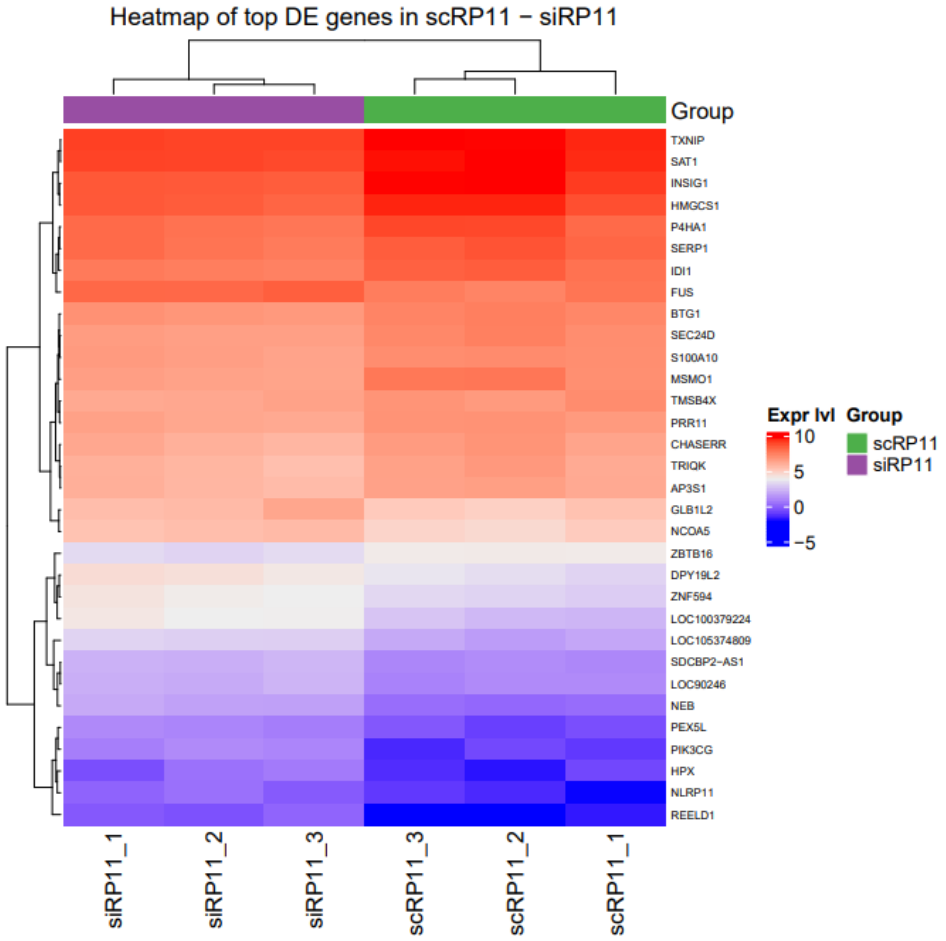

Figure 5.6: Top 50 differentially expressed genes heatmap for circRP11-298P3.4 knockdown

Table 5.3 Differentially expressed genes as result of circRP11-298P3.4 knockdown

Gene Symbol	*Gene Full Name*	*Chr*	*Gene Start*	*Gene End*	*FDR*	*Expression Change*	*Gene Biotype*
MSMO1	Methylsterol Monooxygenase 1	4	165327668	165343163	0.000624	Down	PC
INSIG1	Insulin Induced Gene 1	7	155297877	155310234	0.003514	Down	PC
LOC100379224	Uncharacterized LOC100379224	19	44103007	44113183	0.004606	Up	ncRNA
PIK3CG	Phosphatidylinositol-4,5-Bisphosphate 3-Kinase Catalytic Subunit Gamma	7	106865281	106908979	0.004606	Up	PC
SEC24D	SEC24 Homolog D, COPII Coat Complex Component	4	118722822	118838682	0.011333	Down	PC
TRIQK	Triple QxxK/R Motif Containing	8	92883532	93017673	0.011333	Down	PC
LOC105374809	uncharacterized LOC105374809	2	74928262	74958892	0.011333	Up	ncRNA
HMGCS1	3-Hydroxy-3-Methylglutaryl-CoA Synthase 1	5	43287469	43313476	0.011333	Down	PC
REELD1	Reeler Domain Containing 1	4	146214515	146230878	0.011333	Up	PC
NEB	Nebulin	2	151485333	151734475	0.019549	Up	PC
P4HA1	Prolyl 4-Hydroxylase Subunit Alpha 1	10	73007216	73096865	0.023234	Down	PC
ZNF594	Zinc Finger Protein 594	17	5179535	5191868	0.025563	Up	PC
AP3S1	Adaptor Related Protein Complex 3 Subunit Sigma 1	5	115841605	115914080	0.03609	Down	PC
LOC90246	uncharacterized LOC90246	3	128507835	128510595	0.038888	Up	ncRNA
IDI1	Isopentenyl-Diphosphate Delta Isomerase 1	10	1039151	1056703	0.041739	Down	PC

TMSB4X	Thymosin Beta 4 X-Linked	X	12975109	12977222	0.041739	Down	PC
S100A10	S100 Calcium Binding Protein A10	1	151982914	151993858	0.041739	Down	PC
BTG1	BTG Anti-Proliferation Factor 1	12	92140277	92145845	0.041739	Down	PC
DPY19L2	Dpy-19 Like 2	12	63558912	63669200	0.042666	Up	PC
NLRP11	NLR Family Pyrin Domain Containing 11	19	55789398	55836574	0.042666	Up	PC
GLB1L2	Galactosidase Beta 1 Like 2	11	134331874	134378341	0.044282	Up	PC
SAT1	Spermidine/spermine N1-acetyltransferase 1	X	23783172	23786209	0.044864	Down	PC
PRR11	Proline Rich 11	17	59155732	59206709	0.049921	Down	PC
SDCBP2-AS1	SDCBP2 antisense RNA 1	20	1325405	1378735	0.049921	Up	ncRNA
NCOA5	Nuclear Receptor Coactivator 5	20	46060990	46089961	0.049921	Up	PC
ZBTB16	Zinc Finger and BTB Domain Containing 16	11	114059575	114256769	0.049921	Down	PC
CHASERR	CHD2 Adjacent Suppressive Regulatory RNA	7	92882843	92898747	0.049921	Down	ncRNA
HPX	Hemopexin	11	6431048	6440986	0.049921	Up	PC
FUS	FUS RNA Binding Protein	16	31180109	31194870	0.049921	Up	PC
TXNIP	Thioredoxin Interacting Protein	1	145992434	145996578	0.049921	Down	PC
PEX5L	Peroxisomal Biogenesis Factor 5 Like	3	179794957	180037008	0.049921	Up	PC
SERP1	Stress Associated Endoplasmic Reticulum Protein 1	3	150541997	150546495	0.049921	Down	PC

Position is from GRCh38. Abbreviations: Chr, chromosome; PC, protein coding; ncRNA, non-coding RNA;

5.2.4 circRP11-298P3.4 Pathway Analysis

Utilising the 32 differentially expressed mRNAs identified in section 5.2.3 pathway analysis was conducted using the Reactome database and gene ontology tool GOrilla. Gorilla identified four pathways impacted by the reduced *circRP11-298P3.4* expression (FDR <0.05) as seen in Table 5.4 below and illustrated in Figure 5.7. Whereas the Reactome pathway analysis identified seven differentially expressed pathways as seen in Table 5.5 below.

Table 5.4: Differentially expressed pathways from Gene Ontology pathway analysis from the circRP11-298P3.4 knockdown model

GO Term	*Description*	*FDR*	*Genes*
GO:0006695	cholesterol biosynthetic process	1.84E-02	INSIG1, HMGCS1, MSMO1, IDI1
GO:1902653	secondary alcohol biosynthetic process	9.21E-03	INSIG1, HMGCS1, MSMO1, IDI1
GO:0016126	sterol biosynthetic process	6.14E-03	INSIG1, HMGCS1, MSMO1, IDI1
GO:0006694	steroid biosynthetic process	6.69E-02	INSIG1, HMGCS1, MSMO1, IDI1

Table 5.5: Differentially expressed pathways from Reactome pathway analysis from the circRP11-298P3.4 knockdown model

Pathway ID	*Pathway Name*	*FDR*	*Genes*
R-HSA-1655829	Regulation of cholesterol biosynthesis by SREBP (SREBF)	1.81E-06	IDI1, HMGCS1, INSIG1, SEC24D
R-HSA-8957322	Metabolism of steroids	1.24E-04	IDI1, HMGCS1, INSIG1, MSMO1, SEC24D
R-HSA-2426168	Activation of gene expression by SREBF (SREBP)	4.13E-04	IDI1, HMGCS1
R-HSA-191273	Cholesterol biosynthesis	0.010509833	IDI1, HMGCS1, MSMO1
R-HSA-556833	Metabolism of lipids	0.020189836	IDI1, HMGCS1, INSIG1, MSMO1, SEC24D, PIK3CG
R-HSA-9614085	FOXO-mediated transcription	0.020189836	BTG1, TXNIP
R-HSA-9617828	FOXO-mediated transcription of cell cycle genes	0.020189836	BTG1

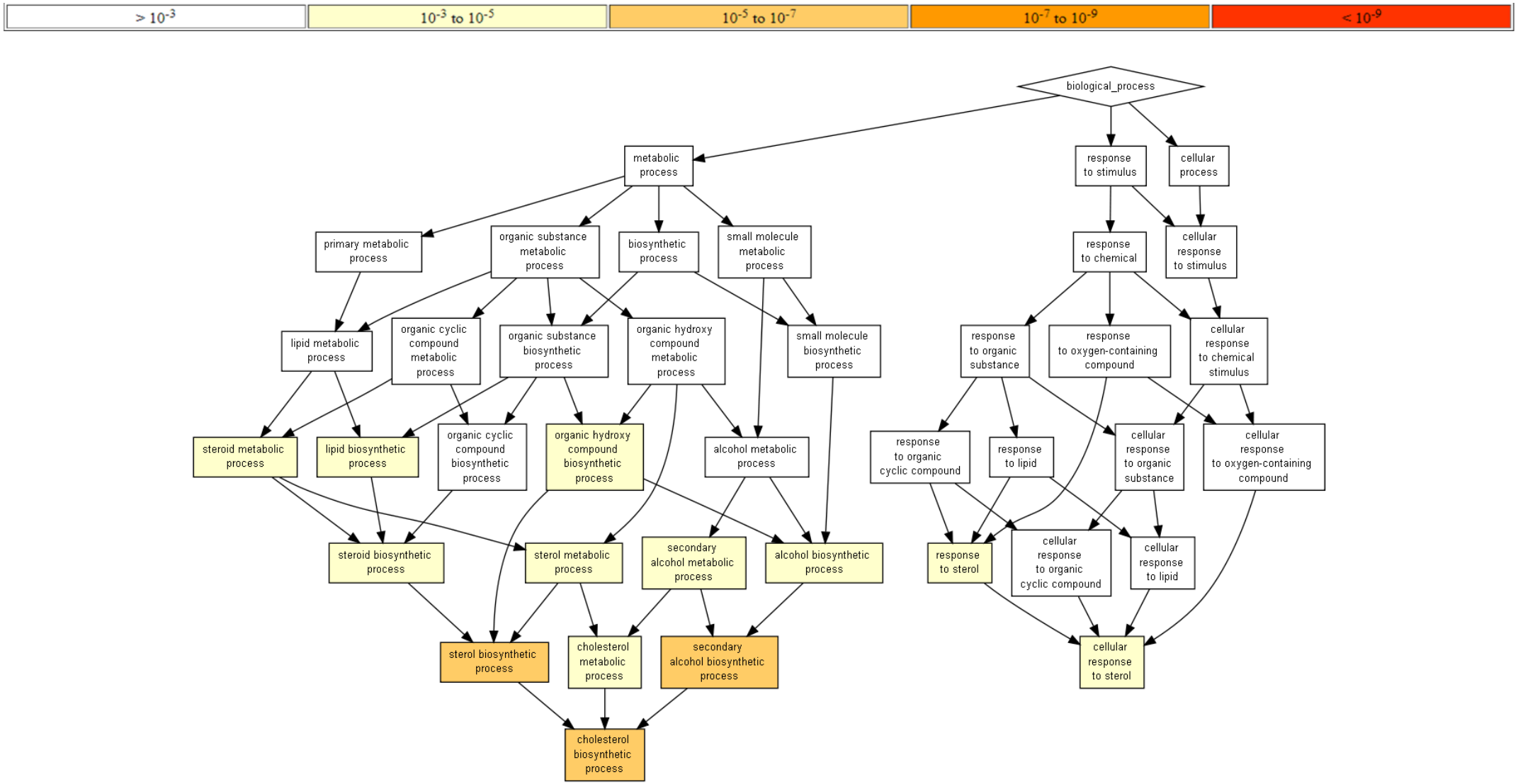

Figure 5.7: Gene Ontology biological process impacted by reduced circRP11-298P3.4 expression . The top bar represents the p-value for each respective pathway.

5.2.5 circZNF91 Pathway Analysis

Utilising the 2288 differentially expressed mRNAs identified in section 5.2.1 pathway analysis was conducted using the Reactome database and gene ontology tool GOrilla. GOrilla identified 46 pathways impacted by the reduced *circZNF91* expression (FDR <0.05) as seen in Table 5.6 below and illustrated in Figure 5.8. Whereas the Reactome pathway analysis identified 58 differentially expressed pathways as seen in Table 5.7 below. The list of genes involved in the differentially expressed pathways listed in Table 5.6 and 5.7 are located appendix 1 and 2, respectively.

Table 5.6: Differentially expressed pathways from Gene Ontology pathway analysis from the *circZNF91* knockdown model

GO Term	*Pathway*	*FDR*	*Genes*
GO:0006614	SRP-dependent cotranslational protein targeting to membrane	1.47E-05	22/2288
GO:0019083	viral transcription	9.08E-06	24/2288
GO:0006613	cotranslational protein targeting to membrane	2.27E-05	21/2288
GO:0045047	protein targeting to ER	3.62E-05	22/2288
GO:0072599	establishment of protein localization to endoplasmic reticulum	2.89E-05	22/2288
GO:0000184	nuclear-transcribed mRNA catabolic process, nonsense-mediated decay	9.46E-05	22/2288
GO:0006612	protein targeting to membrane	2.97E-04	24/2288
GO:0006401	RNA catabolic process	3.98E-04	25/2288
GO:0006413	translational initiation	3.67E-04	22/2288
GO:0044419	interspecies interaction between organisms	3.34E-04	24/2288
GO:0009059	macromolecule biosynthetic process	3.46E-04	60/2288
GO:0070972	protein localization to endoplasmic reticulum	4.63E-04	22/2288
GO:1901576	organic substance biosynthetic process	6.49E-04	90/2288
GO:0044319	wound healing, spreading of cells	6.74E-04	4/2288
GO:0000956	nuclear-transcribed mRNA catabolic process	8.18E-04	23/2288
GO:1901566	organonitrogen compound biosynthetic process	9.03E-04	92/2288
GO:0006412	translation	1.08E-03	24/2288
GO:0006402	mRNA catabolic process	1.09E-03	23/2288
GO:0034645	cellular macromolecule biosynthetic process	1.08E-03	51/2288
GO:0009058	biosynthetic process	1.27E-03	91/2288
GO:0043604	amide biosynthetic process	1.30E-03	51/2288
GO:0016032	viral process	1.49E-03	23/2288
GO:0044403	symbiont process	1.43E-03	23/2288
GO:0006518	peptide metabolic process	2.03E-03	43/2288
GO:0090150	establishment of protein localization to membrane	2.12E-03	26/2288
GO:0044249	cellular biosynthetic process	2.48E-03	85/2288
GO:0051704	multi-organism process	2.56E-03	27/2288
GO:0043043	peptide biosynthetic process	2.65E-03	35/2288
GO:0072594	establishment of protein localization to organelle	2.97E-03	32/2288
GO:0006605	protein targeting	4.12E-03	30/2288
GO:0044271	cellular nitrogen compound biosynthetic process	6.06E-03	67/2288

GO:0070585	protein localization to mitochondrion	6.38E-03	5/2288
GO:0072655	establishment of protein localization to mitochondrion	6.19E-03	5/2288
GO:0034655	nucleobase-containing compound catabolic process	9.31E-03	29/2288
GO:0072657	protein localization to membrane	1.24E-02	35/2288
GO:0046700	heterocycle catabolic process	2.01E-02	29/2288
GO:0043603	cellular amide metabolic process	2.23E-02	58/2288
GO:0044270	cellular nitrogen compound catabolic process	2.49E-02	29/2288
GO:0035295	tube development	2.49E-02	15/2288
GO:0009057	macromolecule catabolic process	3.16E-02	66/2288
GO:0044248	cellular catabolic process	3.28E-02	96/2288
GO:0051649	establishment of localization in cell	3.24E-02	22/2288
GO:1901361	organic cyclic compound catabolic process	3.34E-02	30/2288
GO:0009056	catabolic process	3.98E-02	105/2288
GO:1901575	organic substance catabolic process	4.03E-02	92/2288
GO:0019439	aromatic compound catabolic process	4.20E-02	29/2288

Table 5.7: Differentially expressed pathways from Reactome pathway analysis from the *circZNF91* knockdown model

Pathway ID	*Pathway Name*	*FDR*	*Genes*
R-HSA-9711097	Cellular response to starvation	2.17E-09	56/2288
R-HSA-9633012	Response of EIF2AK4 (GCN2) to amino acid deficiency	1.43E-08	42/2288
R-HSA-156842	Eukaryotic Translation Elongation	4.43E-08	41/2288
R-HSA-72689	Formation of a pool of free 40S subunits	4.43E-08	42/2288
R-HSA-1799339	SRP-dependent cotranslational protein targeting to membrane	5.42E-08	46/2288
R-HSA-156902	Peptide chain elongation	5.42E-08	38/2288
R-HSA-975956	Nonsense Mediated Decay (NMD) independent of the Exon Junction Complex (EJC)	5.42E-08	40/2288
R-HSA-72766	Translation	7.88E-08	93/2288
R-HSA-72764	Eukaryotic Translation Termination	1.84E-07	40/2288
R-HSA-2262752	Cellular responses to stress	2.24E-07	162/2288
R-HSA-72706	GTP hydrolysis and joining of the 60S ribosomal subunit	2.51E-07	53/2288
R-HSA-156827	L13a-mediated translational silencing of Ceruloplasmin expression	2.51E-07	43/2288
R-HSA-927802	Nonsense-Mediated Decay (NMD)	5.92E-07	43/2288
R-HSA-975957	Nonsense Mediated Decay (NMD) enhanced by the Exon Junction Complex (EJC)	5.92E-07	43/2288
R-HSA-8953897	Cellular responses to stimuli	6.61E-07	168/2288
R-HSA-72613	Eukaryotic Translation Initiation	7.75E-07	44/2288
R-HSA-72737	Cap-dependent Translation Initiation	7.75E-07	44/2288
R-HSA-2408557	Selenocysteine synthesis	1.31E-06	39/2288
R-HSA-192823	Viral mRNA Translation	2.04E-06	39/2288
R-HSA-1236977	Endosomal/Vacuolar pathway	5.13E-06	1/2288
R-HSA-983170	Antigen Presentation: Folding, assembly and peptide loading of class I MHC	5.31E-06	6/2288
R-HSA-6791226	Major pathway of rRNA processing in the nucleolus and cytosol	5.67E-06	54/2288
R-HSA-9010553	Regulation of expression of SLITs and ROBOs	9.50E-06	50/2288
R-HSA-168273	Influenza Viral RNA Transcription and Replication	1.31E-05	51/2288
R-HSA-168255	Influenza Infection	1.49E-05	56/2288
R-HSA-8868773	rRNA processing in the nucleus and cytosol	2.09E-05	60/2288
R-HSA-8953854	Metabolism of RNA	7.97E-05	158/2288
R-HSA-376176	Signalling by ROBO receptors	1.41E-04	59/2288
R-HSA-381038	XBP1(S) activates chaperone genes	2.56E-04	18/2288
R-HSA-1236974	ER-Phagosome pathway	3.03E-04	15/2288
R-HSA-422475	Axon guidance	3.54E-04	118/2288
R-HSA-381070	IRE1alpha activates chaperones	7.95E-04	17/2288

R-HSA-1236975	Antigen processing-Cross presentation	7.95E-04	18/2288
R-HSA-72312	rRNA processing	7.95E-04	28/2288
R-HSA-9675108	Nervous system development	8.72E-04	122/2288
R-HSA-983169	Class I MHC mediated antigen processing & presentation	0.001165341	70/2288
R-HSA-392499	Metabolism of proteins	0.002110015	362/2288
R-HSA-2408522	Selenoamino acid metabolism	0.002603348	44/2288
R-HSA-8866652	Synthesis of active ubiquitin: roles of E1 and E2 enzymes	0.008144808	13/2288
R-HSA-199991	Membrane Trafficking	0.010477885	123/2288
R-HSA-174048	APC/C:Cdc20 mediated degradation of Cyclin B	0.014488308	11/2288
R-HSA-174178	APC/C:Cdh1 mediated degradation of Cdc20 and other APC/C:Cdh1 targeted proteins in late mitosis/early G1	0.017859112	21/2288
R-HSA-5674400	Constitutive Signalling by AKT1 E17K in Cancer	0.022067144	11/2288
R-HSA-199977	ER to Golgi Anterograde Transport	0.024331641	37/2288
R-HSA-72695	Formation of the ternary complex, and subsequently, the 43S complex	0.02458317	19/2288
R-HSA-179409	APC-Cdc20 mediated degradation of Nek2A	0.025368207	11/2288
R-HSA-381119	Unfolded Protein Response (UPR)	0.026172426	20/2288
R-HSA-69052	Switching of origins to a post-replicative state	0.035620106	25/2288
R-HSA-8943724	Regulation of PTEN gene transcription	0.037415158	20/2288
R-HSA-5389840	Mitochondrial translation elongation	0.039281298	25/2288
R-HSA-72662	Activation of the mRNA upon binding of the cap-binding complex and eIFs, and subsequent binding to 43S	0.039281298	21/2288
R-HSA-909733	Interferon alpha/beta signalling	0.040973752	6/2288
R-HSA-2426168	Activation of gene expression by SREBF (SREBP)	0.040973752	13/2288
R-HSA-72649	Translation initiation complex formation	0.040973752	20/2288
R-HSA-6807070	PTEN Regulation	0.042120708	38/2288
R-HSA-8849469	PTK6 Regulates RTKs and Their Effectors AKT1 and DOK1	0.046798149	6/2288
R-HSA-9648895	Response of EIF2AK1 (HRI) to heme deficiency	0.04984227	4/2288
R-HSA-174154	APC/C:Cdc20 mediated degradation of Securin	0.04984227	19/2288

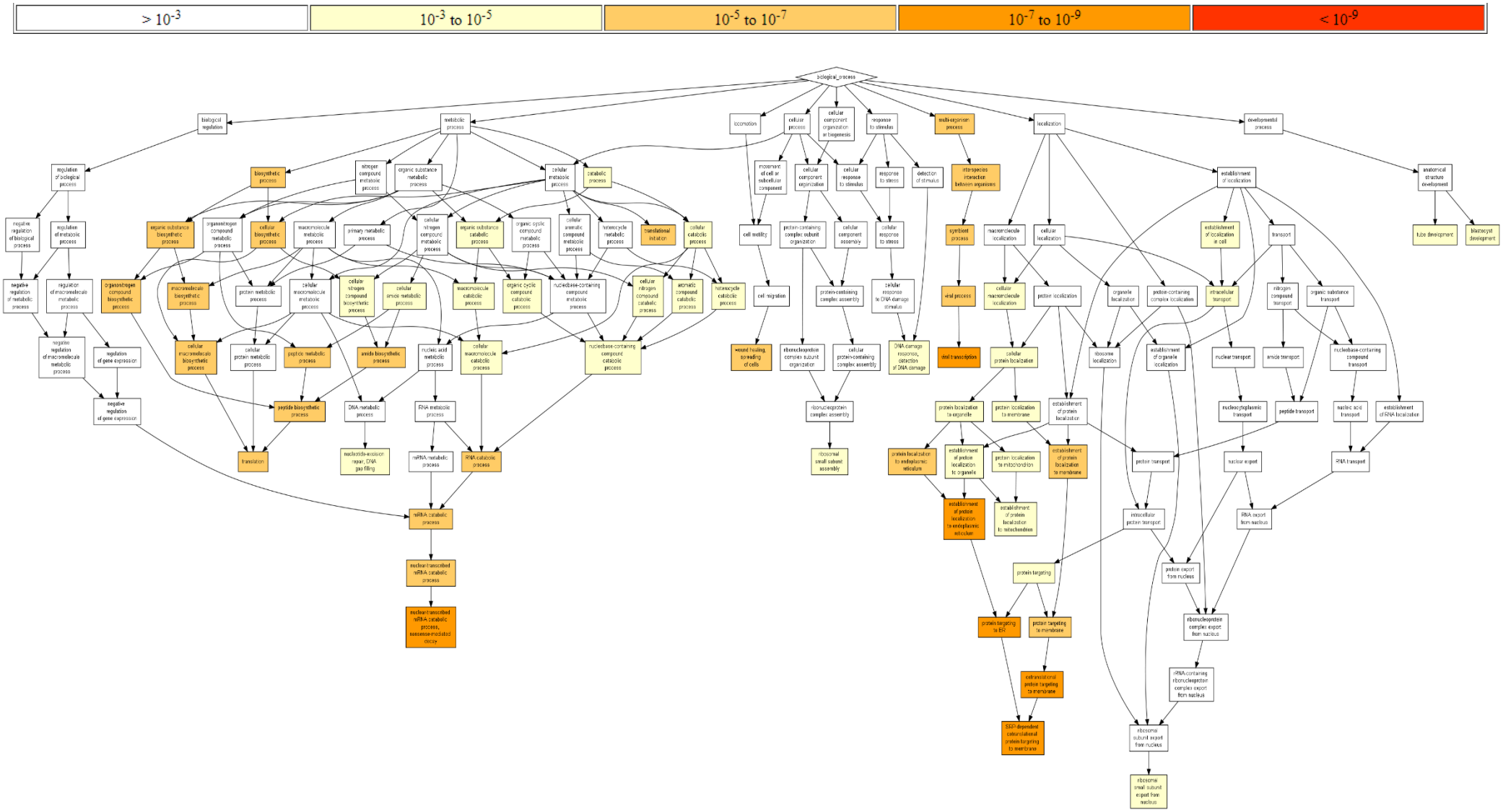

Figure 5.8: Gene Ontology biological process impacted by reduced circZNF91 expression. The top bar represents the p-value for each respective pathway.

5.2.6 circGRB10 Pathway Analysis

Utilising the 2907 differentially expressed mRNAs identified in section 5.2.2 pathway analysis was conducted using the Reactome database and gene ontology tool GOrilla. Gorilla identified 84 pathways impacted by the reduced *circGRB10* expression (FDR <0.05) as seen in Table 5.8 below and illustrated in Figure 5.9. Whereas the Reactome pathway analysis identified 87 differentially expressed pathways as seen in Table 5.9 below. The list of genes involved in the differentially expressed pathways listed in Table 5.8 and 5.9 are located appendix 3 and 4, respectively.

Table 5.8: Differentially expressed pathway using Gene Ontology for *circGRB10* knockdown model

GO Term	*Description*	*FDR*	*Genes*
GO:0044419	interspecies interaction between organisms	5.37E-07	87/2907
GO:0051704	multi-organism process	4.39E-07	161/2907
GO:0016032	viral process	1.37E-06	94/2907
GO:0044403	symbiont process	1.03E-06	93/2907
GO:0000184	nuclear-transcribed mRNA catabolic process, nonsense-mediated decay	1.46E-04	23/2907
GO:0016071	mRNA metabolic process	1.36E-04	71/2907
GO:0019083	viral transcription	4.68E-04	23/2907
GO:0044271	cellular nitrogen compound biosynthetic process	4.24E-04	146/2907
GO:0006413	translational initiation	8.01E-04	22/2907
GO:0045047	protein targeting to ER	9.20E-04	21/2907
GO:0072599	establishment of protein localization to endoplasmic reticulum	8.37E-04	21/2907
GO:0006614	SRP-dependent cotranslational protein targeting to membrane	1.07E-03	20/2907
GO:0072594	establishment of protein localization to organelle	1.44E-03	39/2907
GO:0006401	RNA catabolic process	1.41E-03	26/2907
GO:0006613	cotranslational protein targeting to membrane	1.38E-03	20/2907
GO:0006605	protein targeting	1.31E-03	33/2907
GO:1901576	organic substance biosynthetic process	1.30E-03	213/2907
GO:0009059	macromolecule biosynthetic process	1.30E-03	87/2907
GO:0009894	regulation of catabolic process	1.33E-03	75/2907
GO:0070972	protein localization to endoplasmic reticulum	1.34E-03	22/2907
GO:1901566	organonitrogen compound biosynthetic process	1.54E-03	93/2907
GO:0009058	biosynthetic process	1.53E-03	219/2907
GO:0046907	intracellular transport	1.48E-03	106/2907
GO:0000956	nuclear-transcribed mRNA catabolic process	1.80E-03	24/2907
GO:0006402	mRNA catabolic process	1.73E-03	24/2907
GO:0034645	cellular macromolecule biosynthetic process	2.87E-03	92/2907
GO:0044265	cellular macromolecule catabolic process	3.86E-03	53/2907
GO:0072657	protein localization to membrane	3.76E-03	37/2907
GO:0090150	establishment of protein localization to membrane	3.67E-03	26/2907
GO:0006518	peptide metabolic process	3.64E-03	55/2907
GO:0031329	regulation of cellular catabolic process	3.76E-03	68/2907
GO:0050896	response to stimulus	3.70E-03	62/2907

GO:0008152	metabolic process	3.59E-03	538/2907
GO:0051649	establishment of localization in cell	3.69E-03	116/2907
GO:0044237	cellular metabolic process	4.02E-03	517/2907
GO:0016070	RNA metabolic process	4.00E-03	123/2907
GO:0034641	cellular nitrogen compound metabolic process	3.92E-03	223/2907
GO:0044249	cellular biosynthetic process	3.89E-03	201/2907
GO:0006412	translation	4.33E-03	25/2907
GO:0043604	amide biosynthetic process	4.40E-03	37/2907
GO:0043043	peptide biosynthetic process	5.26E-03	26/2907
GO:0009057	macromolecule catabolic process	5.17E-03	56/2907
GO:0006810	transport	5.56E-03	199/2907
GO:0043933	protein-containing complex subunit organization	5.80E-03	97/2907
GO:0070887	cellular response to chemical stimulus	6.08E-03	21/2907
GO:0006612	protein targeting to membrane	8.17E-03	21/2907
GO:0071840	cellular component organization or biogenesis	8.94E-03	301/2907
GO:0065003	protein-containing complex assembly	8.86E-03	30/2907
GO:0071705	nitrogen compound transport	8.95E-03	113/2907
GO:0051234	establishment of localization	9.78E-03	205/2907
GO:0042221	response to chemical	1.15E-02	27/2907
GO:0000463	maturation of LSU-rRNA from tricistronic rRNA transcript (SSU-rRNA, 5.8S rRNA, LSU-rRNA)	1.14E-02	3/2907
GO:0051716	cellular response to stimulus	1.15E-02	33/2907
GO:0016043	cellular component organization	1.17E-02	297/2907
GO:0022618	ribonucleoprotein complex assembly	1.41E-02	31/2907
GO:0006890	retrograde vesicle-mediated transport, Golgi to ER	1.43E-02	16/2907
GO:0046483	heterocycle metabolic process	1.61E-02	197/2907
GO:0071702	organic substance transport	2.36E-02	120/2907
GO:0000377	RNA splicing, via transesterification reactions with bulged adenosine as nucleophile	1.49E-04	31/2907
GO:0000398	mRNA splicing, via spliceosome	1.49E-04	31/2907
GO:0051641	cellular localization	1.61E-04	142/2907
GO:0015833	peptide transport	1.63E-04	93/2907
GO:0072655	establishment of protein localization to mitochondrion	1.71E-04	14/2907
GO:0006886	intracellular protein transport	1.79E-04	64/2907
GO:0006725	cellular aromatic compound metabolic process	1.81E-04	197/2907
GO:0031331	positive regulation of cellular catabolic process	1.82E-04	26/2907
GO:0051179	localization	2.13E-04	210/2907

GO:0032386	regulation of intracellular transport	2.35E-04	45/2907
GO:0000375	RNA splicing, via transesterification reactions	2.35E-04	30/2907
GO:0006397	mRNA processing	2.37E-04	40/2907
GO:0010033	response to organic substance	2.49E-04	22/2907
GO:0006139	nucleobase-containing compound metabolic process	2.74E-04	189/2907
GO:0045184	establishment of protein localization	2.80E-04	98/2907
GO:0042176	regulation of protein catabolic process	2.84E-04	34/2907
GO:0071826	ribonucleoprotein complex subunit organization	2.97E-04	32/2907
GO:0071704	organic substance metabolic process	3.10E-04	505/2907
GO:0070585	protein localization to mitochondrion	3.60E-04	14/2907
GO:0006396	RNA processing	3.68E-04	74/2907
GO:0045862	positive regulation of proteolysis	3.78E-04	47/2907
GO:1903362	regulation of cellular protein catabolic process	3.82E-04	34/2907
GO:0015031	protein transport	3.94E-04	91/2907
GO:0090304	nucleic acid metabolic process	4.09E-04	157/2907
GO:0009987	cellular process	4.22E-04	505/297
GO:0022904	respiratory electron transport chain	4.31E-04	15/2907

Table 5.9 Differentially expressed pathways from Reactome pathway analysis from the *circGRB10* knockdown model

Pathway ID	*Pathway Name*	*FDR*	*Genes*
R-HSA-1236974	ER-Phagosome pathway	7.75E-14	23/2907
R-HSA-983170	Antigen Presentation: Folding, assembly and peptide loading of class I MHC	7.75E-14	8/2907
R-HSA-1236977	Endosomal/Vacuolar pathway	7.75E-14	3/2907
R-HSA-1236975	Antigen processing-Cross presentation	1.16E-13	25/2907
R-HSA-909733	Interferon alpha/beta signalling	4.21E-11	10/2907
R-HSA-9633012	Response of EIF2AK4 (GCN2) to amino acid deficiency	5.10E-09	53/2907
R-HSA-983169	Class I MHC mediated antigen processing & presentation	1.03E-08	85/2907
R-HSA-422475	Axon guidance	2.77E-08	172/2907
R-HSA-72689	Formation of a pool of free 40S subunits	2.99E-08	53/2907
R-HSA-9711097	Cellular response to starvation	2.99E-08	72/2907
R-HSA-156842	Eukaryotic Translation Elongation	5.38E-08	39/2907
R-HSA-156902	Peptide chain elongation	7.49E-08	58/2907
R-HSA-975956	Nonsense Mediated Decay (NMD) independent of the Exon Junction Complex (EJC)	9.23E-08	59/2907
R-HSA-2262752	Cellular responses to stress	1.56E-07	209/2907
R-HSA-9675108	Nervous system development	1.56E-07	178/2907
R-HSA-8953897	Cellular responses to stimuli	2.11E-07	210/2907
R-HSA-9010553	Regulation of expression of SLITs and ROBOs	2.11E-07	68/2907
R-HSA-1799339	SRP-dependent cotranslational protein targeting to membrane	2.87E-07	53/2907
R-HSA-72764	Eukaryotic Translation Termination	2.87E-07	49/2907
R-HSA-8868773	rRNA processing in the nucleus and cytosol	2.87E-07	77/2907
R-HSA-72706	GTP hydrolysis and joining of the 60S ribosomal subunit	3.34E-07	54/2907
R-HSA-156827	L13a-mediated translational silencing of Ceruloplasmin expression	3.34E-07	54/2907
R-HSA-927802	Nonsense-Mediated Decay (NMD)	3.66E-07	54/2907
R-HSA-975957	Nonsense Mediated Decay (NMD) enhanced by the Exon Junction Complex (EJC)	3.66E-07	54/2907
R-HSA-2408557	Selenocysteine synthesis	5.09E-07	50/2907
R-HSA-6791226	Major pathway of rRNA processing in the nucleolus and cytosol	5.09E-07	71/2907
R-HSA-877300	Interferon gamma signalling	6.12E-07	13/2907
R-HSA-376176	Signalling by ROBO receptors	6.13E-07	82/2907
R-HSA-381038	XBP1(S) activates chaperone genes	9.60E-07	23/2907

R-HSA-72613	Eukaryotic Translation Initiation	1.36E-06	54/2907
R-HSA-72737	Cap-dependent Translation Initiation	1.36E-06	54/2907
R-HSA-381070	IRE1alpha activates chaperones	4.97E-06	24/2907
R-HSA-192823	Viral mRNA Translation	1.01E-05	46/2907
R-HSA-168273	Influenza Viral RNA Transcription and Replication	2.33E-05	64/2907
R-HSA-72766	Translation	2.33E-05	103/2907
R-HSA-913531	Interferon Signalling	2.52E-05	38/2907
R-HSA-168255	Influenza Infection	2.65E-05	71/2907
R-HSA-72312	rRNA processing	3.56E-05	79/2907
R-HSA-8953854	Metabolism of RNA	8.29E-05	192/2907
R-HSA-381119	Unfolded Protein Response (UPR)	1.14E-04	30/2907
R-HSA-199991	Membrane Trafficking	0.001201	160/2907
R-HSA-1640170	Cell Cycle	0.001602	168/2907
R-HSA-453274	Mitotic G2-G2/M phases	0.002327	60/2907
R-HSA-69275	G2/M Transition	0.005209	59/2907
R-HSA-69278	Cell Cycle, Mitotic	0.006243	137/2907
R-HSA-162906	HIV Infection	0.009367	71/2907
R-HSA-2408522	Hellenomania acid metabolism	0.009735	55/2907
R-HSA-174178	APC/C:Cdh1 mediated degradation of Cdc20 and other APC/C:Cdh1 targeted proteins in late mitosis/early G1	0.009735	25/2907
R-HSA-380320	Recruitment of NuMA to mitotic centrosomes	0.010716	30/2907
R-HSA-6811434	COPI-dependent Golgi-to-ER retrograde traffic	0.015668	31/2907
R-HSA-6811442	Intra-Golgi and retrograde Golgi-to-ER traffic	0.015787	59/2907
R-HSA-380270	Recruitment of mitotic centrosome proteins and complexes	0.017859	28/2907
R-HSA-8854518	AURKA Activation by TPX2	0.019163	27/2907
R-HSA-380287	Centrosome maturation	0.024868	28/2907
R-HSA-68867	Assembly of the pre-replicative complex	0.025	22/2907
R-HSA-6807878	COPI-mediated anterograde transport	0.025975	33/2907
R-HSA-75815	Ubiquitin-dependent degradation of Cyclin D	0.025975	20/2907
R-HSA-72695	Formation of the ternary complex, and subsequently, the 43S complex	0.025975	24/2907
R-HSA-9679191	Potential therapeutics for SARS	0.026764	30/2907
R-HSA-2565942	Regulation of PLK1 Activity at G2/M Transition	0.02807	30/2907
R-HSA-6781827	Transcription-Coupled Nucleotide Excision Repair (TC-NER)	0.031117	28/2907
R-HSA-69563	p53-Dependent G1 DNA Damage Response	0.031608	21/2907
R-HSA-69580	p53-Dependent G1/S DNA damage checkpoint	0.031608	21/2907

R-HSA-1280218	Adaptive Immune System	0.037225	153/2907
R-HSA-380284	Loss of proteins required for interphase microtubule organization from the centrosome	0.037225	25/2907
R-HSA-380259	Loss of Nlp from mitotic centrosomes	0.037225	25/2907
R-HSA-8852276	The role of GTSE1 in G2/M progression after G2 checkpoint	0.039406	24/2907
R-HSA-8856688	Golgi-to-ER retrograde transport	0.039744	42/2907
R-HSA-4086400	PCP/CE pathway	0.039744	29/2907
R-HSA-2467813	Separation of Sister Chromatids	0.039865	50/2907
R-HSA-174154	APC/C:Cdc20 mediated degradation of Securin	0.039865	23/2907
R-HSA-9648895	Response of EIF2AK1 (HRI) to heme deficiency	0.039865	6/2907
R-HSA-69615	G1/S DNA Damage Checkpoints	0.040668	21/2907
R-HSA-5676590	NIK-->noncanonical NF-kB signalling	0.041756	20/2907
R-HSA-68882	Mitotic Anaphase	0.043391	61/2907
R-HSA-2979096	NOTCH2 Activation and Transmission of Signal to the Nucleus	0.04351	12/2907
R-HSA-2555396	Mitotic Metaphase and Anaphase	0.045939	62/2907
R-HSA-2682334	EPH-Ephrin signalling	0.048608	34/2907
R-HSA-72649	Translation initiation complex formation	0.048608	26/2907
R-HSA-5607761	Dectin-1 mediated noncanonical NF-kB signalling	0.048608	20/2907
R-HSA-72662	Activation of the mRNA upon binding of the cap-binding complex and eIFs, and subsequent binding to 43S	0.048608	26/2907
R-HSA-6782210	Gap-filling DNA repair synthesis and ligation in TC-NER	0.048608	22/2907
R-HSA-8943724	Regulation of PTEN gene transcription	0.048608	24/2907
R-HSA-174113	SCF-beta-TrCP mediated degradation of Emi1	0.048608	18/2907
R-HSA-8854050	FBXL7 down-regulates AURKA during mitotic entry and in early mitosis	0.048608	18/2907
R-HSA-68886	M Phase	0.048608	96/2907
R-HSA-5696397	Gap-filling DNA repair synthesis and ligation in GG-NER	0.048608	11/2907

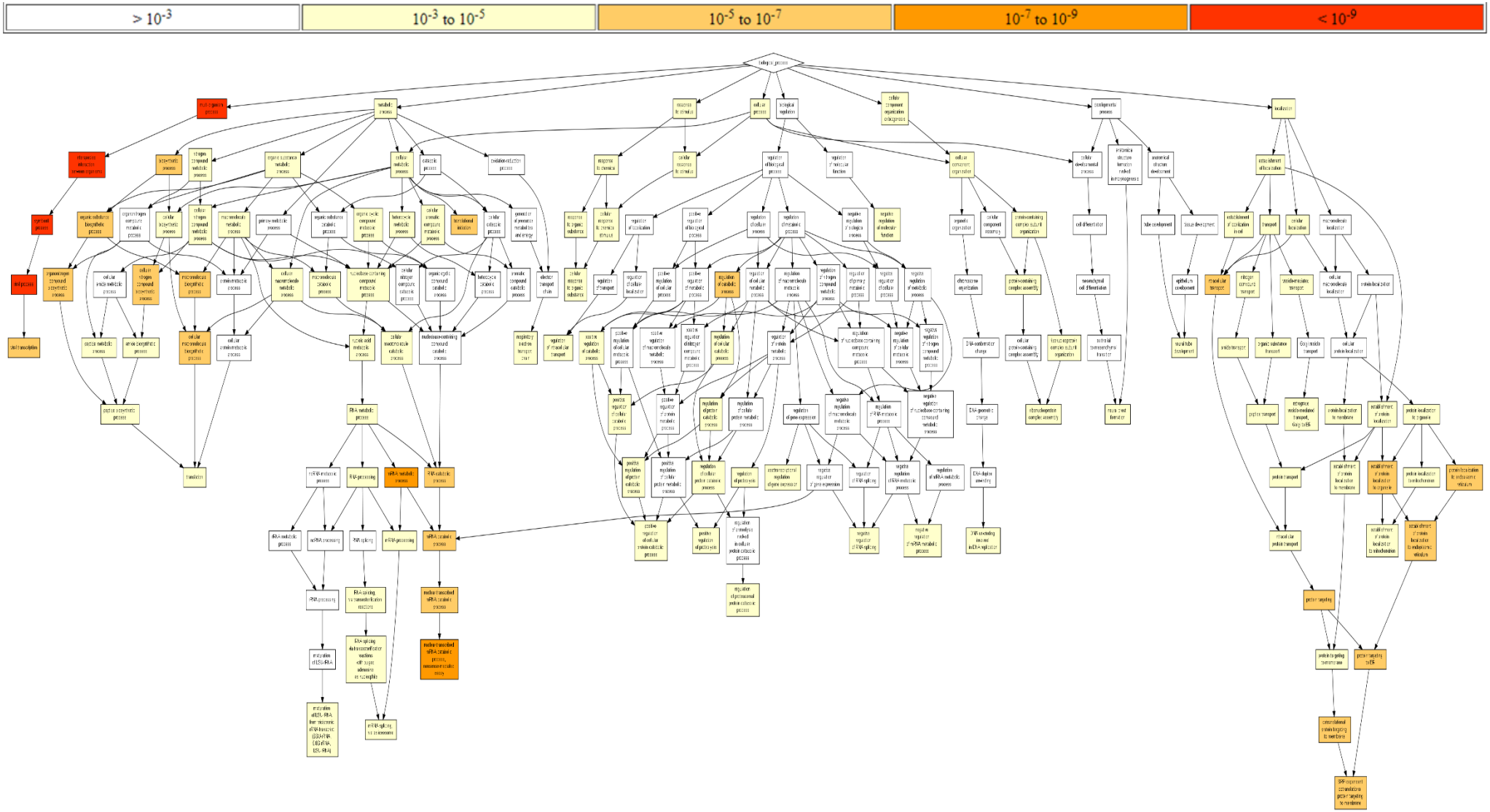

Figure 5.9: Gene Ontology biological process impacted by reduced *circGRB10* expression. The top bar represnets the p-value for each respective pathway.

5.2.7 circRNA – miRNA – mRNA networks of interest for circRP11-298P3.4

RNA and miRNA sequencing of the *circRP11-298P3.4* knockdown model identified several differentially expressed mRNAs and miRNAs (Table 4.3 and 5.3). Utilising this list of differentially expressed mRNAs and miRNAs we were able to identify probable circRNA-miRNA-mRNA networks. This was achieved by applying a similar methodology from section 3.1.9 whereby the predicted miRNA-mRNA interactions were cross-matched with our list of differentially expressed mRNAs and the completed *circRP11-298P3.4* – miRNA – mRNA network is illustrated in Figure 5.10. In addition to this, the functions of the mRNAs of interest are outlined in Table 5.10.

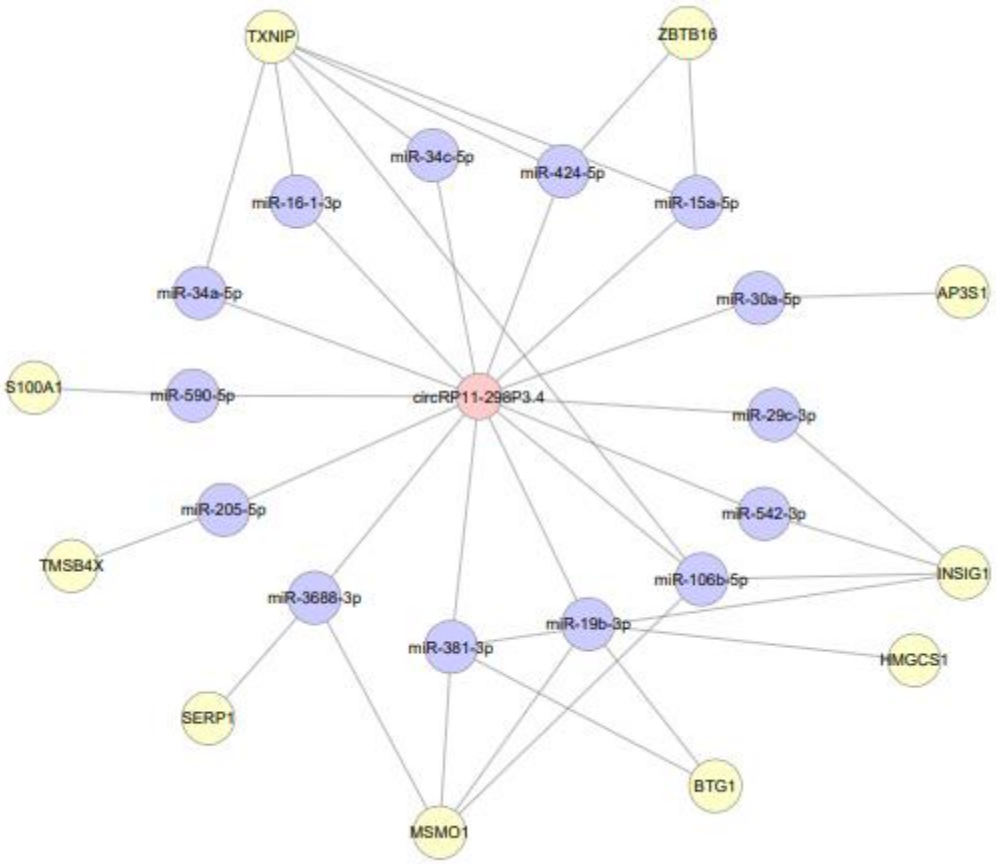

Figure 5.10: Finalised circRNA – miRNA – mRNA network for circRP11-298P3.4 model

Table 5.10 *circRP11-298P3.4* model mRNAs of interest function as per GeneCards

Differentially Expressed Gene	*Function*
AP3S1	It facilitates the budding of vesicles from the Golgi membrane and may be directly involved in trafficking to lysosomes.
BTG1	This gene is a member of an anti-proliferative gene family that regulates cell growth and differentiation. Expression of this gene is highest in the G0/G1 phases of the cell cycle and downregulated when cells progressed through G1.
HMGCS1	Catalyses the condensation of acetyl-CoA with acetoacetyl-CoA to form HMG-CoA, which is converted by HMG-CoA reductase (HMGCR) into mevalonate, a precursor for cholesterol synthesis.
INSIG1	Oxysterol-binding protein that mediates feedback control of cholesterol synthesis by controlling both endoplasmic reticulum to Golgi transport of SCAP and degradation of HMGCR
MSMO1	Catalyses the three-step monooxygenation required for the demethylation of 4,4-dimethyl and 4alpha-methylsterols, which can be subsequently metabolized to cholesterol
S100A1	S100A10 induces the dimerization of ANXA2/p36, it may function as a regulator of protein phosphorylation in that the ANXA2 monomer is the preferred target (in vitro) of tyrosine-specific kinase.
SERP1	Interacts with target proteins during their translocation into the lumen of the endoplasmic reticulum. Protects unfolded target proteins against degradation during ER stress.
TMSB4X	Plays an important role in the organization of the cytoskeleton. Binds to and sequesters actin monomers (G actin) and therefore inhibits actin polymerization.
TXNIP	May act as an oxidative stress mediator by inhibiting thioredoxin activity or by limiting its bioavailability. Interacts with COPS5 and restores COPS5-induced suppression of CDKN1B stability, blocking the COPS5-mediated translocation of CDKN1B from the nucleus to the cytoplasm.
ZBTB16	Acts as a transcriptional repressor.

5.3 Discussion

The concluding chapter of this thesis aimed to shine light on the last component of the circRNA – miRNA -mRNA interaction network. Utilising the same circRNA knockdown models in chapter 4 of this thesis we undertook mRNA sequencing to fully understand the impact of reduced circRNA expression on the mRNA profile. This was subsequently followed by pathway analysis to determine how individual or groups of genes impact on the renal function. RNA sequencing identified several differentially expressed mRNAs for each of our models.

For the *circZNF91* knockdown model we identified 2288 differentially expressed genes in the absence of any differentially expressed miRNAs. Subsequent pathway analysis identifying upwards of 90 pathways (Table 5.6 and 5.7) impacted by the differentially expressed genes. Several genes have published inference in either BP regulation or overall renal function. For example, *GPX4*, a gene that encodes for glutathione peroxidase 4 which is responsible for reduction of hydrogen peroxide was of interest in this model [219]. GPX4 has been shown to be necessary for proper kidney function with disruption leading to ferroptosis causing massive cell death in the tubular epithelia cells [220]. Another differentially expressed mRNA of interest in this model is *RACK1*. *RACK1* encodes the Receptor for activated C kinase 1 protein that organizes interactions between $G\beta_{\gamma}$, $G\alpha_{q}$, and PLC all of which are key components of G protein-coupled receptors. A study by Zhu *et al*., (2016) demonstrated that RACK1 enhanced proliferation of SHR pre-glomerular VSMCs and augments Gq-Gi coincident signalling and contributed to increased renal vasoconstriction in the SHR with the researchers postulating that RACK1 may be a crucial element in the pathogenesis of HT [221]. These two genes are just an example of the differentially expressed genes in this model that are a pre-established association with renal function or BP regulation which serves as the basis for further investigation. When considering the role circRNAs play in this observation

the intermediate target(s) are yet to be determined and are fundamental to fully understanding how reduced *circZNF91* expression is contributing to this list of differentially expressed genes. Further work is required to identify the middle regulator between *circZNF91* and mRNAs, provided miRNAs mediated gene expression is less than likely based on the results obtained in Chapter 4 Section 4.2.3, a pulldown assay would be advantageous to identify circRNA-protein interactions and allow for further investigation into the role these might play in gene expression.

Secondly with the *circGRB10* knockdown model we identified 2907 differentially expressed genes in the absence of any differentially expressed miRNAs. Subsequent pathway analysis identified upwards of 160 pathways (Table 5.8 and 5.9) impacted by the differentially expressed genes. Like the *circZNF91* model, several differentially expressed genes in the circGRB10 model have a published association with either BP regulation or overall renal function. For example, in this model we identified CD151 molecule (Raph Blood Group) as a gene of interest. CD151, a member of the tetraspanin family of membrane proteins, is crucially involved in the formation of the glomerular filtration barrier in humans and mice. A study conducted by Blumenthal *et al*., (2012) demonstrated that CD151 knockdown in podocytes reduced β1-integrin expression and podocyte cell area, indicating diminished adherence and/or spreading [222]. Further to this a study by Sachs *et al*., (2012) identified BP as an important factor in the initiation and progression of CD151 knockout induced nephropathy [223]. Together this has identified CD151 as a gene of interest not only for overall renal function but potentially in BP regulation and subsequent HT development. In the circGRB10 model we also identified FAM3A as a gene of interest. FAM3A was identified as an important regulator of vascular constriction and BP. FAM3A stimulates proliferation and migration of VSMCs by ATP-P2 receptor-mediated activation of PI3K-Akt and ERK1/2 pathways [224]. These are just 2 examples from this model that have a pre-

established association with renal function/BP regulation. Further work is required to identify the middle regulator between *circGRB10* and mRNAs, provided miRNAs mediated gene expression is less than likely based on the results obtained in Chapter 4 Section 4.2.4, a pulldown assay would be advantageous to undertake. This would identify circRNA-protein interactions and allow for further investigation into the role these might play in gene expression.

And lastly, for the *circRP11-298P3.4* model we identified 32 differentially expressed genes after successfully identifying 110 differentially expressed miRNAs with the upregulated ones becoming our miRNAs of interest (Refer section 4.2.5). Subsequent pathway analysis identified 11 pathways (Table 5.4 and 5.5) impacted by the differentially expressed genes. As with the *circZNF91* and *circGRB10* knockdown models, some of the differentially expressed genes have a pre-established association with either BP regulation or overall renal function. For example, PIK3CG was identified as a gene of interest. The PIK3CG gene encodes for the Phosphatidylinositol-4,5-Bisphosphate 3-Kinase Catalytic Subunit Gamma protein which is involved in signalling cascades responsible for cell growth, survival, proliferation, motility, and morphology [225]. A study by Carnevale *et al*., demonstrated inhibition of PIK3CG reduced BP by initiating vasorelaxation via the L-type calcium channel [226]. Additional work by An *et al*., (2020) identified the importance of PIK3CG in renal fibrosis. PIK3CG in Ang-II induced HT facilitates the influx of macrophages, T cells and bone marrow-derived fibroblasts into the kidney resulting in renal injury and fibrosis [227]. Further to PIK3CG, Thioredoxin-interacting protein (TXNIP) was also identified as a gene or interest in the *circRP11-298P3.4* model. TXNIP encodes for the thioredoxin-interacting protein which acts as an important regulator of glucose and lipid metabolism through pleiotropic regulation of β-cell function, hepatic glucose production, peripheral glucose uptake, adipogenesis [228]. Due to TXNIP's involvement in a variety of metabolic processes

this promoted Ferreira *et al*., to investigate the role it might have in metabolic conditions such as HT and diabetes. It was observed that higher TXNIP expression enhanced susceptibility to chronic metabolic conditions such as diabetes and HT [229].

In addition to TXNIP, several of the differentially expressed genes in this model have a pre-established role in either cholesterol metabolism or biogenesis. Furthermore, the GOrilla and Reactome databases identified a number of pathways involved in cholesterol metabolism/biogenesis were impact by our list of differentially expressed genes (Table 5.4 and 5.5). Dysregulation of cholesterol has long been established as a key factor for several pathologies, in particular atherosclerosis and other cardiovascular conditions [230]. In the *circRP11-298P3.4* knockdown model we identified several genes that play a significant role in cholesterol synthesis such as hydroxymethylglutaryl-CoA synthase (HMGCS1) that is a rate limiting enzyme in cholesterol synthesis [231]. Methylsterol mono-oxygenase 1(MSMO1) which catalyses the three-step monooxygenation required for the demethylation of 4,4-dimethyl and 4alpha-methylsterols, which can be subsequently metabolized to cholesterol [232]. Further to this, overexpression of MSMO1 was shown to inhibit differentiation of 3T3-L1 cells and led to the down-regulated expression of adipogenic marker genes, while knockdown of MSMO1 had the opposite effect [233]. Isopentenyl diphosphate isomerase (IDI) a cytoplasmic enzyme that is involved in the synthesis of isoprenoids including cholesterols [234]. And lastly, insulin induced gene 1 (INSIG1) that regulates cholesterol metabolism, lipogenesis, and glucose homeostasis [235]. It binds the sterol-sensing domains of 3-hydroxy-3-methylglutaryl-coenzyme A reductase (HMG-CoA reductase) and is essential for the sterol-mediated trafficking of these two proteins. It promotes the endoplasmic reticulum retention of SCAP and degradation of HMG-CoA reductase [236].

In this model we have observed decreased expression in the beforehand listed genes, however it is important to remember in Chapter 3 we identified an upregulation of *circRP11-298P3.4* instead of a downregulation which was induced via the siRNA transfection. With this information in mind in a hypertensive state we would expect the opposite expression levels for TXNIP, HMGCS1, MSMO1, IDI and INSIG1. In the knockdown model this gene expression profile would result in reduced cholesterol synthesis and the opposite expression profile would result in increased cholesterol synthesis. A study by Zhong *et al*., demonstrates altered cholesterol homeostasis activates pathways in tubular epithelial cells that lead to interstitial accumulation of fluid and harmful particles that promote progressive kidney damage [237]. This fluid retention, although not demonstrated in this article, may also contribute to an increased BP, and warrants further investigation into the specific role renal related cholesterol has in BP regulation.

5.4 Limitations

Throughout this and the subsequent chapters of this thesis, miRNA and mRNAs of interest have been identified with a potential role in either overall renal function or BP regulation. The next step is to confirm these interactions functionally. These interactions can be confirmed via luciferase reporter assays which have been discussed previously in Chapter 4 Section 4.4.

As discussed in Section 5.3 we observed an increased expression of *circRP11-298P3.4* in Chapter 3 however the methodologies utilised to investigate its function centred on a reduced expression model. To fully replicate the hypertensive phenotype an overexpression of *circRP11-298P3.4* would have been more advantageous to link the results to HT more appropriately. Overexpression can be achieved by utilising expression constructs with inverted flanking intronic repeats, such as in Liu *et al*. [238].

Chapter 6
Discussion and Conclusions

6.0 Overview

The major finding of this Thesis are:

1. Ultra-deep RNA sequencing identified 12 differentially expressed circRNAs in hypertensive human kidney samples from the TRANSLATE study **(Chapter 3, Table 3.5)**
    i. Validation of the ultra-deep RNA sequencing confirmed the expression of 7 circRNAs **(Figure 3.5).**
    ii. The linear isoforms for the circRNAs of interest displayed no differential expression indicating circRNA expression is independent of mRNA alterations **(Figure 3.6).**
    iii. *In-silico* analysis identified several predicted miRNA interactions with our circRNAs of interest that have been pre-established in EH development **(Figure 3.7).**
    iv. miRNA expression analysis identified an association between *circZNF91*, *circGRB10* and *circRP11-298P3.4* with miR-145 and miR-217 **(Figure 3.8)**.
    v. In-silico circRNA-miRNA-mRNA network was established displaying a predicted link between our circRNAs of interest and genes with a known role in either BP regulation or EH development **(Figure 3.9)**.
2. Reduced *circZNF91*, *circGRB10* and *circRP11-298P3.4* expression was induced utilising siRNA transfection **(Chapter 4, Figure 4.1)**
    i. The *circZNF91* **(Figure 4.3 and 4.4)** and *circGRB10* **(Figure 4.4 and 4.5)** knockdown models was unsuccessful in identifying differentially expressed miRNAs, suggesting that these circRNAs might not function as a 'miRNA sponge' but through another mechanism.

ii. The *circRP11-298P3.4* model identified 109 differentially expressed miRNAs with the 37 upregulated miRNAs becoming our ones of interest based on interaction mechanics **(Figure 4.2 and Table 4.3).**

iii. Several of the upregulated miRNAs in the *circRP11-298P3.4* model have been identified to play a role in BP regulation **(Table 4.6).**

3. RNA sequencing identified several differentially expressed genes in each of our knockdown models (**Chapter 5**).

i. The *circZNF91* model identified 2288 differentially expressed genes of which 646 were upregulated and 1642 were downregulated **(Figure 5.1 and Table 5.1)**. Subsequent pathway analysis identified several biological processes impacted by the reduced circRNA expression **(Table 5.6 and 5.7)**. Given a differentially gene was observed in absence of an altered miRNA expression profile further work is required to determine how *circZNF91* exerts its function on downstream gene expression.

ii. The *circGRB10* model identified 2907 differentially expressed genes of which 2233 were upregulated and 574 were downregulated **(Figure 5.3 and 5.2)**. Subsequent pathway analysis identified several biological processes impacted by the reduced circRNA expression **(Table 5.8 and 5.9)**. Given a differentially gene was observed in absence of an altered miRNA expression profile further work is required to determine how *circGRB10* exerts its function on downstream gene expression.

iii. The *circRP11-298P3.4* model identified 32 differentially expressed genes of which 15 were upregulated and 17 downregulated **(Figure 5.5 and Table 5.3).** Subsequent pathway analysis identified several biological processes impacted by the reduced circRNA expression **(Table 5.4 and 5.5).** A number of the

genes identified have a common function that centres around cholesterol synthesis.

iv. Based on the direction of gene expression in this knockdown model a decreased cholesterol synthesis phenotype would be observed. However, the original *circRP11-298P3.4* expression observed in Chapter 3 was upregulated indicating that if we observed the same correlation between circRNA-miRNA-mRNA expression in our 'true' hypertensive phenotype we would expect an increase in cholesterol synthesis.

6.2 Discussion

BP is controlled by a variety of systems, and it is the dysregulation of these systems that contribute to EH development. These include the SNS, the RAAS, renal system via electrolyte homeostasis, natriuretic peptide system and vascular system via endothelial dysfunction. The human kidney is recognised as a key organ of BP regulation and plays a significant role in many of the above-mentioned biological systems making it one of the largest contributors to the development of EH. The unknown cause of EH has led researchers to investigate the role of genetics in the development of EH. The role of epigenetics in EH has gained considerable attention as one of the factors bridging the gap between inherited and lifestyle risk factors. This hypothesis has not been extensively tested in renal tissue. Moreover, the role of renal circRNA in gene expression remains largely unstudied and poorly understood. The focus of this thesis was to investigate the role of circRNAs in EH which was examined by 3 studies. The first study investigated the expression of circRNAs in hypertensive human kidney samples by ultra-deep RNA sequencing technology. The second and third studies utilised the results from study 1, aiming to further elucidate the potential role of these circRNAs of interest. These studies utilised siRNA transfection to decrease expression of our circRNAs of interest followed by miRNA and mRNA sequencing to identify potential downstream targets that are impacted by the altered circRNA expression.

Each study was successful in testing their respective aims with study 1 identifying 12 differentially expressed circRNAs in a large cohort (n=65) of hypertensive human kidney samples from the TRANSLATE study and identifying through *in-silico* techniques potential miRNA interactions that have previously established roles in HT development or BP regulation. In addition to testing circRNA expression it was necessary to analyse the expression of the corresponding linear RNA as recommended by Ashwal-Fluss *et al*., predominantly because circRNA biogenesis competes with pre-mRNA splicing due to both

processes requiring the same splicing machinery [130]. This consequently can lead to an inverse relationship between circRNA expression and its mRNA counterpart. The sequencing analysis conducted in chapter 3 did not identify any differential expression in the mRNAs for our circRNAs of interest, these results confirm the differential circRNA expression was independent of mRNA expression and supports our hypothesis that these circRNAs are altered as a result of elevated BP. Post circRNA validation *in silico* analysis of circRNA-miRNA-mRNA interactions was successful in identifying predicted interactions that may have significant implications in BP regulation and ultimately HT development. For example, *circZNF91* was predicted to interact with miR-145 which has long been associated with different forms of HT [239, 240]. One such study by Wang *et al*., postulated this is due to *miR-145* targeting *SLC7A1* an important amino acid transporter that regulates arginine metabolism [239] contributing to an extracellular deficiency and subsequent reduction in NO production. This occurs due to reduced arginine concentrations which is the rate limiting substrate for eNOS [241]. NO is critical for the maintenance of healthy endothelium and a significant reduction in freely available NO is a major contributor to endothelial dysfunction and subsequent HT development [242]. In addition to established miRNA – mRNA interactions further *in-silico* analysis performed identified several unidentified interactions that may have significant implications in BP regulation and/or HT development. For example, it was predicted that *miR-145* interacts with ATPase plasma membrane Ca2+ transporting 1 (ATP2B1). ATP2B1 promotes the hydrolysis of ATP coupled with the transport of calcium thereby aiding in calcium homeostasis [243]. GWAS studies across several populations has identified *ATP2B1* as a gene of interest in HT development [244, 245] and served as the basis for work undertaken by Kobayashi *et al* (2012). In VSMC *ATP2B1* knockout mice Kobayashi *et al*., (2012) observed higher BP than in the wild-type mice, as measured by the tail-cuff method and radio telemetry [246]. Together these results

presents some potential pathway that our circRNAs of interest can regulate BP and potential contribute HT development which can be tested in future experiments.

The novel circRNA – miRNA – mRNA interactions predicted in Chapter 3 served as the basis for further investigation in study 2 and 3 where the aim was to characterize three of our circRNAs of interest *circZNF91*, *circRP11-298P3.4* and *circGRB10*. This was accomplished utilising siRNA induced knockdown subsequently followed by sRNA sequencing. This aimed to elucidate these circRNAs ability to function as a miRNA sponge. These studies provided mixed results and revealed that further work is required to understand the potential function of *circZNF91* and *circGRB10* as we did not observe any differentially expressed miRNAs from the sequencing results. Future research should focus on the other potential functions of circRNA (outlined in Section 1.6.2) and this theory of an alternate circRNA function has been demonstrated in the context of CVD by Garikipati *et al*., who outlined circFndc3b's ability to modulate cardiac repair post MI through interacting with the RBP Fused in sarcomere (FUS) in sarcomeres to regulate VEGF expression and signalling [146]. Outside of RBP and miRNA sequestering other circRNA functions have yet to be correlated to CVD opening an opportunity to investigate how these alternate functions may relate to our circRNAs of interest and their effect on end stage gene expression.

This alternate circRNA function hypothesis was further supported by the results in Chapter 5 where an altered mRNA expression profile was observed in HEK293 cells with knocked down *circZNF91* and *circGRB10* expression. The mRNA expression was unlikely to have been impacted by changes in the miRNA expression profile but instead through alternative means such as sequestering of RBP's or direct impact on linear RNA expression. The mRNA sequencing results identified several genes with pre-established functions relating to either renal function or BP regulation. One such example is *RAP1B* in the *circZNF91* model. *RAP1B* performs a critical role in the regulation of vascular tone and BP by controlling

responses of endothelium and smooth muscle cells to stimuli, both of which are responsible for coordinating the relaxation–contraction mechanism in blood vessels [247]. Further to *RAP1B* role in vasculature function a significant function has been revealed in renal tubules. Xiao *et al*., discovered that *RAP1B* ameliorates renal tubular injury in individuals suffering from diabetic nephropathy [248]. This is therapeutic effect is achieved via C/EBP-β-PGC-1α signalling. In diabetic nephropathy decreased PGC-1α expression via the ERK1/2–C/EBP-b pathway and phosphorylation of Drp-1 induces an imbalance between mitochondrial fission and fusion proteins leading to an overproduction of ROS and subsequent renal tubular apoptosis [248]. These pathways were reversed with *RAP1B* overexpression suggesting it could regulate mitochondrial specific oxidative stress and slow down diabetic nephropathy progression. Together, these independent research pieces suggest a critical role for *RAP1B* in BP regulation through the vasculature and renal function but how *circZNF91* influences these functions requires further work in addition to identifying additional genes of interest in both the *circGRB10* and *circZNF91* models and the mechanisms at large resulting in downstream gene expression regulation

In contrast, *circRP11-298P3.4* knockdown was successful in producing an altered miRNA profile (Table 4.3) and subsequent mRNA sequencing analysis was able to identify a cohort of differential expressed genes as a result of this reduced circRNA expression (Table 5.3). These results together support the hypothesis that *circRP11-298P3.4* functions as a 'miRNA sponge', upon further analysis of both sequencing results several predicted interactions (Figure 5.10) were uncovered and demonstrated potential for regulating BP and even for HT development. Figure 5.10 outlines a number of predicted circRNA – miRNA – mRNA interactions of interest from these studies and such example is the *circRP11-298P3.4 – miR-34a-5p – TXNIP* network. *TXNIP* is a crucial element in cellular redox signalling which in summary is the cells protection against oxidative stress. *TXNIP* inhibits the antioxidative

function of thioredoxin resulting in the accumulation of ROS. As discussed in Section 1.1.3 an accumulation/imbalance of ROS will result in oxidative stress which is a significant contributor to elevated BP and HT development. Further to this *TXNIP* mediated oxidative stress has been demonstrated as a contributor to renal injury. Han *et al*., identified an increase in mitochondrial ROS was accompanied by an upregulation in *TXNIP* which was responsible for renal tubular oxidative injury [249]. These independent pieces of research have illustrated *TXNIP's* role in BP regulation via oxidative stress mechanisms and potentially via renal injury however this requires further work. This is one example of a circRNA – miRNA – mRNA network with potential implications on either BP regulation, overall renal function and HT development.

Further to *TXNIP*, many of the differentially expressed genes in this model had an interrelated function centring around cholesterol metabolism and biosynthesis. As touched on in Chapter 5, cholesterol has long been established as a key component in CVD development such as atherosclerosis. The correlation however is yet to be fully elucidated in HT but Zhong *et al*., displayed impaired cholesterol homeostasis activates fluid retention pathways in the tubular epithelial cells of the kidney [237]. Similar findings were also demonstrated by Honzumi *et al*., who in C57BL/6 mice feed a high-cholesterol diet observed an increased cholesterol load on the kidney which contributed to the decrease of megalin an endocytic receptor contributing to protein reabsorption [250] . In addition to the reduced megalin, the cholesterol overload is take/deposited in the renal tubule epithelial cells which by consequence caused suppression of cell proliferation. In combination these observations may be a contributing factor to renal damage and fluid retention ultimately contributing to abnormal BP regulation and HT development. These predicted networks are the foundation for future work into the role of *circRP11-298P3.4's* in BP regulation and more specifically

its influence on renal cholesterol synthesis and whether or not its differential expression contributes to elevated BP in humans.

This PhD thesis provides new insight into the role of circRNA expression in renal mediated BP regulation and HT development. This thesis identifies novel relationships between circRNA and downstream targets in the human kidney that influence genes implicated in HT; suggesting a significant role for renal circRNA expression in the altered function of various genes that regulate BP. Collectively, the data presented in this thesis supports the overarching hypothesis that alterations in hypertensive kidney circRNA expression plays a fundamental role in modulating gene expression changes with a potential role in BP regulation. The following section will outline future experimentation needed to enhance the results already generated and further confirm the role of these circRNAs of interest in a hypertensive phenotype.

6.4 Future Directions

Throughout the above chapters future methodologies have been outlined as well as adaptations to further enhance the quality of this research. One of significance is outlined in Chapter 5 Section 5.4 where our studies throughout this thesis have centred around reduced circRNA expression induced by siRNA transfection, however this is contradictory to the initial results we observed in Chapter 3. To fully mimic the hypertensive phenotype *in vitro* overexpression of circRNAs via plasmid transfection would be more appropriate. In conjunction with reduced expression model this would further enhance our understanding of these circRNAs by being able to see how both increased and decreased expression alters miRNA and mRNA expression profile.

In addition to this inducing a more stable knockdown model is fundamental for further understanding the role of our circRNAs of interest. As identified in Chapter 4 the variability between samples in the sRNA sequencing could have potentially contributed to the lack of differentially expressed miRNAs observed in the *circZNF91* and *circGRB10* models. A stable circRNA knockdown model can be achieved utilising CRISPR–Cas13 methodology and is considered the gold standard for reducing circRNA expression [217]. This stable knockdown model is important to establish before further investigating the mediator between *circZNF91* and *circGBR10* influence on mRNA expression. If similar miRNA analysis results are obtained with a stable knockdown model, then this further supports the hypothesis that these two circRNAs of interest manipulate downstream gene expression through a function other than acting as a 'miRNA sponge.'

In addition to the circRNA, sRNA and RNA sequencing experiments we have undertaken it would serve beneficial to undertake single cell sequencing of each respective components of the kidney. At this point in time single cell sequencing has yet screen for circRNA

sequencing. If single cell circRNA sequencing is able to be applied this additional work would pinpoint the specific regions where circRNA expression is more abundant and thus providing valuable insight into specific renal mediated functions and how they regulate BP/ result in HT development.

In-silico analysis has been used thoroughly throughout many of the above chapters. This methodology has allowed us to identify predicted circRNA – miRNA – mRNA networks of interest and correlate these networks with possible effects on BP regulation and HT development. Further work is required now to confirm what are now predicted interactions. The main methodology used to confirm circRNA – miRNA – mRNA networks are luciferase assays. Upon confirmation of these networks this will take the guesswork that currently exists with predicted interactions and allow for definitive cause and effect relationship between circRNA expression and phenotype to be established.

Upon confirmation/establishing the before mentioned methodologies the ideal next/final step in this process would be developing an *in vivo* overexpression model. This would hypothetically reproduce the hypertensive phenotype observed in the TRANSLATE study samples and would allow for BP monitoring in real time and determine how increased expression of either *circZNF91*, *circGRB10* and *circRP11-298P3.4* affect other phenotypes.

References

1. Unger, T., et al., *2020 International Society of Hypertension Global Hypertension Practice Guidelines.* Hypertension, 2020. **75**(6): p. 1334-1357.
2. Carretero, O.A. and S. Oparil, *Essential hypertension. Part I: definition and etiology.* Circulation, 2000. **101**(3): p. 329-35.
3. O'Shea, P.M., T.P. Griffin, and M. Fitzgibbon, *Hypertension: The role of biochemistry in the diagnosis and management.* Clin Chim Acta, 2017. **465**: p. 131-143.
4. Chang, A.R., et al., *Blood Pressure Goals in Patients with CKD: A Review of Evidence and Guidelines.* Clin J Am Soc Nephrol, 2019. **14**(1): p. 161-169.
5. Dickson, M.E. and C.D. Sigmund, *Genetic basis of hypertension: revisiting angiotensinogen.* Hypertension, 2006. **48**(1): p. 14-20.
6. Hird, T.R., et al., *Productivity Burden of Hypertension in Australia.* Hypertension, 2019. **73**(4): p. 777-784.
7. Forouzanfar, M.H., et al., *Global Burden of Hypertension and Systolic Blood Pressure of at Least 110 to 115 mm Hg, 1990-2015.* JAMA, 2017. **317**(2): p. 165-182.
8. Newton-Cheh, C., et al., *Genome-wide association study identifies eight loci associated with blood pressure.* Nat Genet, 2009. **41**(6): p. 666-76.
9. World Health Organisation. *A Global Brief on Hypertension, Silent Killer, Global Public Health Crisis.* 2013 October 20, 2020]; Available from: https://apps.who.int/iris/bitstream/handle/10665/79059/WHO_DCO_WHD_2013.2_eng.pdf?sequence=1.
10. Warren, H.R., et al., *Genome-wide association analysis identifies novel blood pressure loci and offers biological insights into cardiovascular risk.* Nat Genet, 2017. **49**(3): p. 403-415.
11. Hoffmann, T.J., et al., *Genome-wide association analyses using electronic health records identify new loci influencing blood pressure variation.* Nat Genet, 2017. **49**(1): p. 54-64.
12. Wain, L.V., et al., *Genome-wide association study identifies six new loci influencing pulse pressure and mean arterial pressure.* Nat Genet, 2011. **43**(10): p. 1005-11.
13. Kato, N., et al., *Meta-analysis of genome-wide association studies identifies common variants associated with blood pressure variation in east Asians.* Nat Genet, 2011. **43**(6): p. 531-8.
14. International Consortium for Blood Pressure Genome-Wide Association, S., et al., *Genetic variants in novel pathways influence blood pressure and cardiovascular disease risk.* Nature, 2011. **478**(7367): p. 103-9.
15. Padmanabhan, S., et al., *Genome-wide association study of blood pressure extremes identifies variant near UMOD associated with hypertension.* PLoS Genet, 2010. **6**(10): p. e1001177.
16. Levy, D., et al., *Genome-wide association study of blood pressure and hypertension.* Nat Genet, 2009. **41**(6): p. 677-87.
17. Evangelou, E., et al., *Genetic analysis of over 1 million people identifies 535 new loci associated with blood pressure traits.* Nat Genet, 2018. **50**(10): p. 1412-1425.
18. Ulrich-Lai, Y.M. and J.P. Herman, *Neural regulation of endocrine and autonomic stress responses.* Nat Rev Neurosci, 2009. **10**(6): p. 397-409.
19. Munoz-Durango, N., et al., *Role of the Renin-Angiotensin-Aldosterone System beyond Blood Pressure Regulation: Molecular and Cellular Mechanisms Involved in End-Organ Damage during Arterial Hypertension.* Int J Mol Sci, 2016. **17**(7).

20. McKie, P.M., T. Ichiki, and J.C. Burnett, Jr., *M-atrial natriuretic peptide: a novel antihypertensive protein therapy.* Curr Hypertens Rep, 2012. **14**(1): p. 62-9.
21. Oparil, S., M.A. Zaman, and D.A. Calhoun, *Pathogenesis of hypertension.* Ann Intern Med, 2003. **139**(9): p. 761-76.
22. Mancia, G. and G. Grassi, *The autonomic nervous system and hypertension.* Circ Res, 2014. **114**(11): p. 1804-14.
23. Bolivar, J.J., *Essential hypertension: an approach to its etiology and neurogenic pathophysiology.* Int J Hypertens, 2013. **2013**: p. 547809.
24. DiBona, G.F. and M. Esler, *Translational medicine: the antihypertensive effect of renal denervation.* Am J Physiol Regul Integr Comp Physiol, 2010. **298**(2): p. R245-53.
25. Head, G.A., et al., *Central nervous system dysfunction in obesity-induced hypertension.* Curr Hypertens Rep, 2014. **16**(9): p. 466.
26. Grassi, G., et al., *Neuroadrenergic and reflex abnormalities in patients with metabolic syndrome.* Diabetologia, 2005. **48**(7): p. 1359-65.
27. Brook, R.D. and S. Julius, *Autonomic imbalance, hypertension, and cardiovascular risk.* Am J Hypertens, 2000. **13**(6 Pt 2): p. 112S-122S.
28. Touyz, R.M., et al., *Vascular smooth muscle contraction in hypertension.* Cardiovasc Res, 2018. **114**(4): p. 529-539.
29. Levick, S.P., et al., *Sympathetic nervous system modulation of inflammation and remodeling in the hypertensive heart.* Hypertension, 2010. **55**(2): p. 270-6.
30. Kelm, M., et al., *Left ventricular mass is linked to cardiac noradrenaline in normotensive and hypertensive patients.* Journal of Hypertension, 1996. **14**(11): p. 1357-1364.
31. Nguyen, G., *Renin, (pro)renin and receptor: an update.* Clin Sci (Lond), 2011. **120**(5): p. 169-78.
32. Fountain, J.H. and S.L. Lappin, *Physiology, Renin Angiotensin System*, in *StatPearls*. 2020: Treasure Island (FL).
33. Guyton, A.C., *Abnormal renal function and autoregulation in essential hypertension.* Hypertension, 1991. **18**(5 Suppl): p. III49-53.
34. Jaisser, F. and N. Farman, *Emerging Roles of the Mineralocorticoid Receptor in Pathology: Toward New Paradigms in Clinical Pharmacology.* Pharmacol Rev, 2016. **68**(1): p. 49-75.
35. Campbell, D.J., *Clinical relevance of local Renin Angiotensin systems.* Front Endocrinol (Lausanne), 2014. **5**: p. 113.
36. Nemecz, M., et al., *Role of MicroRNA in Endothelial Dysfunction and Hypertension.* Curr Hypertens Rep, 2016. **18**(12): p. 87.
37. Flammer, A.J., et al., *The assessment of endothelial function: from research into clinical practice.* Circulation, 2012. **126**(6): p. 753-67.
38. Rajendran, P., et al., *The vascular endothelium and human diseases.* Int J Biol Sci, 2013. **9**(10): p. 1057-69.
39. Sandoo, A., et al., *The endothelium and its role in regulating vascular tone.* Open Cardiovasc Med J, 2010. **4**: p. 302-12.
40. Senoner, T. and W. Dichtl, *Oxidative Stress in Cardiovascular Diseases: Still a Therapeutic Target?* Nutrients, 2019. **11**(9).
41. Magenta, A., et al., *Oxidative stress and microRNAs in vascular diseases.* Int J Mol Sci, 2013. **14**(9): p. 17319-46.
42. Lubos, E., D.E. Handy, and J. Loscalzo, *Role of oxidative stress and nitric oxide in atherothrombosis.* Front Biosci, 2008. **13**: p. 5323-44.

43. Sinha, N. and P.K. Dabla, *Oxidative stress and antioxidants in hypertension-a current review.* Curr Hypertens Rev, 2015. **11**(2): p. 132-42.
44. Fukai, T. and M. Ushio-Fukai, *Superoxide dismutases: role in redox signaling, vascular function, and diseases.* Antioxid Redox Signal, 2011. **15**(6): p. 1583-606.
45. Potter, L.R., S. Abbey-Hosch, and D.M. Dickey, *Natriuretic peptides, their receptors, and cyclic guanosine monophosphate-dependent signaling functions.* Endocr Rev, 2006. **27**(1): p. 47-72.
46. Zois, N.E., et al., *Natriuretic peptides in cardiometabolic regulation and disease.* Nat Rev Cardiol, 2014. **11**(7): p. 403-12.
47. Sarzani, R., et al., *Expression of natriuretic peptide receptors in human adipose and other tissues.* J Endocrinol Invest, 1996. **19**(9): p. 581-5.
48. Volpe, M., M. Carnovali, and V. Mastromarino, *The natriuretic peptides system in the pathophysiology of heart failure: from molecular basis to treatment.* Clin Sci (Lond), 2016. **130**(2): p. 57-77.
49. Cannone, V., et al., *Atrial Natriuretic Peptide: A Molecular Target of Novel Therapeutic Approaches to Cardio-Metabolic Disease.* Int J Mol Sci, 2019. **20**(13).
50. Spiranec, K., et al., *Endothelial C-Type Natriuretic Peptide Acts on Pericytes to Regulate Microcirculatory Flow and Blood Pressure.* Circulation, 2018. **138**(5): p. 494-508.
51. Steinhelper, M.E., K.L. Cochrane, and L.J. Field, *Hypotension in transgenic mice expressing atrial natriuretic factor fusion genes.* Hypertension, 1990. **16**(3): p. 301-7.
52. Ogawa, Y., et al., *Molecular cloning of the complementary DNA and gene that encode mouse brain natriuretic peptide and generation of transgenic mice that overexpress the brain natriuretic peptide gene.* J Clin Invest, 1994. **93**(5): p. 1911-21.
53. Bae, E.H., et al., *Altered regulation of renal nitric oxide and atrial natriuretic peptide systems in angiotensin II-induced hypertension.* Regul Pept, 2011. **170**(1-3): p. 31-7.
54. Ito, T., et al., *Inhibitory effect of natriuretic peptides on aldosterone synthase gene expression in cultured neonatal rat cardiocytes.* Circulation, 2003. **107**(6): p. 807-10.
55. Akabane, S., et al., *Effects of brain natriuretic peptide on renin secretion in normal and hypertonic saline-infused kidney.* Eur J Pharmacol, 1991. **198**(2-3): p. 143-8.
56. Guyton, A.C., *Physiologic regulation of arterial pressure.* Am J Cardiol, 1961. **8**: p. 401-7.
57. Guyton, A.C., T.G. Coleman, and H.J. Granger, *Circulation: overall regulation.* Annu Rev Physiol, 1972. **34**: p. 13-46.
58. Wadei, H.M. and S.C. Textor, *The role of the kidney in regulating arterial blood pressure.* Nat Rev Nephrol, 2012. **8**(10): p. 602-9.
59. Stevens, P.E., A. Levin, and M. Kidney Disease: Improving Global Outcomes Chronic Kidney Disease Guideline Development Work Group, *Evaluation and management of chronic kidney disease: synopsis of the kidney disease: improving global outcomes 2012 clinical practice guideline.* Ann Intern Med, 2013. **158**(11): p. 825-30.
60. McCullough, P.A., et al., *National Kidney Foundation's Kidney Early Evaluation Program (KEEP) annual data report 2010: executive summary.* Am J Kidney Dis, 2011. **57**(3 Suppl 2): p. S1-3.
61. Levey, A.S., et al., *National Kidney Foundation practice guidelines for chronic kidney disease: evaluation, classification, and stratification.* Ann Intern Med, 2003. **139**(2): p. 137-47.
62. DiBona, G.F., *Physiology in perspective: The Wisdom of the Body. Neural control of the kidney.* Am J Physiol Regul Integr Comp Physiol, 2005. **289**(3): p. R633-41.

63. Klein, I.H., et al., *Sympathetic activity is increased in polycystic kidney disease and is associated with hypertension.* J Am Soc Nephrol, 2001. **12**(11): p. 2427-33.
64. Ingelfinger, J.R., et al., *Sodium regulation of angiotensinogen mRNA expression in rat kidney cortex and medulla.* J Clin Invest, 1986. **78**(5): p. 1311-5.
65. Lalouel, J.M. and A. Rohrwasser, *Genetic susceptibility to essential hypertension: insight from angiotensinogen.* Hypertension, 2007. **49**(3): p. 597-603.
66. Thethi, T., M. Kamiyama, and H. Kobori, *The link between the renin-angiotensin-aldosterone system and renal injury in obesity and the metabolic syndrome.* Curr Hypertens Rep, 2012. **14**(2): p. 160-9.
67. Gonzalez, A.A. and M.C. Prieto, *Renin and the (pro)renin receptor in the renal collecting duct: Role in the pathogenesis of hypertension.* Clin Exp Pharmacol Physiol, 2015. **42**(1): p. 14-21.
68. Xue, C. and H.M. Siragy, *Local renal aldosterone system and its regulation by salt, diabetes, and angiotensin II type 1 receptor.* Hypertension, 2005. **46**(3): p. 584-90.
69. Ahn, D., et al., *Collecting duct-specific knockout of endothelin-1 causes hypertension and sodium retention.* J Clin Invest, 2004. **114**(4): p. 504-11.
70. Hynynen, M.M. and R.A. Khalil, *The vascular endothelin system in hypertension--recent patents and discoveries.* Recent Pat Cardiovasc Drug Discov, 2006. **1**(1): p. 95-108.
71. Bruzzi, I., et al., *Time course and localization of endothelin-1 gene expression in a model of renal disease progression.* Am J Pathol, 1997. **151**(5): p. 1241-7.
72. D'Amours, M., et al., *Increased ET-1 and reduced ET(B) receptor expression in uremic hypertensive rats.* Clin Exp Hypertens, 2010. **32**(1): p. 61-9.
73. Alexander, B.T., et al., *Enhanced renal expression of preproendothelin mRNA during chronic angiotensin II hypertension.* Am J Physiol Regul Integr Comp Physiol, 2001. **280**(5): p. R1388-92.
74. Barton, M., et al., *ET(A) receptor blockade prevents increased tissue endothelin-1, vascular hypertrophy, and endothelial dysfunction in salt-sensitive hypertension.* Hypertension, 1998. **31**(1 Pt 2): p. 499-504.
75. Allcock, G.H., R.C. Venema, and D.M. Pollock, *ETA receptor blockade attenuates the hypertension but not renal dysfunction in DOCA-salt rats.* Am J Physiol, 1998. **275**(1): p. R245-52.
76. Guidi, E., et al., *Hypertension may be transplanted with the kidney in humans: a long-term historical prospective follow-up of recipients grafted with kidneys coming from donors with or without hypertension in their families.* J Am Soc Nephrol, 1996. **7**(8): p. 1131-8.
77. Harrap, S.B., et al., *Familial patterns of covariation for cardiovascular risk factors in adults: The Victorian Family Heart Study.* Am J Epidemiol, 2000. **152**(8): p. 704-15.
78. Xu, X., et al., *Genetic and environmental influences on blood pressure variability: a study in twins.* J Hypertens, 2013. **31**(4): p. 690-7.
79. Arnett, D.K. and S.A. Claas, *Omics of Blood Pressure and Hypertension.* Circ Res, 2018. **122**(10): p. 1409-1419.
80. Gandhi, S., F. Ruehle, and M. Stoll, *Evolutionary Patterns of Non-Coding RNA in Cardiovascular Biology.* Noncoding RNA, 2019. **5**(1).
81. Das, A., A. Samidurai, and F.N. Salloum, *Deciphering Non-coding RNAs in Cardiovascular Health and Disease.* Front Cardiovasc Med, 2018. **5**: p. 73.
82. Mitchell, P.S., et al., *Circulating microRNAs as stable blood-based markers for cancer detection.* Proc Natl Acad Sci U S A, 2008. **105**(30): p. 10513-8.
83. Zhu, H. and S.W. Leung, *Identification of microRNA biomarkers in type 2 diabetes: a meta-analysis of controlled profiling studies.* Diabetologia, 2015. **58**(5): p. 900-11.

84. Pisarello, M.J., et al., *MicroRNAs in the Cholangiopathies: Pathogenesis, Diagnosis, and Treatment.* J Clin Med, 2015. **4**(9): p. 1688-712.
85. Bartel, D.P., *MicroRNAs: genomics, biogenesis, mechanism, and function.* Cell, 2004. **116**(2): p. 281-97.
86. Catalanotto, C., C. Cogoni, and G. Zardo, *MicroRNA in Control of Gene Expression: An Overview of Nuclear Functions.* Int J Mol Sci, 2016. **17**(10).
87. Broughton, J.P., et al., *Pairing beyond the Seed Supports MicroRNA Targeting Specificity.* Mol Cell, 2016. **64**(2): p. 320-333.
88. Ardekani, A.M. and M.M. Naeini, *The Role of MicroRNAs in Human Diseases.* Avicenna J Med Biotechnol, 2010. **2**(4): p. 161-79.
89. Marzi, M.J., et al., *Degradation dynamics of microRNAs revealed by a novel pulse-chase approach.* Genome Res, 2016. **26**(4): p. 554-65.
90. Romaine, S.P., et al., *Circulating microRNAs and hypertension--from new insights into blood pressure regulation to biomarkers of cardiovascular risk.* Curr Opin Pharmacol, 2016. **27**: p. 1-7.
91. Cengiz, M., et al., *Circulating miR-21 and eNOS in subclinical atherosclerosis in patients with hypertension.* Clin Exp Hypertens, 2015. **37**(8): p. 643-9.
92. Badawy, H.K., D.M. Abo-Elmatty, and N.M. Mesbah, *Differential expression of MicroRNA let-7e and 296-5p in plasma of Egyptian patients with essential hypertension.* Heliyon, 2018. **4**(11): p. e00969.
93. Baker, M.A., et al., *MiR-192-5p in the Kidney Protects Against the Development of Hypertension.* Hypertension, 2019. **73**(2): p. 399-406.
94. Carr, G., et al., *MicroRNA-153 targeting of KCNQ4 contributes to vascular dysfunction in hypertension.* Cardiovasc Res, 2016. **112**(2): p. 581-589.
95. Cengiz, M., et al., *Differential expression of hypertension-associated microRNAs in the plasma of patients with white coat hypertension.* Medicine (Baltimore), 2015. **94**(13): p. e693.
96. Chen, Z., et al., *Identification of potential candidate genes for hypertensive nephropathy based on gene expression profile.* BMC Nephrol, 2016. **17**(1): p. 149.
97. Dluzen, D.F., et al., *MicroRNAs Modulate Oxidative Stress in Hypertension through PARP-1 Regulation.* Oxid Med Cell Longev, 2017. **2017**: p. 3984280.
98. Huang, Y., et al., *Circulating miR-92a expression level in patients with essential hypertension: a potential marker of atherosclerosis.* J Hum Hypertens, 2017. **31**(3): p. 200-205.
99. Klimczak, D., et al., *Plasma microRNA-155-5p is increased among patients with chronic kidney disease and nocturnal hypertension.* J Am Soc Hypertens, 2017. **11**(12): p. 831-841 e4.
100. Krishnan, R., et al., *Expression and methylation of circulating microRNA-510 in essential hypertension.* Hypertens Res, 2017. **40**(4): p. 361-363.
101. Ling, S., et al., *Modulation of microRNAs in hypertension-induced arterial remodeling through the beta1 and beta3-adrenoreceptor pathways.* J Mol Cell Cardiol, 2013. **65**: p. 127-36.
102. Liu, J., et al., *Preliminary study of microRNA-126 as a novel therapeutic target for primary hypertension.* Int J Mol Med, 2018. **41**(4): p. 1835-1844.
103. Liu, Y., et al., *MicroRNA-214-3p in the Kidney Contributes to the Development of Hypertension.* J Am Soc Nephrol, 2018. **29**(10): p. 2518-2528.
104. Luo, Y., et al., *A potential risk factor of essential hypertension in case-control study: MicroRNAs miR-10a-5p.* Clin Exp Hypertens, 2019: p. 1-7.
105. Marketou, M., et al., *Platelet microRNAs in hypertensive patients with and without cardiovascular disease.* J Hum Hypertens, 2019. **33**(2): p. 149-156.

106. Marques, F.Z., et al., *Signatures of miR-181a on the Renal Transcriptome and Blood Pressure.* Mol Med, 2015. **21**(1): p. 739-748.
107. Tian, X., et al., *MicroRNA-199a-5p aggravates primary hypertension by damaging vascular endothelial cells through inhibition of autophagy and promotion of apoptosis.* Exp Ther Med, 2018. **16**(2): p. 595-602.
108. Yang, Q., et al., *MicroRNA-505 identified from patients with essential hypertension impairs endothelial cell migration and tube formation.* Int J Cardiol, 2014. **177**(3): p. 925-34.
109. Yi, F., et al., *Overexpression of microRNA-506-3p aggravates the injury of vascular endothelial cells in patients with hypertension by downregulating Beclin1 expression.* Exp Ther Med, 2018. **15**(3): p. 2844-2850.
110. Zhang, Z., et al., *Blood pressure and expression of microRNAs in whole blood.* PLoS One, 2017. **12**(3): p. e0173550.
111. Zhang, Z., T. Yang, and J. Xiao, *Circular RNAs: Promising Biomarkers for Human Diseases.* EBioMedicine, 2018. **34**: p. 267-274.
112. Zhao, X., Y. Cai, and J. Xu, *Circular RNAs: Biogenesis, Mechanism, and Function in Human Cancers.* Int J Mol Sci, 2019. **20**(16).
113. Jeck, W.R., et al., *Circular RNAs are abundant, conserved, and associated with ALU repeats.* RNA, 2013. **19**(2): p. 141-57.
114. Chen, I., C.Y. Chen, and T.J. Chuang, *Biogenesis, identification, and function of exonic circular RNAs.* Wiley Interdiscip Rev RNA, 2015. **6**(5): p. 563-79.
115. Black, D.L., *Mechanisms of alternative pre-messenger RNA splicing.* Annu Rev Biochem, 2003. **72**: p. 291-336.
116. Qu, S., et al., *Circular RNA: A new star of noncoding RNAs.* Cancer Lett, 2015. **365**(2): p. 141-8.
117. Holdt, L.M., A. Kohlmaier, and D. Teupser, *Molecular roles and function of circular RNAs in eukaryotic cells.* Cell Mol Life Sci, 2018. **75**(6): p. 1071-1098.
118. Szmulewicz, M.N., G.E. Novick, and R.J. Herrera, *Effects of Alu insertions on gene function.* Electrophoresis, 1998. **19**(8-9): p. 1260-4.
119. Salzman, J., *Circular RNA Expression: Its Potential Regulation and Function.* Trends Genet, 2016. **32**(5): p. 309-316.
120. Holdt, L.M., et al., *Circular non-coding RNA ANRIL modulates ribosomal RNA maturation and atherosclerosis in humans.* Nat Commun, 2016. **7**: p. 12429.
121. Starke, S., et al., *Exon circularization requires canonical splice signals.* Cell Rep, 2015. **10**(1): p. 103-11.
122. Surono, A., et al., *Circular dystrophin RNAs consisting of exons that were skipped by alternative splicing.* Hum Mol Genet, 1999. **8**(3): p. 493-500.
123. Szabo, L., et al., *Statistically based splicing detection reveals neural enrichment and tissue-specific induction of circular RNA during human fetal development.* Genome Biol, 2015. **16**: p. 126.
124. Rybak-Wolf, A., et al., *Circular RNAs in the Mammalian Brain Are Highly Abundant, Conserved, and Dynamically Expressed.* Mol Cell, 2015. **58**(5): p. 870-85.
125. Salzman, J., et al., *Circular RNAs are the predominant transcript isoform from hundreds of human genes in diverse cell types.* PLoS One, 2012. **7**(2): p. e30733.
126. Chen, D., et al., *Circular RNA circHIPK3 promotes cell proliferation and invasion of prostate cancer by sponging miR-193a-3p and regulating MCL1 expression.* Cancer Manag Res, 2019. **11**: p. 1415-1423.
127. Capel, B., et al., *Circular transcripts of the testis-determining gene Sry in adult mouse testis.* Cell, 1993. **73**(5): p. 1019-30.

128. Hansen, T.B., et al., *Natural RNA circles function as efficient microRNA sponges.* Nature, 2013. **495**(7441): p. 384-8.
129. Abdelmohsen, K., et al., *Identification of HuR target circular RNAs uncovers suppression of PABPN1 translation by CircPABPN1.* RNA Biol, 2017. **14**(3): p. 361-369.
130. Ashwal-Fluss, R., et al., *circRNA biogenesis competes with pre-mRNA splicing.* Mol Cell, 2014. **56**(1): p. 55-66.
131. Pamudurti, N.R., et al., *Translation of CircRNAs.* Mol Cell, 2017. **66**(1): p. 9-21 e7.
132. Yang, Y., et al., *Extensive translation of circular RNAs driven by N(6)-methyladenosine.* Cell Res, 2017. **27**(5): p. 626-641.
133. Wu, N., L. Jin, and J. Cai, *Profiling and bioinformatics analyses reveal differential circular RNA expression in hypertensive patients.* Clin Exp Hypertens, 2017. **39**(5): p. 454-459.
134. Bao, X., et al., *Up-regulation of circular RNA hsa_circ_0037909 promotes essential hypertension.* J Clin Lab Anal, 2019: p. e22853.
135. Bao, X., et al., *A potential risk factor of essential hypertension in case-control study: Circular RNA hsa_circ_0037911.* Biochem Biophys Res Commun, 2018. **498**(4): p. 789-794.
136. Liu, L., et al., *Microarray Profiling of Circular RNA Identifies hsa_circ_0126991 as a Potential Risk Factor for Essential Hypertension.* Cytogenet Genome Res, 2019.
137. Zheng, S., et al., *Circular RNA hsa_circ_0014243 may serve as a diagnostic biomarker for essential hypertension.* Exp Ther Med, 2019. **17**(3): p. 1728-1736.
138. Zheng, S., et al., *The up-regulated hsa-circRNA9102-5 may be a risk factor for essential hypertension.* J Clin Lab Anal, 2020: p. e23339.
139. Lu, C., et al., *CircNr1h4 regulates the pathological process of renal injury in salt-sensitive hypertensive mice by targeting miR-155-5p.* J Cell Mol Med, 2020. **24**(2): p. 1700-1712.
140. Yin, L., et al., *Identification of candidate lncRNAs and circRNAs regulating WNT3/beta-catenin signaling in essential hypertension.* Aging (Albany NY), 2020. **12**(9): p. 8261-8288.
141. He, X., et al., *The microarray identification circular RNA hsa_circ_0105015 up-regulated involving inflammation pathway in essential hypertension.* J Clin Lab Anal, 2020: p. e23603.
142. Tao, Z., et al., *Hsa_circ_0037897 may be a risk factor for essential hypertension via hsa-miR-145-5p.* Clin Exp Hypertens, 2020: p. 1-6.
143. Geng, H.H., et al., *The Circular RNA Cdr1as Promotes Myocardial Infarction by Mediating the Regulation of miR-7a on Its Target Genes Expression.* PLoS One, 2016. **11**(3): p. e0151753.
144. Cai, L., et al., *Circular RNA Ttc3 regulates cardiac function after myocardial infarction by sponging miR-15b.* J Mol Cell Cardiol, 2019. **130**: p. 10-22.
145. Huang, S., et al., *Loss of Super-Enhancer-Regulated circRNA Nfix Induces Cardiac Regeneration After Myocardial Infarction in Adult Mice.* Circulation, 2019. **139**(25): p. 2857-2876.
146. Garikipati, V.N.S., et al., *Circular RNA CircFndc3b modulates cardiac repair after myocardial infarction via FUS/VEGF-A axis.* Nat Commun, 2019. **10**(1): p. 4317.
147. Shen, L., et al., *CircRNA0044073 is upregulated in atherosclerosis and increases the proliferation and invasion of cells by targeting miR107.* Mol Med Rep, 2019. **19**(5): p. 3923-3932.

148. Zhang, F., et al., *Comprehensive analysis of circRNA expression pattern and circRNA-miRNA-mRNA network in the pathogenesis of atherosclerosis in rabbits.* Aging (Albany NY), 2018. **10**(9): p. 2266-2283.
149. Yang, L., et al., *Circular RNA circCHFR Facilitates the Proliferation and Migration of Vascular Smooth Muscle via miR-370/FOXO1/Cyclin D1 Pathway.* Mol Ther Nucleic Acids, 2019. **16**: p. 434-441.
150. Shang, L., et al., *MicroRNA-148a-3p promotes survival and migration of endothelial cells isolated from Apoe deficient mice through restricting circular RNA 0003575.* Gene, 2019. **711**: p. 143948.
151. Li, C.Y., L. Ma, and B. Yu, *Circular RNA hsa_circ_0003575 regulates oxLDL induced vascular endothelial cells proliferation and angiogenesis.* Biomed Pharmacother, 2017. **95**: p. 1514-1519.
152. Wang, L., et al., *Identification of circular RNA Hsa_circ_0001879 and Hsa_circ_0004104 as novel biomarkers for coronary artery disease.* Atherosclerosis, 2019. **286**: p. 88-96.
153. Zhao, Z., et al., *Peripheral blood circular RNA hsa_circ_0124644 can be used as a diagnostic biomarker of coronary artery disease.* Sci Rep, 2017. **7**: p. 39918.
154. Lin, F., et al., *circRNAmiRNA association for coronary heart disease.* Mol Med Rep, 2019. **19**(4): p. 2527-2536.
155. Matsuki, K., et al., *The role of transforming growth factor beta1 in the regulation of blood pressure.* Curr Hypertens Rev, 2014. **10**(4): p. 223-38.
156. Kim, Y., et al., *Posttranscriptional Regulation of the Inflammatory Marker C-Reactive Protein by the RNA-Binding Protein HuR and MicroRNA 637.* Mol Cell Biol, 2015. **35**(24): p. 4212-21.
157. Drosos, G., et al., *Serum Creatinine and Chronic Kidney Disease-Epidemiology Estimated Glomerular Filtration Rate: Independent Predictors of Renal Replacement Therapy following Cardiac Surgery.* Am J Nephrol, 2018. **48**(2): p. 108-117.
158. Fang, Y., et al., *MicroRNA-10a regulation of proinflammatory phenotype in athero-susceptible endothelium in vivo and in vitro.* Proc Natl Acad Sci U S A, 2010. **107**(30): p. 13450-5.
159. Robbins, C.S., et al., *Local proliferation dominates lesional macrophage accumulation in atherosclerosis.* Nat Med, 2013. **19**(9): p. 1166-72.
160. Wu, X., et al., *NLRP3 in fl ammasome mediates chronic intermittent hypoxia-induced renal injury implication of the microRNA-155/FOXO3a signaling pathway.* J Cell Physiol, 2018. **233**(12): p. 9404-9415.
161. Liu, D.F., et al., *The involvement of miR-155 in blood pressure regulation in pregnant hypertension rat via targeting FOXO3a.* Eur Rev Med Pharmacol Sci, 2018. **22**(20): p. 6591-6598.
162. Smit, M., A.R. Coetzee, and A. Lochner, *The Pathophysiology of Myocardial Ischemia and Perioperative Myocardial Infarction.* J Cardiothorac Vasc Anesth, 2019.
163. Collaborators, G.B.D.R.F., *Global, regional, and national comparative risk assessment of 79 behavioural, environmental and occupational, and metabolic risks or clusters of risks, 1990-2015: a systematic analysis for the Global Burden of Disease Study 2015.* Lancet, 2016. **388**(10053): p. 1659-1724.
164. Law, M., N. Wald, and J. Morris, *Lowering blood pressure to prevent myocardial infarction and stroke: a new preventive strategy.* Health Technol Assess, 2003. **7**(31): p. 1-94.

165. Wu, H.J., et al., *Microarray Expression Profile of Circular RNAs in Heart Tissue of Mice with Myocardial Infarction-Induced Heart Failure.* Cell Physiol Biochem, 2016. **39**(1): p. 205-16.
166. Li, B., et al., *MicroRNA-7a/b protects against cardiac myocyte injury in ischemia/reperfusion by targeting poly(ADP-ribose) polymerase.* PLoS One, 2014. **9**(3): p. e90096.
167. Nishi, H., et al., *MicroRNA-15b modulates cellular ATP levels and degenerates mitochondria via Arl2 in neonatal rat cardiac myocytes.* J Biol Chem, 2010. **285**(7): p. 4920-30.
168. Gimbrone, M.A., Jr. and G. Garcia-Cardena, *Endothelial Cell Dysfunction and the Pathobiology of Atherosclerosis.* Circ Res, 2016. **118**(4): p. 620-36.
169. Pan, R.Y., et al., *Circular RNA profile in coronary artery disease.* Am J Transl Res, 2019. **11**(11): p. 7115-7125.
170. Yu, F., et al., *Circular RNA expression profiles and bioinformatic analysis in coronary heart disease.* Epigenomics, 2020. **12**(5): p. 439-454.
171. Vilades, D., et al., *Plasma circular RNA hsa_circ_0001445 and coronary artery disease: Performance as a biomarker.* FASEB J, 2020. **34**(3): p. 4403-4414.
172. Dudekula, D.B., et al., *CircInteractome: A web tool for exploring circular RNAs and their interacting proteins and microRNAs.* RNA Biol, 2016. **13**(1): p. 34-42.
173. Panda, A.C. and M. Gorospe, *Detection and Analysis of Circular RNAs by RT-PCR.* Bio Protoc, 2018. **8**(6).
174. Pfaffl, M.W., G.W. Horgan, and L. Dempfle, *Relative expression software tool (REST) for group-wise comparison and statistical analysis of relative expression results in real-time PCR.* Nucleic Acids Res, 2002. **30**(9): p. e36.
175. Messerli, F.H., B. Williams, and E. Ritz, *Essential hypertension.* The Lancet, 2007. **370**(9587): p. 591-603.
176. Zaiou, M., *Circular RNAs in hypertension: challenges and clinical promise.* Hypertens Res, 2019. **42**(11): p. 1653-1663.
177. Kristensen, L.S., et al., *Circular RNAs in cancer: opportunities and challenges in the field.* Oncogene, 2018. **37**(5): p. 555-565.
178. Tomaszewski, M., et al., *Pathway analysis shows association between FGFBP1 and hypertension.* J Am Soc Nephrol, 2011. **22**(5): p. 947-55.
179. Tomaszewski, M., et al., *Renal Mechanisms of Association between Fibroblast Growth Factor 1 and Blood Pressure.* J Am Soc Nephrol, 2015. **26**(12): p. 3151-60.
180. Szabo, L. and J. Salzman, *Detecting circular RNAs: bioinformatic and experimental challenges.* Nat Rev Genet, 2016. **17**(11): p. 679-692.
181. Chen, Y., et al., *SOAPnuke: a MapReduce acceleration-supported software for integrated quality control and preprocessing of high-throughput sequencing data.* Gigascience, 2018. **7**(1): p. 1-6.
182. Glazar, P., P. Papavasileiou, and N. Rajewsky, *circBase: a database for circular RNAs.* RNA, 2014. **20**(11): p. 1666-70.
183. Panda, A.C., et al., *Analysis of Circular RNAs Using the Web Tool CircInteractome.* Methods Mol Biol, 2018. **1724**: p. 43-56.
184. Han, F., et al., *MiR-217 mediates the protective effects of the dopamine D2 receptor on fibrosis in human renal proximal tubule cells.* Hypertension, 2015. **65**(5): p. 1118-25.
185. Hatziioanou, D., et al., *Chloride Intracellular Channel 4 Overexpression in the Proximal Tubules of Kidneys from the Spontaneously Hypertensive Rat: Insight from Proteomic Analysis.* Nephron, 2018. **138**(1): p. 60-70.

186. Xu, Y., et al., *Suppression of CLIC4/mtCLIC enhances hydrogen peroxide-induced apoptosis in C6 glioma cells.* Oncol Rep, 2013. **29**(4): p. 1483-91.
187. Chou, S.Y., et al., *CLIC4 regulates apical exocytosis and renal tube luminogenesis through retromer- and actin-mediated endocytic trafficking.* Nat Commun, 2016. **7**: p. 10412.
188. Wang, B., et al., *Enhanced cadmium-induced testicular necrosis and renal proximal tubule damage caused by gene-dose increase in a Slc39a8-transgenic mouse line.* Am J Physiol Cell Physiol, 2007. **292**(4): p. C1523-35.
189. Zhang, R., et al., *A blood pressure-associated variant of the SLC39A8 gene influences cellular cadmium accumulation and toxicity.* Hum Mol Genet, 2016. **25**(18): p. 4117-4126.
190. Varoni, M.V., et al., *Cadmium as an environmental factor of hypertension in animals: new perspectives on mechanisms.* Vet Res Commun, 2003. **27 Suppl 1**: p. 807-10.
191. Li, X., et al., *AGO2 and its partners: a silencing complex, a chromatin modulator, and new features.* Crit Rev Biochem Mol Biol, 2020. **55**(1): p. 33-53.
192. Yu, C.Y., et al., *The circular RNA circBIRC6 participates in the molecular circuitry controlling human pluripotency.* Nat Commun, 2017. **8**(1): p. 1149.
193. Marques, F.Z. and F.J. Charchar, *microRNAs in Essential Hypertension and Blood Pressure Regulation.* Adv Exp Med Biol, 2015. **888**: p. 215-35.
194. Rahman, R.U., et al., *Oasis 2: improved online analysis of small RNA-seq data.* BMC Bioinformatics, 2018. **19**(1): p. 54.
195. Robinson, M.D., D.J. McCarthy, and G.K. Smyth, *edgeR: a Bioconductor package for differential expression analysis of digital gene expression data.* Bioinformatics, 2010. **26**(1): p. 139-40.
196. de Ronde, M.W.J., et al., *High miR-124-3p expression identifies smoking individuals susceptible to atherosclerosis.* Atherosclerosis, 2017. **263**: p. 377-384.
197. Hijmans, J.G., et al., *Association between hypertension and circulating vascular-related microRNAs.* J Hum Hypertens, 2018. **32**(6): p. 440-447.
198. Tsai, H.Y., et al., *miR-424/322 protects against abdominal aortic aneurysm formation by modulating the Smad2/3/runt-related transcription factor 2 axis.* Mol Ther Nucleic Acids, 2022. **27**: p. 656-669.
199. Hu, J.M., et al., *Antagonist targeting miR106b5p attenuates acute renal injury by regulating renal function, apoptosis and autophagy via the upregulation of TCF4.* Int J Mol Med, 2021. **48**(3).
200. Sun, C.M., et al., *Fer exacerbates renal fibrosis and can be targeted by miR-29c-3p.* Open Med (Wars), 2021. **16**(1): p. 1378-1385.
201. Huang, W., et al., *Bioinformatic gene analysis for possible biomarkers and therapeutic targets of hypertension-related renal cell carcinoma.* Transl Androl Urol, 2020. **9**(6): p. 2675-2687.
202. He, D., et al., *miR-15a-5p regulates myocardial fibrosis in atrial fibrillation by targeting Smad7.* PeerJ, 2021. **9**: p. e12686.
203. Shi, P., et al., *Neutrophil-like cell membrane-coated siRNA of lncRNA AABR07017145.1 therapy for cardiac hypertrophy via inhibiting ferroptosis of CMECs.* Mol Ther Nucleic Acids, 2022. **27**: p. 16-36.
204. Velle-Forbord, T., et al., *Circulating microRNAs as predictive biomarkers of myocardial infarction: Evidence from the HUNT study.* Atherosclerosis, 2019. **289**: p. 1-7.
205. Yang, M., et al., *NRF1-enhanced miR-4458 alleviates cardiac hypertrophy through releasing TTP-inhibited TFAM.* In Vitro Cell Dev Biol Anim, 2020. **56**(2): p. 120-128.

206. He, Y., et al., *miR30a5p inhibits hypoxia/reoxygenationinduced oxidative stress and apoptosis in HK2 renal tubular epithelial cells by targeting glutamate dehydrogenase 1 (GLUD1).* Oncol Rep, 2020. **44**(4): p. 1539-1549.
207. Lin, Z., et al., *MiR-21-3p Plays a Crucial Role in Metabolism Alteration of Renal Tubular Epithelial Cells during Sepsis Associated Acute Kidney Injury via AKT/CDK2-FOXO1 Pathway.* Biomed Res Int, 2019. **2019**: p. 2821731.
208. Zhu, X.S., et al., *miR-381-3p inhibits high glucose-induced vascular smooth muscle cell proliferation and migration by targeting HMGB1.* J Gene Med, 2021. **23**(1): p. e3274.
209. Ling, H., et al., *LncRNA GAS5 inhibits miR-579-3p to activate SIRT1/PGC-1alpha/Nrf2 signaling pathway to reduce cell pyroptosis in sepsis-associated renal injury.* Am J Physiol Cell Physiol, 2021. **321**(1): p. C117-C133.
210. Wang, M., et al., *Down-regulation of lncRNA SNHG5 relieves sepsis-induced acute kidney injury by regulating the miR-374a-3p/TLR4/NF-kappaB pathway.* J Biochem, 2021. **169**(5): p. 575-583.
211. Chen, L., et al., *Sodium Reduction, miRNA Profiling and CVD Risk in Untreated Hypertensives: a Randomized, Double-Blind, Placebo-Controlled Trial.* Sci Rep, 2018. **8**(1): p. 12729.
212. Zhuang, X., et al., *MicroRNA-146b-3p regulates the dysfunction of vascular smooth muscle cells via repressing phosphoinositide-3 kinase catalytic subunit gamma.* Bioengineered, 2021. **12**(1): p. 2627-2638.
213. Tian, S., et al., *The miR-378c-Samd1 circuit promotes phenotypic modulation of vascular smooth muscle cells and foam cells formation in atherosclerosis lesions.* Sci Rep, 2021. **11**(1): p. 10548.
214. Wang, Q., Y. Dong, and H. Wang, *microRNA-19b-3p-containing extracellular vesicles derived from macrophages promote the development of atherosclerosis by targeting JAZF1.* J Cell Mol Med, 2022. **26**(1): p. 48-59.
215. Fan, P., et al., *MiR-590-5p inhibits pathological hypertrophy mediated heart failure by targeting RTN4.* J Mol Histol, 2021. **52**(5): p. 955-964.
216. Bai, Q., et al., *Knockdown of XIST up-regulates 263294miR-340-5p to relieve myocardial ischaemia-reperfusion injury via inhibiting cyclin D1.* ESC Heart Fail, 2021.
217. Koch, L., *CRISPR-Cas13 targets circRNAs.* Nat Rev Genet, 2021. **22**(2): p. 68.
218. Eden, E., et al., *GOrilla: a tool for discovery and visualization of enriched GO terms in ranked gene lists.* BMC Bioinformatics, 2009. **10**: p. 48.
219. Seiler, A., et al., *Glutathione peroxidase 4 senses and translates oxidative stress into 12/15-lipoxygenase dependent- and AIF-mediated cell death.* Cell Metab, 2008. **8**(3): p. 237-48.
220. Friedmann Angeli, J.P., et al., *Inactivation of the ferroptosis regulator Gpx4 triggers acute renal failure in mice.* Nat Cell Biol, 2014. **16**(12): p. 1180-91.
221. Zhu, X. and E.K. Jackson, *RACK1 regulates angiotensin II-induced contractions of SHR preglomerular vascular smooth muscle cells.* Am J Physiol Renal Physiol, 2017. **312**(4): p. F565-F576.
222. Blumenthal, A., et al., *Morphology and migration of podocytes are affected by CD151 levels.* Am J Physiol Renal Physiol, 2012. **302**(10): p. F1265-77.
223. Sachs, N., et al., *Blood pressure influences end-stage renal disease of Cd151 knockout mice.* J Clin Invest, 2012. **122**(1): p. 348-58.
224. Xiang, R., et al., *VSMC-Specific Deletion of FAM3A Attenuated Ang II-Promoted Hypertension and Cardiovascular Hypertrophy.* Circ Res, 2020. **126**(12): p. 1746-1759.

225. Brock, C., et al., *Roles of G beta gamma in membrane recruitment and activation of p110 gamma/p101 phosphoinositide 3-kinase gamma.* J Cell Biol, 2003. **160**(1): p. 89-99.
226. Carnevale, D., et al., *PI3Kgamma inhibition reduces blood pressure by a vasorelaxant Akt/L-type calcium channel mechanism.* Cardiovasc Res, 2012. **93**(1): p. 200-9.
227. An, C., et al., *Phosphoinositide 3-kinase gamma deficiency attenuates kidney injury and fibrosis in angiotensin II-induced hypertension.* Nephrol Dial Transplant, 2020. **35**(9): p. 1491-1500.
228. Alhawiti, N.M., et al., *TXNIP in Metabolic Regulation: Physiological Role and Therapeutic Outlook.* Curr Drug Targets, 2017. **18**(9): p. 1095-1103.
229. Ferreira, N.E., et al., *Thioredoxin interacting protein genetic variation is associated with diabetes and hypertension in the Brazilian general population.* Atherosclerosis, 2012. **221**(1): p. 131-6.
230. Schade, D.S., L. Shey, and R.P. Eaton, *Cholesterol Review: A Metabolically Important Molecule.* Endocr Pract, 2020. **26**(12): p. 1514-1523.
231. Vock, C., F. Doring, and I. Nitz, *Transcriptional regulation of HMG-CoA synthase and HMG-CoA reductase genes by human ACBP.* Cell Physiol Biochem, 2008. **22**(5-6): p. 515-24.
232. Mazein, A., et al., *A comprehensive machine-readable view of the mammalian cholesterol biosynthesis pathway.* Biochem Pharmacol, 2013. **86**(1): p. 56-66.
233. Xin, Y., et al., *RNA-Seq analysis reveals a negative role of MSMO1 with a synergized NSDHL expression during adipogenesis of 3T3-L1.* Biosci Biotechnol Biochem, 2019. **83**(4): p. 641-652.
234. Nakamura, K., et al., *Isopentenyl diphosphate isomerase, a cholesterol synthesizing enzyme, is localized in Lewy bodies.* Neuropathology, 2015. **35**(5): p. 432-40.
235. Dong, X.Y. and S.Q. Tang, *Insulin-induced gene: a new regulator in lipid metabolism.* Peptides, 2010. **31**(11): p. 2145-50.
236. Sever, N., et al., *Accelerated degradation of HMG CoA reductase mediated by binding of insig-1 to its sterol-sensing domain.* Mol Cell, 2003. **11**(1): p. 25-33.
237. Zhong, J., H. Yang, and V. Kon, *Kidney as modulator and target of "good/bad" HDL.* Pediatr Nephrol, 2019. **34**(10): p. 1683-1695.
238. Liu, D., et al., *A Highly Efficient Strategy for Overexpressing circRNAs.* Methods Mol Biol, 2018. **1724**: p. 97-105.
239. Wang, X., et al., *Functional role of arginine during the peri-implantation period of pregnancy. I. Consequences of loss of function of arginine transporter SLC7A1 mRNA in ovine conceptus trophectoderm.* FASEB J, 2014. **28**(7): p. 2852-63.
240. Yue, Y., et al., *miR-143 and miR-145 promote hypoxia-induced proliferation and migration of pulmonary arterial smooth muscle cells through regulating ABCA1 expression.* Cardiovasc Pathol, 2018. **37**: p. 15-25.
241. Ignarro, L.J., et al., *Role of the arginine-nitric oxide pathway in the regulation of vascular smooth muscle cell proliferation.* Proc Natl Acad Sci U S A, 2001. **98**(7): p. 4202-8.
242. Cyr, A.R., et al., *Nitric Oxide and Endothelial Dysfunction.* Crit Care Clin, 2020. **36**(2): p. 307-321.
243. Brini, M. and E. Carafoli, *The plasma membrane Ca(2)+ ATPase and the plasma membrane sodium calcium exchanger cooperate in the regulation of cell calcium.* Cold Spring Harb Perspect Biol, 2011. **3**(2).
244. Althwab, S.A., et al., *ATP2B1 genotypes rs2070759 and rs2681472 polymorphisms and risk of hypertension in Saudi population.* Nucleosides Nucleotides Nucleic Acids, 2021. **40**(11): p. 1075-1089.

245. Xie, M., et al., *ATP2B1 gene polymorphisms rs2681472 and rs17249754 are associated with susceptibility to hypertension and blood pressure levels: A systematic review and meta-analysis.* Medicine (Baltimore), 2021. **100**(15): p. e25530.
246. Kobayashi, Y., et al., *Mice lacking hypertension candidate gene ATP2B1 in vascular smooth muscle cells show significant blood pressure elevation.* Hypertension, 2012. **59**(4): p. 854-60.
247. Lakshmikanthan, S., et al., *Rap1b in smooth muscle and endothelium is required for maintenance of vascular tone and normal blood pressure.* Arterioscler Thromb Vasc Biol, 2014. **34**(7): p. 1486-94.
248. Xiao, L., et al., *Rap1 ameliorates renal tubular injury in diabetic nephropathy.* Diabetes, 2014. **63**(4): p. 1366-80.
249. Han, Y., et al., *Reactive oxygen species promote tubular injury in diabetic nephropathy: The role of the mitochondrial ros-txnip-nlrp3 biological axis.* Redox Biol, 2018. **16**: p. 32-46.
250. Honzumi, S., et al., *The effect of cholesterol overload on mouse kidney and kidney-derived cells.* Ren Fail, 2018. **40**(1): p. 43-50.

Appendix

1) circZNF91 knockdown Gene Ontology pathway analysis

GO Term	*Pathway*	*Genes Involved*
GO:0006614	SRP-dependent cotranslational protein targeting to membrane	RPL35, RPS5, UBA52, RPS26, RPS2, RPLP2, RPLP1, RPS16, RPL18, RPL13, RPLP0, RPS19, RPL10, RPS11, RPS8, RPL41, RPL8, RPS14, RPS15, RPS28, RPL36, RPL28
GO:0019083	viral transcription	RPL35, RPS5, UBA52, NUP43, RPS26, RPS2, RPLP2, RPLP1, RPL18, RPS16, RPL13, RPLP0, RPS19, RPL10, RPS11, AAAS, RPS8, RPL41, RPL8, RPS14, RPS15, RPS28, RPL36, RPL28
GO:0006613	cotranslational protein targeting to membrane	RPL35, RPS5, UBA52, RPS26, RPLP2, RPLP1, RPL18, RPS16, RPL13, RPLP0, RPS19, RPS11, RPL10, RPS8, RPL41, RPL8, RPS14, RPS15, RPS28, RPL36, RPL28
GO:0045047	protein targeting to ER	RPL35, RPS5, UBA52, RPS26, RPS2, RPLP2, RPLP1, RPL18, RPS16, RPL13, RPLP0, RPS19, RPL10, RPS11, RPS8, RPL41, RPL8, RPS14, RPS15, RPS28, RPL36, RPL28
GO:0072599	establishment of protein localization to endoplasmic reticulum	RPL35, RPS5, UBA52, RPS26, RPS2, RPLP2, RPLP1, RPS16, RPL18, RPL13, RPLP0, RPS19, RPS11, RPL10, RPS8, RPL41, RPL8, RPS14, RPS15, RPS28, RPL36, RPL28
GO:0000184	nuclear-transcribed mRNA catabolic process, nonsense-mediated decay	RPL35, RPS5, UBA52, RPS26, RPS2, RPLP2, RPLP1, RPS16, RPL18, RPL13, RPLP0, RPS19, RPS11, RPL10, RPS8, RPL41, RPL8, RPS14, RPS15, RPS28, RPL36, RPL28
GO:0006612	protein targeting to membrane	RPL35, RPS5, UBA52, YIF1B, RPS26, RPS2, RPLP2, RPLP1, RPS16, RPL18, RPL13, RPLP0, RPS19, RPS11, RPL10, RPS8, RPL41, RPL8, NACAD, RPS14, RPS15, RPS28, RPL36, RPL28
GO:0006401	RNA catabolic process	UBA52, RNASEH2A, RPS26, RPL18, RPS16, RPL13, RPS19, RPL10, RPS11, RPS8, RPL8, RPS14, RPS15, RPL35, RPS5, LSM6, RPS2, RPLP2, RPLP1, RPLP0, RPL41, RPS28, RPL36, DEDD2, RPL28
GO:0006413	translational initiation	RPL35, RPS5, UBA52, RPS26, RPS2, RPLP2, RPLP1, RPL18, RPS16, RPL13, RPLP0, RPS19, RPS11, RPL10, RPS8, RPL41, RPL8, RPS14, RPS15, RPS28, RPL36, RPL28
GO:0044419	interspecies interaction between organisms	ITGA5, RPS26, BAD, RPL13, RNGTT, UBC, RPL8, TRIM28, RPS14, RPS15, AP1S2, CPSF4, CD151, HMGA2, SKP1, GNB2L1, NDUFA13, E2F1, HSPB1, GAPDH, FKBP8, MOV10, CUL7, RPL36
GO:0009059	macromolecule biosynthetic process	GTPBP2, TK1, RPL18, RPL13, RPL10, RPL8, TRIM28, FLNA, AGRN, MAD2L2, RPL35, RECQL4, RPS2, RPLP2, MRPL12, RPLP0, MCM5, RPL41, B4GALT2, MCM2, RPL36, TELO2, RPL28, UBA52, RNASEH2A, EEF1G, LIN52, TAF6, RPS26, NPM3, RPS16, EEF1A2, UBC, RNGTT, RPS19, UBB, RPS11, ADRM1 RPS8, DHPS, RPS14, RPS15, SLC10A7, CPSF4, DEAF1, MRPS31, RPS6KB2, MAPK3, GNB2L1, COL4A2, XAB2, MRPS34, E2F1, HSPG2, MRPL54, POLD2, POLD1, RPS28, PNKP, MED12

GO:0070972	protein localization to endoplasmic reticulum	RPL35, RPS5, UBA52, RPS26, RPS2, RPLP2, RPLP1, RPL18, RPS16, RPL13, RPLP0, RPS19, RPL10, RPS11, RPS8, RPL41, RPL8, RPS14, RPS15, RPS28, RPL36, RPL28
GO:1901576	organic substance biosynthetic process	GTPBP2, TK1, RPL18, RPL13, PYCR1, RPL10, RPL8, TRIM28, FLNA, AGRN, DCK, PMM1, GCH1, G6PC3, ENO2, MAD2L2, CAD, RPL35, RECQL4, CPOX, RPS2, NADSYN1, RPLP2, MRPL12, PLA2G6, RPLP0, PPCDC, PFKL, RPL41, B4GALT2, MCM5, MCM2, APRT, GUK1, NT5C, RPL36, G6PD, TELO2, RPL28, UBA52, RNASEH2A, LIN52, EEF1G, TAF6, RPS26, NPM3, RPS16, EEF1A2, PTGDS, RNGTT, UBC, RPS19, UBB, PHGDH, RPS11, RPS8, ADRM1, RPS14, DHPS, RPS15, GPX4, SLC10A7, CPSF4, DEAF1, PMEL, CPNE3, RPS6KB2, MRPS31, INPPL1, MAPK3, GNB2L1, COL4A2, XAB2, MRPS34, E2F1, MRPL54, HSPG2, SLC25A1, GAPDH, POLD2, POLD1, GMPPB, SBF1, SRD5A1, RPS28, CKB, ILVBL, PNKP, BCAT2, DCXR
GO:0044319	wound healing, spreading of cells	ITGA5, RHOC, FLNA, CD151
GO:0000956	nuclear-transcribed mRNA catabolic process	RPL35, LSM6, UBA52, RPS5, RPS26, RPS2, RPLP2, RPLP1, RPS16, RPL18, RPL13, RPS19, RPLP0, RPS11, RPL10, RPS8, RPL8, RPL41, RPS14, RPS15, RPS28, RPL36, RPL28
GO:1901566	organonitrogen compound biosynthetic process	ELOVL2, GSTP1, RPL19, TK1, RPL18A, RPL18, NDUFA7, CHAC1, RPL13, ORMDL3, ABCA2, NME4, MRPS18A, RPL10, PYCR1, ENO3, RPL8, AGRN, GSTZ1, DCK, IMPDH1, ELOVL7, GCH1, ENO2, FASN, RPL35, CAD, RPS5, CPOX, TNIP1, ELOVL5, RPS2, NADSYN1, RPLP2, RPLP1, RPLP0, PPCDC, RPL37A, B4GALT3, PFKL, B4GALT2, RPL41, COASY, MRPL27, APRT, GUK1, RPL36, IDH2, RPL28, RPS26, MRPL24, SLC25A39, GAMT, RPS16, CHPF, EEF1A2, RPS19, SHMT2, PHGDH, RPS11, RPS8, DHPS, RPS14, RPS15, B3GAT3, UCKL1, SLC10A7, HAGH, MRPL41, PRKD2, RPS6KB2, MRPL28, ASL, TGFB1, PEMT, MRPS34, ASS1, HSPG2, PLOD3, SLC25A1, GAPDH, B4GALT6, RPS28, CKB, RPS29, ILVBL, UPRT, MPI, BCAT2, FPGS, SRM, BCAT1
GO:0006412	translation	RPS26, RPL18, RPS16, EEF1A2, RPL13, RPS19, RPL10, RPS11, RPS8, RPL8, DHPS, RPS14, RPS15, RPS6KB2, RPL35, RPS5, RPS2, RPLP2, MRPS34, RPLP0, RPL41, RPS28, RPL36, RPL28
GO:0006402	mRNA catabolic process	RPL35, LSM6, UBA52, RPS5, RPS26, RPS2, RPLP2, RPLP1, RPS16, RPL18, RPL13, RPS19, RPLP0, RPS11, RPL10, RPS8, RPL8, RPL41, RPS14, RPS15, RPS28, RPL36, RPL28
GO:0034645	cellular macromolecule biosynthetic process	GTPBP2, TK1, RPL18, RPL13, RPL10, RPL8, FLNA, MAD2L2, RPL35, RECQL4, RPS2, RPLP2, MRPL12, RPLP0, MCM5, RPL41, MCM2, RPL36, TELO2, RPL28, UBA52, RNASEH2A, EEF1G, LIN52, TAF6, RPS26, NPM3, RPS16, EEF1A2, UBC, RNGTT, RPS19, UBB, RPS11, RPS8, DHPS, RPS14, RPS15, DEAF1, MRPS31, RPS6KB2, GNB2L1, XAB2, COL4A2, MRPS34, E2F1, MRPL54, POLD2, POLD1, RPS28, PNKP
GO:0009058	biosynthetic process	GTPBP2, TK1, RPL18, RPL13, PYCR1, RPL10, RPL8, TRIM28, FLNA, AGRN, DCK, PMM1, GCH1, G6PC3, ENO2, MAD2L2, CAD, RPL35, RECQL4, CPOX, RPS2, NADSYN1, RPLP2, MRPL12, PLA2G6, RPLP0, PPCDC, PFKL, B4GALT2, RPL41, MCM5, MCM2, APRT, GUK1, NT5C, RPL36, G6PD, TELO2, RPL28, UBA52, RNASEH2A, LIN52, EEF1G, TAF6, RPS26, NPM3,

		RPS16, EEF1A2, PTGDS, UBC, RNGTT, RPS19, UBB, PHGDH, RPS11, RPS8, ADRM1, RPS14, DHPS, RPS15, GPX4, SLC10A7, CPSF4, DEAF1, PMEL, CPNE3, RPS6KB2, MRPS31, INPPL1, MAPK3, GNB2L1, COL4A2, XAB2, MRPS34, E2F1, MRPL54, HSPG2, SLC25A1, GAPDH, POLD2, POLD1, GMPPB, SBF1, SRD5A1, RPS28, CKB, ILVBL, MED12, PNKP, BCAT2, DCXR
GO:0043604	amide biosynthetic process	ELOVL2, RPL19, RPL18A, RPL18, NDUFA7, RPL13, CHAC1, ORMDL3, MRPS18A, RPL10, RPL8, ELOVL7, GCH1, FASN, RPL35, RPS5, TNIP1, ELOVL5, RPS2, RPLP2, RPLP1, RPLP0, RPL37A, B4GALT3, RPL41, MRPL27, RPL36, RPL28, RPS26, MRPL24, RPS16, EEF1A2, RPS19, RPS11, RPS8, RPS14, DHPS, RPS15, HAGH, MRPL41, RPS6KB2, ASL, MRPL28, MRPS34, PEMT, ASS1, SLC25A1, B4GALT6, RPS28, RPS29, FPGS
GO:0016032	viral process	NUP43, RPS26, SKP1, GNB2L1, NDUFA13, BAD, UBC, RNGTT, RPL13, E2F1, HSPB1, TRIM28, RPL8, RPS14, RPS15, FKBP8, AP1S2, RPS28, CD151, CPSF4, MOV10, CUL7, RPL36
GO:0044403	symbiont process	NUP43, RPS26, SKP1, GNB2L1, NDUFA13, BAD, RNGTT, UBC, RPL13, E2F1, HSPB1, TRIM28, RPL8, RPS14, RPS15, FKBP8, AP1S2, RPS28, CD151, CPSF4, MOV10, CUL7, RPL36
GO:0006518	peptide metabolic process	APEH, GSTP1, EEF1G, RPS26, MRPL24, RPL18A, RPS16, RPL18, EEF1A2, NDUFA7, RPL13, CHAC1, RPS19, RPS11, RPL10, RPS8, RPL8, RPS14, DHPS, RPS15, GSTZ1, HAGH, MRPL41, TPP1, RPS6KB2, RPL35, RPS5, TNIP1, MRPL28, RPS2, RPLP2, RPLP1, MRPS34, SEC11C, RPLP0, RPL41, MRPL27, RPS28, STUB1, RPS29, RPL36, G6PD, RPL28
GO:0090150	establishment of protein localization to membrane	UBA52, YIF1B, RPS26, RPL18, RPS16, BAD, RPL13, RPS19, RPL10, RPS11, RPS8, RPL8, RPS14, RPS15, RPL35, RPS5, RPS2, RPLP2, RPLP1, NDUFA13, RPLP0, RPL41, NACAD, RPS28, RPL36, RPL28
GO:0044249	cellular biosynthetic process	GTPBP2, TK1, RPL18, RPL13, PYCR1, RPL10, TRIM28, RPL8, FLNA, DCK, PMM1, GCH1, ENO2, MAD2L2, RPL35, CAD, RECQL4, CPOX, RPS2, NADSYN1, RPLP2, MRPL12, PLA2G6, RPLP0, PPCDC, PFKL, B4GALT2, RPL41, MCM5, MCM2, APRT, GUK1, NT5C, RPL36, TELO2, RPL28, UBA52, RNASEH2A, LIN52, EEF1G, TAF6, RPS26, NPM3, RPS16, EEF1A2, PTGDS, UBC, RNGTT, RPS19, UBB, PHGDH, RPS11, RPS8, ADRM1, RPS14, DHPS, RPS15, GPX4, SLC10A7, CPSF4, DEAF1, PMEL, CPNE3, RPS6KB2, MRPS31, INPPL1, MAPK3, GNB2L1, COL4A2, XAB2, MRPS34, E2F1, MRPL54, SLC25A1, GAPDH, POLD2, POLD1, GMPPB, SBF1, SRD5A1, RPS28, ILVBL, MED12, PNKP, BCAT2
GO:0051704	multi-organism process	ITGA5, RPS26, BAD, UBC, RNGTT, RPL13, RPL8, TRIM28, RPS14, FLNA, RPS15, AP1S2, CPSF4, CD151, HMGA2, NUP43, SKP1, GNB2L1, NDUFA13, E2F1, HSPB1, GAPDH, FKBP8, RPS28, MOV10, CUL7, RPL36
GO:0043043	peptide biosynthetic process	RPS26, MRPL24, RPL18A, RPL18, RPS16, EEF1A2, NDUFA7, RPL13, CHAC1, RPS19, RPL10, RPS11, RPS8, RPL8, RPS14, DHPS, RPS15, HAGH, MRPL41, RPS6KB2, RPL35, RPS5, TNIP1, MRPL28, RPS2, RPLP2, RPLP1, MRPS34, RPLP0, RPL41, MRPL27, RPS28, RPS29, RPL36, RPL28
GO:0072594	establishment of protein localization to organelle	FIS1, UBA52, RPS26, RPL18, RPS16, BAD, RPL13, UBC, RPS19, AIP, UBB, TNPO2, RPL10, RPS11, RPS8, RPL8, RPS14, RPS15, TIMM17B, RPL35, RPS5, RPS2, RPLP2, NDUFA13, RPLP1, RPLP0, RPL41, RPS28, VPS4A, RPL36 RUVBL2, RPL28
GO:0006605	protein targeting	FIS1, UBA52, YIF1B, RPS26, RPL18, RPS16, RPL13, UBC, AIP, RPS19, UBB, RPL10, RPS11, RPS8, RPL8, RPS14, RPS15,

		TIMM17B, RPL35, RPS5, RPS2, RPLP1, RPLP0, RPL41, NACAD, HGS, RPS28, RPL36, VPS4A, RPL28
GO:0044271	cellular nitrogen compound biosynthetic process	TK1, RPL18, RPL13, WWTR, RPL10, RPL8, TRIM28, FLNA, SUPT5H, DCK, PMM1, ELOVL7, GCH1 ENO2, MAD2L2, RPL35, CAD, RPS5, CPOX, NADSYN1, RPS2, RPLP2, RPLP1, MRPL12, RPLP0, PPCDC, PFKL, RPL41, APRT, GUK1, NT5C, RPL36, TELO2, RPL28, UBA52, LIN52, TAF6, RPS26, NPM3, RPS16, EEF1A2, RNGTT, UBC, RPS19, UBB, RPS11, ADRM1, DHPS, RPS14, RPS15, CPSF4, DEAF1, RPS6KB2, MED15, MAPK3, XAB2, COL4A2, MRPS34, ASS1, E2F1, SLC25A1, POLD2, GAPDH, POLD1, GMPPB, RPS28, MED12
GO:0070585	protein localization to mitochondrion	TIMM17B, FIS1, NDUFA13, BAD, AIP
GO:0072655	establishment of protein localization to mitochondrion	TIMM17B, FIS1, NDUFA13, BAD, AIP
GO:0034655	nucleobase-containing compound catabolic process	UBA52, RNASEH2A, RPS26, RPL18, RPS16, RPL13, RPS19, RPL10, RPS11, RPS8, RPL8, RPS14, RPS15, ENO2, RPL35, LSM6, RPS5, RPS2, RPLP2, RPLP1, RPLP0, PFKL, RPL41, GAPDH, RPS28, NT5C, RPL36, DEDD2, RPL28
GO:0072657	protein localization to membrane	UBA52, YIF1B, DLG4, RPS26, RPS16, RPL18, BAD, JUP, RPL13, RPS19, RPS11, RPL10, RPS8, RPL8, RPS14, FLNA, RPS15, AGRN, FCHO2, GRIK5, RPL35, RPS5, SSNA1, RPS2, RPLP2, NDUFA13, RPLP1, DVL1, RPLP0, RPL41, NACAD, HGS, RPS28, RPL36, RPL28
GO:0046700	heterocycle catabolic process	UBA52, RNASEH2A, RPS26, RPL18, RPS16, RPL13, RPS19, RPL10, RPS11, RPS8, RPL8, RPS14, RPS15, ENO2, RPL35, LSM6, RPS5, RPS2, RPLP2, RPLP1, RPLP0, PFKL, RPL41, GAPDH, RPS28, NT5C, RPL36, DEDD2, RPL28
GO:0043603	cellular amide metabolic process	APEH, GSTP1, RPL18A, RPL18, RPL13, CHAC1, NDUFA7, ORMDL3, ABCA2, RPL10, RPL8, GSTZ1, ELOVL7, GCH1, FAR1, RPL35, RPS5, TNIP1, ELOVL5, RPS2, RPLP2, RPLP1, RPLP0, RPL41, MRPL27, RPL36, G6PD, RPL28, EEF1G, CLN6, RPS26, MRPL24, RPS16, EEF1A2, RPS19, SHMT2, RPS11, RPS8, DHPS, RPS14, RPS15, HAGH, MRPL41, TPP1, MCCC2, RPS6KB2, MRPL28, PEMT, MRPS34, SEC11C, ASS1, SLC25A1, RPS28, B4GALT6, STUB1, RPS29, FPGS
GO:0044270	cellular nitrogen compound catabolic process	UBA52, RNASEH2A, RPS26, RPL18, RPS16, RPL13, RPS19, RPL10, RPS11, RPS8, RPL8, RPS14, RPS15, ENO2, RPL35, LSM6, RPS5, RPS2, RPLP2, RPLP1, RPLP0, PFKL, RPL41, GAPDH, RPS28, NT5C, RPL36, DEDD2, RPL28
GO:0035295	tube development	PKD1, EPHA2, BRIP1, DCHS1, CRLF1, TGFB1, ZNF358, ASS1, DVL1, UBB, PHGDH, PLOD3, SLC4A2, AMBRA1, TRAF4
GO:0009057	macromolecule catabolic process	CDC20, CAPN1, RPL18A, RPL18, UHRF1, RPL13, USE1, CDC34, WWTR1, RPL10, PYGB, RPL8, PTPN23, FBXW5, AGRN, CUL9, UBE2S, RPL35, RPS5, SPSB3, GAA, RPS2, SKP1, RPLP2, RPLP1, HYAL2, PSMB6, RPLP0, RPL41, PSMD8, UBXN6, RPL36, VPS4A, RPL28, MVB12A, LONP1, UBA52, RNASEH2A, CLN6, RPS26, AURKB, RPS16, USP5, UBC, RPS19, UBB, RPS11, ADRM1, RPS8, RPS14, RPS15, BAP1, TPP1, LSM6, USP11, AP2M1, KLHL25, HSPG2, UBE2W, RNF40, RPS28, STUB1, LYPLA2, CUL7, SHARPIN, DEDD2

GO:0044248	cellular catabolic process	CDC20, CAPN1, RPL18A, RPL18, BCKDK, UHRF1, RPL13, CDC34, WWTR1, RPL10, PYGB, ATP13A2, LDLR, RPL8, ENO3, PTPN23, FBXW5, ECI1, GSTZ1, CUL9, UBE2S, ENO2, ENTPD6, RPL35, RPS5, SPSB3, GAA, SKP1, RPS2, RPLP2, RPLP1, HYAL2, PLA2G6, PSMB6, RPLP0, MAP1S, PFKL, RPL41, PLCG1, PRDX2, NT5C, PSMD8, VPS4A, RPL36, UBXN6, RPL28, MVB12A, LONP1, FIS1, UBA52, VPS51, RNASEH2A, CLN6, RPS26, LRP1, AURKB, TBC1D17, RPS16, USP5, ATG4D, UBC, RPS19, UBB, RPS11, RPS8, ADRM1, RPS14, RPS15, SULT1C4, HAGH, BAP1, ETFB, GRAMD1A, TPP1, MCCC2, LSM6, CHMP6, USP11, WDR45, AP2M1, KLHL25, GAPDH, UBE2W, RNF40, HGS, BCKDHA, STUB1, RPS28, LYPLA2, CUL7, SHARPIN, ILVBL, BCAT2, DEDD2, PRDX5, DCXR
GO:0051649	establishment of localization in cell	TIMM17B, FIS1, DDX39A, NUP43, PLEKHJ1, RPS26, NDUFA13, BAD, PTGDS, RPL13, UBC, AIP, HSPB1, RPL8, FLNA, RPS15, AP1S2, RPS28, COPE, ARHGAP1, RPL36, FCHO2
GO:1901361	organic cyclic compound catabolic process	UBA52, RNASEH2A, RPS26, RPL18, RPS16, RPL13, RPS19, RPL10, RPS11, RPS8, RPL8, RPS14, RPS15, ENO2, RPL35, LSM6, RPS5, RPS2, RPLP2, RPLP1, RPLP0, PFKL, RPL41, GAPDH, SRD5A1, RPS28, NT5C, RPL36, DEDD2, RPL28
GO:0009056	catabolic process	CDC20, BCKDK, UHRF1, CDC34, USE1, WWTR1, LDLR, ENO3, PTPN23, FBXW5, AGRN, ECI1, GSTZ1, ENO2, UBE2S, ENTPD6, RPL35, OCRL, PSMB6, MAP1S, PLCG1, PRDX2, PSMD8, RPL36, UBXN6, MVB12A, FIS1, VPS51, RNASEH2A, ATG4D, SULT1C4, HAGH, BAP1, LSM6, CHMP6, USP11, OC90, WDR45, KLHL25, HSPG2, RNF40, HGS, STUB1, CUL7, SHARPIN, CAPN1, RPL18A, RPL18, RPL13, RPL10, ATP13A2, PYGB, RPL8, CUL9, MAN2C1, RPS5, GAA, SPSB3, RPS2, SKP1, RPLP2, RPLP1, HYAL2, PLA2G6, RPLP0, PFKL, RPL41, NT5C, VPS4A, RPL28, GALE, LONP1, UBA52, CLN6, RPS26, LRP1, TBC1D17, RPS16, BAD, USP5, UBC, RPS19, UBB, RPS11, RPS8, ADRM1, RPS14, RPS15, ETFB, ADAM15, GRAMD1A, MCCC2, TPP1, AP2M1, GAPDH, UBE2W, SRD5A1, BCKDHA, RPS28, LYPLA2, ILVBL, BCAT2, PRDX5, DEDD2, DCXR
GO:1901575	organic substance catabolic process	CDC20, CAPN1, RPL18A, RPL18, BCKDK, UHRF1, RPL13, USE1, CDC34, WWTR1, RPL10, PYGB, RPL8, ENO3, PTPN23, FBXW5, ECI1, AGRN, GSTZ1, CUL9, UBE2S, ENO2, MAN2C1, ENTPD6, RPL35, RPS5, GAA, SPSB3, SKP1, RPS2, RPLP2, RPLP1, OCRL, HYAL2, PLA2G6, PSMB6, RPLP0, PFKL, RPL41, PLCG1, NT5C, PSMD8, VPS4A, UBXN6, RPL36, RPL28, GALE, MVB12A, LONP1, UBA52, RNASEH2A, CLN6, RPS26, LRP1, AURKB, RPS16, BAD, USP5, UBC, RPS19, UBB, RPS11, ADRM1, RPS8, RPS14, RPS15, SULT1C4, HAGH, BAP1, ETFB, TPP1, MCCC2, LSM6, USP11, OC90, AP2M1, KLHL25, HSPG2, GAPDH, UBE2W, RNF40, SRD5A1, BCKDHA, STUB1, RPS28, LYPLA2, CUL7, SHARPIN, ILVBL, BCAT2, DEDD2, DCXR
GO:0019439	aromatic compound catabolic process	UBA52, RNASEH2A, RPS26, RPL18, RPS16, RPL13, RPS19, RPL10, RPS11, RPS8, RPL8, RPS14, RPS15, ENO2, RPL35, LSM6, RPS5, RPS2, RPLP2, RPLP1, RPLP0, PFKL, RPL41, GAPDH, RPS28, NT5C, RPL36, DEDD2, RPL28

2) circZNF91 knockdown Reactome pathway analysis

Pathway ID	*Pathway Name*	*Genes*
R-HSA-9711097	Cellular response to starvation	RPL3, RPL32, RPLP1, RPLP0, RRP1, RPL8, RPS15, RPS14, RPS16, RPL18A, RPS19, MLST8, RPL36, RPLP2, RPL35, RPS11;SEC13;SZT2, ATP6V1G1, RPS7, RPS8, RPS5, RPL13A, DDIT3, RPL37A, TRIB3, RPL29, ATP6V0D1, RPL28, UBA52, ATP6V1B1, RPL10, NPRL2, NPRL3, RPL11, WDR24, UBB, UBC, RPS3, RPL13, SLC38A9, RPS2, RPL18, GCN1, ATP6V1C1, RPL19, RPL41, ASNS, MTOR, RPS26, RPS28, RPS29, CASTOR2, RPL27A, LAMTOR2, FAU, LAMTOR1, LAMTOR4, LAMTOR3
R-HSA-9633012	Response of EIF2AK4 (GCN2) to amino acid deficiency	RPL3, RPL32, RPL10, RPLP1, RPL11, RPLP0, RRP1, RPL8, RPS15, RPS14, RPS16, RPL18A, RPS19, UBB, UBC, RPS3, RPL36, RPLP2, RPL35, RPL13, RPS2, RPL18, RPS11, GCN1, RPL19, RPL41, RPS7, RPS8, RPS5, ASNS, RPL13A, RPS26, RPS28, RPS29, DDIT3, RPL27A, RPL37A, TRIB3, FAU, RPL29, UBA52, RPL28
R-HSA-156842	Eukaryotic Translation Elongation	RPL3, RPL32, RPL10, RPLP1, RPL11, RPLP0, RRP1, RPL8, RPS15, RPS14, RPS16, RPL18A, RPS19, UBB, UBC, RPS3, RPL36, RPLP2, RPL35, RPL13, RPS2, RPL18, RPS11, RPL19, RPL41, RPS7, RPS8, RPS5, RPL13A, EEF2, RPS26, EEF1G, RPS28, RPS29, RPL27A, EEF1A2, RPL37A, FAU RPL29, UBA52, RPL28
R-HSA-72689	Formation of a pool of free 40S subunits	RPL3, RPL32, RPL10, RPLP1, RPL11, RPLP0, RRP1, RPL8, RPS15, RPS14, RPS16, RPL18A, RPS19, UBB, UBC, RPS3, RPL36, RPLP2, RPL35, RPL13, RPS2, RPL18, RPS11, RPL19, RPL41, RPS7, EIF1AX, RPS8, RPS5, RPL13A, RPS26, RPS28, RPS29, RPL27A, RPL37A, EIF3J, EIF3G, FAU;EIF3C, RPL29, UBA52, RPL28
R-HSA-1799339	SRP-dependent cotranslational protein targeting to membrane	TRAM1, RPL3, RPL32, RPL10, WBP1, RPLP1, RPL11, RPLP0, RRP1, RPL8, RPS15, RPS14, RPS16, RPL18A, RPS19, UBB, UBC, RPS3, RPL36, RPLP2, RPL35, RPL13, RPS2, RPL18, RPS11, SEC11C, RPL19, RPL41, RPS7, SSR4, RPS8, RPS5, SSR2, RPL13A, SRP9, DDOST, RPS26, RPS28, RPS29, RPL27A, RPL37A, SRPRA, FAU, RPL29, UBA52, RPL28
R-HSA-156902	Peptide chain elongation	RPL3, RPL32, RPL10, RPLP1, RPL11, RPLP0, RRP1, RPL8, RPS15, RPS14, RPS16, RPL18A, RPS19, UBB, UBC, RPS3, RPL36, RPLP2, RPL35, RPL13, RPS2, RPL18, RPS11, RPL19, RPL41, RPS7, RPS8, RPS5, RPL13A, EEF2, RPS26, RPS28, RPS29, RPL27A, RPL37A, FAU, RPL29, UBA52, RPL28
R-HSA-975956	Nonsense Mediated Decay (NMD) independent of the Exon Junction Complex (EJC)	RPL3, RPL32, RPL10, RPLP1, RPL11, RPLP0, RRP1, RPL8, RPS15, RPS14, RPS16, RPL18A, RPS19, UBB, UBC, RPS3, RPL36, RPLP2, RPL35, RPL13, RPS2, RPL18, RPS11, RPL19, UPF1, RPL41, RPS7, RPS8, RPS5, RPL13A, RPS26, RPS28, RPS29, RPL27A, RPL37A, FAU, RPL29, UBA52, RPL28, EIF4G1

R-HSA-72766	Translation	TRAM1, RPL3, RPL32, RPLP1, RPLP0, RRP1, MRPL38, APEH, RPL8, MRPL41, RPS15, MRPL4, TRMT112, RPS14, MRPL2, RPS16, RPL18A, QARS1, RPS19, RPL36, RPLP2, RPL35, RPS11, MRPS26, RPS7, SSR4, EIF1AX, RPS8, RPS5, SSR2, MARS1, MRPL49, AIP, MRPS2, RPL13A, DARS2, MRPS18A, SRP9, DARS1, DDOST, TUFM, EEF1G, EEF1A2, RPL37A, TARS2, RPL29, CARS1, AURKAIP1, EEF1E1, RPL28, UBA52, AARS1, AARS2, RPL10, WBP1, MRPS35, RPL11, MRPL19, MRPS34, MRPS31, MRPL14, MRPL12, MRPL54, MRPL10, MRPL55, BRIP1, UBB, UBC, RPS3, EIF4EBP1, RPL13, RPS2, RPL18, RPL19, SEC11C, GADD45GIP1, RPL41, MRPL27, MRPL28, EEF2, MRPL24, RPS26, AIMP1, RPS28, RPS29, RPL27A, EIF3J, SRPRA, EIF3G, FAU, FARSA, EIF3C, EIF4G1
R-HSA-72764	Eukaryotic Translation Termination	RPL3;RPL32;RPL10;RPLP1;RPL11;RPLP0;RRP1;APEH;RPL8;RPS15;TRMT112;RPS14;RPS16;RPL18A;RPS19;UBB;UBC;RPS3;RPL36;RPLP2;RPL35;RPL13;RPS2;RPL18;RPS11;RPL19;RPL41;RPS7;RPS8;RPS5;RPL13A;RPS26;RPS28;RPS29;RPL27A;RPL37A;FAU;RPL29;UBA52;RPL28
R-HSA-2262752	Cellular responses to stress	CRTC2;RPL3;RPL32;RRP1;UBE2D1;KEAP1;RPL8;CCAR2;RPS15;PSMD8;RPS14;RPS16;RPL18A;RPS19;PSMD4;TUBB3;PSMD2;PSMD3;SCMH1;RPL36;RPL35;CHAC1;RPS11;SKP1;MAP2K3;ATP6V1G1;SZT2;RPS7;RPS8;DDX11;RPS5;PRKCD;UBE2E1;CYBA;COX6B1;MAPKAPK3;DDIT3;TRIB3;PREB;ATP6V0D1;RPL29;TLN1;UBA52;RPL28;ASF1A;ANAPC2;VCP;CUL7;PSMD12;ANAPC15;RPS19BP1;NPRL2;HSPA4L;NPRL3;AAAS;DEDD2;ANAPC11;HELZ2;PRDX2;RAI1;PRDX5;BAG2;UBB;UBC;SERPINH1;COX11;SLC38A9;GCN1;ATP6V1C1;ZBTB17;ACD;RPL41;PHC2;UBE2C;CBX2;HMGA1;ASNS;HMGA2;H1-2;RPS26;MOV10;RPS28;RPS29;UBE2S;RPL27A;AGO2;SRPRA;CYCS;TPP1;CALR;BAP1;H2AX;ACADVL;CDKN1A;GSK3A;COX4I1;RPLP1;RPLP0;HSPB1;BMI1;MYDGF;TUBA1C;TUBA1B;SIN3B;NUP62;MLST8;RPLP2;ELOB;ATP7A;NDC1;COX8A;SEC13;MINK1;PPP2R5B;RPL13A;SIRT1;ARFGAP1;NCOR2;RPL37A;BLVRB;ATP6V1B1;PPP1R15A;HDAC3;DCTN2;RPL10;DCTN1;GSTP1;DCTN3;RPL11;WDR24;RELA;HDAC6;PSMB6;FZR1;PSMB5;MAPK7;RPS3;E2F1;RPL13;NUP43;RPS2;TBL1X;RBBP7;RPL18;EXTL3;RPL19;MAPK3;EGLN1;TXNRD2;PTGES3;SYVN1;TUBB4B;ATOX1;YIF1A;MTOR;MAPK11;RAD50;CCS;PC;PSMC3;CASTOR2;CARM1;LAMTOR2;FAU;LAMTOR1;P4HB;LAMTOR4;LAMTOR3
R-HSA-72706	GTP hydrolysis and joining of the 60S ribosomal subunit	RPL3;RPL32;RPL10;RPLP1;RPL11;RPLP0;RRP1;RPL8;RPS15;RPS14;RPS16;RPL18A;RPS19;UBB;UBC;RPS3;RPL36;RPLP2;RPL35;RPL13;RPS2;RPL18;RPS11;RPL19;RPL41;RPS7;EIF1AX;RPS8;RPS5;RPL13A;RPS26;RPS28;RPS29;RPL27A;RPL37A;EIF3J;EIF3G;FAU;EIF3C;RPL29;UBA52;RPL28;EIF4G1

R-HSA-156827	L13a-mediated translational silencing of Ceruloplasmin expression	RPL3;RPL32;RPL10;RPLP1;RPL11;RPLP0;RRP1;RPL8;RPS15;RPS14;RPS16;RPL18A;RPS19;UBB;UBC;RPS3;RPL36;RPLP2;RPL35;RPL13;RPS2;RPL18;RPS11;RPL19;RPL41;RPS7;EIF1AX;RPS8;RPS5;RPL13A;RPS26;RPS28;RPS29;RPL27A;RPL37A;EIF3J;EIF3G;FAU;EIF3C;RPL29;UBA52;RPL28;EIF4G1
R-HSA-927802	Nonsense-Mediated Decay (NMD)	RPL3;RPL32;RPL10;RPLP1;RPL11;RPLP0;RRP1;RPL8;SMG5;RPS15;RPS14;RPS16;RPL18A;RPS19;UBB;PPP2R1A;UBC;RPS3;RPL36;RPLP2;RPL35;RPL13;RPS2;RPL18;RPS11;RPL19;UPF1;RPL41;RPS7;RPS8;RPS5;RPL13A;RPS26;RPS28;RPS29;RPL27A;RPL37A;RNPS1;FAU;RPL29;UBA52;RPL28;EIF4G1
R-HSA-975957	Nonsense Mediated Decay (NMD) enhanced by the Exon Junction Complex (EJC)	RPL3;RPL32;RPL10;RPLP1;RPL11;RPLP0;RRP1;RPL8;SMG5;RPS15;RPS14;RPS16;RPL18A;RPS19;UBB;PPP2R1A;UBC;RPS3;RPL36;RPLP2;RPL35;RPL13;RPS2;RPL18;RPS11;RPL19;UPF1;RPL41;RPS7;RPS8;RPS5;RPL13A;RPS26;RPS28;RPS29;RPL27A;RPL37A;RNPS1;FAU;RPL29;UBA52;RPL28;EIF4G1
R-HSA-8953897	Cellular responses to stimuli	CRTC2;RPL3;RPL32;RRP1;UBE2D1;KEAP1;RPL8;CCAR2;RPS15;PSMD8;RPS14;RPS16;RPL18A;RPS19;PSMD4;TUBB3;PSMD2;PSMD3;SCMH1;RPL36;RPL35;CHAC1;RPS11;SKP1;MAP2K3;ATP6V1G1;SZT2;RPS7;RPS8;DDX11;RPS5;PRKCD;UBE2E1;CYBA;COX6B1;MAPKAPK3;DDIT3;TRIB3;PREB;ATP6V0D1;RPL29;TLN1;UBA52;RPL28;ASF1A;ANAPC2;VCP;CUL7;PSMD12;ANAPC15;RPS19BP1;NPRL2;HSPA4L;NPRL3;AAAS;DEDD2;ANAPC11;HELZ2;PRDX2;RAI1;PRDX5;BAG2;UBB;UBC;SERPINH1;COX11;SLC38A9;GCN1;ATP6V1C1;ZBTB17;ACD;RPL41;PHC2;UBE2C;CBX2;HMGA1;ASNS;HMGA2;H1-2;RPS26;MOV10;RPS28;RPS29;UBE2S;RPL27A;AGO2;SRPRA;CYCS;TPP1;CALR;BAP1;H2AX;ACADVL;CDKN1A;GSK3A;COX4I1;RPLP1;RPLP0;HSPB1;BMI1;MYDGF;TUBA1C;TUBA1B;SIN3B;NUP62;MLST8;RPLP2;ELOB;ATP7A;NDC1;COX8A;SEC13;MINK1;PPP2R5B;RPL13A;SIRT1;ARFGAP1;NCOR2;RPL37A;BLVRB;ATP6V1B1;PPP1R15A;HDAC3;DCTN2;RPL10;DCTN1;GSTP1;DCTN3;RPL11;WDR24;RELA;HDAC6;PSMB6;FZR1;PSMB5;MAPK7;RPS3;E2F1;RPL13;NUP43;RPS2;TBL1X;RBBP7;RPL18;EXTL3;RPL19;MAPK3;EGLN1;TXNRD2;PTGES3;SYVN1;TUBB4B;ATOX1;YIF1A;MTOR;MAPK11;RAD50;CCS;PC;PSMC3;CASTOR2;CARM1;LAMTOR2;FAU;LAMTOR1;P4HB;LAMTOR4;LAMTOR3
R-HSA-72613	Eukaryotic Translation Initiation	RPL3;RPL32;RPL10;RPLP1;RPL11;RPLP0;RRP1;RPL8;RPS15;RPS14;RPS16;RPL18A;RPS19;UBB;UBC;RPS3;EIF4EBP1;RPL36;RPLP2;RPL35;RPL13;RPS2;RPL18;RPS11;RPL19;RPL41;RPS7;EIF1AX;RPS8;RPS5;RPL13A;RPS26;RPS28;RPS29;RPL27A;RPL37A;EIF3J;EIF3G;FAU;EIF3C;RPL29;UBA52;RPL28;EIF4G1
R-HSA-72737	Cap-dependent Translation Initiation	RPL3;RPL32;RPL10;RPLP1;RPL11;RPLP0;RRP1;RPL8;RPS15;RPS14;RPS16;RPL18A;RPS19;UBB;UBC;RPS3;EIF4EBP1;RPL36;RPLP2;RPL35;RPL13;RPS2;RPL18;RPS11;RPL19;RPL41;RPS7;EIF1AX;RPS8;RPS5;RPL1

		3A;RPS26;RPS28;RPS29;RPL27A;RPL37A;EIF3J;EIF3G;FAU;EIF3C;RPL29;UBA52;RPL28;EIF4G1
R-HSA-2408557	Selenocysteine synthesis	RPL3;RPL32;RPL10;RPLP1;RPL11;RPLP0;RRP1;RPL8;RPS15;RPS14;RPS16;RPL18A;RPS19;UBB;UBC;RPS3;RPL36;RPLP2;RPL35;RPL13;RPS2;RPL18;RPS11;RPL19;EEFSEC;RPL41;RPS7;RPS8;RPS5;RPL13A;RPS26;RPS28;RPS29;RPL27A;RPL37A;FAU;RPL29;UBA52;RPL28
R-HSA-192823	Viral mRNA Translation	RPL3;RPL32;RPL10;RPLP1;RPL11;RPLP0;RRP1;RPL8;RPS15;RPS14;RPS16;RPL18A;RPS19;UBB;UBC;RPS3;RPL36;RPLP2;RPL35;RPL13;RPS2;RPL18;RPS11;RPL19;RPL41;RPS7;RPS8;RPS5;RPL13A;RPS26;RPS28;RPS29;RPL27A;RPL37A;FAU;GRSF1;RPL29;UBA52;RPL28
R-HSA-1236977	Endosomal/Vacuolar pathway	HLA-B
R-HSA-6791226	Major pathway of rRNA processing in the nucleolus and cytosol	DDX49;RPL3;RPL32;RPLP1;RPLP0;RRP1;RPL8;RRP9;RPS15;RPS14;RPS16;RPL18A;RPS19;DBT;RPL36;RPLP2;RPL35;RPS11;WDR36;RPS7;UTP11;RPS8;RPS5;RPL13A;CSNK1D;RPL37A;RPL29;RPL28;UBA52;RPL10;LRP1;RPL11;RRP7A;UBB;UBC;RPS3;RPL13;RPS2;RPL18;DCAF13;RPL19;RPL41;WDR18;BYSL;RPS26;BOP1;RPS28;TBL3;RPS29;RPL27A;MPHOSPH10;FAU;NOL12;MPHOSPH6
R-HSA-9010553	Regulation of expression of SLITs and ROBOs	RPL3;RPL32;RPLP1;RPLP0;RRP1;RPL8;PSMD8;RPS15;RPS14;RPS16;RPL18A;PSMD4;RPS19;PSMD2;PSMD3;RPL36;RPLP2;RPL35;ELOB;RPS11;RPS7;RPS8;RPS5;RPL13A;RPL37A;RPL29;RPL28;UBA52;PSMD12;RPL10;RPL11;PSMB6;PSMB5;UBB;UBC;RPS3;ZSWIM8;RPL13;RPS2;RPL18;RPL19;RPL41;RPS26;RPS28;PSMC3;RPS29;RPL27A;RNPS1;FAU;EIF4G1
R-HSA-168273	Influenza Viral RNA Transcription and Replication	RPL3;RPL32;RPLP1;RPLP0;RRP1;RPL8;RPS15;RPS14;RPS16;RPL18A;RPS19;NUP62;RPL36;RPLP2;RPL35;RPS11;NDC1;SEC13;RPS7;RPS8;RPS5;RPL13A;GTF2F1;RPL37A;RPL29;RPL28;UBA52;RPL10;RPL11;AAAS;UBB;POLR2A;UBC;RPS3;RPL13;NUP43;RPS2;POLR2I;RPL18;POLR2J;POLR2K;POLR2L;RPL19;RPL41;MTOR;RPS26;RPS28;RPS29;RPL27A;FAU;GRSF1
R-HSA-168255	Influenza Infection	RPL3;RPL32;RPLP1;RPLP0;RRP1;RPL8;RPS15;RPS14;RPS16;RPL18A;RPS19;NUP62;RPL36;RPLP2;RPL35;KPNA5;RPS11;NDC1;SEC13;RPS7;RPS8;RPS5;RPL13A;GTF2F1;CANX;RPL37A;RPL29;RPL28;UBA52;RPL10;RPL11;AAAS;UBB;POLR2A;UBC;RPS3;RPL13;NUP43;RPS2;POLR2I;RPL18;POLR2J;POLR2K;POLR2L;RPL19;CPSF4;RPL41;TGFB1;MTOR;RPS26;RPS28;RPS29;RPL27A;CALR;FAU;GRSF1
R-HSA-8868773	rRNA processing in the nucleus and cytosol	DDX49;RPL3;RPL32;RPLP1;RPLP0;RRP1;RPL8;RRP9;RPS15;TRMT112;RPS14;RPS16;RPL18A;RPS19;DBT;RPL36;RPLP2;RPL35;RPS11;WDR36;RPS7;UTP11;DIMT1;RPS8;RPS5;RPL13A;CSNK1D;RPL37A;RPL29;RPL28;UBA52;RPL10;LRP1;RPL11;RRP7A;UBB;UBC;RPS3;RPL13;RPS2;RPL18;DCAF13;RPL19;RPL41;WDR18;BYSL;RPS26;BOP1;RPS28;TBL3;RPS29;RPL27A;MPHOSPH10;FAU;NOL12;MPHOSPH6

R-HSA-8953854	Metabolism of RNA	POP7;RPL3;RPL32;RRP1;RTCB;RPL8;TSEN54;RRP9;EDC3;PSMD8;RPS15;EDC4;RPS14;RPS16;RPL18A;SNRPD2;PSMD4;RPS19;PPP2R1A;PSMD2;PSMD3;RPL36;AKT1;RPL35;RPS11;RPS7;METTL1;DIMT1;RPS8;PUS1;RPS5;PRKCD;CSNK1D;THOC5;GTF2F1;THOC6;DDX39A;CLNS1A;RBP1;SNRPG;GEMIN4;CD2BP2;SNRNP25;SNRPF;RPL29;UBA52;RPL28;SNRPA;SNRPB;PSMD12;RNPC3;AAAS;RRP7A;UBB;UBC;SYMPK;DHX38;C2orf49;RBM10;CPSF4;RPL41;CPSF6;CPSF1;ALYREF;SUPT5H;LSM4;LSM3;RPS26;RPS28;TBL3;LSM7;LSM6;RPS29;RPL27A;CNOT3;TRMT13;MPHOSPH10;RNPS1;NOL12;EIF4G1;DDX49;RPLP1;RPLP0;HSPB1;PPWD1;SMG5;PQBP1;TRMT112;SART1;PCF11;DBT;NUP62;RPLP2;TNKS1BP1;TNPO1;NDC1;UPF1;WDR36;SEC13;UTP11;RPL13A;QTRT1;GCFC2;CTU2;CTU1;RPL37A;DNAJC8;SLU7;SF3B5;RPL10;LRP1;POLDIP3;URM1;DDX23;RPL11;SRRT;DDX20;HSD17B10;LAGE3;U2AF1L4;PSMB6;PSMB5;POLR2A;U2AF2;RPS3;RPL13;NUP43;SNRPB2;RPS2;POLR2I;RPL18;POLR2J;DCAF13;POLR2K;POLR2L;PAIP1;RPL19;TRMT10C;SF3A2;RNGTT;WDR18;TRMT1;U2SURP;MTOR;BYSL;NUDT21;MAPK11;XAB2;BOP1;PSMC3;TRMT5;ERCC2;FAU;TRMT61A;PPIL4;MPHOSPH6
R-HSA-376176	Signalling by ROBO receptors	RPL3;RPL32;RPLP1;MAST1;RPLP0;RRP1;RPL8;PSMD8;RPS15;RPS14;RPS16;RPL18A;PSMD4;RPS19;PSMD2;PSMD3;RPL36;RPLP2;RPL35;ELOB;RPS11;RPS7;RPS8;RPS5;RPL13A;ENAH;RPL37A;EVL;RPL29;PFN1;RPL28;UBA52;PSMD12;RPL10;SRC;RPL11;PSMB6;PSMB5;UBB;UBC;RPS3;ZSWIM8;RPL13;RPS2;RPL18;PAK4;RPL19;RPL41;MYO9B;RPS26;RPS28;PSMC3;RPS29;RPL27A;RNPS1;FAU;EIF4G1
R-HSA-381038	XBP1(S) activates chaperone genes	ZBTB17;ACADVL;CUL7;GSK3A;DCTN1;DDX11;SYVN1;PPP2R5B;YIF1A;ARFGAP1;MYDGF;SRPRA;PREB;TPP1;TLN1;ATP6V0D1;EXTL3
R-HSA-1236974	ER-Phagosome pathway	PSMD12;HLA-B;PSMB6;PSMD8;PSMB5;PSMD4;PSMC3;UBB;PSMD2;PSMD3;UBC;STX4;CALR;IKBKG;UBA52
R-HSA-422475	Axon guidance	RPL3;PLXND1;RPL32;RRP1;RPL8;RPS6KA4;PSMD8;RPS15;RPS14;RPS6KA6;RPS6KA5;RPS16;RPL18A;PSMD4;RPS19;TUBB3;PSMD2;PSMD3;RPL36;RPL35;RPS11;AP2M1;MAP2K2;RPS7;RPS8;RPS5;CACNB1;DOK1;MYL6;CACNB3;COL4A2;RPL29;PFN1;TLN1;UBA52;RPL28;EPHA2;PSMD12;EFNA4;CACNA1H;APH1A;EFNB1;RRAS;UBB;UBC;PIP5K1C;PLCG1;SCN3B;RPL41;RDX;RPS26;EFNA1;RPS28;EFNA3;CDK5;RPS29;DLG4;RPL27A;PLXNB1;RNPS1;REEP6;EIF4G1;GSK3A;CNTNAP1;RPLP1;RPLP0;MAST1;CLTB;TUBA1C;TUBA1B;RPLP2;ELOB;ITGAV;SPTAN1;GIT1;PSENEN;LYPLA2;ACTR2;ITGA2;TRPC1;RPL13A;RHOC;DNM2;RGMA;ENAH;COL6A2;COL6A1;RPL37A;SCN4A;EVL;ITGA5;DOCK1;RPL10;SRC;ROCK2;RPL11;PSMB6;PTPA;MAPK7;PSMB5;ZSWIM8;RPS3;RPL13;RPS2;RPL18;PDLIM7;MAPK3;PAK4;RPL19;LAMB2;MYO9B;TUBB4B;MAPK12;MAPK11;PSMC3;FAU;AGRN

R-HSA-381070	IRE1alpha activates chaperones	ZBTB17;ACADVL;CUL7;GSK3A;DCTN1;DDX11;SYVN1;PPP2R5B;YIF1A;ARFGAP1;MYDGF;SRPRA;PREB;TPP1;TLN1;ATP6V0D1;EXTL3
R-HSA-1236975	Antigen processing-Cross presentation	PSMD12;HLA-B;CYBA;PSMB6;PSMD8;MRC2;PSMB5;PSMD4;PSMC3;UBB;PSMD2;PSMD3;UBC;ITGAV;STX4;CALR;IKBKG;UBA52
R-HSA-72312	rRNA processing	DDX49;RPL3;RPL32;RPLP1;RPLP0;RRP1;RPL8;RRP9;RPS15;TRMT112;RPS14;RPS16;RPL18A;RPS19;DBT;RPL36;RPLP2;RPL35;RPS11;WDR36;RPS7;UTP11;DIMT1;RPS8;RPS5;RPL13A;CSNK1D;RPL37A;RPL29;RPL28;UBA52;RPL10;LRP1;RPL11;HSD17B10;RRP7A;UBB;UBC;RPS3;RPL13;RPS2;RPL18;DCAF13;RPL19;RPL41;TRMT10C;WDR18;BYSL;RPS26;BOP1;RPS28;TBL3;RPS29;RPL27A;MPHOSPH10;FAU;NOL12;MPHOSPH6
R-HSA-9675108	Nervous system development	RPL3;PLXND1;RPL32;RRP1;RPL8;RPS6KA4;PSMD8;RPS15;RPS14;RPS6KA6;RPS6KA5;RPS16;RPL18A;PSMD4;RPS19;TUBB3;PSMD2;PSMD3;RPL36;RPL35;RPS11;AP2M1;MAP2K2;RPS7;RPS8;RPS5;CACNB1;DOK1;MYL6;CACNB3;COL4A2;RPL29;PFN1;TLN1;UBA52;RPL28;EPHA2;PSMD12;EFNA4;CACNA1H;APH1A;EFNB1;RRAS;UBB;UBC;PIP5K1C;PLCG1;SCN3B;WWTR1;RPL41;RDX;SMARCA4;RPS26;EFNA1;RPS28;EFNA3;CDK5;RPS29;DLG4;RPL27A;PLXNB1;RNPS1;REEP6;EIF4G1;GSK3A;CNTNAP1;RPLP1;RPLP0;MAST1;CLTB;TAZ;TUBA1C;TUBA1B;RPLP2;ELOB;ITGAV;SPTAN1;GIT1;PSENEN;TEAD4;LYPLA2;ACTR2;ITGA2;TRPC1;RPL13A;RHOC;SREBF2;DNM2;RGMA;ENAH;COL6A2;COL6A1;RPL37A;SCN4A;EVL;ITGA5;DOCK1;RPL10;SRC;ROCK2;RPL11;PSMB6;PTPA;MAPK7;PSMB5;ZSWIM8;RPS3;RPL13;RPS2;RPL18;PDLIM7;MAPK3;PAK4;RPL19;LAMB2;MYO9B;TUBB4B;MAPK12;MAPK11;PSMC3;FAU;AGRN
R-HSA-983169	Class I MHC mediated antigen processing & presentation	LRSAM1;UBE2D1;KEAP1;CDC20;PSMD8;MRC2;PSMD4;UBE2Q2;PSMD2;PSMD3;TOM1;FBXO6;ELOB;ITGAV;IKBKG;SKP1;FBXW4;SEC13;FBXW5;FBXW9;UBE2E1;HLA-B;CYBA;LRRC41;TRAF7;RNF123;CDC34;CANX;UBE2V2;RBCK1;UBA52;THOP1;TRIM11;ANAPC2;CUL7;PSMD12;CUL5;SAR1B;UBA5;FBXO44;ANAPC11;PSMB6;FZR1;PSMB5;UBB;RNF138;UBC;POC1A;RBBP6;STX4;BCAP31;KLHL25;UBE2C;RNF25;FBXL19;BTBD6;FBXL12;UBE2W;UBOX5;PSMC3;UBE2S;UBE2O;STUB1;UBA1;CALR;UBE2K;KBTBD8;UBE2M;RNF220
R-HSA-392499	Metabolism of proteins	RPL3;RPL32;RRP1;KEAP1;SMC5;SMC6;RPL8;CDC20;RPS15;PSMD8;RPS14;NUB1;LGALS1;RPS16;RPL18A;RPS19;PSMD4;TRIM28;PSMD2;PSMD3;RPL36;RPL35;FBXO6;RPS11;SKP1;ALG6;HLA-B;MRPS18A;COG1;MOGS;CSNK1D;P3H3;TMEM170B;HSPG2;HCFC1;RNF123;CDC34;CD109;TARS2;PREB;AURKAIP1;RPL29;UBA52;RPL28;OBSL1;ALG10B;AARS1;AARS2;L3MBTL2;KLK1;SAR1B;EIF5A2;DCUN1D4;MRPL19;TGFA;GATA4;MRPL14;AAAS;MRPL12;ADAMTS10;MRPL10;APH1A;BRIP1;RCE1;EDEM3;

		RPL41;PHC2;PMM1;ABCA3;MRPL27;RAB39A;MRPL28;MRPL24;RPS26;AIMP1;RPS28;RPS29;RPL27A;PAF1;CALR;FARSA;BAP1;H2AX;TRAM1;PIGT;UBXN1;GPAA1;PIGQ;RPLP1;RPLP0;MRPL38;CHM;IDE;BMI1;BABAM1;MRPL41;TUBA1C;TRMT112;TUBA1B;QARS1;TMED3;GNPNAT1;RPLP2;ELOB;QSOX1;IKBKG;TIMP1;TMED7;CTSD;SPTAN1;PSENEN;NDC1;MRPS26;TMED9;SEC13;SSR4;EXOC7;PRMT1;SSR2;ACTL6A;MRPL49;ANO8;MRPS2;SRP9;LRRC41;DDB2;COMMD5;NCOR2;KAT2A;CANX;PIGK;VWA1;KIFC3;GAS6;MFGE8;EEF1E1;ARF5;NAPA;NAPB;MRPS35;RPL10;GPS1, MRPS34;RPL11, MRPS31, DERL2, MRPL54,RELA, MRPL55, PSMB6, GGA1, PSMB5, GGA3, RNF139, LMAN2, MGAT3, RPS3, STX5, RPL13, RPS2, RPL18, RPL19, MBD6, MCRS1, NR1H2, GBF1, SYVN1, NR1H3, DOHH, TUBB4B, PEX14, SPSB3, AGBL5, PSMC3, AGBL3, MSRB2, NUCB1, FAU, COPG1, KBTBD8, PNPLA2, RAB3C, RAB3A, MPI, TNC, UBE2D1, APEH, MANEA, POFUT2, TUBB3, SCMH1,NUDT14, LARGE2, FBXW4, RAB2A, SLC30A6, FBXW5, TRAPPC2L, RPS7, USP5, USP4, RPS8, EIF1AX, RPS5, FBXW9, USP2, IGFBP2, AIP, UBE2E1, SHISA5, MUL1, ALG12, ALG10, RNF40, TUFM, DPM1, DPM2, DOK1, RAB31, HGS, RAB34, EEF1A2, FKBP8, UBE2V2, SCG3, CARS1, CUL9, VCP, INO80E, RAB5B, CUL7, PSMD12, CUL5, UBA5, ARL2, DNAJC24, FBXO44, ATXN3, UBB, UBC, PSAP, TMEM129, EIF4EBP1, NAE1, WDTC1, TMEM132E, TRAPPC1, CBX5, TGFB1, KLHL25, UBE2C, SEC16A, CBX2, TBCB, BTBD6, EEF2, UBE2W, TMEM115, UBE2S, GNAQ, GNB2, TADA3, SRPRA, RNF181, UBA1, CCDC22, TAB1, CNIH2, UBE2K, COPE, UBE2M, EIF4G1, B4GALT2, B4GALT3, MCFD2, THRA, PRKCSH, CHD3, ETFB, GMPPB, MRPL4, MRPL2, SUMO1, MAN1A2, PPP6R1, UBE2Q2, GMPPA, NUP62, DHPS, MARS1, PLAUR, AXIN1, RPL13A, DARS2, RAD23A, TRAF2, POMGNT2, RANGAP1, ADRA2C, POMGNT1, BET1L, DARS1, ARFGAP1, DDOST, ARFGAP2, EEF1G, TRAPPC6A, RPL37A, NAF1, MVD, B4GALT6, PFDN5, GAPDH, ST6GALNAC4, OTUB1, ST6GALNAC6, HDAC3, DCTN2, WBP1, DCTN1, ABRAXAS1, USP11, RAB1B, DCTN3, TULP4, FURIN, USP19, AURKB, HDAC7, AP3M1, DCAF17, GANAB, MTA1, GNG4, TDG, GNA11, RAB24, POC1A, NUP43, RBBP7, UGGT2, DCAF13, SEC11C, OPCML, GADD45GIP1, SLC35A1, USP20, LAMB2, FEM1B, GALNT1, FBXL19, ADRM1, MTOR, FBXL12, ASXL1, PC, NAGK, TNIP1, TNIP2, ASXL2, EIF3J, EIF3G, P4HB, EIF3C, BET1
R-HSA-2408522	Selenoamino acid metabolism	RPL3, RPL32, RPL10, RPLP1, RPL11, RPLP0, RRP1, RPL8, RPS15, RPS14, RPS16, RPL18A, RPS19, QARS1, UBB, UBC, RPS3, RPL36, RPLP2, RPL35, RPL13, RPS2, RPL18, RPS11, RPL19, EEFSEC, RPL41, RPS7, RPS8, RPS5, MARS1, RPL13A, DARS1, AIMP1,

		RPS26, RPS28, RPS29, RPL27A, RPL37A, FAU, RPL29, EEF1E1, UBA52, RPL28
R-HSA-8866652	Synthesis of active ubiquitin: roles of E1 and E2 enzymes	USP5, UBE2C, UBE2E1, UBE2D1, UBE2W, CDC34, UBB, UBE2Q2, UBE2S, UBC, UBA1, UBA52, UBE2K
R-HSA-199991	Membrane Trafficking	RAB3A, GCC2, TUBB3, AKT2, AP1S2, AKT1, ARFIP2, SBF1, VPS36, TBC1D10A, AP2M1, TBC1D10B, SH3GL1, GABARAPL2, TRAPPC2L, SYTL1, AP1B1, TSC2, COG1, OCRL, CSNK1D, RAB31, HGS, ZW10, TBC1D25, PREB, UBA52, VPS28, FTL, RAB5B, SAR1B, RHOBTB3, ARL1, TGFA, PLA2G6, KLC4, BLOC1S6, GRK2, KLC2, UBB, KIF3A, BLOC1S1, UBC, DVL2, PACSIN3, PIP5K1C, TBC1D17, AP1M1, TBC1D16, TRAPPC1, DENND4B, SEC16A, ASPSCR1, RAB39A, SNF8, TMEM115, CHMP2A, CNIH2, COPE, MON1A, PICALM, MCFD2, GDI1, CLTB, CHM, USE1, TUBA1C, TUBA1B, AP1G2, MAN1A2, PPP6R1, TMED3, KIF1A, TMED7, SPTAN1, POLG, ACTR2, SEC13, TMED9, EXOC7, RAB3IL1, KIF22, EPN1, BET1L, ARFGAP1, DNM2, ARFGAP2, TRAPPC6A, NAA38, DNASE2, CHMP6, PAFAH1B3, ARF5, ARF6, NAPA, NAPB, DCTN2, DCTN1, SRC, RAB1B, GPS1, VPS4A, DCTN3, STX10, CYTH2, GGA1, GGA3, VPS51, LMAN2, FCHO2, REPS2, MVB12A, STX5, STX4, LDLR, GALNT1, GBF1, TUBB4B, SNX18, MYO1C, NECAP1, COPG1, BET1
R-HSA-174048	APC/C:Cdc20 mediated degradation of Cyclin B	CDC20, ANAPC15, UBB, UBE2S, UBE2C, UBC, UBE2E1, UBE2D1, UBA52, ANAPC11, ANAPC2
R-HSA-174178	APC/C:Cdh1 mediated degradation of Cdc20 and other APC/C:Cdh1 targeted proteins in late mitosis/early G1	PSMD12, ANAPC15, UBE2C, UBE2E1, UBE2D1, AURKB, ANAPC11, PSMB6, CDC20, PSMD8, FZR1, PSMB5, PSMD4 PSMC3, UBB, UBE2S, PSMD2, PSMD3, UBC, UBA52, ANAPC2
R-HSA-5674400	Constitutive Signalling by AKT1 E17K in Cancer	CASP9, NR4A1, CDKN1A, GSK3A, BAD, AKT2, RPS6KB2, MLST8, TSC2, AKT1, MTOR
R-HSA-199977	ER to Golgi Anterograde Transport	NAPA, NAPB, MCFD2, DCTN2, DCTN1, SAR1B, RAB1B, DCTN3, TGFA, TUBA1C, TUBA1BTUBB3, PPP6R1, LMAN2, TMED3, STX5, TMED7, SPTAN1, SEC13, TMED9, TRAPPC2L, TRAPPC1, SEC16A, GBF1, COG1, CSNK1D, TUBB4B, BET1L, ARFGAP1, ARFGAP2, TRAPPC6A, TMEM115, PREB, COPG1, CNIH2, ARF5, COPE, BET1
R-HSA-72695	Formation of the ternary complex, and subsequently, the 43S complex	RPS7, EIF1AX, RPS8, RPS5, RPS26, RPS15, RPS14, RPS28, RPS16, UBB, RPS19, RPS29, EIF3J, EIF3G, RPS3, FAU, RPS2, EIF3C, RPS11
R-HSA-179409	APC-Cdc20 mediated degradation of Nek2A	CDC20, ANAPC15, UBB, UBE2S, UBE2C, UBC, UBE2E1, UBE2D1, UBA52, ANAPC11, ANAPC2
R-HSA-381119	Unfolded Protein Response (UPR)	ZBTB17, ACADVL, CUL7, GSK3A, DCTN1, DDX11, SYVN1, PPP2R5B, ASNS, YIF1A, ARFGAP1, MYDGF, DDIT3, SRPRA, PREB, TPP1, CALR, TLN1, ATP6V0D1, EXTL3

R-HSA-69052	Switching of origins to a post-replicative state	PSMD12, ANAPC15, MCM7, UBE2D1, ANAPC11, PSMB6, PSMD8, FZR1, PSMB5, PSMD4, UBB, PSMD2, PSMD3, ORC2, UBC, SKP1, CDT1, UBE2C, UBE2E1, PSMC3, UBE2S, MCM5, UBA52, ANAPC2, MCM2
R-HSA-8943724	Regulation of PTEN gene transcription	HDAC5, PHC2, HDAC3, CBX2, ATN1, CHD3, BMI1, MTOR, HDAC7, MTA1;PC, SCMH1, MLST8, LAMTOR2, SLC38A9, LAMTOR1, RBBP7, LAMTOR4, LAMTOR3, BAP1, MAPK3
R-HSA-5389840	Mitochondrial translation elongation	MRPS35, MRPL19, MRPS34, MRPS31, MRPL38, MRPL14, MRPL12, MRPL54, MRPL10, MRPL55, MRPL41, MRPL4, BRIP1, MRPL2, GADD45GIP1, MRPS26, MRPL49, MRPL27, AIP, MRPL28, MRPS2, MRPS18A, MRPL24, TUFM, AURKAIP1
R-HSA-72662	Activation of the mRNA upon binding of the cap-binding complex and eIFs, and subsequent binding to 43S	RPS7, EIF1AX, RPS8, RPS5, RPS26, RPS15, RPS14, RPS28, RPS16, UBB, RPS19, RPS29, EIF3J, EIF3G, EIF4EBP1, RPS3, FAU, RPS2, EIF3C, RPS11, EIF4G1
R-HSA-909733	Interferon alpha/beta signalling	BST2, IFITM3, IFITM1, HLA-B, IRF8, TYK2
R-HSA-2426168	Activation of gene expression by SREBF (SREBP)	FDPS, SREBF1, MVK, LSS, SREBF2, HELZ2, FASN, CARM1, PMVK, MVD, DHCR7, TBL1X, FDFT1
R-HSA-72649	Translation initiation complex formation	RPS7, EIF1AX, RPS8, RPS5, RPS26, RPS15, RPS14, RPS28, RPS16, UBB, RPS19, RPS29, EIF3J, EIF3G, RPS3, FAU, RPS2, EIF3C, RPS11, EIF4G1
R-HSA-6807070	PTEN Regulation	HDAC5, PSMD12, HDAC3, ATN1, CHD3, BMI1, HDAC7, PSMB6, PSMD8, MTA1, PSMB5, PSMD4, UBB, PSMD2, AKT2, PSMD3, SCMH1, UBC, MLST8, AKT1, SLC38A9, RBBP7, MAPK3, PHC2, CBX2, MTOR, MOV10, PC, PSMC3, AGO2, LAMTOR2, STUB1, LAMTOR1, LAMTOR4, UBA52, LAMTOR3, BAP1, FRK
R-HSA-8849469	PTK6 Regulates RTKs and Their Effectors AKT1 and DOK1	DOK1, UBB;UBC, AKT1, ARAP1, UBA52
R-HSA-9648895	Response of EIF2AK1 (HRI) to heme deficiency	PPP1R15A, DDIT3, ASNS, TRIB3, CHAC1
R-HSA-174154	APC/C:Cdc20 mediated degradation of Securin	PSMD12, ANAPC15, UBE2C, UBE2E1, UBE2D1, ANAPC11, PSMB6, CDC20, PSMD8, PSMB5, PSMD4, PSMC3, UBB, UBE2S, PSMD2, PSMD3, UBC, UBA52, ANAPC2

3) circGRB10 knockdown Gene Ontology pathway analysis

GO Term	*Description*	*Genes Involved*
GO:0044419	interspecies interaction between organisms	ZC3H7B, AP1B1, SEC13, IKBKG, MCRS1, CANX , USF2, ADRBK1, RPL13, SUPT6H, RPL10, TLN1, NUP62, TRIM28, RPL8, BSG, CD151, UPF1, CD81, BANF1, PHB, EIF3G, EPHA2, RPL35, RPS5, HLA-B, SCARB1, TUFM, RPS2, SLC1A5, RPLP2, RPLP1, ALYREF, PSMB6, ATP6V0C, FURIN, RPLP0, RAD23A, RPL41, PSMC3, CARM1, FKBP8, PPP1CA, EIF4G1, VPS4A, RPL36, RPL28, BAX, RAB1B, UBA52, RPS26, PPIB, GADD45GIP1, PTBP1, RPS16, BAD, RPS19, UBB, RPS11, RPS8, AAAS, KRT8, RPS15, AUP1, CPSF4, SMARCA4, USP11, MAPK3, GNB2L1, NDUFA13, AP2M1, SND1, E2F1, PHB2, HSPB1, SYNGR2, GAPDH, SRCAP, HMGA1, SGTA, RPS28, TCEB2, BCAP31, POLR2E, IRAK1, POLR2A
GO:0051704	multi-organism process	ZC3H7B, EXOSC5, SEC13, IKBKG, GTF2F1, NUP62, BSG, FLNA, CD151, UPF1, BANF1, CD81, EPHA2, RPL35, TUFM, SCARB1, TRIM11, ALYREF, PSMB6, FURIN, PSMC3, RPL36, RAB1B, EEF1G, PPIB, GADD45GIP1, PTBP1, KRT8, PQBP1, CPSF4, SMARCA4, USP11, NDUFA13, E2F1, HSPB1, SRCAP, SYNGR2, BCAP31, TCEB2, POLR2E, IRAK1, AP1B1, MCRS1, CANX, USF2, RPL13, ADRBK1, SUPT6H, RPL10, TLN1, RPL8, COTL1, EIF3G, PHB, CAD, RPS5, HLA-B, RPS2, RPLP2, SLC1A5, RPLP1, DVL1, RPLP0, ATP6V0C, RAD23A, RPL41, CARM1, FAM3A, FKBP8, PPP1CA, VPS4A, RPL28, BAX, UBA52, RPS26, RPS16, BAD, RPS19, UBB, RPS11, AAAS, RPS8, RPS15, AUP1, MAPK11, MAP3K14, MAPK3, GNB2L1, IGFBP2, AP2M1, SND1, PHB2, GAPDH, HMGA1, SGTA, RPS28, VPS13A
GO:0016032	viral process	ZC3H7B, AP1B1, SEC13, IKBKG, MCRS1, CANX, RPL18A, USF2, ADRBK1, RPL13, SUPT6H, RPL10, TLN1, NUP62, TRIM28, RPL8, CD151, SUV39H1, UPF1, BANF1, EIF3G, RPL35, RPS5, HLA-B, TUFM, RPS2, RPLP2, RPLP1, ALYREF, PSMB6, ARF1, ATP6V0C, FURIN, RPLP0, RAD23A, RPL41, PSMC3, CARM1, FKBP8, PPP1CA, EIF4G1, VCP, VPS4A, RPL36, RPL28, BAX, MVB12A, RAB1B, UBA52, RPS26, GADD45GIP1, PTBP1, PI4KB, RPS16 , BAD, AKAP8L, RPS19, UBB, RPS11, RPS8, AAAS, UBXN1, KRT8, RPS15, AUP1, CPSF4, RPS7, KRT18, HCFC1, CHMP1A, USP11, E4F1, MVB12B, MAPK3, GNB2L1, NDUFA13, AP2M1, SND1, E2F1, PHB2, HSPB1, SYNGR2, SRCAP, HMGA1, SGTA, RPS28, TCEB2, BCAP31, RPTOR, CUL7, POLR2E, IRAK1, POLR2A
GO:0044403	symbiont process	ZC3H7B, AP1B1, SEC13, IKBKG, MCRS1, CANX, RPL18A, USF2, RPL13, ADRBK1, SUPT6H, RPL10, TLN1, NUP62, TRIM28, RPL8, CD151, SUV39H1, UPF1, BANF1, EIF3G, RPL35, RPS5, HLA-B, TUFM, RPS2, RPLP2, RPLP1, ALYREF, PSMB6, ARF1, ATP6V0C, FURIN, RPLP0, RAD23A, RPL41, PSMC3, CARM1, FKBP8, PPP1CA, EIF4G1, VCP, VPS4A, RPL36, RPL28, BAX, MVB12A, RAB1B, UBA52, RPS26, GADD45GIP1, PTBP1, PI4KB, RPS16, BAD, AKAP8L, RPS19, UBB, RPS11, AAAS, RPS8, UBXN1, KRT8, RPS15, AUP1, CPSF4, RPS7, KRT18, HCFC1, CHMP1A, USP11, E4F1, MVB12B, MAPK3, GNB2L1, NDUFA13, AP2M1, SND1, E2F1, PHB2, HSPB1, SYNGR2, SRCAP, HMGA1, SGTA, RPS28, TCEB2, BCAP31, RPTOR, CUL7, POLR2E, IRAK1, POLR2A
GO:0000184	nuclear-transcribed mRNA catabolic process, nonsense-	RPL35, UBA52, RPS5, RPS26, RPS2, RPLP2, RPLP1, PPP2R1A, RPS16, SMG5, RPL13, RPLP0, RPS19, RPS11, RPL10, RPS8, RPL41, RPL8, RPS15, RPS28, UPF1, RPL36, RPL28

	mediated decay	
GO:0016071	mRNA metabolic process	EXOSC5, SYMPK, RPL18A, RPL13, PRPF6, ARL6IP4, RALY, SF3A2, GTF2F1, SUPT6H, RPL10, RPL8, FLNA, SUPT5H, UPF1, CNOT3, PRPF19, RPL35, RPS5, EDC3, RPS2, RPLP2, RPLP1, PPP2R1A, SART1, ALYREF, RPLP0, RPL41, AURKAIP1, DDX23, TBRG4, NHP2L1, EIF4G1, RPL36, PDCD11, RPL28, UBA52, DDX39A, SNRPD2, POLDIP3, RPS26, PTBP1, RPS16, AKAP8L, RPS19, SNRPB, RPS11, RPS8, RPS15, PQBP1, CPSF4, SF3B5, RPS7, SNRNP200, RBM10, POLR2L, U2AF2, SRRT, POLR2J, XAB2, WDR83, SMG5, LSM4, TUT1, PCIF1, ZMAT5, RPS28, POLR2F, POLR2E, CD2BP2, POLR2A
GO:0019083	viral transcription	RPL35, UBA52, RPS5, SEC13, RPS26, RPS2, RPLP2, RPLP1, RPS16, USF2, RPL13, RPS19, RPLP0, RPS11, RPL10, AAAS, RPS8, RPL8, RPL41, RPS15, RPS28, RPL36, RPL28
GO:0044271	cellular nitrogen compound biosynthetic process	FOXK2, MED24, RFC2, TCOF1, SYMPK, ELOF1, NDUFA7, CHAC1, ABCA2, MRPS18A, GTF2F1, DRAP1, TRIM28, FLNA, IMPDH1, PMM1, ENO1, ENTPD6, RPL35, OAZ1, NADSYN1, BRF1, GTF3C1, FURIN, COASY, APRT, EIF4G1, GUK1, RPL36, TELO2, TAF6, TPI1, EEF1A2, SNRPB, TECR, CPSF4, DEAF1, RPAP1, HAGH, PTMA, CDK4, POLRMT, MRPL2, MRPL28, ASL, TSPO, POLR2L, POLR2J, XAB2, COL4A2, MRPS34, ASS1, E2F1, SLC25A1, POLD2, GMPPB, POLD1, AGPAT2, TCEB2, POLR2F, POLR2E, SCAF1, POLR2A, DRG2, NAT14, NADK, UROD, TK1, RPL19, RPL18A, RPL18, CNDP2, RPL13, UAP1L1, SUPT6H, RPL10, RPL8, SUPT5H, GPI, PPP5C, UPP1, MAD2L2, FASN, PHB, CAD, RPS5, AKT1, RPS2, RPLP2, MED16, RPLP1, MRPL12, ACD, ATP6V0C, RPLP0, MRPS2, PFKL, B4GALT3, RPL41, STOML2, NR2C2AP, NT5C, VCP, IDH2, RPL28, BAX, UBA52, RPS26, ZNF768, SLC25A39, NPM3, RPS16, UBC, RPS19, SHMT2, UBB, RPS11, RPS8, ADRM1, ESRRA, DHPS, RPS14, RPS15, HIRA, ITPA, FLAD1, CYB5R3, PKM, MRPL11, RPS7, RPS6KB2, MED15, GTF3C5, TGFB1, GCN1L1, SRRT, MAPK3, ACOT7, PEMT, GAPDH, RPS28, MED12, INTS1, FPGS, CERS1, SRM
GO:0006413	translational initiation	RPL35, RPS5, UBA52, RPS26, RPS2, RPLP2, RPLP1, RPS16, RPL13, RPLP0, RPS19, RPS11, RPL10, RPS8, RPL41, RPL8, RPS15, RPS28, RPL36, RPL28, EIF6, EIF3G
GO:0045047	protein targeting to ER	RPL35, UBA52, RPS5, RPS26, RPS2, RPLP2, RPLP1, RPS16, RPL13, RPLP0, RPS19, RPS11, RPL10, RPS8, RPL41, RPL8, RPS15, RPS28, SGTA, RPL36, RPL28
GO:0072599	establishment of protein localization to endoplasmic reticulum	RPL35, UBA52, RPS5, RPS26, RPS2, RPLP2, RPLP1, RPS16, RPL13, RPLP0, RPS19, RPS11, RPL10, RPS8, RPL41, RPL8, RPS15, SGTA, RPS28, RPL36, RPL28
GO:0006614	SRP-dependent cotranslational protein targeting to membrane	RPL35, UBA52, RPS5, RPS26, RPS2, RPLP2, RPLP1, RPS16, RPL13, RPLP0, RPS19, RPS11, RPL10, RPS8, RPL41, RPL8, RPS15, RPS28, RPL36, RPL28
GO:0072594	establishment of protein localization to organelle	BAX, UBA52, TOMM40, FIS1, SEC13, RPS26, BRCA2, RPS16, BAD, RPL13, RPS19, AIP, TIMM13, RPS11, RPL10, RPS8, RPL8, RPS15, TIMM17B, RPL35, RPS5, PINK1, RPS2, RPLP2, NDUFA13, RPLP1, RPLP0, PHB2, RPL41, AP3D1, HGS, CALM3, SGTA, RPS28, RPL36, VPS4A, VPS13A, RUVBL2, RPL28

GO:0006401	RNA catabolic process	UBA52, EXOSC5, RNASEH2A, RPS26, RPS16, RPL13, RPS19, RPL10, RPS11, RPS8, RPL8, RPS15, UPF1, RPL35, RPS5, RPS2, RPLP2, RPLP1, PPP2R1A, SMG5, RPLP0, SND1, RPL41, RPS28, RPL36, RPL28
GO:0006613	cotranslational protein targeting to membrane	RPL35, UBA52, RPS5, RPS26, RPS2, RPLP2, RPLP1, RPS16, RPL13, RPLP0, RPS19, RPS11, RPL10, RPS8, RPL41, RPL8, RPS15, RPS28, RPL36, RPL28
GO:0006605	protein targeting	TOMM40, UBA52, FIS1, RPS26, RPS16, RPL13, AIP, RPS19, TIMM13, OS9, RPL10, RPS11, RPS8, RPL8, RPS15, GIPC1, TIMM17B, RPL35, RPS5, RPS2, RPLP2, RPLP1, RPLP0, CDC37, RPL41, AP3D1, HGS, RPS28, SGTA, VPS4A, RPL36, VPS13A, RPL28
GO:1901576	organic substance biosynthetic process	RFC2, SYMPK, NDUFA7, CHAC1, ELOF1, ABCA2, TRIM28, PMM1, G6PC3, DPM2, UPF1, ENO1, TUFM, AKR1A1, ALG12, GTPBP1, EIF4G1, MRPL49, EEF2, EEF1G, TPI1, EEF1A2, SNRPB, TECR, CPSF4, POLRMT, POLR2L, E4F1, TSPO, POLR2J, COL4A2, XAB2, MRPS34, MVD, CACNA1H, E2F1, MRPL54, HSPG2, SLC25A1, POLD2, POLD1, GMPPB, POLR2F, POLR2E, SCAF1, POLR2A, NAT14, NADK, RPL19, RPL18A, CNDP2, RPL18, RPL13, SUPT6H, UAP1L, RPL10, RPL8, SUPT5H, PPP5C, UPP1, PNPLA2, FASN, MAD2L2, CAD, ZNF598, RPS5, AKT1, RPS2, MED16, RPLP2, RPLP1, MRPL12, ACD, RPLP0, MRPS2, B4GALT3, B4GALT2, RPL41, FADS2, NR2C2AP, AURKAIP1, VCP, MECR, G6PD, RPL28, UBA52, ERAL1, RPS26, ZNF768, NPM3, GAMT, RPS16, UBC, RPS19, UBB, RPS11, ADRM1, RPS8, ESRRA, RPS14, RPS15, HIRA, MRPL38, ITPA, MRPL11, RPS7, RPS6KB2, SLC44A2, GTF3C5, GCN1L1, MAPK3, GNB2L1, PEMT, CCDC88A, GAPDH, RPS28, ILVBL, MED12, CDIPT, SRM, DCXR, FOXK2, MED24, GSTP1, TCOF1, SDSL, MRPS18A, GTF2F1, DRAP1, FLNA, AGRN, IMPDH1, PRPF19, ENTPD6, RPL35, OAZ1, SCARB1, NADSYN1, ARF1, BRF1, GTF3C1, FURIN, FDX1L, COASY, DPM3, APRT, GUK1, RPL36, DGKZ, TELO2, MCM7, RNASEH2A, TAF6, GADD45GIP1, MDH2, RPAP1, DEAF1, HAGH, HSD17B10, CDK4, PTMA, MRPL2, MRPL28, PTMS, ASL, ASS1, MRPL4, SBF1, AGPAT2, IP6K1, TCEB2, DRG2, TK1, TKT, PGD, PYCR1, GPI, PHB, TM7SF2, SLC25A11, PIGQ, ATP6V0C, PFKL, MCM5, STOML2, MCM2, NT5C, IDH2, BAX, GRWD1, SLC25A39, PI4KB, ETNK2, EBP, SHMT2, PHGDH, DHPS, B3GAT3, GPX4, FLAD1, CYB5R3, PKM, MED15, TGFB1, SRRT, ACOT7, PLOD3, CKB, B4GALT7, INTS1, BCAT2, CERS1, FPGS
GO:0009059	macromolecule biosynthetic process	MED24, TCOF1, SYMPK, TK1, ELOF1, NDUFA7, RPL13, DRAP1, GTF2F1, MRPS18A, SUPT6H, RPL10, TRIM28, RPL8, FLNA, SUPT5H, AGRN, UPF1, PHB, RPL35, RPS5, TUFM, RPS2, MED16, RPLP2, RPLP1, MRPL12, RPLP0, B4GALT3, MCM5, GTPBP1, RPL41, MCM2, NR2C2AP, AURKAIP1, EIF4G1, RPL36, RPL28, BAX, MRPL49, EEF2, UBA52, MCM7, RNASEH2A, EEF1G, RPS26, GRWD1, ZNF768, NPM3, GADD45GIP1, RPS16, EEF1A2, RPS19, UBB, SNRPB, RPS11, RPS8, ADRM1, ESRRA, DHPS, RPS15, B3GAT3, CPSF4, DEAF1, RPS6KB2, POLRMT, MRPL2, GTF3C5, MRPL28, PTMS, GCN1L1, MAPK3, POLR2J, GNB2L1, COL4A2, XAB2, MRPS34, E2F1, MRPL4, MRPL54, POLD2, POLD1, RPS28, TCEB2, POLR2F, POLR2E, POLR2A
GO:0009894	regulation of catabolic process	TIMP1, EXOSC5, CDC20, SEC13, IKBKG, TMEM259, OS9, JMJD8, NUP62, FLNA, ATP6V0D1, SUPT5H, GIPC1, UPF1, MAD2L2, CD81, MLST8, PHB, ATP6V0B, PINK1, GIT1, OAZ1, SCARB1, DVL1, PCBP4, PSMB6, ATP6V0C, FURIN, RAD23A, GTPBP1, PSMC3, PPP1CA, TBRG4, EIF4G1, VCP, PSMD8, AMBRA1, PSMD4, PSMD3, BAX, RAB1B, UBA52, PKP3, USP19, LRP1, BAD, PIN1, EEF1A2, USP5, UBB, AAAS, LAMTOR4, DDX49, EIF6, DAPK3, RBM10, TSPO, MAPK3, GNB2L1, NDUFA13,

		HSPBP1, E2F1, PHB2, HSPB1, CDC37, GAPDH, RNF40, HGS, SGTA, STUB1, TCEB2, BCAP31, HMOX1, GSK3A, NUPR1
GO:0070972	protein localization to endoplasmic reticulum	RPL35, RPS5, UBA52, RPS26, RPS2, RPLP2, RPLP1, RPS16, PPP1R15A, RPL13, RPS19, RPLP0, RPS11, RPL10, RPS8, RPL8, RPL41, RPS15, SGTA, RPS28, RPL36, RPL28
GO:1901566	organonitrogen compound biosynthetic process	DRG2, FOXK2, GSTP1, NADK, UROD, TK1, RPL18A, RPL18, CNDP2, RPL1, CHAC1, NDUFA7, SDSL, ABCA2, MRPS18A, PYCR1, RPL10, RPL8, AGRN, IMPDH1, UPP1, FASN, ENO1, RPL35, CAD, RPS5, AKT1, OAZ1, NADSYN1, RPS2, RPLP2, RPLP1, AKR1A1, ATP6V0C, FURIN, RPLP0, MRPS2, PFKL, B4GALT3, B4GALT2, RPL41, COASY, STOML2, APRT, EIF4G1, GUK1, RPL36, IDH2, RPL28, TPI1, RPS26, SLC25A39, GAMT, RPS16, EEF1A2, RPS19, SHMT2, PHGDH, TECR, RPS11, RPS8, DHPS, RPS15, B3GAT3, HAGH, FLAD1, PKM, MRPL11, RPS7, RPS6KB2, SLC44A2, MRPL2, MRPL28, ASL, TSPO, TGFB1, GCN1L1, ACOT7, MRPS34, PEMT, ASS1, HSPG2, PLOD3, SLC25A1, GAPDH, AGPAT2, RPS28, CKB, B4GALT7, ILVBL, BCAT2, CERS1, SRM
GO:0009058	biosynthetic process	RFC2, SYMPK, NDUFA7, CHAC1, ELOF1, ABCA2, TRIM28, PMM1, DPM2, UPF1, G6PC3, ENO1, TUFM, AKR1A1, ALG12, GTPBP1, EIF4G1, MRPL49, EEF2, EEF1G, TPI1, EEF1A2, SNRPB, TECR, CPSF4, POLRMT, POLR2L, TSPO, E4F1, POLR2J, COL4A2, XAB2, MRPS34, MVD, CACNA1H, E2F1, MRPL54, HSPG2, SLC25A1, POLD2, POLD1, GMPPB, POLR2F, POLR2E, SCAF1, POLR2A, NAT14, NADK, UROD, RPL19, RPL18A, CNDP2, RPL18, RPL13, SUPT6H, UAP1L1, RPL10, RPL8, SUPT5H, PPP5C, UPP1, PNPLA2, FASN, MAD2L2, CAD, ZNF598, RPS5, AKT1, RPS2, MED16, RPLP2, RPLP1, MRPL12, ACD, RPLP0, MRPS2, B4GALT3, B4GALT2, RPL41, FADS2, NR2C2AP, AURKAIP1, VCP, G6PD, MECR, CYBA, RPL28, UBA52, ERAL1, RPS26, ZNF768, NPM3, GAMT, RPS16, UBC, RPS19, UBB, RPS11, ADRM1, RPS8, ESRRA, RPS14, RPS15, HIRA, MRPL38, ITPA, MRPL11, RPS7, RPS6KB2, SLC44A2, GTF3C5, GCN1L1, SERPINH1, MAPK3, GNB2L1, PEMT, CCDC88A, GAPDH, RPS28, ILVBL, MED12, CDIPT, DCXR, SRM, FOXK2, MED24, GSTP1, TCOF1, SDSL, GTF2F1, MRPS18A, DRAP1, FLNA, AGRN, IMPDH1, PRPF19, ENTPD6, RPL35, OAZ1, SCARB1, NADSYN1, BRF1, ARF1, FURIN, GTF3C1, FDX1L, COASY, DPM3, APRT, GUK1, RPL36, TELO2, DGKZ, MCM7, LEPREL2, RNASEH2A , TAF6, MDH2, GADD45GIP1, DEAF1, RPAP1, HAGH, HSD17B10, CDK4, PTMA, MRPL2, PTMS, MRPL28, ASL, ASS1, MRPL4, SBF1, IP6K1, AGPAT2, TCEB2, DRG2, TK1, TKT, PGD, PYCR1, GPI, PHB, TM7SF2, GCAT, SLC25A11, PIGQ, ATP6V0C, PFKL, MCM5, STOML2, MCM2, NT5C, IDH2, BAX, GRWD1, SLC25A39, PI4KB, ETNK2, EBP, SHMT2, PHGDH, DHPS, B3GAT3, GPX4, FLAD1, CYB5R3, PKM, MED15, TGFB1, SRRT, ACOT7, PLOD3, CKB, B4GALT7, INTS1, BCAT2, FPGS, CERS1
GO:0046907	intracellular transport	SEC13, KDELR1, SYMPK, ARFGAP2, OS9, SCAP, NUP62, DCTN1, PTPN23, FLNA, LMAN2, TBC1D10A, UPF1, REEP2, BANF1, RPL35, TRAPPC2L, ALYREF, BET1L, RAB11B, UBXN6, RPL36, MVB12A, RAB1B, FIS1, SNRPD2, DDX39A, SNRPB, ARF5, CPSF4, YIF1A, ARHGAP1, EIF6, TIMM17B, ARFIP2, CHMP1A, SSNA1, TSPO, PLEKHJ1, NDUFA13, SMG5, HSPB1, CDC37, AP3D1, RAMP1, HGS, BCAP31, TOMM40, AP1B1, MICALL1, RPL18A, RPL13, TBC1D13, TIMM13, RPL10, TIMM10, SUN2, RPL8, TMED9, GIPC1, KIF1C, RPS5, STX10, RPS2, RPLP2, RPLP1, RPLP0, NOL6, CALR, RPL41, STOML2, TUBA1C, RAB5C, VCP, TMEM115, VPS4A, RPL28, UBA52, POLDIP3, RPS26, COPG1, RPS16, RPS19, AIP, UBB, SSR2, RPS11, AAAS, RPS8, RPS15,

		CLTB, AUP1, KIF1A, PEF1, TGFB1, U2AF2, DNM2, AP2M1, NAPA, PHB2, ERGIC3, HMGA1, SGTA, RPS28, COPE, VPS13A
GO:0000956	nuclear-transcribed mRNA catabolic process	RPL35, UBA52, RPS5, EXOSC5, RPS26, RPS2, RPLP2, RPLP1, RPS16, PPP2R1A, SMG5, RPL13, RPS19, RPLP0, RPS11, RPL10, RPS8, RPL8, RPL41, RPS15, RPS28, UPF1, RPL36, RPL28
GO:0006402	mRNA catabolic process	RPL35, UBA52, RPS5, EXOSC5, RPS26, RPS2, RPLP2, RPLP1, RPS16, PPP2R1A, SMG5, RPL13, RPS19, RPLP0, RPS11, RPL10, RPS8, RPL8, RPL41, RPS15, RPS28, UPF1, RPL36, RPL28
GO:0034645	cellular macromolecule biosynthetic process	TCOF1, TK1, RPL18A, RPL13, NDUFA7, DRAP1, GTF2F1, MRPS18A, SUPT6H, RPL10, RPL8, FLNA, SUPT5H, UPF1, PPP5C, MAD2L2, PHB, RPL35, RPS5, AKT1, TUFM, RPS2, RPLP2, MED16, RPLP1, MRPL12, ACD, GTF3C1, RPLP0, MRPS2, MCM5, GTPBP1, RPL4, MCM2, AURKAIP1, EIF4G1, VCP, RPL36, TELO2, RPL28, MRPL49, EEF2, UBA52, MCM7, RNASEH2A, EEF1G, TAF6, RPS26, GRWD1, ZNF768, NPM3, GADD45GIP1, RPS16, EEF1A2, RPS19, UBB, RPS1, RPS8, DHPS, RPS, B3GAT3, DEAF1, RPAP1, MRPL38, RPS7, RPS6KB2, PTMA, POLRMT, MRPL2, GTF3C5, MRPL28, PTMS, E4F1, POLR2L, GCN1L1, SRRT, POLR2J, GNB2L1, XAB2, COL4A2, MRPS34,E2F1, MRPL4, MRPL54, POLD2, POLD1, RPS28, TCEB2, POLR2F, POLR2E, B4GALT7, INTS1, POLR2A
GO:0044265	cellular macromolecule catabolic process	EXOSC5, CDC20, RPL13, CDC34, OS9, RPL10, RPL8, PTPN23, FBXW5, UPF1, UBE2s, RPL35, RPS5, PINK1, SPSB3, RPS2, RPLP2, RPLP1, PPP2R1A, PSMB6, RPLP0, RAD23A, RPL41, PSMC3, PSMD8, RPL36, PSMD4, VPS4A, RPL28, PSMD3, LONP1 UBA52, RNASEH2A, RPS26, USP19, RPS16, USP5, FBXW4, RPS19, RPS11, RPS8, ADRM1, RPS15, BAP1, AP2M1, SMG5, SND1, RNF40, SGTA, STUB1, RPS28, GSK3A, VPS13A
GO:0072657	protein localization to membrane	BAX, UBA52, PKP3, RPS26, RPS16, BAD, RPL13, RPS19, TIMM13, RPS11, RPL10, RPS8, RPL8, BSG, FLNA, RPS15, FLOT2, AGRN, REEP2, CD81, EPHA2, RPL35, RPS5, RPS2, RPLP2, NDUFA13, RPLP1, DVL1, RPLP0, RPL41, AP3D1, RAMP1, RPS28, SGTA, RPL36, PALM, RPL28
GO:0090150	establishment of protein localization to membrane	BAX, UBA52, RPS26, RPS16, BAD, RPL13, RPS19, TIMM13, RPL10, RPS11, RPS8, RPL8, RPS15, REEP2, RPL35, RPS5, RPS2, RPLP2, RPLP1, NDUFA13, RPLP0, RPL41, SGTA, RPS28, RPL36, RPL28
GO:0006518	peptide metabolic process	[DRG2, APEH, PSENEN, GSTP1, RPL19, RPL18A, CNDP2, RPL18, RPL13, NDUFA7, CHAC1, MRPS18A, RPL10, RPL8, RPL35, RPS5 , AKT1, RPS2, RPLP2, RPLP1, FURIN, RPLP0, PTGES2, MRPS2, RPL41, APH1A, EIF4G1, RPL36, G6PD, RPL28, EEF1G, RPS26, RPS16, EEF1A2, RPS19, RPS11, RPS8, DHPS, RPS14, RPS15, HM13, HAGH, RPS7, MRPL11, RPS6KB2, MRPL2, MRPL28, GCN1L1, MRPS34, THOP1, GDAP1L1, RPS28, STUB, ECE1
GO:0031329	regulation of cellular catabolic process	TIMP1, EXOSC5, CDC20, SEC13, IKBKG, TMEM259, OS9, JMJD8, NUP62, ATP6V0D1, SUPT5H, GIPC1, UPF1, CD81, MLST8, ATP6V0B, PINK1, GIT1, SCARB1, DVL1, PCBP4, PSMB6, ATP6V0C, FURIN, RAD23A, GTPBP1, PSMC3, PPP1CA, TBRG4, EIF4G1, VCP, PSMD8, AMBRA1, PSMD4, PSMD3, BAX, UBA52, RAB1B, PKP3, USP19, LRP1, BAD, EEF1A2, USP5, UBB, AAAS, LAMTOR4, DDX49, EIF6, DAPK3, RBM10, TSPO, MAPK3, GNB2L1, HSPBP1, E2F1, PHB2, HSPB1, CDC37, GAPDH, RNF40, SGTA, STUB1, TCEB2, BCAP31, HMOX1, GSK3A, NUPR1

GO:0050896	response to stimulus	EMD, GSTP1, COX4I1, PYCR1, TLN1, SFN, SDF4, PRMT1, TRIM28, RPL8, ATP6V0D1, COTL1, FASN, SCYL1, HLA-B, EIF4EBP1, TUFM, PLOD1, RAD23A, MCM5, FAM3A, STOML2, MCM2, PRDX2, APRT, PSMD8, LONP1, MCM7, RNASEH2A, EEF1G, RANGAP1, MDK, BAD, EEF1A2, LRP5, MYBL2, KRT8, PQBP1, LAMTOR4, GPX4, YIF1A, PEF1, BAP1, PTK7, COL6A2, IGFBP2, NDUFA13, XAB2, PPP1R15A, PKN1, HSPB1, POLD2, RNF40, RAMP1, HMGA1, NDUFS8, NOC2L, SGTA, TCEB2, HMOX1, SRM, RUVBL2
GO:0008152	metabolic process	COX6B1, AGAP3, SYMPK, COX4I1, ELOF1, ABCA2, ABCA3, SF3A2, ARL6IP4, OS9, ABL1, NUP62, COX8A, CLPP, PMM1, FTSJ3, TRAF4, PNPLA6, PLOD1, ACO2, CD320, OTUB1, GTPBP1, TRMT1, AMBRA1, CRABP2, MARK4, SNRPD2, USP20, USP19, PPIB, HDAC11, ATG4D, SNRPB, CTDSP1, TECR, CPSF4, BAP1, MMP24, POLRMT, ARFIP2, RBM10, POLR2L, USP11, POLR2J, TEX264, COL4A2, PPP1R15A, PLD3, MRPL54, POR, SLC25A1, CACTIN, POLD2, SRCAP, POLD1, NAA10, POLR2F, POLR2E, LAMB2, RUVBL2, POLR2A, SHC2, CNDP2, ADRBK1, PRPF6, SUPT6H, KHK, SUPT5H, SUV39H1, PPP5C, MAPKAPK3, AKT1, PPP4C, STX1A, CTSD, GAA, SDF2L1, PPP2R1A, NUDT14, KIF22, MRPS2, FKBP8, APH1A, FADS2, DDX23, PPP1CA, PPM1G, CYC1, G6PD, CYBA, GALE, RNF181, C12orf44, LONP1, POLDIP3, ZNF768, SHISA5, GAMT, PI4KAP2, USP5, KCTD17, SLC25A25, KMT2D, AAAS, ADRM1, AGBL5, BRMS1, MAP2K2, MAPK11, GTF3C5, GCN1L1, MAPK3, PGLS, COPS6, WDR83, PRKCSH, CSK, LSM4, PKN1, CCDC88A, CSNK1D, GAPDH, RNF123, VPS25, SLC27A4, NSUN5, ILVBL, SF3B2, PRDX5, SRM, DCXR, APEH, GSTP1, DDOST, STK40, SDHA, MRPS18A, GTF2F1, MAP3K10, DDB1, PTPN23, TBC1D10A, MAP3K11, APBB1, RPL35, SCYL1, NADSYN1, P4HB, ARF1, FURIN, GTF3C1, OBSCN, RAB11B, MSRB1, TBRG4, APRT, GUK1, RPL36, WDR18, BRPF1, MCM7, ADAM11, GADD45GIP1, MDH2, SERINC2, RPAP1, HAGH, HSD17B10, HCFC1, DAPK3, CHMP1A, ASL, PLEKHJ1, WDR45, CDK16, ASS1, MFGE8, MAPK12, SBF1, HGS, MBD3, DRG2, RRP9, IRF2BP1, PGD, FAM207A, MAN2B1, PHB, PEX14, PIGQ, SART1, ATP6V0C, SLC3A2, PFKL, MCM5, MCM2, GEN1, SLC5A3, BAX, PKD1, GRK6, GRWD1, SLC25A39, LRP1, PI4KB, BAD, PIN1, ETNK2, FBXW4, GPS1, LRP5, AIP, SHMT2, PHGDH DHPS, UBE2M, B3GAT3, AUP1, GPX4, PEF1, CYB5R3, PKM, GRAMD1A, MAP3K14, MED15, MVB12B, U2AF2, SRRT, DNM2, ACOT7, PHB2, PLOD3, SGTA, BCKDHA, LYPLA2, GSK3A, B4GALT7, INTS1, BCAT2, PIGT, DNAJB2, EXOSC5, RFC2, BRCA2, NDUFA7, CHAC1, RALY, SLC29A1, SCAP, PRMT1, TRIM28, BSG, TMEM208, G6PC3, UPF1, DPM2 ENO1, NUBP1, BANF1, EPHA2, TUFM, TRIM11, ALYREF, AKR1A1, ALG12, BLVRB, EIF4G1, URM1, PDCD11, MRPL49, MVB12A, RAB1B, EEF2, LAS1L, DDX39A, VPS51, EEF1G, TPI1, EEF1A2, MYH9, PQBP1, DDX54, SF3B5, ERI3, SNRNP200, CHID1, E4F1, TSPO, XAB2, MVD, MRPS34, WDTC1, CACNA1H, E2F1, HSPG2, GDAP1L1, GMPPB, RAMP1, VKORC1, STUB1, SHARPIN, ECE1, UQCRC1, NAT14, TOMM40, NADK, LMF2, UROD, CAPN1, MCRS1, RPL19, RPL18A, NEK5, RPL18, RPL13, UAP1L1, RPL10, EIF3D, RPL8, ALDH4A1, HDAC5, UPP1, FARSA, CARS, PNPLA2, FASN, PUSL1, MAD2L2, EIF3I, EIF3G, LAMTOR2, CAD, ZNF598, RPS5, PINK1, SPSB3, RPS2, MED16, RPLP2, RPLP1, MRPL12, ADCK2, ACD, RPLP0, TADA3, NOL6, CALR, JMJD4, B4GALT3, RPL41, B4GALT2, CAMK4, VAV1, CARM1, NR2C2AP, AURKAIP1, NDUFA11, STK25, VCP, LRRC41, RPL28, TTLL12, KIF14, UBA52, ERAL1, RPS26, NPM3, RPS16, NTMT1, UBA1, GPAA1, UBC, RPS19, UBB, GDPD5, RPS11, NT5DC2, RPS8, ESRRA, RPS14, HIRA, RPS15, TYRO3, HM13, MRPL38, ETFB, ADAM15,

		GANAB, MRPL11, RPS7, RPS6KB2, SLC44A2, UBXN11, BABAM1, SERPINH1, GNB2L1, PHPT1, PEMT, RRP12, TUT1, RPS28, HMOX1, NUPR1, MPG, CD2BP2, MED12, CDIPT, VPS13A, ZC3H7B, PSENEN, FOXK2, MED24, CDC20, TCOF1, TCN2, IKBKG, SDSL, USE1, CDC34, DRAP1, BOP1, FLNA, FBXW5, AGRN, PSKH1, IMPDH1, UBE2S, PRPF19, CD81, RRP7A, CDCA5, ENTPD6, OAZ1, SCARB1, ADAT2, PSMB6, CAMK1, FDX1L, PSMC3, COASY, PRDX2, DPM3, PSMD8, UBXN6, PSMD4, TELO2, DGKZ, PSMD3, FIS1, LEPREL2, RNASEH2A, TAF6, ESYT1, PTBP1, DAB2IP, CHMP2A, MYBBP1A, RRP1, UBXN1, NUCB1, CIB1, TARBP1, DEAF1, PTK7, EIF6, NOSIP, PTMA, MRPL2, MRPL28, PTMS, NDUFA13, THAP4, SMG5, KLHL25, MRPL4, RNF40, ZMAT5, PTPRA, IP6K1, AGPAT2, NRTN, TCEB2, CUL7, IRAK1, PTPRF, TIMP1, NOP2, TK1, TEX15, TKT, PYCR1, ATP13A2, PYGB, ESPL1, CNOT3, TM7SF2, GCAT, NGFR, EDC3, SLC25A11, KMT2B, TONSL, PTGES2, DUS1L, RAD23A, STOML2, NKTR, NHP2L1, NT5C, VPS4A, IDH3G, SETD1A, DDX56, IDH2, NDUFB11, DDIT4, RANGAP1, AKAP8L, EBP, PES1, FLAD1, DDX49, NDUFB8, TRMT2A, TGFB1, MAPK8IP2, IGFBP2, PELP1, AP2M1, SND1, THOP1, PCIF1, NDUFS8, NDUFS6, CKB, NDUFV1, CERS1
GO:0051649	establishment of localization in cell	SEC13, SYMPK, KDELR1, IKBKG, ARFGAP2, OS9, SCAP, NUP62, DCTN1, FLNA, PTPN23, LMAN2, TBC1D10A, UPF1, REEP2, BANF1, RPL35, TRAPPC2L, ALYREF, PPFIA3, BET1L, RAB11B, RPL36, UBXN6, MVB12A, RAB1B, FIS1, SNRPD2, DDX39A, SNRPB, ARF5, CPSF4, YIF1A, ARHGAP1, EIF6, TIMM17B, ARFIP2, CHMP1A, SSNA1, TSPO, PLEKHJ1, NDUFA13, SMG5, HSPB1, CDC37, AP3D1, RAMP1, HGS, BCAP31, TOMM40, AP1B1, MICALL1, RPL18A, CANX, RPL13, TBC1D13, TIMM13, RPL10, TIMM10, SUN2, RPL8, TMED9, GIPC1, ESPL1, KIF1C, RPS5, STX10, RPS2, RPLP2, RPLP1, DVL1, RPLP0, KIF22, NOL6, CALR, RPL41, STOML2, CALM3, RAB5C, TUBA1C, TMEM115, VCP, VPS4A, RPL28, BAX, UBA52, POLDIP3, RPS26, COPG1, RPS16, BAD, AIP, RPS19, UBB, SSR2, ITPR3, RPS11, RPS8, AAAS, RPS15, CLTB, AUP1, KIF1A, PEF1, U2AF2, TGFB1, DNM2, AP2M1, NAPA, PHB2, ERGIC3, HMGA1, SGTA, RPS28, COPE, VPS13A
GO:0044237	cellular metabolic process	COX6B1, AGAP3, SYMPK, COX4I1, ELOF1, ABCA2, ABCA3, SF3A2, ARL6IP4, OS9, ABL1, NUP62, COX8A, PMM1, FTSJ3, TRAF4, PNPLA6, PLOD1, ACO2, CD320, OTUB1, GTPBP1, TRMT1, AMBRA1, CRABP2, MARK4, SNRPD2, USP20, USP19, PPIB, HDAC11, ATG4D, SNRPB, CTDSP1, TECR, CPSF4, BAP1, POLRMT, ARFIP2, RBM10, USP11, POLR2L, POLR2J, TEX264, COL4A2, PPP1R15A, PLD3, MRPL54, POR, CACTIN, SLC25A1, POLD2, SRCAP, POLD1, NAA10, POLR2F, POLR2E, LAMB2, RUVBL2, POLR2A, SHC2, CNDP2, ADRBK1, PRPF6, SUPT6H, KHK, SUPT5H, SUV39H1, PPP5C, MAPKAPK3, AKT1, PPP4C, STX1A, GAA, SDF2L1, PPP2R1A, NUDT14, KIF22, MRPS2, FADS2, APH1A, FKBP8, DDX23, PPP1CA, PPM1G, CYC1, G6PD, CYBA, RNF181, LONP1, C12orf44, POLDIP3, ZNF768, SHISA5, GAMT, PI4KAP2, USP5, KCTD17, SLC25A25, KMT2D, ADRM1, AAAS, AGBL5, BRMS1, MAP2K2, MAPK11, GTF3C5, GCN1L1, MAPK3, PGLS, COPS6, WDR83, PRKCSH, CSK, LSM4, CCDC88A, PKN1, CSNK1D, GAPDH, RNF123, VPS25, SLC27A4, NSUN5, ILVBL, SF3B2, PRDX5, SRM, DCXR, APEH, GSTP1, DDOST, STK40, SDHA, GTF2F1, MRPS18A, MAP3K10, DDB1, PTPN23, MAP3K11, APBB1, RPL35, SCYL1, NADSYN1, P4HB, ARF1, GTF3C1, FURIN, OBSCN, RAB11B, TBRG4, MSRB1, APRT, GUK1, RPL36, WDR18, BRPF1, MCM7, MDH2, GADD45GIP1, SERINC2, RPAP1, HAGH, HSD17B10, HCFC1, DAPK3, ASL, PLEKHJ1, WDR45, CDK16, ASS1, MFGE8, MAPK12, SBF1, HGS, MBD3, DRG2, RRP9, IRF2BP1, PGD,

		FAM207A, MAN2B1, PHB, PEX14, PIGQ, SART1 ATP6V0C, PFKL, MCM5, MCM2, GEN1, SLC5A3, BAX, PKD1, GRK6, GRWD1, SLC25A39, LRP1, PI4KB, PIN1, BAD, ETNK2, FBXW4, GPS1, AIP, SHMT2, PHGDH, DHPS, B3GAT3, UBE2M , AUP1, GPX4, PEF1, CYB5R3, PKM, GRAMD1A, MED15, MAP3K14, U2AF2, MVB12B, SRRT, DNM2, ACOT7, PHB2, PLOD3, BCKDHA, SGTA, LYPLA2, GSK3A, B4GALT7, BCAT2, INTS1, PIGT, DNAJB2, EXOSC5, RFC2, BRCA2, CHAC1, NDUFA7, RALY, SLC29A1, SCAP, PRMT1, TRIM28, BSG, TMEM208, G6PC3, DPM2, UPF1, ENO1, NUBP1, BANF1, EPHA2, TUFM, TRIM11, ALYREF, AKR1A1, ALG12, BLVRB, EIF4G1, URM1, PDCD11, MRPL49, MVB12A, RAB1B, EEF2, LAS1L, VPS51, DDX39A, EEF1G, TPI1, EEF1A2, PQBP1, DDX54, SF3B5, ERI3, SNRNP200, E4F1, TSPO, XAB2, MVD, MRPS34, WDTC1, CACNA1H, E2F1, HSPG2, GDAP1L1, GMPPB, RAMP1, VKORC1, STUB1, SHARPIN, ECE1, UQCRC1, NAT14, TOMM40, NADK, UROD, CAPN1, MCRS1, RPL19, NEK5, RPL18A, RPL18, RPL13, UAP1L1, RPL10, EIF3D, RPL8, ALDH4A1, UPP1, HDAC5, FARSA, CARS, PNPLA2, FASN, MAD2L2, PUSL1, EIF3I, EIF3G, LAMTOR2, CAD, ZNF598, RPS5, PINK1, SPSB3, RPS2, MED16, RPLP2, RPLP1, MRPL12, ADCK2, ACD, RPLP0, TADA3, NOL6, JMJD4, B4GALT3, B4GALT2, CAMK4, RPL41, VAV1, CARM1, AURKAIP1, NR2C2AP, NDUFA11, STK25, VCP, LRRC41, RPL28, TTLL12, KIF14, UBA52, ERAL1, RPS26, NPM3, RPS16, NTMT1, UBA1, GPAA1, UBC, RPS19, UBB, RPS11, RPS8, NT5DC2, ESRRA, RPS14, HIRA, RPS15, TYRO3, HM13, MRPL38, ETFB, GANAB, RPS7, MRPL11, RPS6KB2, UBXN11, SLC44A2, BABAM1, GNB2L1, PHPT1, PEMT, RRP12, TUT1, RPS28, HMOX1, NUPR1, MPG, CD2BP2, MED12, CDIPT, VPS13A, ZC3H7B, PSENEN, FOXK2 MED24, CDC20, TCOF1, TCN2, IKBKG, SDSL, CDC34, DRAP1, BOP1, FLNA, FBXW5, AGRN, IMPDH1, PSKH1, UBE2S, PRPF19, CD81, RRP7A, CDCA5, ENTPD6, OAZ1, SCARB1, ADAT2, PSMB6, CAMK1, FDX1L, PSMC3, COASY, PRDX2, DPM3, PSMD8, UBXN6, PSMD4, TELO2, DGKZ, PSMD3, FIS1, LEPREL2, RNASEH2A, TAF6, ESYT1, PTBP1, DAB2IP, CHMP2A, MYBBP1A, RRP1, UBXN1, NUCB1, CIB1, TARBP1, DEAF1, EIF6, PTK7, NOSIP, PTMA, MRPL2, PTMS, MRPL28, NDUFA13, THAP4, SMG5, KLHL25, MRPL4, RNF40, ZMAT5, PTPRA, IP6K1, AGPAT2, NRTN, TCEB2, CUL7, IRAK1, PTPRF, TIMP1, NOP2, TK1, TEX15, TKT, PYCR1, ATP13A2, PYGB, CNOT3, GCAT, EDC3, KMT2B, TONSL, PTGES2, DUS1L, RAD23A, STOML2, NKTR, NHP2L1, NT5C, IDH3G, VPS4A, SETD1A, DDX56, IDH2, NDUFB11, DDIT4, RANGAP1, AKAP8L, PES1, FLAD1, DDX49, NDUFB8, TRMT2A, TGFB1, MAPK8IP2, PELP1, IGFBP2, AP2M1, SND1, THOP1, PCIF1, NDUFS8, NDUFS6, CKB, NDUFV1, CERS1
GO:0016070	RNA metabolic process	ZC3H7B, EXOSC5, MED24, TCOF1, SYMPK, ELOF1, SF3A2, RALY, ARL6IP4, DRAP1, GTF2F1, BOP1, TRIM28, FLNA, UPF1, PRPF19, FTSJ3, RRP7A, RPL35, ALYREF, GTF3C1, TBRG4, TRMT1, EIF4G1, PDCD11, RPL36, WDR18, DDX39A, SNRPD2, RNASEH2A, TAF6, PTBP1, SNRPB, RRP1, DDX54, PQBP1, TARBP1, CPSF4, RPAP1, DEAF1, SF3B5, HSD17B10, EIF6, SNRNP200, PTMA, POLRMT, RBM10, POLR2L, POLR2J, XAB2, COL4A2, SMG5, E2F1, ZMAT5, TCEB2, POLR2F, POLR2E, POLR2A, NOP2, RPL18A, PRPF6, RPL13, SUPT6H, RPL10, RPL8, SUPT5H, SUV39H1, CNOT3, PPP5C, CARS, FARSA, PUSL1, RPS5, EDC3, RPS2, RPLP2, MED16, RPLP1, PPP2R1A, SART1, MRPL12, RPLP0, NOL6, DUS1L, RPL41, NR2C2AP, AURKAIP1, DDX23, NHP2L1, RPL28, BAX, UBA52, POLDIP3, RPS26, ZNF768, NPM3, RPS16, AKAP8L, RPS19, RPS11, ADRM1, RPS8, ESRRA, RPS15, PES1, RPS7, DDX49, TRMT2A,

		GTF3C5, U2AF2, SRRT, MAPK3, PELP1, WDR83, SND1, LSM4, RRP12, TUT1, PCIF1, RPS28, NSUN5, CD2BP2, INTS1
GO:0034641	cellular nitrogen compound metabolic process	EXOSC5, SYMPK, BRCA2, ELOF1, NDUFA7, ABCA2, ARL6IP4, SF3A2, RALY, ABL1, TRIM28, PMM1, UPF1, BANF1, FTSJ3, EPHA2, ALYREF, OTUB1, GTPBP1, BLVRB, TRMT1, EIF4G1, PDCD11, SNRPD2, DDX39A, EEF1G, TPI1, EEF1A2, SNRPB, TECR, PQBP1, DDX54, CPSF4, SF3B5, SNRNP200, POLRMT, RBM10, POLR2L, TSPO, E4F1, POLR2J, COL4A2, XAB2, MRPS34, PLD3, E2F1, SLC25A1, GDAP1L1, POLD2, POLD1, STUB1, POLR2F, POLR2E, ECE1, POLR2A, RUVBL2, UQCRC1, UROD, MCRS1, RPL18A, CNDP2, PRPF6, RPL13, SUPT6H, RPL10, RPL8, SUPT5H, SUV39H1, PPP5C, UPP1, CARS, FARSA, PUSL1, FASN, MAD2L2, CAD, RPS5, AKT1, RPS2, MED16, RPLP2, RPLP1, PPP2R1A, MRPL12, ACD, NUDT14, KIF22, RPLP0, MRPS2, NOL6, B4GALT3, RPL41, DDX23, NR2C2AP, AURKAIP1, VCP, G6PD, RPL28, LONP1, UBA52, POLDIP3, RPS26, ZNF768, NPM3, RPS16, RPS19, SLC25A25, UBB, RPS11, ADRM1, RPS8, ESRRA, RPS15, HM13, RPS7, RPS6KB2, GTF3C5, BABAM1, GCN1L1, PGLS, MAPK3, WDR83, LSM4, RRP12, GAPDH, TUT1, RPS28, HMOX1, NSUN5, MPG, CD2BP2, DCXR, SRM, ZC3H7B, APEH, PSENEN, MED24, GSTP1, TCOF1, CDC34, GTF2F1, MRPS18A, DRAP1, BOP1, FLNA, IMPDH1, PRPF19, RRP7A, RPL35, OAZ1, NADSYN1, GTF3C1, FURIN, TBRG4, APRT, GUK1, RPL36, WDR18, TELO2, MCM7, RNASEH2A, TAF6, MDH2, PTBP1, RRP1, CIB1, TARBP1, DEAF1, RPAP1, HAGH, HSD17B10, EIF6, PTMA, MRPL2, PTMS, MRPL28, ASL, SMG5, ASS1, ZMAT5, AGPAT2, MBD3, TCEB2, NOP2, TK1, TEX15, TKT, PGD, CNOT3, PHB, EDC3, SART1, TONSL, ATP6V0C, DUS1L, RAD23A, MCM5, STOML2, MCM2, NHP2L1, BAX, GRWD1, SLC25A39, BAD, AKAP8L, GPS1, SHMT2, DHPS, PES1, CYB5R3, PKM, DDX49, TRMT2A, TGFB1, U2AF2, SRRT, ACOT7, PELP1, SND1, THOP1, PCIF1, GSK3A, INTS1
GO:0044249	cellular biosynthetic process	RFC2, SYMPK, CHAC1, NDUFA7, ELOF1, ABCA2, TRIM28, PMM1, DPM2, UPF1, ENO1, TUFM, AKR1A1, GTPBP1, EIF4G1, MRPL49, EEF2, EEF1G, TPI1, EEF1A2, SNRPB, TECR, CPSF4, POLRMT, POLR2L, E4F1, TSPO, POLR2J, COL4A2, XAB2, MRPS34, MVD, CACNA1H, E2F1, MRPL54, SLC25A1, POLD2, POLD1, GMPPB, POLR2F, POLR2E, SCAF1, POLR2A, NAT14, NADK, UROD, RPL19, RPL18A, CNDP2, RPL18, RPL13, SUPT6H, UAP1L1, RPL10, RPL8, SUPT5H, PPP5C, UPP1, FASN, PNPLA2, MAD2L2, CAD, ZNF598, RPS5, AKT1, RPS2, RPLP2, MED16, RPLP1, MRPL12, ACD, RPLP0, MRPS2, B4GALT3, B4GALT2, RPL41, FADS2, AURKAIP1, NR2C2AP, VCP, MECR, CYBA, RPL28, UBA52, ERAL1, RPS26, ZNF768, NPM3, GAMT, RPS16, UBC, RPS19, UBB, RPS11, ADRM1, RPS8, ESRRA, RPS14, RPS15, HIRA, MRPL38, ITPA, MRPL11, RPS7, RPS6KB2, SLC44A2, GTF3C5, GCN1L1, MAPK3, GNB2L1, PEMT, CCDC88A, GAPDH, RPS28, ILVBL, MED12, CDIPT, SRM, FOXK2, MED24, GSTP1, TCOF1, SDSL, MRPS18A, GTF2F1, DRAP1, FLNA, IMPDH1, ENTPD6, RPL35, SCARB1, OAZ1, NADSYN1, ARF1, BRF1, FURIN, GTF3C1, FDX1L, COASY, DPM3, APRT, GUK1, RPL36, DGKZ, TELO2, MCM7, RNASEH2A, TAF6, GADD45GIP1, RPAP1, DEAF1, HAGH, HSD17B10, CDK4, PTMA, MRPL2, ASL, PTMS, MRPL28, ASS1, MRPL4, SBF1, AGPAT2, TCEB2, DRG2, TK1, TKT, PYCR1, GPI, PHB, PIGQ, ATP6V0C, PFKL, MCM5, STOML2, MCM2, NT5C, IDH2, BAX, GRWD1, SLC25A39, PI4KB, ETNK2, SHMT2, PHGDH, DHPS, B3GAT3, GPX4, FLAD1, CYB5R3, PKM, MED15, TGFB1, SRRT, ACOT7, PLOD3, B4GALT7, INTS1, BCAT2, CERS1, FPGS

GO:0006412	translation	RPS26, RPS16, EEF1A2, RPL13, RPS19, MRPS18A, RPL10, RPS11, RPS8, RPL8, DHPS, RPS15, RPS6KB2, RPL35, RPS5, MRPL28, GCN1L1, RPS2, RPLP2, RPLP1, RPLP0, RPL41, RPS28, RPL36, RPL28
GO:0043604	amide biosynthetic process	RPS26, CNDP2, RPS16, EEF1A2, RPL13, NDUFA7, RPS19, MRPS18A, RPL10, RPS11, TECR, RPS8, RPL8, DHPS, RPS15, FASN, RPS6KB2, RPL35, RPS5, MRPL2, ASL, MRPL28, GCN1L1, RPS2, RPLP2, RPLP1, MRPS34, ASS1, FURIN, RPLP0, SLC25A1, B4GALT3, RPL41, RPS28, EIF4G1, RPL36, RPL28
GO:0043043	peptide biosynthetic process	RPS26, CNDP2, RPS16, EEF1A2, RPL13, RPS19, MRPS18A, RPL10, RPS11, RPS8, RPL8, DHPS, RPS15, RPS6KB2, RPL35, RPS5, MRPL28, GCN1L1, RPS2, RPLP2, RPLP1, RPLP0, RPL41, RPS28, RPL36, RPL28
GO:0009057	macromolecule catabolic process	EXOSC5, CDC20, RPL13, CDC34, OS9, RPL10, RPL8, PTPN23, FBXW5, AGRN, UPF1, UBE2S, PRPF19, RPL35, RPS5, PINK1, CTSD, SPSB3, RPS2, SDF2L1, RPLP2, RPLP1, PPP2R1A, PSMB6, RPLP0, RAD23A, RPL41, PSMC3, PSMD8, VPS4A, RPL36, PSMD4, RPL28, PSMD3, LONP1, UBA52, RNASEH2A, RPS26, RPS16, FBXW4, USP5, RPS19, RPS11, RPS8, ADRM1, RPS15, BAP1, AP2M1, SMG5, SND1, RNF40, SGTA, STUB1, RPS28, GSK3A, VPS13A
GO:0006810	transport	COX6B1, SYMPK, KDELR1, COX4I1, ARFGAP2, OS9, SCAP, NUP62, NCOR2, COX8A, LMAN2, G6PC3, UPF1, REEP2, BANF1, APBA3, CD320, ALYREF, BET1L, SLC7A5, MVB12A, EEF2, RAB1B, SNRPD2, DDX39A, EPN1, ATG4D, SNRPB, KXD1, AHI1, CPSF4, YIF1A, TIMM17B, ARFIP2, CHID1, TSPO, TEX264, CACNA1H, HSPB1, SLC25A1, AP3D1, RAMP1, GPR108, BCAP31, TOMM40, AP1B1, FTL, RPL18A, CANX, ADRBK1, RPL13, SUPT6H, TIMM13, RPL10, TIMM10, SDF4 - stromal cell derived factor 4, SUN2 - sad1 and unc84 domain containing 2, RPL8, CAD, RPS5, HLA-B, PINK1, CTSD, GAA, STX10, RPS2, RPLP2, RPLP1, KIF22, RPLP0, NOL6, CALR, RPL41, TUBA1C, TMEM115, VCP, RPL28, UBA52, POLDIP3, RPS26, RPS16, JUP, RPS19, SLC25A25, UBB, ITPR3, SSR2, RPS11, AAAS, RPS8, RPS15, TUBB4B, SLC25A22, SLC44A2, MAPK3, MVP, KLC2, NAPA, ATP13A1, HMGA1, RPS28, SLC27A4, VPS13A, APEH, GSTP1, SEC13, TCN2, DDOST, DCTN1, PTPN23, FLNA, TBC1D10A, IMPDH1, CD81, RPL35, SCYL1, TRAPPC2L, SCAMP4, SCARB1, PSMB6, FURIN, PPFIA3, RAB11B, PSMC3, APRT, PSMD8, RPL36, PSMD4, UBXN6, PSMD3, FXYD5, FIS1, ARF5, ARHGAP1, EIF6, CHMP1A, SSNA1, PLEKHJ1, CDK16, NDUFA13, SMG5, MFGE8, CDC37, SYNGR2, HGS, TIMP1, MICALL1, TMED3, ATP1A3, TBC1D13, PYGB, TLN1, TMED9, ATP6V0D1, COTL1, GIPC1, KIF1C, MAN2B1, PHB, NCS1, ATP6V0B, SLC1A5, SLC25A11, DVL1, ATP6V0C, SLC4A2, STOML2, PRELID1, RAB5C, VPS4A, LTBP4, BAX, LRPAP1, LRP1, COPG1, PI4KB, LRP5, AIP, TAGLN2, CLTB, AUP1, GRN, KIF1A, PEF1, CYB5R3, PKM, GRAMD1A, ZFPL1, TGFB1, U2AF2, DNM2, PDAP1, AP2M1, ATAD3B, TMEM120A, PHB2, ERGIC3, SGTA, COPE
GO:0043933	protein-containing complex subunit organization	APEH, SEC13, IKBKG, CDT1, DHX30, NDUFA7, SF3A2, MRPS18A, SCAP, PRMT1, BOP1, UBE2S, NCKAP5L, PRPF19, RRP7A, TRAPPC2L, SCARB1, P4HB, ECSIT, PSMD4, MRPL49, RAB1B, SNRPD2, MCM7, GADD45GIP1, SNRPB, HSD17B10, EIF6, SMARCA4, MRPL2, MRPL28, NDUFA13, SHKBP1, XAB2, MRPS34, MRPL54, MRPL4, SRCAP, TCEB2, RUVBL2, TK1, PRPF6, SUPT6H, RPL10, TLN1, FARSA, TSPAN4, EIF3G, RPS5, SLC1A5, PPP2R1A, MRPL12, SART1, DVL1, DVL2, RPLP0, CALR, MCM5, MCM2, STOML2, AURKAIP1, PPP1CA, NDUFA11, VCP, VPS4A, NDUFB11, LONP1, UBA52, GRWD1, PSMG3, BAD, GPAA1, RPS19, UBB, KMT2D, ADRM1, RPS15, CLTB, GPX4, PEF1, NDUFB8, SERPINH1, TGFB1, MAPK3, DNM2, AP2M1, LSM4, TMEM120A, PLOD3, HMGA1, NDUFS8, RPS28, NDUFS6, NUPR1, NDUFV1, CD2BP2, SH3GL1

GO:0070887	cellular response to chemical stimulus	LONP1, EMD, GSTP1, EIF4EBP1, RANGAP1, NDUFA13, BAD, MYBL2, HSPB1, PYCR1, RPL8, MCM2, PQBP1, PRDX2, LAMTOR4, APRT, HMOX1, FASN, PTK7, RUVBL2, SRM
GO:0006612	protein targeting to membrane	RPL35, RPS5, UBA52, RPS26, RPS2, RPLP2, RPLP1, RPS16, RPL13, RPS19, RPLP0, RPS11, RPL10, RPS8, RPL8, RPL41, RPS15, RPS28, SGTA, RPL36, RPL28
GO:0071840	cellular component organization or biogenesis	EMD, AKT1S1, EMP3, BRCA2, ARFGAP2, CDT1, DHX30, NDUFA7, ELOF1, ABCA2, SF3A2, ABCA3, SCAP, PRMT1, ABL1, TRIM28, NUP62, BSG, LMAN2, UPF1, REEP2, NCKAP5L, BANF1, EPHA2, NCAPH2, HPS1, SORBS3, TUBG1, ECSIT, BET1L, MYO1C, AMBRA1, PARVB, SNTA1, MRPL49, MVB12A, RAB1B, GOLGA8A, AXIN1, SNRPD2, CENPM, HDAC11, EPN1, SNRPB, MYBL2, KRT8, PQBP1, AHI1, BAP1, SNRNP200, KRT18, POLRMT, COL6A2, ARFIP2, SMARCA4, TSPO, BSN, PLXNB2, TEX264, SHKBP1, XAB2, E2F4, COL4A2, MRPS34, WDTC1, PPP1R15A, E2F1, MRPL54, SRCAP, POLD2, AP3D1, POLD1, NAA10, SHARPIN, LAMB2, RUVBL2, PPRC1, SYP, EML2, CAPN1, MCRS1, PRPF6, TIMM13, SUPT6H, TIMM10, RPL10, SUN2, SUV39H1, PPP5C, HDAC5, FARSA, BAIAP2, PNPLA2, MAD2L2, HAX1, EIF3G, RPS5, PINK1, AKT1, STX10, GAA, PPP2R1A, MRPL12, ACD, RPLP0, KIF22, TADA3, MRPS2, CALR, MPV17L2, VAV1, CARM1, CALM3, AURKAIP1, DDX23, PPP1CA, NDUFA11, TUBA1C, STK25, MTCH1, VCP, TTLL12, LONP1, C12orf44, UBA52, NPM3, RPS16, PSMG3, NTMT1, GPAA1, JUP, KCTD17, RPS19, UBB, CORO1B, KMT2D, ADRM1, AAAS, ESRRA, RPS15, BRMS1, TUBB4B, MRPL38, TUBB3, SYCP2, ADAM15, RPS7, PLEKHM2, BABAM1, SERPINH1, MAPK3, NAPA, LSM4, CSK, PKN1, MAP7D1, GAPDH, HMGA1, RPS28, WDR62, NUPR1, CD2BP2, VPS13A, APEH, CDC20, SEC13, IKBKG, ZNF385A, MRPS18A, STMN3, BOP1, DCTN1, FLNA, PTPN23, FLNC, FLOT2, AGRN, CD151, UBE2S, PRPF19, C12orf57, APBB1, RRP7A, SMCR7L, TRAPPC2L, SCARB1, P4HB, ARF1, FURIN, PPFIA3, POC1A, ATAD3A, PSMD4, PALM, CLUH, TELO2, FIS1, FXYD5, PKP3, MCM7, TAF6, MDK, GADD45GIP1, NUMA1, RHOC, MYBBP1A, CIB1, LAMTOR4, HSD17B10, PTK7, EIF6, HCFC1, DAPK3, CHMP1A, MRPL2, MRPL28, PLEKHJ1, WDR45, CDK16, NDUFA13, MFGE8, MRPL4, SYNGR2, AAR2, RNF40, HGS, CDC42EP1, NRTN, MBD3, TCEB2, RPTOR, CUL7, PTPRF, TIMP1, NOP2, MICALL1, TMED3, TK1, ATP1A3, FAM50A, TEX15, TLN1, SFN, TMED9, CEP290, ATP6V0D1, COTL1, ESPL1, SLC12A4, TSPAN4, PHB, EDC3, PEX14, SLC1A5, SART1, DVL1, DVL2, MCM5, STOML2, MCM2, RAC3, PRELID1, VPS4A, SETD1A, TNNT1, PKD1, BAX, NDUFB11, DDIT4, GRWD1, PIN1, BAD, GPS1, AKAP8L, SHMT2, PHGDH, PES1, CLTB, GPX4, AUP1, GRN, LTBP3, PEF1, GRAMD1A, TWF2, NDUFB8, TGFB1, DNM2, GOLGA8B, AP2M1, ATAD3B, TMEM120A, PHB2, PLOD3, NDUFS8, NOC2L, NDUFS6, NDUFV1, GSK3A, B4GALT7, SH3GL1
GO:0065003	protein-containing complex assembly	LONP1, RAB1B, MCM7, BAD, GPAA1, SF3A2, ADRM1, PRMT1, BOP1, TLN1 RPS15, GPX4, PEF1, FARSA, HSD17B10, RPS5, SLC1A5, NDUFA13, PPP2R1A, XAB2, AP2M1, MCM5, STOML2, MCM2, NDUFS8, NDUFS6, RPS28, NDUFA11, TCEB2, RUVBL2
GO:0071705	nitrogen compound transport	TCN2, SEC13, KDELR1, SYMPK, ARFGAP2, OS9, NUP62, PTPN23, LMAN2, TBC1D10A, UPF1, REEP2, RPL35, APBA3, SCAMP4, CD320, ALYREF, PPFIA3, BET1L, SLC7A5, RAB11B, RPL36, MVB12A, RAB1B, FIS1, DDX39A, ATG4D, ARF5, CPSF4, YIF1A, ARHGAP1, KRT18, EIF6, TIMM17B, ARFIP2, CHMP1A, TSPO, CDK16, NDUFA13, SMG5, HSPB1, CDC37, AP3D1, RAMP1, HGS, BCAP31, TOMM40, AP1B1, MICALL1, TMED3, CANX, RPL18A, RPL13, TBC1D13, TIMM13, SUPT6H, TIMM10,

		RPL10, RPL8, TMED9, ATP6V0D1, GIPC1, ATP6V0B, RPS5, AKT1, STX10, RPS2, RPLP2, SLC1A5, RPLP1, RPLP0, ATP6V0C, NOL6, CALR, RPL41, RAB5C, VCP, TMEM115, VPS4A, RPL28 , LTBP4, UBA52, POLDIP3, RPS26, LRP1, COPG1, RPS16, AIP, RPS19, SLC25A25, UBB, SSR2, RPS11, AAAS, RPS8, RPS15, CLTB, AUP1, KIF1A, SLC25A22, SLC44A2, TGFB1, U2AF2, DNM2, MVP, AP2M1, NAPA, PHB2, SGTA, RPS28, COPE, VPS13A
GO:0051234	establishment of localization	COX6B1, KDELR1, SYMPK, BRCA2, ARFGAP2, COX4I1, OS9, SCAP, NUP62, NCOR2, COX8A, LMAN2, G6PC3, UPF1, REEP2, BANF1, APBA3, CD320, ALYREF, BET1L, SLC7A5, MVB12A, RAB1B, EEF2, SNRPD2, DDX39A, EPN1, ATG4D, SNRPB, KXD1, AHI1, CPSF4, YIF1A, TIMM17B, ARFIP2, CHID1, TSPO, TEX264, CACNA1H, HSPB1, SLC25A1, RAMP1, AP3D1, BCAP31, GPR108, RUVBL2, TOMM40, AP1B1, FTL, CANX, RPL18A, ADRBK1, RPL13, SUPT6H, TIMM13, TIMM10, RPL10, SUN2, SDF4, RPL8, CAD, RPS5, PINK1, HLA-B, CTSD, GAA, STX10, RPS2, RPLP2, RPLP1, KIF22, RPLP0, NOL6, CALR, RPL41, CALM3, TUBA1C, TMEM115, VCP, RPL28, UBA52, POLDIP3, RPS26, RPS16, JUP, RPS19, SLC25A25, UBB, SSR2, ITPR3, RPS11, AAAS, RPS8, RPS15, TUBB4B, SLC25A22, SLC44A2, MAPK3, MVP, KLC2, NAPA, ATP13A1, HMGA1, RPS28, SLC27A4, VPS13A, APEH, GSTP1, SEC13, TCN2, IKBKG, DDOST, DCTN1, PTPN23, FLNA, TBC1D10A, IMPDH1, CD81, RPL35, SCYL1, TRAPPC2L, SCAMP4, SCARB1, PSMB6, FURIN, PPFIA3, RAB11B, PSMC3, APRT, PSMD8, RPL36, UBXN6, PSMD4, PSMD3, FXYD5, FIS1, ARF5, ARHGAP1, EIF6, CHMP1A, SSNA1, PLEKHJ1, CDK16, NDUFA13, SMG5, MFGE8, CDC37, SYNGR2, HGS, TIMP1, MICALL1, TMED3, ATP1A3, TBC1D13, TLN1, PYGB, TMED9, ATP6V0D1, COTL1, ESPL1, GIPC1, KIF1C, MAN2B1, NCS1, PHB, ATP6V0B, SLC25A11, SLC1A5, DVL1, ATP6V0C, SLC4A2, STOML2, PRELID1, RAB5C, VPS4A, LTBP4, BAX, LRPAP1, LRP1, COPG1, PI4KB, BAD, LRP5, AIP, TAGLN2, CLTB, AUP1, GRN, KIF1A, PEF1, CYB5R3, PKM, GRAMD1A, ZFPL1, TGFB1, U2AF2, DNM2, PDAP1, AP2M1, ATAD3B, TMEM120A, PHB2, ERGIC3, SGTA, COPE
GO:0042221	response to chemical	LONP1, EMD, GSTP1, RANGAP1, COX4I1, BAD, EEF1A2, MYBL2, PYCR1, RPL8, PQBP1, LAMTOR4, PEF1, FASN, PTK7, COL6A2, EIF4EBP1, TUFM, NDUFA13, HSPB1, MCM2, PRDX2, SGTA, APRT, HMOX1, SRM, RUVBL2
GO:0000463	maturation of LSU-rRNA from tricistronic rRNA transcript (SSU-rRNA, 5.8S rRNA, LSU-rRNA)	RPL35, BOP1, PES1
GO:0051716	cellular response to stimulus	LONP1, EMD, MCM7, GSTP1, RNASEH2A, RANGAP1, BAD, MYBL2, PYCR1, SFN, PRMT1, RPL8, PQBP1, LAMTOR4, FASN, PTK7, EIF4EBP1, NDUFA13, XAB2, PPP1R15A, HSPB1, RAD23A, POLD2, PRDX2, MCM2, HMGA1, NOC2L, SGTA, APRT, HMOX1, PSMD8, SRM, RUVBL2
GO:0016043	cellular component organization	EMD, AKT1S1, EMP3, BRCA2, ARFGAP2, CDT1, DHX30, NDUFA7, ELOF1, ABCA2, SF3A2, ABCA3, SCAP, PRMT1, ABL1, TRIM28, NUP62, BSG, LMAN2, UPF1, REEP2, NCKAP5L, BANF1, EPHA2, NCAPH2, HPS1, SORBS3, TUBG1, ECSIT, BET1L, MYO1C, AMBRA1, PARVB,

		SNTA1, MRPL49, MVB12A, RAB1B, GOLGA8A, AXIN1, SNRPD2, CENPM, HDAC11, EPN1, SNRPB, MYBL2, KRT8, PQBP1, AHI1, BAP1, SNRNP200, KRT18, POLRMT, COL6A2, ARFIP2, SMARCA4, TSPO, BSN, PLXNB2, TEX264, SHKBP1, XAB2, E2F4, COL4A2, MRPS34, WDTC1, PPP1R15A, E2F1, MRPL54, SRCAP, POLD2, AP3D1, POLD1, NAA10, SHARPIN, LAMB2, RUVBL2, PPRC1, SYP, EML2, CAPN1, MCRS1, PRPF6, TIMM13, SUPT6H, RPL10, TIMM10, SUN2, SUV39H1, PPP5C, FARSA, HDAC5, BAIAP2, PNPLA2, MAD2L2, HAX1, EIF3G, RPS5, PINK1, AKT1, STX10, GAA, PPP2R1A, MRPL12, ACD, RPLP0, KIF22, TADA3, MRPS2, CALR, MPV17L2, VAV1, CARM1, AURKAIP1, CALM3, DDX23, PPP1CA, NDUFA11, TUBA1C, STK25, MTCH1, VCP, TTLL12, LONP1, C12orf44, UBA52, NPM3, PSMG3, NTMT1, GPAA1, JUP, KCTD17, RPS19, UBB, CORO1B, KMT2D, AAAS, ADRM1, ESRRA, RPS15, BRMS1, TUBB4B, MRPL38, TUBB3, ADAM15, SYCP2, PLEKHM2, BABAM1, SERPINH1, MAPK3, NAPA, LSM4, CSK, PKN1, GAPDH, MAP7D1, HMGA1, RPS28, WDR62, NUPR1, CD2BP2, VPS13A, APEH, CDC20, SEC13, IKBKG, ZNF385A, MRPS18A, STMN3, BOP1, DCTN1, FLNA, PTPN23, FLNC, FLOT2, AGRN, CD151, UBE2S, PRPF19, C12orf57, APBB1, SMCR7L, RRP7A, TRAPPC2L, SCARB1, P4HB, ARF1, FURIN, PPFIA3, POC1A, ATAD3A, PSMD4, PALM, CLUH, TELO2, FIS1, FXYD5, PKP3, MCM7, TAF6, MDK, GADD45GIP1, NUMA1, RHOC, CIB1, LAMTOR4, HSD17B10, PTK7, EIF6, HCFC1, DAPK3, CHMP1A, MRPL2, MRPL28, PLEKHJ1, WDR45, CDK16, NDUFA13, MFGE8, MRPL4, AAR2, SYNGR2, RNF40, HGS, CDC42EP1, NRTN, MBD3, TCEB2, RPTOR, CUL7, PTPRF, TIMP1, NOP2, MICALL1, TMED3, TK1, ATP1A3, FAM50A, TEX15, TLN1, SFN, TMED9, CEP290, ATP6V0D1, COTL1, ESPL1, SLC12A4, TSPAN4, PHB, EDC3, PEX14, SLC1A5, SART1, DVL1, DVL2, MCM5, STOML2, MCM2, RAC3, PRELID1, VPS4A, SETD1A, TNNT1, PKD1, BAX, NDUFB11, DDIT4, GRWD1, PIN1, BAD, GPS1, AKAP8L, SHMT2, PHGDH, CLTB, GPX4, AUP1, GRN, LTBP3, PEF1, GRAMD1A, TWF2, NDUFB8, TGFB1, DNM2, GOLGA8B, AP2M1, ATAD3B, TMEM120A, PHB2, PLOD3, NDUFS8, NOC2L, NDUFS6, NDUFV1, GSK3A, B4GALT7, SH3GL1
GO:0022618	ribonucleoprotein complex assembly	SNRPD2, ERAL1, NOP2, DHX30, PRPF6, RPS19, SF3A2, SNRPB, RPL10, EIF3D, BOP1, RPS15, PRPF19, EIF3I, EIF3G, RRP7A, EIF6, SNRNP200, RPS5, EDC3, XAB2, SART1, RPLP0, LSM4, MRPS2, MPV17L2, AAR2, DDX23, RPS28, CD2BP2, RUVBL2
GO:0006890	retrograde vesicle-mediated transport, Golgi to ER	RAB1B, SCYL1, KDELR1, TMED3, COPG1, ARFGAP2, KLC2, NAPA, KIF22, ERGIC3, LMAN2, TMED9, ARF5, COPE, TMEM115, KIF1C
GO:0046483	heterocycle metabolic process	EXOSC5, SYMPK, BRCA2, ELOF1, RALY, ARL6IP4, SF3A2, ABL1, TRIM28, PMM1, UPF1, BANF1, FTSJ3, EPHA2, ALYREF, CD320, OTUB1, GTPBP1, BLVRB, EIF4G1, TRMT1, PDCD11, DDX39A, SNRPD2, TPI1, SNRPB, TECR, DDX54, PQBP1, CPSF4, SF3B5, SNRNP200, POLRMT, RBM10, POLR2L, TSPO, E4F1, POLR2J, COL4A2, XAB2, PLD3, E2F1, SLC25A1, POLD2, POLD1, STUB1, POLR2F, POLR2E, RUVBL2, POLR2A, UQCRC1, UROD, MCRS1, RPL18A, PRPF6, RPL13, SUPT6H, RPL10, RPL8, SUPT5H, SUV39H1, PPP5C, FARSA, CARS, UPP1, MAD2L2, FASN, PUSL1, CAD, RPS5, RPS2, MED16, RPLP2, RPLP1, PPP2R1A, MRPL12, ACD, NUDT14, KIF22, RPLP0, NOL6, RPL41, DDX23, NR2C2AP, AURKAIP1, VCP, G6PD, RPL28, LONP1, UBA52, POLDIP3, RPS26, ZNF768, NPM3, RPS16, RPS19, SLC25A25, UBB,

		RPS11, ADRM1, RPS8, ESRRA, RPS15, RPS7, GTF3C5, BABAM1, PGLS, MAPK3, WDR83, LSM4, RRP12, GAPDH TUT1, RPS28, HMOX1, NSUN5, MPG, CD2BP2, DCXR, ZC3H7B, MED24, TCOF1, TCN2, CDC34, GTF2F1, DRAP1, BOP1, FLNA, IMPDH1, PRPF19, RRP7A, RPL35, NADSYN1, GTF3C1, TBRG4, APRT, GUK1, RPL36, WDR18, TELO2, MCM7, RNASEH2A, TAF6, MDH2, PTBP1, RRP1, CIB1, TARBP1, RPAP1, DEAF1, HSD17B10, EIF6, PTMA, PTMS, SMG5, ZMAT5, AGPAT2, MBD3, TCEB2, NOP2, TK1, TEX15, TKT, PGD, PYCR1, CNOT3, PHB, EDC3, SART1, TONSL, ATP6V0C, DUS1L, RAD23A, MCM5, MCM2, STOML2, NHP2L1, BAX, GRWD1, SLC25A39, BAD, GPS1, AKAP8L, SHMT2, PES1, PKM, DDX49, TRMT2A, TGFB1, U2AF2, SRRT, ACOT7, PELP1, SND1, PCIF1, GSK3A, INTS1
GO:0071702	organic substance transport	TCN2, SEC13, KDELR1, SYMPK, ARFGAP2, OS9, NUP62, PTPN23, LMAN2, TBC1D10A, G6PC3, UPF1, REEP2, RPL35, APBA3, SCAMP4, SCARB1, CD320, ALYREF, PPFIA3, BET1L, SLC7A5, RAB11B, RPL36, MVB12A, RAB1B, FIS1, DDX39A, ATG4D, ARF5, CPSF4, YIF1A, ARHGAP1, KRT18, EIF6, TIMM17B, ARFIP2, CHMP1A, TSPO, CDK16, NDUFA13, SMG5, HSPB1, SLC25A1, CDC37, RAMP1, AP3D1, HGS, BCAP31, TOMM40, AP1B1, MICALL1, TMED3, CANX, RPL18A, RPL13, TBC1D13, TIMM13, SUPT6H, RPL10, TIMM10, RPL8, TMED9, ATP6V0D1, GIPC1, ATP6V0B, RPS5, AKT1, STX10, RPS2, SLC1A5, SLC25A11, RPLP2, RPLP1, ATP6V0C, RPLP0, NOL6, CALR, SLC4A2, RPL41, PRELID1, RAB5C, TMEM115, VCP, VPS4A, RPL28, LTBP4, UBA52, POLDIP3, RPS26, LRP1, COPG1, RPS16, AIP, RPS19, SLC25A25, UBB, SSR2, RPS11, AAAS, RPS8, RPS15, CLTB, AUP1, KIF1A, GRAMD1A, SLC25A22, SLC44A2, TGFB1, U2AF2, DNM2, MVP, AP2M1, NAPA, PHB2, SGTA, RPS28, COPE, SLC27A4, VPS13A
GO:0000377	RNA splicing, via transesterification reactions with bulged adenosine as nucleophile	DDX39A, SNRPD2, SYMPK, PTBP1, PRPF6, SF3A2, RALY, SNRPB, GTF2F1 PQBP1, CPSF4, SF3B5, PRPF19, SNRNP200, RBM10, POLR2L, U2AF2, POLR2J, SRRT, XAB2, SART1, WDR83, ALYREF, LSM4, ZMAT5, DDX23, NHP2L1, POLR2F, POLR2E, CD2BP2, POLR2A
GO:0000398	mRNA splicing, via spliceosome	DDX39A, SNRPD2, SYMPK, PTBP1, PRPF6, SF3A2, RALY, SNRPB, GTF2F1, PQBP1, CPSF4, SF3B5, PRPF19, SNRNP200, RBM10, POLR2L, U2AF2, POLR2J, SRRT, XAB2, SART1, WDR83, ALYREF, LSM4, ZMAT5, DDX23, NHP2L1, POLR2F, POLR2E, CD2BP2, POLR2A
GO:0051641	cellular localization	SEC13, IKBKG, KDELR1, SYMPK, BRCA2, ZNF385A, ARFGAP2, OS9, SCAP, DCTN1, NUP62, FLNA, PTPN23, BSG, LMAN2, FLOT2, TBC1D10A, AGRN, UPF1, REEP2, PRPF19, CD81, BANF1, EPHA2, RPL35, SCYL1, TRAPPC2L, ALYREF, PPFIA3, BET1L, RAB11B, UBXN6, RPL36, PALM, CLUH, MVB12A, FIS1, RAB1B, PKP3, SNRPD2, DDX39A, SNRPB, KXD1, LAMTOR4, ARF5, AHI1, CPSF4, YIF1A, ARHGAP1, EIF6, KRT18, TIMM17B, CHMP1A, ARFIP2, SSNA1, TSPO, PLEKHJ1, NDUFA13, SMG5, PPP1R15A, HSPB1, CDC37, RAMP1, AP3D1, HGS, BCAP31, RUVBL2, TOMM40, AP1B1, MICALL1, TMED3, RPL18A, RPL13, TBC1D13, TIMM13, RPL10, TIMM10, SUN2, RPL8, TMED9, ESPL1, GIPC1, KIF1C, RPS5, PINK1, AKT1, STX10, RPS2, RPLP2, RPLP1, PPP2R1A, DVL1, DVL2, KIF22, RPLP0, NOL6, CALR, RPL41, STOML2, CALM3, RAB5C, TUBA1C, STK25, VCP, TMEM115, VPS4A, RPL28,

		BAX, UBA52, POLDIP3, RPS26, COPG1, RPS16, BAD, JUP, RPS19, AIP, UBB, CORO1B, SSR2, RPS11, RPS8, AAAS, RPS15, CLTB, AUP1, TUBB4B, KIF1A, PEF1, PLEKHM2, TGFB1, U2AF2, DNM2, AP2M1, NAPA, PHB2, ERGIC3, HMGA1, RPS28, SGTA, COPE, VPS13A
GO:0015833	peptide transport	TOMM40, AP1B1, MICALL1, SEC13, TMED3, KDELR1, CANX, RPL18A, ARFGAP2, RPL13, TBC1D13, OS9, TIMM13, TIMM10, RPL10, NUP62, RPL8, PTPN23, TMED9, LMAN2, ATP6V0D1, TBC1D10A, GIPC1, REEP2, ATP6V0B, RPL35, APBA3, RPS5, SCAMP4, AKT1, STX10, RPS2, RPLP2, RPLP1, ATP6V0C, RPLP0, BET1L, CALR, RAB11B, RPL41, RAB5C, TMEM115, VCP, VPS4A, RPL36, RPL28, LTBP4, MVB12A, FIS1, RAB1B, UBA52, RPS26, LRP1, COPG1, RPS16, ATG4D, AIP, RPS19, UBB, SSR2, RPS11, RPS8, RPS15, CLTB, AUP1, ARF5, KIF1A, YIF1A, ARHGAP1, EIF6, KRT18, TIMM17B, CHMP1A, ARFIP2, TSPO, TGFB1, DNM2, MVP, CDK16, NDUFA13, AP2M1, NAPA, PHB2, HSPB1, CDC37, AP3D1, RAMP1, HGS, SGTA, RPS28, BCAP31, COPE, VPS13A
GO:0072655	establishment of protein localization to mitochondrion	BAX, TIMM17B, FIS1, TOMM40, PINK1, AKT1, TSPO, NDUFA13, BAD, AIP, TIMM13, TIMM10, CALM3, BCAP31
GO:0006886	intracellular protein transport	TOMM40, AP1B1, MICALL1, SEC13, RPL13, TBC1D13, OS9, TIMM13, RPL10, TIMM10, NUP62, RPL8, TMED9, TBC1D10A, GIPC1, REEP2, RPL35, RPS5, STX10, RPS2, RPLP2, RPLP1, RPLP0, CALR, RPL41, RAB5C, VCP, RPL36, VPS4A, RPL28, RAB1B, FIS1, UBA52, RPS26, COPG1, RPS16, RPS19, AIP, UBB, SSR2, RPS11, RPS8, RPS15, CLTB, AUP1, ARF5, KIF1A, EIF6, TIMM17B, ARFIP2, TSPO, TGFB1, NDUFA13, AP2M1, PHB2, HSPB1, CDC37, AP3D1, RAMP1, HGS, RPS28, SGTA, BCAP31, VPS13A
GO:0006725	cellular aromatic compound metabolic process	EXOSC5, SYMPK, BRCA2, ELOF1, RALY, ARL6IP4, SF3A2, ABL1, TRIM28, PMM1, UPF1, BANF1, FTSJ3, EPHA2, ALYREF, CD320, OTUB1, GTPBP1, BLVRB, EIF4G1, TRMT1, PDCD11, DDX39A, SNRPD2, TPI1, SNRPB, TECR, PQBP1, DDX54, CPSF4, SF3B5, SNRNP200, POLRMT, RBM10, POLR2L, TSPO, E4F1, POLR2J, COL4A2, XAB2, PLD3, E2F1, SLC25A1, POLD2, POLD1, STUB1, POLR2F, POLR2E, POLR2, RUVBL2, UQCRC1, UROD, MCRS1, RPL18A, PRPF6, RPL13, SUPT6H, RPL10, RPL8, SUPT5H, SUV39H1, PPP5C, CARS, FARSA, UPP1, PUSL1, FASN, MAD2L2, CAD, RPS5, RPS2, RPLP2, MED16, RPLP1, PPP2R1A, MRPL12, ACD, NUDT14, KIF22, RPLP0, NOL6, RPL41, DDX23, NR2C2AP, AURKAIP1, VCP, G6PD, RPL28, LONP1, UBA52, POLDIP3, RPS26, ZNF768, NPM3, RPS16, RPS19, SLC25A25, UBB, RPS11, ADRM1, RPS8, ESRRA, RPS15, RPS7, GTF3C5, BABAM1, MAPK3, PGLS, WDR83, LSM4, RRP12, GAPDH, TUT1, RPS28, HMOX1, NSUN5, MPG, CD2BP2, DCXR, ZC3H7B, MED24, TCOF1, TCN2, CDC34, GTF2F1, DRAP1, BOP1, FLNA, IMPDH1, PRPF19, RRP7A, RPL35, NADSYN1, GTF3C1, TBRG4, APRT, GUK1, RPL36, WDR18, TELO2, MCM7, RNASEH2A, TAF6, MDH2, PTBP1, RRP1, CIB1, TARBP1, RPAP1, DEAF1, HSD17B10, EIF6, PTMA, PTMS, THAP4, SMG5, ZMAT5, AGPAT2, MBD3, TCEB2, NOP2, TK1, TEX15, TKT, PGD, CNOT3, PHB, EDC3, SART1, TONSL, ATP6V0C, DUS1L, RAD23A, MCM5, MCM2, STOML2, NHP2L1, BAX, GRWD1, SLC25A39, BAD, GPS1, AKAP8L, SHMT2, PES1, PKM, DDX49, TRMT2A, TGFB1, U2AF2, SRRT, ACOT7, PELP1, SND1, PCIF1, GSK3A, INTS1

GO:0031331	positive regulation of cellular catabolic process	BAX, CDC20, IKBKG, LRP1, USP5, BAD, SUPT5H, UPF1, CD81, PINK1, MAPK3, GNB2L1, DVL1, PHB2, RAD23A, GTPBP1, CDC37, PSMC3, RNF40, STUB1, SGTA, HMOX1, TCEB2, NUPR1, GSK3A, AMBRA1
GO:0051179	localization	COX6B1, KDELR1, SYMPK, BRCA2, COX4I1, OS9, SCAP, NUP62, BSG, LMAN2, COX8A, UPF1, G6PC3, REEP2, BANF1, EPHA2, APBA3, CD320, ALYREF, BET1L, SLC7A5, RAB1B, EEF2, DDX39A, SNRPD2, EPN1, ATG4D, SNRPB, KXD1, CPSF4, YIF1A, TIMM17B, ARFIP2, CHID, TSPO, BSN, TEX264, PPP1R15A, HSPB1, SLC25A1, AP3D1, RAMP1, BCAP31, GPR108, RUVBL2, TOMM40, AP1B1, FTL, CANX, RPL13, ADRBK1, PRPF6, TIMM13, SUPT6H, RPL10, TIMM10, SUN2, SDF4, RPL8, CAD, RPS5, HLA-B, PINK1, CTSD, STX10, GAA, RPS2, RPLP2, RPLP1, PPP2R1A, RPLP0, KIF22, NOL6, CALR, RPL41, CALM3, TUBA1C, TMEM115, VCP, RPL28, UBA52, POLDIP3, RPS26, RPS16, GPAA1, JUP, RPS19, UBB, SSR2, ITPR3, CORO1B, RPS11, RPS8, AAAS, RPS15, TUBB4B, SLC25A22, PLEKHM2, SLC44A2, MVP, MAPK3, KLC2, ATP13A1, HMGA1, RPS28, SLC27A4, VPS13A, APEH, GSTP1, SEC13, IKBKG, DDOST, ZNF385A, DCTN1, FLNA, PTPN23, FLOT2, TBC1D10A, AGRN, IMPDH1, PRPF19, CD81, RPL35, TRAPPC2L, SCYL1, SCAMP4, SCARB1, PSMB6, FURIN, RAB11B, PSMC3, APRT, PSMD8, UBXN6 PSMD4, RPL36, PALM, PSMD3, FIS1, FXYD5, PKP3, ARF5, LAMTOR4, ARHGAP1, EIF6, SSNA1, CDK16, NDUFA13, SMG5, CDC37, SYNGR2, HGS, TIMP1, MICALL1, ATP1A3, TBC1D13, TLN1, PYGB, TMED9, ATP6V0D1, COTL1, ESPL1, GIPC1, KIF1C, MAN2B1, NCS1, PHB, ATP6V0B, SLC25A11, SLC1A5, DVL1, DVL2, ATP6V0C, SLC4A2, STOML2, PRELID1, RAB5C, VPS4A, BAX, LTBP4, LRPAP1, RANGAP1, LRP1, COPG1, PI4KB, BAD, LRP5, AIP, TAGLN2, CLTB, AUP1, GRN, KIF1A, PEF1, CYB5R3, PKM, TWF2, ZFPL1, TGFB1, U2AF2, DNM2, PDAP1, AP2M1, ATAD3B, PHB2, TMEM120A, PLOD3, ERGIC3, SGTA, COPE
GO:0032386	regulation of intracellular transport	EMD, FIS1, SYP, RANGAP1, AKAP8L, JUP, ABCA2, OS9, NUMA1, SUPT6H, AAAS, SFN, NUP62, TRIM28, PTPN23, FLNA, B3GAT3, CEP290, CIB1, NUCB1, GIPC1, RIMS4, REEP2, BAP1, ARHGAP1, MAP2K2, HAX1, CD81, NCS1, SMCR7L, PINK1, TGFB1, GIT1, OAZ1, MAPK3, NAPA, DVL1, ARF1, CAMK1, RAB11B, CALM3, HMOX1, MYO1C, BCAP31, GSK3A
GO:0000375	RNA splicing, via transesterification reactions	DDX39A, SNRPD2, SYMPK, PTBP1, PRPF6, SF3A2, RALY, SNRPB, GTF2F1, PQBP1, CPSF4, SF3B5, PRPF19, SNRNP200, RBM10, POLR2L, U2AF2,POLR2J, SRRT, XAB2, SART1, WDR83, ALYREF, LSM4, ZMAT5, DDX23, NHP2L1, POLR2F, POLR2E, CD2BP2, POLR2A
GO:0006397	mRNA processing	DDX39A, SNRPD2, POLDIP3, SYMPK, PTBP1 AKAP8L, PRPF6, SF3A2, RALY, ARL6IP4, SNRPB, GTF2F1, SUPT6H, PQBP1, SUPT5H, CPSF4, SF3B5, PRPF19, SNRNP200, RBM10, POLR2L, U2AF2, POLR2J, SRRT, XAB2, WDR83, SART1, ALYREF, LSM4, TUT1, ZMAT5, DDX23, AURKAIP1, TBRG4, NHP2L1, POLR2F, POLR2E, CD2BP2, PDCD11, POLR2A
GO:0010033	response to organic substance	LONP1, EMD, COL6A2, GSTP1, EIF4EBP1, RANGAP1, TUFM, NDUFA13, BAD, MYBL2, HSPB1, RPL8, MCM2, PRDX2, PQBP1, LAMTOR4, SGTA, APRT, FASN, PTK7, RUVBL2, SRM
GO:0006139	nucleobase-containing compound	ZC3H7B, MED24, EXOSC5, TCOF1, SYMPK, BRCA2, ELOF1, CDC34, ARL6IP4, SF3A2 RALY, DRAP1, GTF2F1, BOP1, ABL1, TRIM28, FLNA, IMPDH1, PMM1, UPF1, PRPF19, BANF1, RRP7A, FTSJ3, EPHA2, RPL35,

	metabolic process	NADSYN1, ALYREF, GTF3C1, OTUB1, GTPBP1, TBRG4, TRMT1, APRT, EIF4G1, GUK1, RPL36, PDCD11, WDR18, TELO2, SNRPD2, MCM7, DDX39A, RNASEH2A, TAF6, TPI1, PTBP1, MDH2, SNRPB, TECR, RRP1, CIB1, PQBP1, DDX54, TARBP1, CPSF4, DEAF1, RPAP1, SF3B5, HSD17B10, EIF6, SNRNP200, PTMA, POLRMT, RBM10, PTMS, E4F1, POLR2L, POLR2J, XAB2, COL4A2, SMG5, PLD3, E2F1, SLC25A1, POLD2, ZMAT5, POLD1, AGPAT2, STUB1, MBD3, TCEB2, POLR2F, POLR2E, RUVBL2, POLR2A, UQCRC1, NOP2, TK1, MCRS1, RPL18A, TEX15, TKT, PGD, RPL13, PRPF6, SUPT6H, RPL10, RPL8, SUPT5H, SUV39H1, CNOT3, PPP5C, UPP1, FARSA, CARS, MAD2L2, FASN, PUSL1, PHB, CAD, RPS5, EDC3, RPS2, MED16, RPLP2, RPLP1, PPP2R1A, MRPL12, SART1, ACD, TONSL, NUDT14, RPLP0, KIF22, ATP6V0C, NOL6, DUS1L, RAD23A, RPL41, MCM5, STOML2, MCM2, NR2C2AP, AURKAIP1, DDX23, NHP2L1, VCP, G6PD, RPL28, BAX, LONP1, UBA52, POLDIP3, RPS26, ZNF768, GRWD1, NPM3, RPS16, BAD, AKAP8L, GPS1, RPS19, UBB, SLC25A25, SHMT2, RPS11, RPS8, ADRM1, ESRRA, RPS15, PES1, PKM, RPS7, DDX49, TRMT2A, GTF3C5, BABAM1, TGFB1, U2AF2, MAPK3, PGLS, SRRT, ACOT7, PELP1, WDR83, SND1, LSM4, RRP12, TUT1, GAPDH, PCIF1, RPS28, NSUN5, GSK3A, MPG, CD2BP2, INTS1, DCXR
GO:0045184	establishment of protein localization	SEC13, KDELR1, BRCA2, ARFGAP2, OS9, NUP62, FLNA, PTPN23, LMAN2, TBC1D10A, REEP2, RPL35, APBA3, SCAMP4, BET1L, RAB11B, RPL36, MVB12A, RAB1B, FIS1, ATG4D, ARF5, YIF1A, ARHGAP1, KRT18, EIF6, TIMM17B, ARFIP2, CHMP1A, TSPO, NDUFA13, HSPB1, CDC37, AP3D1, RAMP1, HGS, BCAP31, RUVBL2, TOMM40, AP1B1, MICALL1, TMED3, CANX, RPL18A, RPL13, TBC1D13, TIMM13, RPL10, TIMM10, RPL8, TMED9, ATP6V0D1, GIPC1, ATP6V0B, RPS5, PINK1, AKT1, STX10, RPS2, RPLP2, RPLP1, RPLP0, ATP6V0C, CALR, RPL41, CALM3, RAB5C, TMEM115, VCP, VPS4A, RPL28, BAX, UBA52, RPS26, LRP1, COPG1, RPS16, BAD, RPS19, AIP, UBB, SSR2, RPS11, RPS8, RPS15, CLTB, AUP1, KIF1A, TGFB1, MVP, DNM2, AP2M1, NAPA, PHB2, RPS28, SGTA, COPE, VPS13A
GO:0042176	regulation of protein catabolic process	TIMP1, CDC20, USP19, TMEM259, LRP1, EEF1A2, USP5, PIN1, UBB, OS9, FLNA, GIPC, MAD2L2, CD81, PHB, PINK1, OAZ1, GNB2L1, NDUFA13, HSPBP1, DVL1, FURIN, RAD23A, PSMC3, RNF40, HGS, SGTA, STUB1, BCAP31, TCEB2, NUPR1, GSK3A, VCP, PSMD3
GO:0071826	ribonucleoprotein complex subunit organization	SNRPD2, ERAL1, NOP2, DHX30, PRPF6, RPS19, SF3A2, SNRPB, RPL10, EIF3D, BOP1, RPS15, EIF3I, PRPF19, SNRNP200, RRP7A, EIF3G, EIF6, RPS5, EDC3, XAB2, SART1, RPLP0, LSM4, MRPS2, MPV17L2, AAR2, DDX23, RPS28, VCP, CD2BP2, RUVBL2
GO:0071704	organic substance metabolic process	AGAP3, SYMPK, ELOF1, ABCA2, ABCA3, SF3A2, ARL6IP4, OS9, ABL1, NUP62, CLPP, PMM1, FTSJ3, TRAF4, PNPLA6, PLOD1, ACO2, CD320, OTUB1, GTPBP1, TRMT1, CRABP2, MARK4, SNRPD2, USP20, USP19, PPIB, HDAC11, ATG4D, SNRPB, CTDSP1, TECR, CPSF4, BAP1, MMP24, POLRMT, RBM10, USP11, POLR2L, POLR2J, COL4A2, PPP1R15A, PLD3, MRPL54, CACTIN, SLC25A1, SRCAP, POLD2, POLD1, NAA10, POLR2F, POLR2E, LAMB2, RUVBL2, POLR2A, SHC2, CNDP2, ADRBK1, PRPF6, SUPT6H, KHK, SUPT5H, SUV39H1, PPP5C, MAPKAPK3, PPP4C, AKT1, STX1A, CTSD, GAA, SDF2L1, PPP2R1A, NUDT14, KIF22, MRPS2, FKBP8, APH1A, FADS2, DDX23, PPP1CA, PPM1G, G6PD, GALE, RNF181, LONP1, POLDIP3, ZNF768, SHISA5, GAMT, PI4KAP2, USP5, KCTD17, SLC25A25, KMT2D, ADRM1, AAAS, AGBL5, BRMS1, MAP2K2, MAPK11, GTF3C5, GCN1L1, MAPK3, PGLS, COPS6, WDR83,

		PRKCSH, CSK, LSM4, CCDC88A, PKN1, CSNK1D, GAPDH, RNF123, SLC27A4, NSUN5, ILVBL, SF3B2, SRM, DCXR, APEH, GSTP1, DDOST, STK40, SDHA, GTF2F1, MRPS18A, MAP3K10, DDB1, PTPN23, TBC1D10A, MAP3K11, APBB1, RPL35, SCYL1, NADSYN1, P4HB, ARF1, GTF3C1, FURIN, OBSCN, RAB11B, TBRG4, MSRB1, APRT, GUK1, RPL36, WDR18, BRPF1, MCM7, ADAM11, GADD45GIP1, MDH2, SERINC2, RPAP1, HAGH, HSD17B10, HCFC1, DAPK3, CHMP1A, ASL, PLEKHJ1, WDR45, CDK16, ASS1, MFGE8, MAPK12, HGS, SBF1, MBD3, DRG2, RRP9, IRF2BP1, PGD, FAM207A, MAN2B1, PHB, PEX14, PIGQ, SART1, ATP6V0C, SLC3A2, PFKL, MCM5, MCM2, GEN1, SLC5A3, PKD1, BAX, GRK6, GRWD1, SLC25A39, LRP1, PI4KB, PIN1, ETNK2, BAD, FBXW4, GPS1, LRP5, AIP, SHMT2, PHGDH, DHPS, UBE2M, B3GAT3, AUP1, GPX4, PEF1, CYB5R3, PKM, MED15, MAP3K14 U2AF2, MVB12B, DNM2, SRRT, ACOT7, PLOD3, BCKDHA, SGTA, LYPLA2, GSK3A, B4GALT7, BCAT2, INTS1, PIGT, DNAJB2, EXOSC5, RFC2, BRCA2, CHAC1, NDUFA7, RALY, SLC29A1, SCAP, PRMT1, TRIM28, BSG, TMEM208, DPM2, UPF1, G6PC3, BANF1, ENO1, EPHA2, TUFM, TRIM11, ALYREF, AKR1A1, ALG12, BLVRB, EIF4G1, URM1, PDCD11, MRPL49, MVB12A, RAB1B, EEF2, LAS1L, DDX39A, EEF1G, TPI1, EEF1A2, MYH9, PQBP1, DDX54, SF3B5, ERI3, SNRNP200, CHID1, E4F1, TSPO, XAB2, MVD, MRPS34, WDTC1, CACNA1H, E2F1, HSPG2, GDAP1L1, GMPPB, RAMP1, VKORC1, STUB1, SHARPIN, ECE1, UQCRC1, NAT14, CAPNS1, NADK, UROD, LMF2, CAPN1, MCRS1, RPL19, NEK5, RPL18A, RPL18, RPL13, UAP1L1, RPL10, RPL8, ALDH4A1, UPP1, FARSA, HDAC5, CARS, PNPLA2, FASN, MAD2L2, PUSL1, LAMTOR2, CAD, ZNF598, RPS5, PINK1, SPSB3, RPS2, MED16, RPLP2, RPLP1, MRPL12, ADCK2, ACD, RPLP0, TADA3, NOL6, CALR, JMJD4, B4GALT3, CAMK4, B4GALT2, RPL41, CARM1, NR2C2AP, AURKAIP1, STK25, VCP, LRRC41, RPL28, TTLL12, KIF14, UBA52, ERAL1, RPS26, NPM3, RPS16, NTMT1, UBA1, GPAA1, UBC, RPS19, UBB, GDPD5, RPS11, RPS8, ESRRA, RPS14, HIRA, RPS15, TYRO3, HM13, MRPL38, ETFB, ADAM15, GANAB, MRPL11, RPS7, RPS6KB2, SLC44A2, UBXN11, BABAM1, SERPINH1, GNB2L1, PHPT1, PEMT, RRP12, TUT1, RPS28, HMOX1, NUPR1, MPG, CD2BP2, MED12, CDIPT, VPS13A, ZC3H7B, PSENEN, FOXK2, MED24, CDC20, TCOF1, TCN2, IKBKG, SDSL, USE1, CDC34, DRAP1, BOP1, FLNA, FBXW5, AGRN, PSKH1, IMPDH1, UBE2S, PRPF19, CD81, RRP7A, CDCA5, ENTPD6, OAZ1, SCARB1, ADAT2, PSMB6, CAMK1, FDX1L, PSMC3, COASY, DPM3, PSMD8, UBXN6, PSMD4, TELO2, PSMD3, DGKZ, LEPREL2, RNASEH2A, TAF6, ESYT1, PTBP1, DAB2IP, RRP1, UBXN1, NUCB1, CIB1, TARBP1, DEAF1, EIF6, PTK7, NOSIP, PTMA, MRPL2, PTMS, MRPL28, THAP4, SMG5, KLHL25, MRPL4, RNF40, ZMAT5, PTPRA, IP6K1, AGPAT2, NRTN, TCEB2, CUL7, IRAK1, PTPRF, TIMP1, NOP2, TK1, TEX15, TKT, PYCR1, ATP13A2, PYGB, CNOT3, ESPL1, TM7SF2, GCAT, EDC3, NGFR, SLC25A11, KMT2B, TONSL, PTGES2, DUS1L, RAD23A, STOML2, NKTR, NHP2L1, NT5C, VPS4A, IDH3G, SETD1A, DDX56, IDH2, RANGAP1, AKAP8L, EBP, PES1, FLAD1, DDX49, TRMT2A, TGFB1, MAPK8IP2, PELP1, IGFBP2, AP2M1, SND1, THOP1, PCIF1, CKB, CERS1
GO:0070585	protein localization to mitochondrion	BAX, TIMM17B, FIS1, TOMM40, PINK1, AKT1, TSPO, NDUFA13, BAD, AIP, TIMM13, TIMM10, CALM3, BCAP31

GO:0006396	RNA processing	ZC3H7B, EXOSC5, NOP2, SYMPK, PRPF6, ARL6IP4, RALY, SF3A2, GTF2F1, SUPT6H, BOP1, SUPT5H, SUV39H1, PRPF19, PUSL1, FTSJ3, RRP7A, RPL35, RPS2, PPP2R1A, SART1, ALYREF, NOL6, DUS1L, AURKAIP1, DDX23, TBRG4, NHP2L1, TRMT1, PDCD11, WDR18, SNRPD2, DDX39A, POLDIP3, NPM3, PTBP1, RPS16, AKAP8L, RPS19, SNRPB, RPS8, RRP1, RPS15, PES1, PQBP1, DDX54, TARBP1, CPSF4, SF3B5, RPS7, HSD17B10, DDX49, EIF6, SNRNP200, RBM10, TRMT2A, POLR2L, U2AF2, SRRT, POLR2J, PELP1, XAB2, WDR83, LSM4, RRP12, TUT1, ZMAT5, RPS28, POLR2F, NSUN5, POLR2E, CD2BP2, INTS1, POLR2A
GO:0045862	positive regulation of proteolysis	BAX, PSENEN, DNAJB2, FIS1, CDC20, AXIN1, MUL1, CLN6, TMEM259, USP5, BAD, MYH9, DAB2IP, ADRM1, TBC1D10A, GRN, EFNA3, ENO1, PHB, PINK1, NGFR, AKT1, CTSD, GNB2L1, NDUFA13, HSPBP1, DVL1, FURIN, PACSIN3, MAPK12, RAD23A, CSNK1D, PSMC3, FZR1, RNF40, APH1A, AURKAIP1, PRELID1, STUB1, SGTA, BCAP31, TCEB2, MTCH1, GSK3A, NUPR1, VCP, KEAP1
GO:1903362	regulation of cellular protein catabolic process	PKD1, DNAJB2, CDC20, AXIN1, USP19, TMEM259, LRP1, USP5, ABCA2, UBB, OS9, DAB2IP, ATP13A2, UBXN1, GIPC1, RPS7, CD81, PINK1, AKT1, GNB2L1, HSPBP1, DVL1, FURIN, RAD23A, CSNK1D, PSMC3, RNF40, SGTA, STUB1, TCEB2, BCAP31, GSK3A, NUPR1, VCP
GO:0015031	protein transport	TOMM40, AP1B1, MICALL1, SEC13, TMED3, KDELR1, RPL18A, CANX, ARFGAP2, RPL13, TBC1D13, OS9, TIMM13, TIMM10, RPL10, NUP62, RPL8, PTPN23, TMED9, LMAN2, ATP6V0D1, TBC1D10A, GIPC1, REEP2, ATP6V0B, RPL35, APBA3, RPS5, SCAMP4, AKT1, STX10, RPS2, RPLP2, RPLP1, ATP6V0C, RPLP0, BET1L, CALR, RAB11B, RPL41, RAB5C, TMEM115, VCP, VPS4A, RPL36, RPL28, MVB12A, FIS1, RAB1B, UBA52, RPS26, LRP1, COPG1, RPS16, ATG4D, AIP, RPS19, UBB, SSR2, RPS11, RPS8, RPS15, CLTB, AUP1, ARF5, KIF1A, YIF1A, ARHGAP1, EIF6, KRT18, TIMM17B, CHMP1A, ARFIP2, TSPO, TGFB1, DNM2, MVP, NDUFA13, AP2M1, NAPA, PHB2, HSPB1, CDC37, RAMP1, AP3D1, HGS, SGTA, RPS28, BCAP31, COPE, VPS13A
GO:0090304	nucleic acid metabolic process	ZC3H7B, MED24, EXOSC5, TCOF1, SYMPK, BRCA2, ELOF1, CDC34, ARL6IP4, SF3A2, RALY, DRAP1, GTF2F1, BOP1, ABL1, TRIM28, FLNA, UPF1, PRPF19, BANF1, RRP7A, FTSJ3, RPL35, ALYREF, GTF3C1, OTUB1, TBRG4, TRMT1, EIF4G1, RPL36, PDCD11, WDR18, TELO2, MCM7, SNRPD2, DDX39A, RNASEH2A, TAF6, PTBP1, SNRPB, RRP1, CIB1, DDX54, PQBP1, TARBP1, CPSF4, DEAF1, RPAP1, SF3B5, HSD17B10, EIF6, SNRNP200, PTMA, POLRMT, RBM10, PTMS, POLR2L, E4F1, POLR2J, COL4A2, XAB2, SMG5, PLD3, E2F1, POLD2, ZMAT5, POLD1, MBD3, STUB1, TCEB2, POLR2F, POLR2E, RUVBL2, POLR2A, NOP2, TK1, MCRS1, RPL18A, TEX15, PRPF6, RPL13, SUPT6H, RPL10, RPL8, SUPT5H, SUV39H1, CNOT3, PPP5C, FARSA, CARS, MAD2L2, PUSL1, PHB, RPS5, EDC3, RPS2, MED16, RPLP2, RPLP1, PPP2R1A, .SART1, MRPL12, ACD, TONSL, KIF22, RPLP0, NOL6, DUS1L, RAD23A, MCM5, RPL41, MCM2, AURKAIP1, NR2C2AP, DDX23 NHP2L1, VCP, RPL28, BAX, LONP1, UBA52, POLDIP3, RPS26, ZNF768, GRWD1, NPM3, RPS16, AKAP8L, GPS1, RPS19, UBB, RPS11, RPS8, ADRM1, ESRRA, RPS15, PES1, RPS7, DDX49, TRMT2A, GTF3C5, BABAM1, U2AF2, MAPK3, SRRT, PELP1, WDR83, SND1, LSM4, RRP12, TUT1, PCIF1, RPS28, NSUN5, CD2BP2, MPG, INTS1
GO:0009987	cellular process	AKT1S1, COX6B1, AGAP3, KDELR1, SYMPK, AAMP, ARFGAP2, COX4I1, ELOF1, ABCA2, ARL6IP4, ABCA3, SF3A2, OS9, ABL1, NUP62, LMAN2, COX8A, PMM1, REEP2, NCKAP5L, TRAF4, FTSJ3, APBA3, PLOD1, ECSIT, ACO2, CD320, BTBD2, BET1L, OTUB1, GTPBP1,

SLC7A5, HES4, TRMT1, AMBRA1, SNTA1, SNRPD2, AXIN1, PPIB, USP19, HDAC11, ATG4D, SNRPB, CTDSP1, TECR, KRT8, CPSF4, YIF1A, BAP1, KRT18, POLRMT, COL6A2, ARFIP2, SMARCA4, GNG4, RBM10, GNB2, POLR2L, USP11, PLXNB2, TEX264, POLR2J, COL4A2, HSPBP1, PPP1R15A, PLD3, POR, MRPL54, SLC25A1, POLD2, SRCAP, POLD1, NAA10, POLR2F, POLR2E, LAMB2, RUVBL2, POLR2A, EML2, FTL, MYL6B, CNDP2, ADRBK1, PRPF6, SUPT6H, SDF4, SUN2, SUPT5H, SUV39H1, PPP5C, PPP4C, AKT1, CTSD, GAA, SDF2L1, PPP2R1A, NUDT14, KIF22, MRPS2, MPV17L2, FADS2, FKBP8, DDX23, PPP1CA, TUBA1C, PPM1G, MTCH1, CYC1, G6PD, RNF181, LONP1, C12orf44, POLDIP3, ZNF768, SHISA5, PSMG3, GAMT, USP5, JUP, KCTD17, SLC25A25, ITPR3, KMT2D, AAAS, ADRM1, AGBL5, BRMS1, MAP2K2, MAPK11, GTF3C5, GCN1L1, MAPK3, PGLS, WDR83, PRKCSH, LSM4, CSK1, PKN1, CCDC124, GAPDH, MAP7D1, SLC27A4, NSUN5, PRDX5, DCXR, SRM, APEH, GSTP1, SEC13, DDOST, ZNF385A, STK40, SDHA, MAP3K10, GTF2F1, MRPS18A, ZBTB17, DCTN1, PTPN23, MAP3K11, APBB1, RPL35, KREMEN1, TRAPPC2L, SCYL1, NADSYN1, P4HB, ARF1, GTF3C1, FURIN, RAB11B, TBRG4, ATAD3A, APRT, GUK1, RPL36, PALM, WDR18, FXYD5, MCM7, PKP3, MDK, MDH2, GADD45GIP1, RHOC, SERINC2, LAMTOR4, ARHGDIA, RPAP1, HAGH, ARHGAP1, HSD17B10, HCFC1, DAPK3, CHMP1A, ASL, PLEKHJ1, WDR45, CDK16, ASS1, MFGE8, CDC37, SYNGR2, AAR2, HGS, SBF1, CDC42EP1, MBD3, RPTOR, ARHGEF1, MICALL1, ATP1A3, FAM50A, IRF2BP1, PGD, ATN1, SFN, ATP6V0D1, DOCK6, MAN2B1, SLC12A4, PHB, ATP6V0B, PEX14, SLC1A5, PIGQ, SART1, DVL1, DVL2, ATP6V0C, SLC4A2, MCM5, MCM2, BAX, GRK6, LRPAP1, GRWD1, LRP1, SLC25A39, COPG1, PI4KB, BAD, PIN1, ETNK2, FBXW4, GPS1, LRP5, AIP, SHMT2, PHGDH, DHPS, B3GAT3, GPX4, AUP1, GRN LTBP3, KIF1A, PEF1, CYB5R3, PKM, GRAMD1A, TWF2, MAP3K14, U2AF2, MVB12B, SRRT, DNM2, ACOT7, HCN2, PDAP1, GOLGA8B, ATAD3B, GRINA, TMEM120A, PHB2, PLOD3, NOC2L, BCKDHA, SGTA, LYPLA2, GSK3A, B4GALT7, BCAT2, INTS1, PIGT, SH3GL1, EMD, EXOSC5, EMP3, BRCA2, CDT1, DHX30, NDUFA7, RALY, SCAP, PRMT1, TRIM28, BSG, PPDPF, DPM2, UPF1, G6PC3, BANF1, NCAPH2, HPS1, EPHA2, SORBS3, TUBG1, EIF4EBP1, TUFM, TRIM11, ALYREF, TMEM214, MYL6, BLVRB, MYO1C, EIF4G1, PDCD1, PARVB, MRPL49, MVB12A, RAB1B, GOLGA8A, EEF2, DDX39A, EEF1G, TPI1, CENPM, EPN1, EEF1A2, MYBL2, PQBP1, DDX54, AHI1, ARMC6, SF3B5, SNRNP200, CHID1, TSPO, E4F1, BSN, SHKBP1, XAB2, E2F4, MRPS34, CACNA1H, WDTC1, E2F1, HSPB1, GDAP1L1, AP3D1, RAMP1, VKORC1, STUB1, BCAP31, SHARPIN, ECE1, NENF, TRAP1, PPRC1, UQCRC1, TOMM40, UROD, CAPN1, MCRS1, TMEM259, RPL18A, CANX, USF2, RPL13, TIMM13, TIMM10, RPL10, RPL8, AGTRAP, HDAC5, CARS, BAIAP2, FARSA, UPP1, PUSL1, MAD2L2, FASN, HAX1, EIF3G, CAD, RPS5, PINK1, HLA-B, GIT1, STX10, SPSB3, RPS2, MED16, RPLP2, RPLP1, MRPL12, ACD, PCBP4, RPLP0, TADA3, NOL6, CALR, B4GALT3, B4GALT2, RPL41, CARM1, VAV1, AURKAIP1, NR2C2AP, CALM3, NDUFA11, VAT1, STK25, VCP, RPL28, TTLL12, UBA52, RPS26, EDF1, NPM3, RPS16, NTMT1, GPAA1, UBA1, RPS19, UBB, CORO1B, RPS11, NT5DC2, RPS8, ESRRA, RPS15, TUBB4B, HM13, MRPL38, TUBB3, ADAM15, SYCP2, ETFB, RPS7, RPS6KB2, PLEKHM2, UBXN11, SLC44A2, BABAM1, SERPINH1, MVP, GNB2L1, KLC2, PHPT1, NAPA, ATP13A1, RRP12, TUT1, HMGA1, RPS28, HMOX1, WDR62, NUPR1, RRAS, MPG, CD2BP2, CDIPT, VPS13A, ZC3H7B, PSENEN, MED24, CDC20, TCOF1, TCN2, IKBKG, CDC34, SDSL, DRAP1, STMN3, BOP1,

		FLNA, FBXW5, FLNC, FLOT2, AGRN, CD151, IMPDH1, PSKH1, UBE2S, PRPF19, CD81, RRP7A, SMCR7L, C12orf57, OAZ1, SCARB1, MALAT1, PSMB6, PPFIA3, TOR2A, CAMK1, FDX1L, PSMC3, PRDX2, DPM3, PSMD8, UBXN6, PSMD4, CSRNP1, CLUH, TELO2, DGKZ, PSMD3, FIS1, RNASEH2A, TAF6, PTBP1, NUMA1, MYBBP1A, RRP1, UBXN1, NUCB1, CIB1, TARBP1, DEAF1, EIF6, PTK7, NOSIP, PTMA, MRPL2, SSNA1, PTMS, MRPL28, NDUFA13, UNC45A, THAP4, SMG5, RFXANK, MRPL4, RNF40, PTPRA, ZMAT5, AGPAT2, NRTN, TCEB2, NRGN, CUL7, IRAK1, PTPRF, TIMP1, NOP2, TMED3, TK1, TEX15, TKT, PYCR1, PYGB, TLN1, TMED9, CEP290, COTL1, CNOT3, ESPL1, GIPC1, KIF1C, TSPAN4, MLST8, NCS1, EDC3, TONSL, DUS1L, RAD23A, STOML2, RAC3, PRELID1, NHP2L1, RAB5C, VPS4A, IDH3G, SETD1A, TNNT1, LTBP4, NDUFB11, DDIT4, RALGDS, RANGAP1, AKAP8L, TAGLN2, CLPTM1, CLTB, PES1, RAP1GAP, DDX49, NDUFB8, TRMT2A, TGFB1, IGFBP2, PELP1, AP2M1, SND1, THOP1, PCIF1, NDUFS8, NDUFS6, CKB, NDUFV1, TBCB
GO:0022904	respiratory electron transport chain	NDUFB11, UQCRC1, NDUFB8, COX6B1, PINK1, COX4I1, NDUFA13, NDUFA7, COX8A, NDUFS8, NDUFS6, NDUFA11, NDUFV1, CYC1, ETFB

4) circGRB10 knockdown Reactome pathway analysis

Pathway ID	*Pathway Name*	*Genes*
R-HSA-1236974	ER-Phagosome pathway	HLA-B;HLA-C;HLA-A;PSMB10;PSMA7;PSMB6;PSMD8;SEC61A1;PSMB7;PSMD9;PSMC5;PSMB4;PSMB5;PSMC3;PSMD4;UBB;PSMD2;PSMD3;UBC;STX4;CALR;IKBKG;UBA52
R-HSA-983170	Antigen Presentation: Folding, assembly and peptide loading of class I MHC	BCAP31;SEC13;ERAP2;CANX;HLA-B;HLA-C;CALR;HLA-A
R-HSA-1236977	Endosomal/Vacuolar pathway	HLA-B;HLA-C;HLA-A
R-HSA-1236975	Antigen processing-Cross presentation	PSMB10;PSMA7;PSMB6;PSMD8;MRC2;SEC61A1;PSMB7;PSMD9;PSMB4;PSMB5;PSMD4;UBB;PSMD2;PSMD3;UBC;STX4;IKBKG;HLA-B;HLA-C;CYBA;HLA-A;PSMC5;PSMC3;CALR;UBA52
R-HSA-909733	Interferon alpha/beta signalling	IFITM3;IFITM1;IFITM2;IRF3;IRF1;HLA-B;HLA-C;ISG15;TYK2;HLA-A
R-HSA-9633012	Response of EIF2AK4 (GCN2) to amino acid deficiency	RPL3;RPL32;RPL31;RPLP1;RPLP0;RRP1;RPL10A;RPL8;RPS15;RPS14;RPS16;RPL18A;RPS19;RPL36;RPL35;RPLP2;RPS11;RPS7;RPS8;RPS5;RPL13A;RPSA;DDIT3;CRY2;RPL37A;RPL27;TRIB3;RPL29;RPL28;UBA52;ATF4;RPL10;RPL12;RPL11;UBB;UBC;RPS3;RPL13;RPS2;RPL18;GCN1;RPL19;RPL41;ASNS;RPS26;RPS28;EEF1AKMT4;RPS29;RPL27A;FAU;RPS21;RPL26L1
R-HSA-983169	Class I MHC mediated antigen processing & presentation	LRSAM1;KEAP1;CDC20;PSMD8;MRC2;HERC4;SEC61A1;PSMD9;PSMD4;PSMD2;PSMD3;TOM1;ELOB;IKBKG;FBXO9;FBXW4;SEC13;FBXW5;WSB1;FBXW9;HLA-B;HLA-C;CYBA;HLA-A;FBXO10;LRRC41;TRAIP;TRAF7;RNF123;RNF126;CDC34;CANX;RBCK1;UBA52;THOP1;TRIM11;ANAPC2;CUL7;CUL5;MGRN1;UBE2J2;PSMB10;PSMA7;ANAPC11;PSMB6;PSMB7;PSMB4;FZR1;PSMB5;HECTD2;UBB;HECTD3;RNF217;UBC;POC1A;STX4;BCAP31;KLHL25;ERAP2;UBE2C;RNF25;CCDC14;FBXL19;MIB2;FBXL18;FBXL15;BTBD6;FBXO31;FBXL12;PSMC5;PSMC3;UBE2S;ASB6;UBE2O;STUB1;UBA1;CALR;FBXL4;DZIP3;UBE2M;RNF220;SPSB4
R-HSA-422475	Axon guidance	RPL3;PLXND1;RPL32;RPL31;RRP1;MSI1;RPL10A;RPL8;RPS6KA4;PSMD8;RPS15;RPS14;PSMD9;ALCAM;RPS16;DPYSL4;RPL18A;PSMD4;RPS19;DPYSL5;TUBB3;PSMD2;CFL1;PSMD3;DAG1;RPL36;RPL35;NRTN;EPHB2;RPS11;EPHB4;AP2M1;MAP2K2;UNC5A;RPS7;UNC5B;RPS8;RPS5;ADAM10;ALG3;RPSA;CACNB1;DOK1;SHTN1;MYL6;COL4A2;RPL27;RPL29;PFN1;TLN1;UBA52;RPL28;NGEF;EPHA2;SPTBN4;SHC1;PSEN2;PIK3R2;EFNA4;RAP1GAP;CACNA1H;APH1A;EFNB1;NCSTN;RRAS;UBB;UBC;ABL1;PLXNA2;MYH14;PLXNA1;PIP5K1C;PLCG1;SPTBN2;VASP;RAP1GAP2;RPL41;RPS26;EFNA1;RPS28;EFNA3;DLG1;CDK5;RPS29;RPL27A;RNPS1;RPS21;FGFR1;EIF4G1;GSK3A;LDB1;RPLP1;ARPC1A;RPLP0;MAST1;CLTB;AP2A1;A

		P2A2;TUBA1C;TUBA1B;TUBA1A;RPLP2;ELOB;SPTAN1;GIT1;PSENEN;LYPLA2;TRPC3;ITGA2;MMP2;ITGA1;RPL13A;GAB2;RHOC;SPTB;VAV2;DNM2;RGMA;RASA1;COL6A2;CRY2;COL6A1;RPL37A;MYH9;SCN4A;EVL;ITGA5;SOS1;RPL10;ROCK1;SRC;ROCK2;SEMA3A;RPL12;RPL11;CRMP1;NTN1;PSMA7;PSMB10;PSMB6;PTPA;PSMB7;PSMB4;MAPK7;PSMB5;GPC1;ERBB2;ZSWIM8;RPS3;SLIT1;AP2S1;RPL13;RPS2;PAK3;RPL18;PDLIM7;MAPK3;PAK4;RPL19;LAMB2;LIMK2;LIMK1;MYO9B;TUBB4B;MAPK12;MAPK11;PSMC5;EEF1AKMT4;PSMC3;FAU;AGRN;RPL26L1
R-HSA-72689	Formation of a pool of free 40S subunits	RPL3;RPL32;RPL31;RPLP1;RPLP0;RRP1;RPL10A;RPL8;RPS15;RPS14;RPS16;RPL18A;RPS19;RPL36;RPL35;RPLP2;RPS11;RPS7;RPS8;RPS5;RPL13A;RPSA;CRY2;RPL37A;RPL27;RPL29;RPL28;UBA52;RPL10;RPL12;RPL11;UBB;UBC;RPS3;RPL13;RPS2;RPL18;RPL19;RPL41;RPS26;RPS28;EEF1AKMT4;RPS29;RPL27A;EIF3I;EIF3G;FAU;EIF3C;EIF3D;RPS21;RPL26L1;EIF3B
R-HSA-9711097	Cellular response to starvation	RPL3;RPL32;RPL31;RPLP1;RPLP0;RRP1;RPL10A;RPL8;RPS15;RPTOR;RPS14;FLCN;RPS16;RPL18A;RPS19;MLST8;RPL36;RPL35;RPLP2;RPS11;SEC13;SZT2;ATP6V0B;RPS7;RPS8;RPS5;RPL13A;RPSA;DDIT3;CRY2;RPL37A;RPL27;TRIB3;RPL29;ATP6V0D1;RPL28;UBA52;ATP6V0C;ATF4;RPL10;RPL12;NPRL3;RPL11;WDR24;UBB;UBC;RPS3;RPL13;RPS2;RPL18;ATP6V0E2;GCN1;RPL19;ATP6V1F;RPL41;ASNS;MTOR;RPS26;RPS28;EEF1AKMT4;RPS29;RPL27A;LAMTOR2;FAU;LAMTOR1;LAMTOR4;RPS21;RPL26L1
R-HSA-156842	Eukaryotic Translation Elongation	RPL3;RPL32;RPL31;RPLP1;RPLP0;RRP1;RPL10A;RPL8;RPS15;RPS14;RPS16;RPL18A;RPS19;RPL36;RPL35;RPLP2;RPS11;RPS7;RPS8;RPS5;RPL13A;RPSA;EEF1G;EEF1A2;CRY2;RPL37A;RPL27;RPL29;RPL28;UBA52;RPL10;RPL12;RPL11;UBB;UBC;RPS3;RPL13;RPS2;RPL18;RPL19;RPL41;EEF2;RPS26;RPS28;EEF1AKMT4;RPS29;RPL27A;FAU;RPS21;RPL26L1
R-HSA-156902	Peptide chain elongation	RPL3;RPL10;RPL32;RPL31;RPL12;RPLP1;RPLP0;RPL11;RRP1;RPL10A;RPL8;RPS15;RPS14;RPS16;RPL18A;RPS19;UBB;UBC;RPS3;RPL36;RPL35;RPLP2;RPL13;RPS2;RPL18;RPS11;RPL19;RPL41;RPS7;RPS8;RPS5;RPL13A;RPSA;EEF2;RPS26;RPS28;EEF1AKMT4;RPS29;RPL27A;CRY2;RPL37A;RPL27;FAU;RPL29;UBA52;RPL28;RPS21;RPL26L1
R-HSA-975956	Nonsense Mediated Decay (NMD) independent of the Exon Junction Complex (EJC)	RPL3;RPL32;RPL31;RPLP1;RPLP0;RRP1;RPL10A;RPL8;RPS15;RPS14;RPS16;RPL18A;RPS19;RPL36;RPL35;RPLP2;RPS11;UPF1;RPS7;RPS8;RPS5;RPL13A;RPSA;CRY2;RPL37A;RPL27;RPL29;RPL28;UBA52;RPL10;RPL12;RPL11;UBB;UBC;RPS3;RPL13;RPS2;RPL18;RPL19;RPL41;RPS26;RPS28;EEF1AKMT4;RPS29;RPL27A;FAU;RPS21;RPL26L1;EIF4G1
R-HSA-2262752	Cellular responses to stress	RPL3;RPL32;RPL31;RRP1;KEAP1;RPL8;CCAR2;RPS15;PSMD8;RPS14;PSMD9;RPS16;RPL18A;RPS19;PSMD4;KAT5;PSMD2;PSMD3;RPL36;RPL35;CHAC1;RPS11;NUP210;DDX11;PRKCD;NUP93;SCO2;DDIT3;TRIB3;RPL27;PREB;ATP6V0D1;RPL29;TLN1;CLOCK;UBA52;RPL28;ATF4;POM121;ANAPC15;NPRL3;AAAS;DE

		DD2;ANAPC11;PRDX2;PRDX5;SERPINH1;HMOX1;ACD;RPL41;PHC2;H1-2;RPS26;MOV10;RPS28;RPS29;RPL27A;CREBRF;ATM;HYOU1;CALR;RPS21;BAP1;CDKN1A;RPLP1;RPLP0;RPTOR;MYDGF;TUBA1C;TUBA1B;ACTR1A;TUBA1A;RPLP2;ELOB;COX8A;ATP6V0B;SEC13;MINK1;NCOR2;ATP6V0C;RPL10;GSTP1;RPL12;RPL11;COX5B;WDR24;RELA;PSMA7;PSMB6;PSMB7;HIRA;PSMB4;EXOSC5;PSMB5;EXOSC4;LMNA;RPS3;RPL13;RPS2;ATP6V0E2;RPL18;MEF2D;EXTL3;RPL19;CDKN2D;RANBP2;SYVN1;TUBB4B;YIF1A;PSMC5;EEF1AKMT4;PSMC3;HDGF;LAMTOR2;FAU;LAMTOR1;LAMTOR4;CRTC2;CRTC1;TACO1;RORA;RPL10A;TXN2;TUBB3;SCMH1;MAP2K3;SZT2;RPS7;RPS8;RPS5;RPSA;CYBA;COX6B1;MAPKAPK3;MAPKAPK2;ERF;FKBP4;ANAPC2;VCP;CUL7;RPS19BP1;SHC1;RAI1;STIP1;UBB;BAG3;TPR;UBC;COX14;MAP2K7;GCN1;ATP6V1F;KLHDC3;ZBTB17;CBX6;UBE2C;CBX2;HMGA1;ASNS;CDK4;UBE2S;SRPRA;MDM4;ACADVL;GSK3A;CHD9;COX4I1;HSPB1;CABIN1;FLCN;CAPZB;NUP62;MLST8;ACP2;KDM6B;GPX1;PPP2R5B;RPL13A;ARFGAP1;CTDSP2;AKT1S1;CRY2;RPL37A;BLVRB;PPP1R15A;CAMK2B;SMARCD3;HDAC3;DCTN2;DCTN1;HM13;DCTN3;CXXC1;HDAC6;PSMB10;FZR1;MAPK7;E2F1;MAPK3;TXNRD2;ATOX1;MTOR;MAPK11;RAD50;PC;CARM1;P4HB;RPL26L1
R-HSA-9675108	Nervous system development	RPL3;PLXND1;RPL32;RPL31;RRP1;MSI1;RPL10A;RPL8;RPS6KA4;PSMD8;RPS15;RPS14;PSMD9;ALCAM;RPS16;DPYSL4;RPL18A;PSMD4;RPS19;DPYSL5;TUBB3;PSMD2;CFL1;PSMD3;DAG1;RPL36;RPL35;NRTN;EPHB2;RPS11;EPHB4;AP2M1;MAP2K2;UNC5A;RPS7;UNC5B;RPS8;RPS5;ADAM10;ALG3;RPSA;CACNB1;DOK1;SHTN1;MYL6;COL4A2;RPL27;RPL29;PFN1;TLN1;UBA52;RPL28;NGEF;EPHA2;SPTBN4;SHC1;PSEN2;PIK3R2;EFNA4;RAP1GAP;CACNA1H;APH1A;EFNB1;NCSTN;RRAS;UBB;UBC;ABL1;PLXNA2;MYH14;PLXNA1;PIP5K1C;PLCG1;SPTBN2;VASP;RAP1GAP2;RPL41;SMARCA4;RPS26;EFNA1;RPS28;EFNA3;DLG1;CDK5;RPS29;RPL27A;RNPS1;RPS21;FGFR1;EIF4G1;GSK3A;LDB1;RPLP1;ARPC1A;RPLP0;MAST1;CLTB;AP2A1;TAZ;AP2A2;TUBA1C;TUBA1B;TUBA1A;RPLP2;ELOB;SPTAN1;GIT1;PSENEN;TEAD4;LYPLA2;TRPC3;ITGA2;MMP2;ITGA1;RPL13A;GAB2;RHOC;SPTB;SREBF2;VAV2;DNM2;RGMA;RASA1;COL6A2;CRY2;COL6A1;RPL37A;MYH9;SCN4A;EVL;ITGA5;SOS1;RPL10;ROCK1;SRC;ROCK2;SEMA3A;RPL12;RPL11;CRMP1;NTN1;PSMA7;PSMB10;PSMB6;PTPA;PSMB7;PSMB4;MAPK7;PSMB5;GPC1;ERBB2;ZSWIM8;RPS3;SLIT1;AP2S1;RPL13;RPS2;PAK3;RPL18;PDLIM7;MAPK3;PAK4;RPL19;LAMB2;LIMK2;LIMK1;MYO9B;TUBB4B;MAPK12;MAPK11;PSMC5;EEF1AKMT4;PSMC3;FAU;AGRN;RPL26L1
R-HSA-8953897	Cellular responses to stimuli	RPL3;RPL32;RPL31;RRP1;KEAP1;RPL8;CCAR2;RPS15;PSMD8;RPS14;PSMD9;MT2A;RPS16;RPL18A;RPS19;PSMD4;KAT5;PSMD2;PSMD3;RPL36;RPL35;CHAC

		1;RPS11;NUP210;DDX11;PRKCD;NUP93;SCO2;DDIT3;TRIB3;RPL27;PREB;ATP6V0D1;RPL29;TLN1;CLOCK;UBA52;RPL28;ATF4;POM121;ANAPC15;NPRL3;AAAS;DEDD2;ANAPC11;PRDX2;PRDX5;SERPINH1;HMOX1;ACD;RPL41;PHC2;H1-2;RPS26;MOV10;RPS28;RPS29;RPL27A;CREBRF;ATM;HYOU1;CALR;RPS21;BAP1;CDKN1A;RPLP1;RPLP0;RPTOR;MYDGF;TUBA1C;TUBA1B;ACTR1A;TUBA1A;CSRP1;RPLP2;ELOB;COX8A;ATP6V0B;SEC13;MINK1;NCOR2;ATP6V0C;RPL10;GSTP1;RPL12;RPL11;COX5B;WDR24;RELA;PSMA7;PSMB6;PSMB7;HIRA;PSMB4;EXOSC5;PSMB5;EXOSC4;LMNA;RPS3;RPL13;RPS2;ATP6V0E2;RPL18;MEF2D;EXTL3;RPL19;CDKN2D;RANBP2;SYVN1;TUBB4B;YIF1A;PSMC5;EEF1AKMT4;PSMC3;HDGF;LAMTOR2;FAU;LAMTOR1;LAMTOR4;CRTC2;CRTC1;TACO1;RORA;RPL10A;TXN2;TUBB3;SCMH1;MAP2K3;SZT2;RPS7;RPS8;RPS5;RPSA;CYBA;COX6B1;MAPKAPK3;MAPKAPK2;ERF;FKBP4;ANAPC2;VCP;CUL7;RPS19BP1;SHC1;RAI1;STIP1;UBB;BAG3;TPR;UBC;COX14;MAP2K7;GCN1;ATP6V1F;KLHDC3;ZBTB17;CBX6;UBE2C;CBX2;HMGA1;ASNS;CDK4;UBE2S;SRPRA;MDM4;ACADVL;GSK3A;CHD9;COX4I1;HSPB1;CABIN1;FLCN;CAPZB;NUP62;MLST8;ACP2;KDM6B;GPX1;PPP2R5B;RPL13A;ARFGAP1;CTDSP2;AKT1S1;CRY2;RPL37A;BLVRB;PPP1R15A;CAMK2B;SMARCD3;HDAC3;DCTN2;DCTN1;HM13;DCTN3;CXXC1;HDAC6;PSMB10;FZR1;MAPK7;E2F1;MAPK3;TXNRD2;ATOX1;MTOR;MAPK11;RAD50;PC;CARM1;P4HB;RPL26L1
R-HSA-9010553	Regulation of expression of SLITs and ROBOs	RPL3;RPL32;LDB1;RPL31;RPLP1;RPLP0;RRP1;MSI1;RPL10A;RPL8;PSMD8;RPS15;RPS14;PSMD9;RPS16;RPL18A;PSMD4;RPS19;PSMD2;PSMD3;DAG1;RPL36;RPL35;RPLP2;ELOB;RPS11;RPS7;RPS8;RPS5;RPL13A;RPSA;CRY2;RPL37A;RPL27;RPL29;RPL28;UBA52;RPL10;RPL12;RPL11;PSMB10;PSMA7;PSMB6;PSMB7;PSMB4;PSMB5;UBB;UBC;RPS3;SLIT1;ZSWIM8;RPL13;RPS2;RPL18;RPL19;RPL41;RPS26;PSMC5;RPS28;EEF1AKMT4;PSMC3;RPS29;RPL27A;RNPS1;FAU;RPS21;RPL26L1;EIF4G1
R-HSA-1799339	SRP-dependent cotranslational protein targeting to membrane	RPL3;RPL32;RPL31;RPLP1;RPLP0;RRP1;RPL10A;RPL8;RPS15;SEC61A1;RPS14;RPS16;RPL18A;RPS19;RPL36;RPL35;RPLP2;RPS11;RPS7;SSR4;RPS8;SSR2;RPS5;RPL13A;RPSA;DDOST;CRY2;RPL37A;RPL27;RPL29;RPL28;UBA52;RPL10;RPL12;RPL11;UBB;UBC;RPS3;RPL13;RPS2;RPL18;RPL19;RPL41;SRP68;RPS26;RPS28;EEF1AKMT4;RPS29;RPL27A;SRPRA;FAU;RPS21;RPL26L1
R-HSA-72764	Eukaryotic Translation Termination	RPL3;RPL32;RPL31;RPLP1;RPLP0;RRP1;APEH;RPL10A;RPL8;RPS15;TRMT112;RPS14;RPS16;RPL18A;RPS19;RPL36;RPL35;RPLP2;RPS11;RPS7;RPS8;RPS5;RPL13A;RPSA;CRY2;RPL37A;RPL27;RPL29;RPL28;UBA52;RPL10;RPL12;RPL11;UBB;UBC;RPS3;RPL13;RPS2;RPL18;RPL19;RPL41;RPS26;RPS28;EEF1AKMT4;RPS29;RPL27A;FAU;RPS21;RPL26L1

R-HSA-8868773	rRNA processing in the nucleus and cytosol	DDX49;RPL3;RPL32;RPL31;RPLP1;RPLP0;RRP1;NAT10;RPL10A;RPL8;RRP9;RPS15;TRMT112;RPS14;RPS16;RPL18A;RPS19;RPL36;RPL35;RPLP2;BUD23;RPS11;PELP1;RPS7;RPS8;RPS5;RPL13A;RPSA;CSNK1D;FTSJ3;EBNA1BP2;XRN1;CRY2;RPL37A;NHP2;RPL27;RPL29;RPL28;UBA52;RPL10;LRP1;RPL12;NOP2;RPL11;TSR3;SNU13;NOL6;RRP7A;EXOSC5;EXOSC4;PDCD11;UBB;PES1;UBC;DHX37;RPS3;RPL13;RPS2;RPL18;RPL19;NOP14;RPL41;WDR18;BYSL;RPS26;BOP1;RPS28;TBL3;EEF1AKMT4;LAS1L;RPS29;RPL27A;FAU;NOL12;RPS21;RPL26L1;NOP10
R-HSA-72706	GTP hydrolysis and joining of the 60S ribosomal subunit	RPL3;RPL32;RPL31;RPLP1;RPLP0;RRP1;RPL10A;RPL8;RPS15;RPS14;RPS16;RPL18A;RPS19;RPL36;RPL35;RPLP2;RPS11;RPS7;RPS8;RPS5;RPL13A;RPSA;CRY2;RPL37A;RPL27;RPL29;RPL28;UBA52;RPL10;RPL12;RPL11;UBB;UBC;RPS3;RPL13;RPS2;RPL18;RPL19;RPL41;RPS26;RPS28;EEF1AKMT4;RPS29;RPL27A;EIF3I;EIF3G;FAU;EIF3C;EIF3D;RPS21;RPL26L1;EIF4G1;EIF3B
R-HSA-156827	L13a-mediated translational silencing of Ceruloplasmin expression	RPL3;RPL32;RPL31;RPLP1;RPLP0;RRP1;RPL10A;RPL8;RPS15;RPS14;RPS16;RPL18A;RPS19;RPL36;RPL35;RPLP2;RPS11;RPS7;RPS8;RPS5;RPL13A;RPSA;CRY2;RPL37A;RPL27;RPL29;RPL28;UBA52;RPL10;RPL12;RPL11;UBB;UBC;RPS3;RPL13;RPS2;RPL18;RPL19;RPL41;RPS26;RPS28;EEF1AKMT4;RPS29;RPL27A;EIF3I;EIF3G;FAU;EIF3C;EIF3D;RPS21;RPL26L1;EIF4G1;EIF3B
R-HSA-927802	Nonsense-Mediated Decay (NMD)	RPL3;RPL32;RPL31;RPLP1;RPLP0;RRP1;SMG9;RPL10A;RPL8;SMG5;SMG6;RPS15;RPS14;RPS16;RPL18A;RPS19;PPP2R1A;RPL36;RPL35;RPLP2;RPS11;UPF1;RPS7;RPS8;RPS5;RPL13A;RPSA;CRY2;RPL37A;RPL27;RPL29;RPL28;UBA52;RPL10;RPL12;RPL11;UBB;UBC;RPS3;RPL13;RPS2;RPL18;RPL19;RPL41;RPS26;RPS28;EEF1AKMT4;RPS29;RPL27A;RNPS1;FAU;RPS21;RPL26L1;EIF4G1
R-HSA-975957	Nonsense Mediated Decay (NMD) enhanced by the Exon Junction Complex (EJC)	RPL3;RPL32;RPL31;RPLP1;RPLP0;RRP1;SMG9;RPL10A;RPL8;SMG5;SMG6;RPS15;RPS14;RPS16;RPL18A;RPS19;PPP2R1A;RPL36;RPL35;RPLP2;RPS11;UPF1;RPS7;RPS8;RPS5;RPL13A;RPSA;CRY2;RPL37A;RPL27;RPL29;RPL28;UBA52;RPL10;RPL12;RPL11;UBB;UBC;RPS3;RPL13;RPS2;RPL18;RPL19;RPL41;RPS26;RPS28;EEF1AKMT4;RPS29;RPL27A;RNPS1;FAU;RPS21;RPL26L1;EIF4G1
R-HSA-2408557	Selenocysteine synthesis	RPL3;RPL32;RPL31;RPLP1;RPLP0;RRP1;RPL10A;RPL8;RPS15;RPS14;RPS16;RPL18A;RPS19;RPL36;RPL35;RPLP2;RPS11;RPS7;RPS8;RPS5;RPL13A;RPSA;SARS1;CRY2;RPL37A;RPL27;RPL29;RPL28;UBA52;DCTPP1;RPL10;RPL12;RPL11;UBB;UBC;RPS3;RPL13;RPS2;RPL18;RPL19;EEFSEC;RPL41;RPS26;RPS28;EEF1AKMT4;RPS29;RPL27A;FAU;RPS21;RPL26L1
R-HSA-6791226	Major pathway of rRNA processing in the nucleolus and cytosol	DDX49;RPL3;RPL32;RPL31;RPLP1;RPLP0;RRP1;RPL10A;RPL8;RRP9;RPS15;RPS14;RPS16;RPL18A;RPS19;RPL36;RPL35;RPLP2;BUD23;RPS11;PELP1;RPS7;RPS8;RPS5;RPL13A;RPSA;CSNK1D;FTSJ3;EBNA1BP2;XRN1;CRY2;RPL37A;RPL27;RPL29;RPL28;UBA52;RPL

		10;LRP1;RPL12;RPL11;SNU13;NOL6;RRP7A;EXOSC5;EXOSC4;PDCD11;UBB;PES1;UBC;DHX37;RPS3;RPL13;RPS2;RPL18;RPL19;NOP14;RPL41;WDR18;BYSL;RPS26;BOP1;RPS28;TBL3;EEF1AKMT4;LAS1L;RPS29;RPL27A;FAU;NOL12;RPS21;RPL26L1
R-HSA-877300	Interferon gamma signalling	CAMK2B;PRKCD;HLA-B;HLA-C;HLA-A;IFI30;PML;MT2A;IRF3;IRF1;TRIM68;JAK2;GBP3
R-HSA-376176	Signalling by ROBO receptors	RPL3;RPL32;LDB1;RPL31;RPLP1;MAST1;RPLP0;RRP1;MSI1;RPL10A;RPL8;PSMD8;RPS15;RPS14;PSMD9;RPS16;RPL18A;PSMD4;RPS19;PSMD2;PSMD3;DAG1;RPL36;RPL35;RPLP2;ELOB;RPS11;RPS7;RPS8;RPS5;RPL13A;RPSA;CRY2;RPL37A;RPL27;EVL;RPL29;PFN1;SOS1;RPL28;UBA52;RPL10;SRC;RPL12;RPL11;NTN1;PSMB10;PSMA7;PSMB6;PSMB7;PSMB4;PSMB5;UBB;GPC1;UBC;RPS3;SLIT1;ABL1;ZSWIM8;RPL13;RPS2;PAK3;RPL18;PAK4;RPL19;VASP;RPL41;MYO9B;RPS26;PSMC5;RPS28;EEF1AKMT4;PSMC3;RPS29;RPL27A;RNPS1;FAU;RPS21;RPL26L1;EIF4G1
R-HSA-381038	XBP1(S) activates chaperone genes	ZBTB17;KLHDC3;ACADVL;CUL7;GSK3A;DCTN1;SHC1;DDX11;CXXC1;SYVN1;PPP2R5B;YIF1A;ARFGAP1;MYDGF;CTDSP2;LMNA;SRPRA;HDGF;HYOU1;PREB;TLN1;ATP6V0D1;EXTL3
R-HSA-72613	Eukaryotic Translation Initiation	RPL3;RPL32;RPL31;RPLP1;RPLP0;RRP1;RPL10A;RPL8;RPS15;RPS14;RPS16;RPL18A;RPS19;RPL36;RPL35;RPLP2;RPS11;RPS7;RPS8;RPS5;RPL13A;RPSA;CRY2;RPL37A;RPL27;RPL29;RPL28;UBA52;RPL10;RPL12;RPL11;UBB;UBC;RPS3;EIF4EBP1;RPL13;RPS2;RPL18;RPL19;RPL41;RPS26;RPS28;EEF1AKMT4;RPS29;RPL27A;EIF3I;EIF3G;FAU;EIF3C;EIF3D;RPS21;RPL26L1;EIF4G1;EIF3B
R-HSA-72737	Cap-dependent Translation Initiation	RPL3;RPL32;RPL31;RPLP1;RPLP0;RRP1;RPL10A;RPL8;RPS15;RPS14;RPS16;RPL18A;RPS19;RPL36;RPL35;RPLP2;RPS11;RPS7;RPS8;RPS5;RPL13A;RPSA;CRY2;RPL37A;RPL27;RPL29;RPL28;UBA52;RPL10;RPL12;RPL11;UBB;UBC;RPS3;EIF4EBP1;RPL13;RPS2;RPL18;RPL19;RPL41;RPS26;RPS28;EEF1AKMT4;RPS29;RPL27A;EIF3I;EIF3G;FAU;EIF3C;EIF3D;RPS21;RPL26L1;EIF4G1;EIF3B
R-HSA-381070	IRE1alpha activates chaperones	ZBTB17;KLHDC3;ACADVL;CUL7;GSK3A;DCTN1;SHC1;DDX11;CXXC1;SYVN1;PPP2R5B;YIF1A;ARFGAP1;MYDGF;CTDSP2;LMNA;SRPRA;HDGF;HYOU1;PREB;TLN1;ATP6V0D1;EXTL3
R-HSA-192823	Viral mRNA Translation	RPL3;RPL10;RPL32;RPL31;RPL12;RPLP1;RPLP0;RPL11;RRP1;RPL10A;RPL8;RPS15;RPS14;RPS16;RPL18A;RPS19;UBB;UBC;RPS3;RPL36;RPL35;RPLP2;RPL13;RPS2;RPL18;RPS11;RPL19;RPL41;RPS7;RPS8;RPS5;RPL13A;RPSA;RPS26;RPS28;EEF1AKMT4;RPS29;RPL27A;CRY2;RPL37A;RPL27;FAU;RPL29;UBA52;RPL28;RPS21;RPL26L1
R-HSA-168273	Influenza Viral RNA Transcription and Replication	RPL3;RPL32;RPL31;RPLP1;RPLP0;RRP1;RPL10A;RPL8;RPS15;RPS14;RPS16;RPL18A;RPS19;NUP62;RPL36;RPL35;RPLP2;RPS11;SEC13;NUP210;RPS7;RPS8;RPS5;RPL13A;RPSA;GTF2F1;NUP93;CRY2;RPL37A;RPL27;RPL29;RPL28;UBA52;POM121;RPL10;RPL12;RPL11;AAAS;UBB;POLR2A;TPR;UBC;POLR2E;RPS3;POL

		R2F;RPL13;POLR2G;RPS2;POLR2I;RPL18;POLR2J;POLR2L;RPL19;RANBP2;RPL41;MTOR;RPS26;RPS28;EEF1AKMT4;RPS29;RPL27A;FAU;RPS21;RPL26L1
R-HSA-72766	Translation	RPL3;RPL32;RPL31;RRP1;APEH;RPL10A;YARS1;RPL8;RPS15;RPS14;RPS16;RPL18A;RPS19;RPL36;RPL35;RPS11;RPS7;RPS8;RPS5;AIP;MRPS18A;RPSA;TUFM;EEF1A2;RPL27;TARS2;CARS1;AURKAIP1;RPL29;UBA52;RPL28;AARS1;AARS2;MRPL14;MRPL12;MRPL10;MRPL11;UBB;UBC;EIF4EBP1;RPL41;MRPL27;MRPL28;ERAL1;EEF2;MRPL24;MRPL21;RPS26;RPS28;RPS29;RPL27A;SRPRA;FARSA;RPS21;EIF4G1;RPLP1;RPLP0;MRPL38;MRPL36;MRPL37;MRPL41;MRPL4;TRMT112;SEC61A1;MRPL2;MRPL40;QARS1;RPLP2;MRPS26;SSR4;SSR2;MARS1;MRPL49;MRPS2;MRPS21;RPL13A;DDOST;MRPL52;EEF1G;SARS1;MRPL51;CRY2;RPL37A;RPL10;RPL12;MRPS34;RPL11;MRPL54;MRPL55;RPS3;RPL13;RPS2;RPL18;RPL19;GADD45GIP1;SRP68;EEF1AKMT4;EIF3I;EIF3G;FAU;EIF3C;EIF3D;RPL26L1;EIF3B
R-HSA-913531	Interferon Signalling	IFITM3;CAMK2B;IFITM1;POM121;IFITM2;AAAS;IFI30;MT2A;UBB;NUP62;TPR;UBC;TRIM68;FLNA;FLNB;KPNA5;PLCG1;JAK2;GBP3;MAPK3;RANBP2;SEC13;NUP210;PRKCD;HLA-B;HLA-C;ISG15;TYK2;HLA-A;PML;MTOR;NUP93;IRF3;IRF1;PIN1;UBA52;EIF4G1
R-HSA-168255	Influenza Infection	RPL3;RPL32;RPL31;RPLP1;RPLP0;RRP1;RPL10A;RPL8;RPS15;RPS14;RPS16;RPL18A;RPS19;NUP62;RPL36;RPL35;RPLP2;KPNA5;RPS11;SEC13;NUP210;RPS7;RPS8;RPS5;RPL13A;RPSA;GTF2F1;NUP93;CRY2;CANX;RPL37A;RPL27;RPL29;RPL28;UBA52;POM121;RPL10;RPL12;RPL11;AAAS;UBB;POLR2A;TPR;UBC;POLR2E;RPS3;POLR2F;RPL13;POLR2G;RPS2;POLR2I;RPL18;POLR2J;POLR2L;RPL19;RANBP2;CPSF4;RPL41;TGFB1;ISG15;MTOR;RPS26;RPS28;EEF1AKMT4;RPS29;RPL27A;CALR;FAU;RPS21;RPL26L1
R-HSA-72312	rRNA processing	DDX49;RPL3;RPL32;RPL31;RPLP1;RPLP0;RRP1;NAT10;RPL10A;RPL8;RRP9;RPS15;TRMT112;RPS14;RPS16;RPL18A;RPS19;RPL36;RPL35;RPLP2;BUD23;RPS11;PELP1;RPS7;RPS8;ELAC2;RPS5;RPL13A;RPSA;CSNK1D;FTSJ3;EBNA1BP2;XRN1;CRY2;RPL37A;NHP2;RPL27;RPL29;RPL28;UBA52;RPL10;LRP1;RPL12;NOP2;RPL11;TSR3;SNU13;HSD17B10;NOL6;RRP7A;EXOSC5;EXOSC4;PDCD11;UBB;PES1;UBC;DHX37;RPS3;RPL13;RPS2;RPL18;RPL19;NOP14;RPL41;WDR18;BYSL;RPS26;BOP1;RPS28;TBL3;EEF1AKMT4;LAS1L;RPS29;RPL27A;FAU;NOL12;RPS21;RPL26L1;NOP10
R-HSA-8953854	Metabolism of RNA	POP7;RPL3;RPL32;RPL31;RTCB;RRP1;RPL10A;RPL8;TSEN54;RRP9;EDC3;EFTUD2;LSM10;PSMD8;RPS15;EDC4;RPS14;PSMD9;RPS16;RPL18A;SNRPD2;PSMD4;RPS19;PPP2R1A;PSMD2;SAP130;PSMD3;RPL36;AKT1;RPL35;RPS11;NUP210;RPS7;RPS8;PUS1;RPS5;PRKCD;RPSA;CSNK1D;TRNT1;THOC5;GTF2F1;THOC6;FTSJ3;NUP93;EBNA1BP2;DDX39A;PRPF6;HNRNPUL1;XRN1;MAPKAPK2;GEMIN4;NHP2;CD2BP2;RPL27;SNRNP25;RPL29;SNRNP200;UBA52;RPL28;SNRPA;SNRPB;SRSF9;POM121;NOP2;SNU13;RNPC3;AAAS;RR

		P7A;PDCD11;UBB;PCBP1;ZMAT5;TPR;UBC;DHX37;SYMPK;DHX38;RBM10;APOBEC3C;CPSF4;NOP14;RPL41;ALYREF;SUPT5H;LSM4;RPS26;RPS28;TBL3;LSM7;LAS1L;RPS29;RPL27A;HNRNPF;CNOT3;TRMT13;RNPS1;NOL12;RPS21;NOP10;EIF4G1;APOBEC3B;NXT1;DDX49;RPLP1;RPLP0;WDR4;HSPB1;NAT10;SMG9;PRPF19;SMG5;PQBP1;SMG6;TRMT112;PTBP1;SART1;PCM1;NUP62;RPLP2;TNKS1BP1;BUD23;CTNNBL1;PELP1;UPF1;SEC13;ELAC2;RPL13A;TFIP11;QTRT1;CTU2;CRY2;RPL37A;SF3B5;SF3B2;RPL10;LRP1;POLDIP3;RPL12;URM1;DDX23;PRCC;RPL11;TSR3;SRRT;HSD17B10;LAGE3;PSMA7;PSMB10;NOL6;U2AF1L4;PSMB6;PSMB7;PSMB4;EXOSC5;PSMB5;EXOSC4;POLR2A;U2AF2;PES1;POLR2E;RPS3;POLR2F;RPL13;POLR2G;RPS2;POLR2I;RPL18;POLR2J;SRSF11;POLR2L;RPL19;RANBP2;SF3A1;SF3A2;GPKOW;BRF1;WDR18;TRMT1;MTOR;BYSL;ADAT2;MAPK11;XAB2;BOP1;PSMC5;EEF1AKMT4;PSMC3;ERCC2;FAU;TRMT61A;RPL26L1
R-HSA-381119	Unfolded Protein Response (UPR)	ACADVL;CUL7;GSK3A;DCTN1;SHC1;CXXC1;MYDGF;EXOSC5;EXOSC4;LMNA;EXTL3;ZBTB17;KLHDC3;DDX11;SYVN1;PPP2R5B;ASNS;YIF1A;ARFGAP1;CTDSP2;DDIT3;SRPRA;CREBRF;HDGF;HYOU1;PREB;CALR;TLN1;ATP6V0D1;ATF4
R-HSA-199991	Membrane Trafficking	APP;KDELR1;GCC2;GOLGA2;GOLGA4;TUBB3;KIF5C;AP1S1;AKT1;ARFIP2;KIF21B;SBF1;TBC1D10A;AP2M1;TBC1D10B;SH3GL1;PRKAB2;TRAPPC2L;WNT5A;SYTL1;AP1B1;TSC2;CSNK1D;PRKAB1;HGS;BIN1;MADD;RAB35;PREB;RIN3;KIF20B;UBA52;VPS25;VPS28;FTL;SPTBN4;RAB5C;COPS7B;COPS7A;PLA2G6;KLC4;GRK2;KLC2;UBB;DPH1;MAN2A1;BLOC1S1;BLOC1S3;UBC;DVL2;TBC1D13;PACSIN3;SFN;PIP5K1C;SPTBN2;AP1M1;TBC1D16;TBC1D8B;TRAPPC1;DENND4B;DENND4A;SEC16A;HPS1;TRAPPC5;ASPSCR1;TRAPPC8;SNF8;COPS6;KIF18A;KIF18B;TMEM115;GOLGB1;CHMP2A;CALM3;COPE;MON1A;C2CD5;ARF1;GDI1;ARPC1A;CLTB;AP2A1;ARRB2;PIK3C2A;AP2A2;USE1;RABEPK;AP4M1;TUBA1C;ACTR1A;TUBA1B;TUBA1A;CAPZB;MAN1A2;PPP6R1;TMED3;KIF1C;ACP2;KIF1A;SPTAN1;SEC13;TMED9;SGIP1;EXOC7;VPS37D;RAB3IL1;EPS15L1;KIF22;SPTB;EPN1;BET1L;KIF27;ARFGAP1;DNM2;ARFGAP2;GAK;TRAPPC6A;KIF2A;MYH9;NAA38;DNASE2;EXOC5;CHMP6;VAMP4;PAFAH1B3;ARF5;NAPA;TMF1;DCTN2;DCTN1;SRC;RAB1B;GPS1;VPS4A;DCTN3;STX10;CYTH2;ARFRP1;VPS51;CBS;LMAN2;FCHO2;MVB12B;AP2S1;MVB12A;VPS54;STX5;STX4;YKT6;GALNT2;GBF1;TUBB4B;RAB11B;CENPE;NECAP2;MYO1C;RAB13;TRIP10;TRIP11;COPG1
R-HSA-1640170	Cell Cycle	CCP110;SMC4;CDC20;PSMD8;GOLGA2;PSMD9;KAT5;PSMD4;PPP2R1A;TUBB3;RUVBL2;PSMD2;PSMD3;AKT1;RCC1;KNTC1;BANF1;GTSE1;PIAS4;CEP135;ESCO1;NUP210;LIG1;CEP131;CSNK1D;KNL1;VRK2;CDC25B;NUP93;SGO2;MAU2;ZNF91;AKAP9;NHP2;UBA52;MAD1L1;ANAPC2;POM121;ANAPC15;TUBGCP2

		;CDCA5;HMMR;AAAS;PKMYT1;PMF1;ANAPC11;UBB;PCBP4;TPR;UBC;ABL1;SFN;CEP78;CDT1;ACD;UBE2C;NCAPH2;PLK1;KIF18A;CDK4;UBE2S;CHMP2A;TUBGCP6;ATM;MDM4;NOP10;RAD9A;WRAP53;GSK3A;FEN1;CDKN1A;SYCP2;MCM7;NUMA1;MAST1;BRCA1;FOXM1;BRCA2;BABAM1;TUBA1C;ACTR1A;PCM1;TUBA1B;TUBA1A;MIS18BP1;NUP62;MYBL2;TK1;JAK2;POLE;EMD;CEP290;ZNF385A;OFD1;SUN2;NUDC;SEC13;RMI1;RFC2;ATRX;PPP2R5B;HAUS3;PPP2R5D;TEX15;RANGAP1;TUBG1;RBL2;MZT2A;DBF4;ESPL1;KIF2A;MCM3;MCM5;CHMP6;MCM2;DCTN2;LIN37;DCTN1;SRC;RAB1B;SSNA1;VPS4A;DCTN3;CAPG;PSMA7;AURKB;PSMB10;PSMB6;CLN3;POLD4;PSMB7;PSMB4;FZR1;CDC45;PSMB5;POLR2A;HAUS7;POLD1;POLD2;LMNA;E2F1;POLR2E;POLR2F;RAD54L;POLR2G;E2F4;POLR2I;POLR2J;MAPK3;POLR2L;CDKN2D;RANBP2;MPP2;CENPX;CEP152;FBXL18;TUBB4B;MTOR;PPP1CA;CENPE;RAD50;PSMC5;PSMC3;CENPJ;CENPM;CENPQ;CEP43;SPC24
R-HSA-453274	Mitotic G2-G2/M phases	CDKN1A;MAST1;CCP110;FOXM1;PSMD8;PSMD9;TUBA1C;ACTR1A;PCM1;TUBA1B;TUBA1A;PSMD4;TUBB3;PPP2R1A;PSMD2;PSMD3;MYBL2;GTSE1;CEP290;OFD1;CEP135;CEP131;HAUS3;CSNK1D;TUBG1;CDC25B;MZT2A;AKAP9;UBA52;DCTN2;LIN37;DCTN1;TUBGCP2;SSNA1;DCTN3;HMMR;PKMYT1;AURKB;PSMB10;PSMA7;PSMB6;PSMB7;PSMB4;PSMB5;UBB;HAUS7;UBC;E2F1;CEP78;MPP2;CEP152;PLK1;FBXL18;TUBB4B;PPP1CA;PSMC5;PSMC3;CENPJ;TUBGCP6;CEP43
R-HSA-69275	G2/M Transition	CDKN1A;MAST1;CCP110;FOXM1;PSMD8;PSMD9;TUBA1C;ACTR1A;PCM1;TUBA1B;TUBA1A;PSMD4;TUBB3;PPP2R1A;PSMD2;PSMD3;MYBL2;GTSE1;CEP290;OFD1;CEP135;CEP131;HAUS3;CSNK1D;TUBG1;CDC25B;MZT2A;AKAP9;UBA52;DCTN2;LIN37;DCTN1;TUBGCP2;SSNA1;DCTN3;HMMR;PKMYT1;AURKB;PSMB10;PSMA7;PSMB6;PSMB7;PSMB4;PSMB5;UBB;HAUS7;UBC;CEP78;MPP2;CEP152;PLK1;FBXL18;TUBB4B;PPP1CA;PSMC5;PSMC3;CENPJ;TUBGCP6;CEP43
R-HSA-69278	Cell Cycle, Mitotic	CCP110;SMC4;CDC20;PSMD8;GOLGA2;PSMD9;PSMD4;PPP2R1A;TUBB3;PSMD2;PSMD3;AKT1;RCC1;KNTC1;BANF1;GTSE1;CEP135;ESCO1;NUP210;LIG1;CEP131;CSNK1D;KNL1;VRK2;CDC25B;NUP93;SGO2;MAU2;AKAP9;UBA52;MAD1L1;ANAPC2;POM121;ANAPC15;TUBGCP2;CDCA5;HMMR;AAAS;PKMYT1;PMF1;ANAPC11;UBB;TPR;UBC;ABL1;CEP78;CDT1;UBE2C;NCAPH2;PLK1;KIF18A;CDK4;UBE2S;CHMP2A;TUBGCP6;GSK3A;FEN1;CDKN1A;MCM7;NUMA1;MAST1;FOXM1;TUBA1C;ACTR1A;PCM1;TUBA1B;TUBA1A;NUP62;MYBL2;TK1;JAK2;POLE;EMD;CEP290;OFD1;NUDC;SEC13;RFC2;PPP2R5B;HAUS3;PPP2R5D;RANGAP1;TUBG1;RBL2;MZT2A;DBF4;ESPL1;KIF2A;MCM3;MCM5;CHMP6;MCM2;DCTN2;LIN37;DCTN1;SRC;RAB1B;SSNA1;VPS4A;DCTN3;CAPG;PSMA7;AURKB;PSMB10;PSMB6;CLN3;POLD4;PSMB7;PS

		MB4;FZR1;CDC45;PSMB5;HAUS7;POLD1;POLD2;LMNA;E2F1;E2F4;MAPK3;CDKN2D;RANBP2;MPP2;CEP152;FBXL18;TUBB4B;MTOR;PPP1CA;CENPE;PSMC5;PSMC3;CENPJ;CENPM;CENPQ;CEP43;SPC24
R-HSA-162906	HIV Infection	FEN1;ARF1;ELL;AP2A1;AP2A2;PSMD8;PSMD9;PCM1;PSMD4;PSMD2;PSMD3;NUP62;AP1S1;RCC1;ELOA;ELOB;BANF1;NELFB;NELFA;AP2M1;SEC13;NUP210;LIG1;AP1B1;VPS37D;HLA-A;GTF2F1;RANGAP1;NUP93;CHMP6;UBA52;VPS28;POM121;CTDP1;CUL5;VPS4A;FURIN;AAAS;PSMB10;PSMA7;PSMB6;PSMB7;PSMB4;PSMB5;UBB;POLR2A;MVB12B;TPR;UBC;POLR2E;AP2S1;MVB12A;POLR2F;POLR2G;POLR2I;POLR2J;POLR2L;AP1M1;RANBP2;XRCC6;TAF10;HMGA1;SSRP1;SUPT5H;MTOR;PSMC5;PSMC3;ERCC2;NMT1;CHMP2A;TAF6
R-HSA-2408522	Hellenomania acid metabolism	RPL3;RPL32;RPL31;RPLP1;RPLP0;RRP1;RPL10A;RPL8;RPS15;RPS14;RPS16;RPL18A;QARS1;RPS19;RPL36;RPL35;RPLP2;RPS11;RPS7;RPS8;RPS5;MARS1;RPL13A;RPSA;SARS1;CRY2;RPL37A;RPL27;RPL29;RPL28;UBA52;DCTPP1;AHCY;RPL10;RPL12;RPL11;UBB;CBS;UBC;RPS3;RPL13;RPS2;RPL18;RPL19;EEFSEC;RPL41;CBSL;RPS26;RPS28;EEF1AKMT4;RPS29;RPL27A;FAU;RPS21;RPL26L1
R-HSA-174178	APC/C:Cdh1 mediated degradation of Cdc20 and other APC/C:Cdh1 targeted proteins in late mitosis/early G1	ANAPC15;AURKB;PSMB10;PSMA7;ANAPC11;PSMB6;PSMD8;CDC20;PSMB7;PSMD9;PSMB4;FZR1;PSMB5;PSMD4;UBB;PSMD2;PSMD3;UBC;UBE2C;PLK1;PSMC5;PSMC3;UBE2S;UBA52;ANAPC2
R-HSA-380320	Recruitment of NuMA to mitotic centrosomes	NUMA1;DCTN2;DCTN1;TUBGCP2;SSNA1;MAST1;DCTN3;CCP110;TUBA1C;PCM1;ACTR1A;TUBA1B;TUBA1A;TUBB3;PPP2R1A;HAUS7;CEP290;CEP78;OFD1;CEP135;CEP152;PLK1;CEP131;HAUS3;CSNK1D;TUBG1;TUBB4B;MZT2A;CENPJ;AKAP9;TUBGCP6;CEP43
R-HSA-6811434	COPI-dependent Golgi-to-ER retrograde traffic	NAPA;ARF1;KDELR1;RAB1B;USE1;TUBA1C;KLC4;TUBA1B;TUBA1A;KLC2;TUBB3;KIF5C;TMED3;KIF1C;KIF1A;KIF21B;TMED9;GBF1;KIF22;TUBB4B;KIF27;ARFGAP1;ARFGAP2;CENPE;KIF18A;KIF18B;KIF2A;COPG1;KIF20B;ARF5;COPE
R-HSA-6811442	Intra-Golgi and retrograde Golgi-to-ER traffic	ARF1;KDELR1;GCC2;USE1;RABEPK;TUBA1C;ACTR1A;GOLGA4;TUBA1B;TUBA1A;CAPZB;MAN1A2;TUBB3;KIF5C;TMED3;ARFIP2;KIF1C;ACP2;KIF1A;KIF21B;TMED9;KIF22;BET1L;KIF27;ARFGAP1;ARFGAP2;KIF2A;NAA38;VAMP4;KIF20B;PAFAH1B3;ARF5;NAPA;TMF1;DCTN2;DCTN1;RAB1B;DCTN3;PLA2G6;STX10;ARFRP1;KLC4;CYTH2;KLC2;VPS51;MAN2A1;CBS;VPS54;STX5;YKT6;GALNT2;GBF1;TUBB4B;CENPE;KIF18A;KIF18B;TRIP11;COPG1;COPE
R-HSA-380270	Recruitment of mitotic centrosome proteins and complexes	DCTN2;DCTN1;TUBGCP2;SSNA1;MAST1;DCTN3;CCP110;PCM1;ACTR1A;TUBA1A;PPP2R1A;HAUS7;CEP290;CEP78;OFD1;CEP135;CEP152;PLK1;CEP131;HAUS3;CSNK1D;TUBG1;TUBB4B;MZT2A;CENPJ;AKAP9;TUBGCP6;CEP43
R-HSA-8854518	AURKA Activation by TPX2	DCTN2;DCTN1;SSNA1;MAST1;DCTN3;CCP110;HMMR;AURKB;PCM1;ACTR1A;TUBA1A;PPP2R1A;HAU

		S7;CEP290;CEP78;OFD1;CEP135;CEP152;PLK1;CEP131;HAUS3;CSNK1D;TUBG1;TUBB4B;CENPJ;AKAP9;CEP43
R-HSA-380287	Centrosome maturation	DCTN2;DCTN1;TUBGCP2;SSNA1;MAST1;DCTN3;CCP110;PCM1;ACTR1A;TUBA1A;PPP2R1A;HAUS7;CEP290;CEP78;OFD1;CEP135;CEP152;PLK1;CEP131;HAUS3;CSNK1D;TUBG1;TUBB4B;MZT2A;CENPJ;AKAP9;TUBGCP6;CEP43
R-HSA-68867	Assembly of the pre-replicative complex	CDT1;MCM7;PSMB10;PSMA7;PSMB6;PSMD8;PSMB7;PSMD9;PSMC5;PSMB4;PSMB5;PSMC3;PSMD4;UBB;PSMD2;PSMD3;UBC;MCM3;E2F1;MCM5;UBA52;MCM2
R-HSA-6807878	COPI-mediated anterograde transport	NAPA;SPTBN4;ARF1;DCTN2;DCTN1;KDELR1;RAB1B;DCTN3;GOLGA2;TUBA1C;ACTR1A;TUBA1B;TUBA1A;CAPZB;TUBB3;TMED3;STX5;ACP2;SPTAN1;YKT6;SPTBN2;TMED9;GBF1;TUBB4B;SPTB;BET1L;ARFGAP1;ARFGAP2;TMEM115;GOLGB1;COPG1;ARF5;COPE
R-HSA-75815	Ubiquitin-dependent degradation of Cyclin D	GSK3A;PSMB10;PSMA7;PSMB6;PSMD8;CLN3;PSMB7;PSMD9;PSMC5;PSMB4;PSMB5;PSMC3;PSMD4;UBB;CDK4;PSMD2;PSMD3;UBC;UBA52
R-HSA-72695	Formation of the ternary complex, and subsequently, the 43S complex	RPS7;RPS8;RPS5;RPSA;RPS15;RPS26;RPS14;RPS28;RPS16;EEF1AKMT4;UBB;RPS19;RPS29;EIF3I;CRY2;EIF3G;RPS3;FAU;RPS2;EIF3C;RPS11;EIF3D;RPS21;EIF3B
R-HSA-9679191	Potential therapeutics for SARS	CNTFR;ROCK1;ROCK2;ARID4A;ATP1A3;ARID4B;AP2A1;FURIN;CHD3;ATP1A1;COMT;AP2A2;MTA1;TBK1;AP2S1;JAK2;MTA2;AP2M1;MBD3;ITGA4;SIGMAR1;TYK2;GATAD2A;REST;BRMS1;IMPDH1;BIN1;IMPDH2;FXYD6;FKBP4
R-HSA-2565942	Regulation of PLK1 Activity at G2/M Transition	DCTN2;DCTN1;SSNA1;MAST1;DCTN3;CCP110;AURKB;PCM1;ACTR1A;TUBA1A;UBB;PPP2R1A;HAUS7;UBC;CEP290;CEP78;OFD1;CEP135;CEP152;PLK1;CEP131;HAUS3;CSNK1D;TUBG1;TUBB4B;PPP1CA;CENPJ;AKAP9;UBA52;CEP43
R-HSA-6781827	Transcription-Coupled Nucleotide Excision Repair (TC-NER)	ELL;GPS1;COPS7B;COPS7A;PRPF19;POLD4;UBB;POLR2A;POLD1;POLD2;UBC;POLR2E;POLR2F;POLR2G;POLK;POLR2I;POLR2J;POLE;POLR2L;LIG1;RFC2;XRCC1;DDB1;XAB2;COPS6;ERCC1;ERCC2;UBA52
R-HSA-69563	p53-Dependent G1 DNA Damage Response	CDKN1A;PSMB10;PSMA7;PSMB6;PSMD8;PSMB7;PSMD9;PSMC5;PSMB4;PSMB5;PSMC3;PSMD4;UBB;PCBP4;PSMD2;PSMD3;UBC;ATM;MDM4;UBA52;ZNF385A
R-HSA-69580	p53-Dependent G1/S DNA damage checkpoint	CDKN1A;PSMB10;PSMA7;PSMB6;PSMD8;PSMB7;PSMD9;PSMC5;PSMB4;PSMB5;PSMC3;PSMD4;UBB;PCBP4;PSMD2;PSMD3;UBC;ATM;MDM4;UBA52;ZNF385A
R-HSA-1280218	Adaptive Immune System	IFITM3;IFITM1;CD81;KEAP1;IFI30;PVR;CDC20;PSMD8;HERC4;PSMD9;PSMD4;PPP2R1A;TUBB3;KIF5C;PSMD2;PSMD3;TOM1;AP1S1;AKT1;AP2M1;FBXO9;FBXW4;FBXW5;WSB1;FBXW9;HLA-B;AP1B1;HLA-C;CYBA;HLA-A;FBXO10;TRAIP;RNF123;RNF126;CDC34;STIM1;ORAI2;SPNS1;TRIB3;RBCK1;UBA52;TRIM11;ANAPC2;CUL7;CUL5;ITPR2;ITPR3;PIK3R2;UBE2J2;RAP1GAP;

		ANAPC11;KLC4;KLC2;UBB;RNF217;UBC;PLCG1;SPTBN2;AP1M1;BTNL9;VASP;RAP1GAP2;KLHL25;UBE2C;CCDC14;BTBD6;FBXO31;KIF18A;UBE2S;UBE2O;UBA1;CALM3;CALR;NFKBIE;FBXL4;MAP3K14;DZIP3;UBE2M;RNF220;ARF1;LRSAM1;AP2A1;AP2A2;MRC2;SEC61A1;TUBA1C;ACTR1A;TUBA1B;ACTR1B;TUBA1A;CAPZB;MLST8;ACP2;ELOB;IKBKG;CTSD;SEC13;ITGA4;PPP2R5B;PPP2R5D;KIF22;VAV1;LRRC41;DNM2;TRAF7;KIF2A;CANX;EVL;SOS1;THOP1;RAPGEF3;DCTN2;DCTN1;MGRN1;SRC;DCTN3;WAS;PSMA7;RELA;PSMB10;PSMB6;PSMB7;PSMB4;FZR1;PSMB5;HECTD2;HECTD3;POC1A;AP2S1;RICTOR;CSK;STX4;PAK3;NPDC1;BCAP31;ERAP2;RNF25;FBXL19;MIB2;FBXL18;FBXL15;TUBB4B;MTOR;FBXL12;CENPE;PSMC5;PSMC3;ASB6;STUB1;NECTIN2;SIPA1;SPSB4
R-HSA-380284	Loss of proteins required for interphase microtubule organization from the centrosome	DCTN2;DCTN1;SSNA1;MAST1;DCTN3;CCP110;PCM1;ACTR1A;TUBA1A;PPP2R1A;HAUS7;CEP290;CEP78;OFD1;CEP135;CEP152;PLK1;CEP131;HAUS3;CSNK1D;TUBG1;TUBB4B;CENPJ;AKAP9;CEP43
R-HSA-380259	Loss of Nlp from mitotic centrosomes	DCTN2;DCTN1;SSNA1;MAST1;DCTN3;CCP110;PCM1;ACTR1A;TUBA1A;PPP2R1A;HAUS7;CEP290;CEP78;OFD1;CEP135;CEP152;PLK1;CEP131;HAUS3;CSNK1D;TUBG1;TUBB4B;CENPJ;AKAP9;CEP43
R-HSA-8852276	The role of GTSE1 in G2/M progression after G2 checkpoint	CDKN1A;PLK1;TUBB4B;PSMB10;PSMA7;PSMB6;PSMD8;TUBA1C;PSMB7;PSMD9;PSMC5;PSMB4;TUBA1B;PSMB5;TUBA1A;PSMC3;PSMD4;UBB;TUBB3;PSMD2;PSMD3;UBC;GTSE1;UBA52
R-HSA-8856688	Golgi-to-ER retrograde transport	NAPA;ARF1;DCTN2;DCTN1;KDELR1;RAB1B;DCTN3;PLA2G6;USE1;TUBA1C;KLC4;ACTR1A;TUBA1B;TUBA1A;KLC2;CAPZB;TUBB3;KIF5C;TMED3;KIF1C;ACP2;KIF1A;KIF21B;TMED9;GALNT2;GBF1;KIF22;TUBB4B;KIF27;ARFGAP1;ARFGAP2;CENPE;KIF18A;KIF18B;KIF2A;COPG1;KIF20B;PAFAH1B3;ARF5;COPE
R-HSA-4086400	PCP/CE pathway	CLTB;AP2A1;ARRB2;AP2A2;PSMB10;PSMA7;PSMB6;PSMD8;PSMB7;PSMD9;PSMB4;PSMB5;PSMD4;UBB;PSMD2;DVL1;PSMD3;UBC;AP2S1;DVL2;RAC3;AP2M1;FZD3;WNT5B;WNT5A;PSMC5;PSMC3;PFN1;UBA52
R-HSA-2467813	Separation of Sister Chromatids	MAST1;CDC20;PSMD8;PSMD9;TUBA1C;TUBA1B;TUBA1A;PSMD4;TUBB3;PPP2R1A;PSMD2;PSMD3;KNTC1;NUDC;SEC13;PPP2R5B;PPP2R5D;KNL1;RANGAP1;SGO2;ESPL1;KIF2A;UBA52;MAD1L1;ANAPC2;ANAPC15;CDCA5;PMF1;AURKB;PSMB10;PSMA7;ANAPC11;PSMB6;PSMB7;PSMB4;PSMB5;UBB;UBC;RANBP2;UBE2C;PLK1;TUBB4B;CENPE;PSMC5;KIF18A;PSMC3;UBE2S;CENPM;CENPQ;SPC24
R-HSA-174154	APC/C:Cdc20 mediated degradation of Securin	ANAPC15;UBE2C;PSMB10;PSMA7;ANAPC11;PSMB6;CDC20;PSMD8;PSMB7;PSMD9;PSMC5;PSMB4;PSMB5;PSMC3;PSMD4;UBB;UBE2S;PSMD2;PSMD3;UBC;UBA52;ANAPC2
R-HSA-9648895	Response of EIF2AK1 (HRI) to heme deficiency	PPP1R15A;DDIT3;ASNS;TRIB3;CHAC1;ATF4

R-HSA-69615	G1/S DNA Damage Checkpoints	CDKN1A;PSMB10;PSMA7;PSMB6;PSMD8;PSMB7;PSMD9;PSMC5;PSMB4;PSMB5;PSMC3;PSMD4;UBB;PCBP4;PSMD2;PSMD3;UBC;ATM;MDM4;UBA52;ZNF385A
R-HSA-5676590	NIK-->noncanonical NF-kB signalling	PSMB10;RELA;PSMA7;NFKB2;PSMB6;PSMD8;PSMB7;PSMD9;PSMC5;PSMB4;PSMB5;PSMC3;PSMD4;UBB;PSMD2;PSMD3;UBC;UBA52;MAP3K14;UBE2M
R-HSA-68882	Mitotic Anaphase	MAST1;CDC20;PSMD8;PSMD9;TUBA1C;TUBA1B;TUBA1A;PSMD4;TUBB3;PPP2R1A;PSMD2;PSMD3;NUP62;RCC1;KNTC1;BANF1;EMD;NUDC;SEC13;PPP2R5B;PPP2R5D;KNL1;VRK2;RANGAP1;NUP93;SGO2;ESPL1;KIF2A;CHMP6;UBA52;MAD1L1;ANAPC2;POM121;ANAPC15;CDCA5;VPS4A;PMF1;AURKB;PSMB10;PSMA7;ANAPC11;PSMB6;PSMB7;PSMB4;PSMB5;UBB;LMNA;UBC;RANBP2;UBE2C;PLK1;TUBB4B;CENPE;PSMC5;KIF18A;PSMC3;UBE2S;CHMP2A;CENPM;CENPQ;SPC24
R-HSA-2979096	NOTCH2 Activation and Transmission of Signal to the Nucleus	APH1A;PSENEN;NCSTN;UBB;MDK;UBC;NEURL1;PSEN2;MIB2;ADAM10;ALG3;UBA52
R-HSA-2555396	Mitotic Metaphase and Anaphase	MAST1;CDC20;PSMD8;PSMD9;TUBA1C;TUBA1B;TUBA1A;PSMD4;TUBB3;PPP2R1A;PSMD2;PSMD3;NUP62;RCC1;KNTC1;BANF1;EMD;NUDC;SEC13;PPP2R5B;PPP2R5D;KNL1;VRK2;RANGAP1;NUP93;SGO2;ESPL1;KIF2A;CHMP6;UBA52;MAD1L1;ANAPC2;POM121;ANAPC15;CDCA5;VPS4A;PMF1;AURKB;PSMB10;PSMA7;ANAPC11;PSMB6;PSMB7;PSMB4;PSMB5;UBB;LMNA;UBC;RANBP2;UBE2C;PLK1;TUBB4B;CENPE;PSMC5;KIF18A;PSMC3;UBE2S;CHMP2A;CENPM;CENPQ;SPC24
R-HSA-2682334	EPH-Ephrin signalling	ROCK1;ROCK2;SRC;ARPC1A;CLTB;PSEN2;AP2A1;AP2A2;EFNA4;APH1A;EFNB1;NCSTN;CFL1;AP2S1;MYH14;PAK3;EPHB2;GIT1;AP2M1;EPHB4;PSENEN;MMP2;LIMK2;LIMK1;ADAM10;ALG3;VAV2;EFNA1;MYL6;EFNA3;RASA1;MYH9;NGEF;EPHA2
R-HSA-72649	Translation initiation complex formation	RPS15;RPS14;RPS16;RPS19;UBB;RPS3;RPS2;RPS11;RPS7;RPS8;RPS5;RPSA;RPS26;RPS28;EEF1AKMT4;RPS29;EIF3I;CRY2;EIF3G;FAU;EIF3C;EIF3D;RPS21;EIF3B;EIF4G1
R-HSA-5607761	Dectin-1 mediated noncanonical NF-kB signalling	PSMB10;RELA;PSMA7;NFKB2;PSMB6;PSMD8;PSMB7;PSMD9;PSMC5;PSMB4;PSMB5;PSMC3;PSMD4;UBB;PSMD2;PSMD3;UBC;UBA52;MAP3K14;UBE2M
R-HSA-72662	Activation of the mRNA upon binding of the cap-binding complex and eIFs, and subsequent binding to 43S	RPS15;RPS14;RPS16;RPS19;UBB;RPS3;EIF4EBP1;RPS2;RPS11;RPS7;RPS8;RPS5;RPSA;RPS26;RPS28;EEF1AKMT4;RPS29;EIF3I;CRY2;EIF3G;FAU;EIF3C;EIF3D;RPS21;EIF3B;EIF4G1
R-HSA-6782210	Gap-filling DNA repair synthesis and ligation in TC-NER	LIG1;RFC2;XRCC1;PRPF19;DDB1;XAB2;POLD4;UBB;POLR2A;POLD1;POLD2;ERCC2;UBC;POLR2E;POLR2F;POLR2G;POLK;POLR2I;POLR2J;UBA52;POLE;POLR2L
R-HSA-8943724	Regulation of PTEN gene transcription	MBD3;HDAC5;CBX6;PHC2;HDAC3;CBX2;ATN1;CHD3;MTOR;HDAC7;GATAD2A;RPTOR;REST;MTA1;PC;SCMH1;MLST8;LAMTOR2;LAMTOR1;MAF1;MTA2;LAMTOR4;BAP1;MAPK3

R-HSA-174113	SCF-beta-TrCP mediated degradation of Emi1	PSMB10;PSMA7;PSMB6;CDC20;PSMD8;PSMB7;PSMD9;PSMC5;PSMB4;FZR1;PSMB5;PSMC3;PSMD4;UBB;PSMD2;PSMD3;UBC;UBA52
R-HSA-8854050	FBXL7 down-regulates AURKA during mitotic entry and in early mitosis	FBXL18;PSMB10;AURKB;PSMA7;PSMB6;PSMD8;PSMB7;PSMD9;PSMC5;PSMB4;PSMB5;PSMC3;PSMD4;UBB;PSMD2;PSMD3;UBC;UBA52
R-HSA-68886	M Phase	NUMA1;MAST1;CCP110;SMC4;CDC20;PSMD8;GOLGA2;PSMD9;TUBA1C;ACTR1A;PCM1;TUBA1B;TUBA1A;PSMD4;TUBB3;PPP2R1A;PSMD2;PSMD3;NUP62;RCC1;KNTC1;BANF1;CEP290;EMD;OFD1;NUDC;SEC13;CEP135;NUP210;CEP131;PPP2R5B;HAUS3;CSNK1D;PPP2R5D;KNL1;VRK2;TUBG1;RANGAP1;NUP93;MZT2A;SGO2;MAU2;ESPL1;KIF2A;AKAP9;CHMP6;UBA52;MAD1L1;ANAPC2;POM121;ANAPC15;DCTN2;DCTN1;TUBGCP2;RAB1B;SSNA1;CDCA5;VPS4A;DCTN3;CAPG;AAAS;PMF1;AURKB;PSMB10;PSMA7;ANAPC11;PSMB6;PSMB7;PSMB4;PSMB5;UBB;HAUS7;LMNA;TPR;UBC;MAPK3;CEP78;RANBP2;UBE2C;CEP152;NCAPH2;PLK1;TUBB4B;MTOR;CENPE;PSMC5;KIF18A;PSMC3;UBE2S;CENPJ;CHMP2A;CENPM;TUBGCP6;CENPQ;CEP43;SPC24
R-HSA-5696397	Gap-filling DNA repair synthesis and ligation in GG-NER	POLD4;UBB;LIG1;RFC2;POLD1;POLD2;UBC;XRCC1;POLK;UBA52;POLE